

**The Role of Cohesin Associated Factors, Pds5, Scc3,
and Wpl1 during Cohesion Establishment and
Maintenance in Budding Yeast**

Dissertation

der Mathematisch-Naturwissenschaftlichen Fakultät

der Eberhard Karls Universität Tübingen

zur Erlangung des Grades eines

Doktors der Naturwissenschaften

(Dr. rer. nat.)

vorgelegt von

Irina Kulemzina

aus Rovno, Ukraine

Tübingen

2012

Tag der mündlichen Qualifikation:

15.10.2012

Dekan:

Prof. Dr. Wolfgang Rosenstiel

1. Berichterstatter:

Dr. Dmitri Ivanov

2. Berichterstatter:

Prof. Dr. Doron Rapaport

ACKNOWLEDGEMENTS

I would like to thank Prof. Dr. Doron Rapaport, Dr. Dmitri Ivanov, Prof. Dr. Detlef Weigel, Dr. Adrian Streit, Dr. Antonio Virgilio Failla, Dr. Christa Lanz, Dr. Gunnar Rätch, Berit Lochmann, Allana Schooley, Susanne Hanel, Olaf-Oliver Wolz, Olga Zhukova, Vipin Sreedharan, Stephanie Heinrich, Andrei Fadeev and Vikash Verma who helped me to overcome the short and steep way from the beginning of my project to its happy end. Thank you!

I am very grateful to my university supervisor Prof. Dr. Doron Rapaport and my direct supervisor Dr. Dmitri Ivanov for giving me the opportunity to work on the interesting and challenging project and for doing their best to help me to finish it successfully. I also would like to thank Prof. Dr. Detlef Weigel and Dr. Adrian Streit, the members of my thesis advisory committee, for their helpful comments and support.

I highly appreciate the collaboration with Dr. Christa Lanz, Dr. Gunnar Rätch and Vipin Sreedharan, which allowed to obtain important ChIP-Seq data for my project. I thank Olga Zhukova and Dr. Adrian Streit, who helped me a lot with qPCR, Berit and Stephanie, who helped me a lot with writing the summary in German.

I would like to thank all members of our group, the AG Ivanov, since during all the time I felt like I was at the right place and was doing right things. Thank you Dmitri, for being the best supervisor and giving me a chance to appreciate the importance of standard deviation and become a PhD student. Thank you Berit, you saved me so many times and made my life as a foreigner in Germany and in the lab smooth, enjoyable, and easy going. Thank you Susanne and Olli for sharing your knowledge, good mood, and relaxing chocolate-breaks with me. Thank you Allana for improving our paper and putting articles and thoughts in my head to their right places and order. Thank you Virgilio for teaching me microscopy and supporting my self-confidence. I think doing science in company of those people is awesome.

I am very grateful to all members of my family, who are always encouraging and supportive in important moments for me. Thank you Olga Vakhrusheva, Evgenii Leushkin, Olga Lisitzuna, Berit Lochmann, and Allana Schooley, my old and new friends!

TABLE OF CONTENTS

| | | |
|-----------|--|-----------|
| 1 | INTRODUCTION | 1 |
| 1.1 | The mechanisms ensuring accurate sister chromatid segregation during cell division | 1 |
| 1.2 | Spindle tension ensures bi-orientation of sister chromatids | 4 |
| 1.3 | Sister chromatid cohesion contributes to the formation of the spindle tension | 4 |
| 1.3.1 | Cohesin complex maintains sister chromatid cohesion | 5 |
| 1.3.1.1 | Structure of the cohesin complex | 6 |
| 1.3.1.2 | Additional proteins associate with cohesin complex | 7 |
| 1.3.1.2.1 | Scc3 | 8 |
| 1.3.1.2.2 | Pds5 | 9 |
| 1.3.1.2.3 | Wapl | 11 |
| 1.3.1.3 | Models for sister chromatid cohesion | 11 |
| 1.3.2 | Sister chromatid cohesion could be mediated by DNA | 15 |
| 1.4 | Fate of cohesin during the cell cycle | 17 |
| 1.4.1 | Loading of cohesin on DNA | 17 |
| 1.4.2 | Establishment of sister chromatid cohesion..... | 21 |
| 1.4.3 | Cohesin removal from chromosomal arms in vertebrate cells during prophase | 26 |
| 1.4.4 | Cohesin removal from chromosomes at the anaphase onset..... | 29 |
| 1.4.5 | Cohesin after anaphase | 31 |
| 1.5 | Non-mitotic functions of the cohesin ring | 34 |
| 1.5.1 | Cohesin role in DNA damage repair..... | 34 |
| 1.5.2 | Cohesin role in apoptosis | 38 |
| 1.5.3 | Cohesin role in meiosis..... | 39 |
| 1.5.4 | Cohesin role in centrosomes duplication and separation | 41 |
| 1.5.5 | Cohesin role in interphase genome organization, regulation of gene expression and development | 42 |
| 1.6 | Aim of this study | 49 |
| 2 | RESULTS | 51 |
| 2.1 | Contributions | 51 |
| 2.2 | Approaches for Pds5 and Scc3 depletion | 51 |
| 2.2.1 | N-terminal DHFR-based degron..... | 51 |
| 2.2.2 | C-terminal Eco1-derived degron..... | 56 |

| | |
|---|-----------|
| 2.3 Stoichiometric amounts of Pds5, Scc3, and Wpl1 are not required to maintain the stable association of cohesin with chromosomes | 61 |
| 2.3.1 Cohesin complexes devoid of Pds5 and Scc3 maintain their association with DNA .61 | |
| 2.3.2 Depletion of Pds5, Scc3 or Wpl1 does not affect the stability of cohesin association with the chromosomes..... | 63 |
| 2.4 Pds5 and Scc3 are stable subunits of the cohesin ring in vivo | 68 |
| 2.5 Depletion of Pds5, Scc3 or Wpl1 does not affect the genome-wide distribution of the cohesin..... | 69 |
| 2.6 Cohesin rings devoid of Scc3 and Pds5 topologically embrace DNA..... | 74 |
| 2.7 Pds5 and Scc3 depletion affects sister chromatid cohesion..... | 76 |
| 2.7.1 Pds5 and Scc3 depletion via Eco1-derived degron results in cohesion defect..... | 77 |
| 2.7.2 Pds5 and Scc3 depletion with DHFR-degron in a single cell cycle experiment results in a modest cohesion defect..... | 78 |
| 3 DISCUSSION..... | 83 |
| 3.1 Are Pds5 and Scc3 cohesin maintenance factors? | 83 |
| 3.1.1 Pds5 and Scc3 are stably bound to the cohesin ring in vivo | 84 |
| 3.1.2 Does the depletion of Pds5 and Scc3 release cohesin from DNA?..... | 85 |
| 3.2 What is the function of Pds5 and Scc3 in sister chromatid cohesion? | 87 |
| 3.2.1 Are Pds5 and Scc3 cohesion establishment factors?..... | 87 |
| 3.2.2 Are Pds5 and Scc3 cohesin recruitment factors? | 91 |
| 3.3 What is the function of Wpl1 in budding yeast?..... | 92 |
| 3.4 Methods employed to address Scc3 and Pds5 function in budding yeast: advantages and limitations..... | 93 |
| 4 MATERIALS AND METHODS..... | 97 |
| 4.1 Molecular biology techniques | 97 |
| 4.1.1 Polymerase chain reaction (PCR) | 97 |
| 4.1.2 Transformation of competent <i>E.coli</i> cells | 97 |
| 4.1.3 Isolation of plasmid DNA from <i>E.coli</i> | 97 |
| 4.1.4 Restriction digest of plasmid DNA | 99 |
| 4.1.5 Analysis of DNA by agarose gel electrophoresis..... | 99 |
| 4.1.6 Extraction of DNA fragments from agarose gels..... | 99 |
| 4.1.7 DNA Ligation | 99 |
| 4.1.8 DNA sequencing..... | 99 |

| | | |
|------------|--|------------|
| 4.2 | Yeast techniques | 100 |
| 4.2.1 | Budding yeast cultivation and storage of yeast strains | 100 |
| 4.2.2 | Budding yeast media..... | 100 |
| 4.2.2.1 | Liquid media | 100 |
| 4.2.2.2 | Solid media..... | 101 |
| 4.2.2.3 | Drop out solutions | 102 |
| 4.2.3 | Cell cycle arrest | 102 |
| 4.2.3.1 | Arrest in G1 with pheromone α -factor | 102 |
| 4.2.3.2 | Arrest in G2/M with nocodazole and benomyl | 103 |
| 4.2.4 | Flow cytometry analysis of DNA content in arrested yeast cells | 103 |
| 4.2.5 | Transformation of budding yeast..... | 103 |
| 4.2.6 | Stability assay for strains transformed with the minichromosome | 104 |
| 4.2.7 | Isolation of genomic DNA..... | 104 |
| 4.2.8 | Crossing of budding yeast..... | 104 |
| 4.2.9 | Tetrad dissection and analysis | 105 |
| 4.2.10 | Budding yeast strain construction..... | 105 |
| 4.2.10.1 | Construction of strains with endogenous genes tagged C-terminally | 105 |
| 4.2.10.2 | Construction of strains with endogenous genes tagged N-terminally | 105 |
| 4.2.10.3 | Constructing strains with array of LacO repeats in URA3 locus | 106 |
| 4.2.10.4 | List of strains..... | 106 |
| 4.2.11 | Induction of DHFR-based degron..... | 111 |
| 4.2.11.1 | In strains with tetO2 promoter | 111 |
| 4.2.11.2 | In strains with CUP1 promoter..... | 112 |
| 4.3 | Fluorescence microscopy | 112 |
| 4.3.1 | Fixation of <i>S.cerevisiae</i> cells for microscopy | 112 |
| 4.3.2 | Assay for sister chromatid cohesion employing strains with Eco1-derived degron . | 113 |
| 4.3.3 | Assay for sister chromatid cohesion employing strains with DHFR-based degron.. | 113 |
| 4.3.4 | Fluorescence recovery after photobleaching (FRAP)..... | 113 |
| 4.4 | Biochemical techniques | 114 |
| 4.4.1 | Chromatin immunoprecipitation experiments | 114 |
| 4.4.2 | ChIP qPCR analysis..... | 115 |
| 4.4.3 | ChIP Seq | 116 |
| 4.4.4 | Minichromosome immunoprecipitation..... | 117 |
| 4.4.5 | Southern blot analysis: capillary transfer and radioactive detection..... | 118 |
| 4.4.6 | Isolation of proteins from <i>S. cerevisiae</i> with Trichloroacetic acid | 118 |
| 4.4.7 | Western blot analysis | 119 |

| | | |
|-------|--|-----|
| 4.4.8 | Preparation of yeast chromatin pellets | 120 |
| 5 | REFERENCES | 123 |
| 6 | SUPPLEMENTAL DATA | 146 |
| 7 | APPENDIX..... | 148 |

LIST OF FIGURES

| | |
|--|----|
| Figure 1.1 Different modes of kinetochore attachment to the spindle poles in budding yeast. | 3 |
| Figure 1.2 Structure of the cohesin complex associated with three additional factors. . | 11 |
| Figure 1.3 Models of how cohesin might hold sister chromatids together..... | 14 |
| Figure 1.4 Cohesin complexes form a cylindrical array between sister kinetochores in metaphase..... | 22 |
| Figure 1.5 Fate of the cohesin ring during the cell cycle of budding yeast..... | 33 |
| Figure 1.6 Multiple functions of cohesin..... | 49 |
| Figure 2.1 Mechanism of the heat-inducible degradation of a DHFR-based degnon-protein fusion. | 52 |
| Figure 2.2 An induction of the N-terminal DHFR-based degnon results in efficient and complete degradation of Pds5 and Scc3. | 55 |
| Figure 2.3 Pds5 and Scc3 are efficiently depleted with a C-terminal Eco1-derived degnon. | 58 |
| Figure 2.4 Efficiency of Pds5 and Scc3 depletion with a C-terminal Eco1-derived degnon. | 59 |
| Figure 2.5 Pds5 and Scc3 depletion with a C-terminal Eco1-derived degnon is complete. | 60 |
| Figure 2.6 Chromatin-associated fraction of cohesin is not affected by the depletion of Scc3, Pds5 or Wpl1..... | 62 |
| Figure 2.7 ChIP-qPCR assay of Scc1..... | 64 |
| Figure 2.8 Depletion of Scc3, Pds5 or Wpl1 does not induce cohesin turnover on chromosomes. | 67 |
| Figure 2.9 Pds5 and Scc3 stably bind to the chromatin in vivo. | 69 |
| Figure 2.10 Depletion of Pds5, Scc3 or Wpl1 does not affect cohesin genome-wide distribution. | 70 |
| Figure 2.11 Cohesin distribution in the pericentromeric regions of chromosome III and V in the strains depleted of Pds5, Scc3 or Wpl1..... | 71 |
| Figure 2.12 Reproducibility of ChIP-Seq experiments. | 72 |
| Figure 2.13 Cohesin distribution at the tDNA loci of chromosome VII in the strains depleted of Pds5, Scc3 or Wpl1..... | 73 |

| | |
|---|----|
| Figure 2.14 Cohesin complexes devoid of Scc3 or Pds5 topologically embrace minichromosomes. | 75 |
| Figure 2.15 Sister chromatid cohesion defect in yeast depleted of Scc3 and Pds5 with the Eco1-derived degron. | 77 |
| Figure 2.16 Sister chromatid cohesion in yeast depleted of Scc3 and Pds5 with the DHFR-based degron..... | 80 |
| Figure 3.1 Cohesin rings depleted of Pds5, Scc3 or Wpl1 are defective in embracing both sister chromatids..... | 88 |
| Figure 3.2 Scc3 and Pds5 function to ensure that two sister chromatids are captured inside a single cohesin ring during the cohesion establishment..... | 89 |
| Figure 3.3 Pds5, Scc3, and Wpl1 might facilitate Eco1 recruitment to the cohesin complex..... | 90 |

LIST OF TABLES

| | |
|--|-----|
| Table 4.1 List of plasmids..... | 97 |
| Table 4.2 List of yeast strains used in this study | 107 |
| Table 4.3 Primary and secondary antibodies used in this study for Western blot analysis..... | 119 |
| Table 6.1 Summary of ChIP-Seq reads alignment against the <i>Saccharomyces cerevisiae</i> genome. | 146 |

ABBREVIATIONS

| | |
|--------|--|
| A, Ala | Alanine |
| aa | Amino acid |
| Amp | Ampicilin |
| APC/C | Anaphase promoting complex/cyclosome |
| ARM | Armadillo repeats |
| ARS | Autonomously Replicating Sequence |
| bp | Base pair |
| BSA | Bovine serum albumine |
| C, Cys | Cysteine |
| CARs | Cohesin associated regions |
| CDE | CEN DNA element |
| Cdk | Cyclin dependent kinase |
| CEN | Centromeric DNA |
| ChIP | Chromatin immunoprecipitation |
| D, Asp | Aspartate |
| dCTP | Deoxycytidine triphosphate |
| DHFR | Dihydrofolate reductase |
| DIG | Digoxygenin |
| DMSO | Dimethyl sulfoxide |
| DNA | Desoxyribonucleic acid |
| dNTP's | Deoxyribonucleotides |
| DSB | Double strand break |
| DTT | Dithiothreitol |
| EC | Embryonic cells |
| ECL | Enhanced chemiluminescence |
| ECR | Ecdysone receptor |
| EDTA | Ethylenediaminetetraacetic acid |
| ER | Estrogen receptor |
| FRET | Fluorescence resonance energy transfer |
| FRAP | Fluorescence recovery after photobleaching |
| g | Gramm |
| GFP | Green fluorescent protein |

| | |
|-----------------|---|
| h | Hour |
| HA | Hemagglutinin |
| HEAT | Huntingtin/Elongation factor 3/protein phosphatase 2A/Tor1 repeats |
| HEPES | 4-(2-hydroxyethyl)-1-piperazineethanesulfonic acid |
| Hph | Hygromycin |
| HR | Homologous recombination |
| HRP | Horse radish peroxidase |
| IP | Immunoprecipitation |
| K, Lys | Lysine |
| Kan | Kanamycin |
| kb | Kilo base |
| l | litre |
| L, Leu | leucine |
| LB | Luria Broth |
| leu | Leucine |
| LiAc | Lithium acetate |
| M | Molarity g/mol |
| MAT | Mating type |
| MCC | Mitotic checkpoint complex |
| mg | Milligram |
| min | Minute |
| ml | Millilitre |
| MQ | Milli Q |
| MT | Microtubules |
| Myc | Epitope tag originating from c-Myc |
| NAT | Antibiotic nourseothricin |
| NHEJ | Non-homologous end-joining |
| noc | Nocodazole |
| o/n | Overnight |
| OD _x | Optical density at x nm |
| ORC | Origin recognition complex |
| PAGE | Polyacrylamide gel electrophoresis |

| | |
|---------|--|
| PBS | Phosphate Buffered Saline |
| PCNA | Proliferating cell nuclear antigen |
| PCR | Polymerase chain reaction |
| Pds5 | Precocious dissociation of sister |
| PEG | Poly ethylene glycol |
| PIC | Protease inhibitor cocktail |
| PICH | Plk1-interacting checkpoint helicase |
| Plk1 | Polo-like kinase 1 |
| PMSF | Phenylmethylsulphonyl fluoride |
| pre-RCs | Pre-replication complexes |
| PP2A | Protein phosphatase 2A |
| qPCR | Quantitative polymerase chain reaction |
| RNAi | RNA interference |
| Rnase | Ribonuclease |
| RPA | Replication protein A |
| rpm | Rounds per minute |
| RSC | Remodels the structure of chromatin |
| RT | Room temperature |
| s | Second |
| S, Ser | Serine |
| SA | Stromal antigen |
| SAC | Spindle assembly checkpoint |
| SAP | Shrimp alkaline phosphatase |
| SC | Synaptonemal complex |
| SCC | Sister chromatid cohesion |
| SDS | Sodium dodecylsulfate |
| SPB | Spindle pole bodies |
| SSC | Saline-sodium citrate buffer |
| ssDNA | Salmon sperm DNA |
| T100 | Zymolyase |
| TAE | Tris-acetate-EDTA buffer |
| TE | Tris-EDTA buffer |
| TEV | Tobacco etch virus |

| | |
|--------|---------------------------------|
| Tris | Tris(hydroxymethyl)aminomethane |
| trp | Tryptophan |
| TX-100 | Triton X 100 |
| UV | Ultraviolet |
| V | Volt |
| w/ | With |
| WAPL | Wings apart-like |
| w/o | Without |
| YE | Yeast extract |
| μl | Microlitre |

SUMMARY

During cell division, each daughter cell receives only one of two identical copies of each parental chromosome. Proper chromosomal segregation in mitosis is dependent on sister chromatid cohesion. Identical copies of parental chromosome, termed sister chromatids, are tightly associated with each other, i.e. cohesed, from DNA replication until sister chromatid segregation to the daughter nuclei during the cell division. Sister chromatid cohesion is mediated by a protein complex, called cohesin. Cohesin consists of three core subunits, Smc1, Smc3, and Scc1, which form a ring-shaped structure capable of trapping two DNA molecules inside. The ring can embrace either one or two DNA molecules and acetylation of cohesin by the acetyltransferase, Eco1, ensures that both sister chromatids are captured inside the ring. The function of three additional factors, namely Pds5, Scc3, and Wpl1, which associate with the cohesin subunit Scc1, is less clear. The essential proteins Pds5 and Scc3 were proposed to be cohesin maintenance factors, that might lock cohesin rings on the DNA and prevent them from opening during G2 and early stages of mitosis or meiosis. Pds5 and Scc3 recruit a non-essential protein, called Wpl1, and all three factors are characterized by the cohesion “anti-establishment” activity, which is neutralized through the cohesin acetylation by Eco1.

We investigated Pds5, Scc3, and Wpl1 function in cohesion establishment and/or maintenance employing new experimental approaches. Pds5 and Scc3, which are essential for viability in budding yeast, were destabilized *in vivo* via a newly characterized degron sequence derived from the Eco1 protein, as well as the previously described DHFR-based degron. The consequences of protein depletion were carefully analyzed. Contrary to the prevailing hypothesis, we discovered that Pds5 and Scc3 are not required for locking cohesin complexes on DNA, or for cohesin association with specific chromosomal loci. However, both proteins are important for sister chromatid cohesion. Based on our results, we propose, that Pds5 and Scc3 function in cohesion establishment. Both proteins facilitate entrapment of both sister chromatids inside the cohesin ring, potentially by promoting acetylation of the Smc3 head domain by Eco1.

We show that the Eco1-derived degron is more selective in inducing protein degradation than the previously described degron and thus might provide a useful tool to study the function of essential proteins.

ZUSAMMENFASSUNG

Während der Zellteilung erhält jede der zwei Tochterzellen genau eine Kopie der genetischen Information. Die genetische Information einer Zelle ist in Chromosomen verpackt. Ein Chromosom besteht aus zwei identischen Kopien, genannt Schwesterchromatiden, die miteinander assoziiert sind. Für die akkurate Verteilung der Schwesterchromatiden ist es notwendig diese von der Replikation der DNS bis zum Zeitpunkt der Trennung durch Kohäsion zusammenzuhalten. Für die Kohäsion von Schwesterchromatiden ist der Proteinkomplex Cohesin essentiell. Cohesin besteht aus den drei Untereinheiten Smc1, Smc3 und Scc1, die eine ringförmige Struktur bilden und zwei DNS-Moleküle umschließen können. Die Acetylierung des Ringes durch die Acetyltransferase Eco1 stellt sicher, dass beide Chromatiden umschlossen werden. Die Funktion von drei weiteren Cohesin-assoziierten Proteinen, Pds5, Scc3 und Wpl1, die an Scc1 binden, ist dagegen weniger bekannt. Es wurde vorgeschlagen, dass die essentiellen Proteine Pds5 und Scc3 Faktoren für die Aufrechterhaltung eines geschlossenen Cohesinringes sind. Pds5 und Scc3 könnten eine zu frühe Öffnung von Cohesin während der G2 Phase des Zellzykluses und in der frühen Mitose bzw. Meiose verhindern. Pds5 und Scc3 sind verantwortlich für Rekrutierung des nicht-essentiellen Proteins Wpl1. Alle drei Proteine zeigen jedoch auch eine entgegengesetzte Aktivität, welche die Etablierung von Kohäsion verhindert und durch die Acetylierung von Cohesin durch Eco1 neutralisiert wird.

Wir haben die Funktion von Pds5, Scc3 und Wpl1 in der Etablierung und Aufrechterhaltung von Kohäsion der Schwesterchromatiden mit neuen experimentellen Ansätzen untersucht. Die essentiellen Proteine Pds5 und Scc3 wurden dafür mit zwei verschiedenen Degronsystemen analysiert, welche die Proteine *in vivo* nach der Induktion des Degrons abbauen. Eine der Degronsequenzen stammt von dem Protein Eco1, während das andere Degronsystem auf dem Protein DHFR basiert. Entgegen der bestehenden Theorien zeigen unsere Ergebnisse, dass Pds5 und Scc3 nicht essentiell sind für die Aufrechterhaltung eines geschlossenen Cohesinringes oder dessen Assoziation mit bestimmten Chromosomenarm-Regionen. Aus diesen Ergebnissen schließen wir, dass Pds5 und Scc3 eine wichtige Funktion in der Schaffung von Kohäsion zwischen den Schwesterchromatiden haben und eventuell erst die Umschließung von beiden Schwesterchromatiden ermöglichen, da beide Proteine die Acetylierung von Smc3 durch Eco1 fördern.

Wir zeigen zudem, dass eine Eco1-basierte Degronsequenz selektiver ist bei dem Abbau von Proteinen als das DHFR-basierende Degronsystem und ein nützliches System für zukünftige Funktionsanalysen essentieller Proteine liefert.

1 Introduction

1.1 The mechanisms ensuring accurate sister chromatid segregation during cell division

Genetic information of cell is stored in the form of DNA. Parental cell replicates DNA and during the process of cell division distributes it equally between daughter cells, supplying each with one and only copy of parental DNA. Eukaryotic cells have individual DNA molecules assembled together with associated proteins into large linear structures, termed chromosomes. During the replication stage of the cell cycle the parental chromosomes are used as templates by replication machinery to create two identical copies. The resulting identical structures, called sister chromatids, stay associated with each other until they are segregated to the daughter nuclei.

How do sister chromatids segregate to the daughter nuclei? Cell possesses several tools to ensure proper sister chromatid segregation. Each sister chromatid harbors a specific chromosomal locus, termed centromere, which are marked by centromere-specific histone variants and modifications (for review see (Verdaasdonk and Bloom, 2011)). The role of the centromere in chromatid segregation was discovered in the experiments with budding yeast circular plasmids. A plasmid, harboring short centromeric sequence was stably inherited during mitosis and meiosis (Clarke and Carbon, 1980). In budding yeast, centromeres of all 16 chromosomes are characterized by a specific DNA sequence, which consists of three conserved parts CDE I, II, and III (Centromere DNA Element) (Clarke and Carbon, 1983; Fitzgerald-Hayes et al., 1982). CDE II and CDE III are essential for chromosome segregation, while CDE I contributes to the high fidelity of chromosomal segregation (Hieter et al., 1985; McGrew et al., 1986). In several steps coordinated with cell cycle, centromeric DNA is able to recruit the components of a huge multiprotein complex, named kinetochore. In vertebrates, mitotic kinetochore consists of inner, middle and outer kinetochores, which could be detected as three distinct layers by electron microscopy (Brinkley and Stubblefield, 1966; Jokelainen, 1967). Kinetochore is believed to be the organizer of chromosomal movement during the segregation process. Indeed, outer kinetochore was shown to contain several protein complexes, which are able to recognize and anchor plus ends of microtubules, as well as motor proteins, e.g., CENP-E and dynein, involved in transport along the microtubules (Pfarr et al., 1990; Steuer et al., 1990; Yen et al., 1992). Microtubules (MTs) are long cylindrically shaped polymers, built of $\alpha\beta$ tubulin head-

to-tail heterodimers. MT have plus and minus ends, where, respectively, β or α tubulin subunits are exposed. These polymers are highly unstable, i.e. they are characterized by phases of growth, mainly happening at the plus end of the MT alternated with the phases of sudden disassembly, which could happen at both MT ends.

MT binding site within outer kinetochore is composed of highly conserved KMN network, which is built of KNL1, MIS12, and NDC80 complexes (Cheeseman and Desai, 2008; Santaguida and Musacchio, 2009). One of the NDC80 complex subunits possesses a positively charged “toe”-domain, which recognizes a negatively charged toe-print site on the surface of a microtubule, thus generating primary contacts between microtubule and kinetochore (Alushin et al., 2010; Sundin et al., 2011; Tooley et al., 2011). In budding yeast this interaction is further enforced by DAM1 complex, which was shown *in vitro* to oligomerize and form rings around MT and hence, can slide along its surface, driven by the conformational changes of MT upon its plus end depolymerization. Thus, DAM1 together with the motor proteins contributes to the movement of chromosomes along the microtubules. Kinetochore is able to convert ATP-dependent forces of motor proteins as well as GTP-dependent forces generated by assembling and disassembling microtubules, into directed chromosomal movement (Westermann et al., 2007). This directed movement of chromosomes to the opposite poles of the cell is guided by a spindle apparatus, which is formed of MTs together with centrioles and pericentriolar proteinaceous material. Centrioles together with the pericentriolar proteinaceous material form spindle poles, which are located at the opposite poles of the cells and are able to nucleate microtubules during the cell division. There are three types of MTs in the spindle, namely astral MTs, which play a role in positioning of the spindle poles in the cell, kinetochore MTs, which connect spindle poles to kinetochores and segregate chromosomes during anaphase, and pole-to-pole MTs, which play a role in establishment of spindle bipolarity.

According to the dominating “search and capture” model, dynamic microtubules grow from the centrosomes and randomly encounter with their lateral surface the kinetochores of duplicated chromosomes (Kirschner and Mitchison, 1986; McIntosh et al., 2002). The captured kinetochore then moves along the side of the microtubule to the spindle pole (Hayden et al., 1990; Rieder and Alexander, 1990). As kinetochore approaches the spindle pole the lateral attachment is converted to an end-on attachment. Alternatively, microtubules could be nucleated at the kinetochores and upon their

growth due to plus-end-biased polymerization at the kinetochores, their minus ends could be captured by astral microtubules and incorporated in the spindle pole (Khodjakov et al., 2002; Maiato et al., 2004).

In budding yeast the kinetochores of a pair of sister chromatids might attach to microtubules originating from the same pole (syntelic attachment) or from the opposite spindle poles (amphitelic attachment, also known as bipolar orientation) (Figure 1.1). However, only if sister chromatids are attached to the opposite spindle poles can they be correctly segregated to daughter cells. Therefore the syntelic mode of attachment has to be recognized and converted to the amphitelic mode.

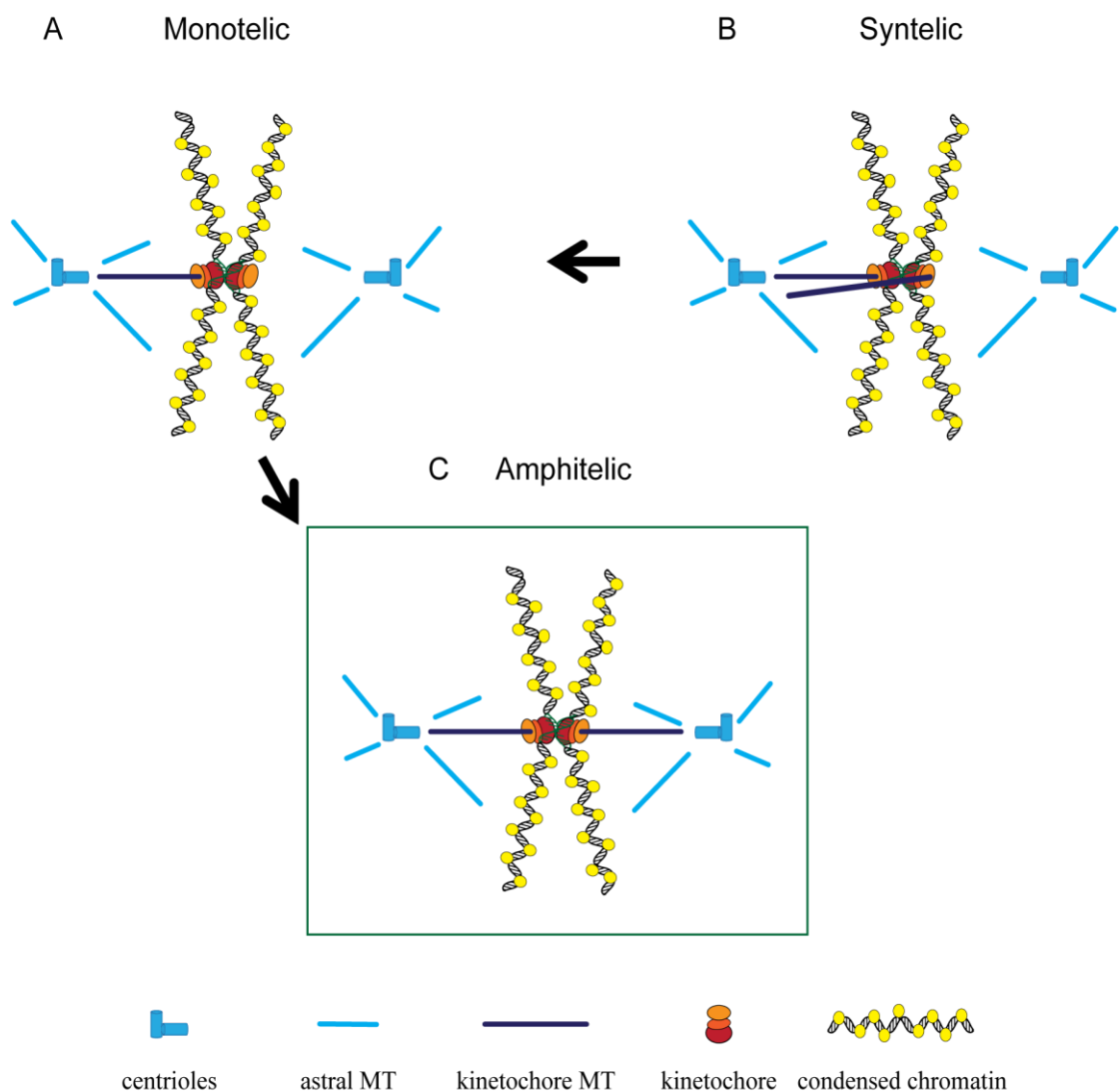


Figure 1.1 Different modes of kinetochore attachment to the spindle poles in budding yeast.

In case of monotelic attachment, only one out of two sister kinetochores is bound to a microtubule and another remains unattached (**A**). Syntelic attachment is characterized by both sister kinetochores bound to kinetochore microtubules, which originate from the same spindle pole (**B**). As monotelic and syntelic attachments will result in chromosomal segregation errors, they need to be corrected to amphitelic attachment (**C**) where sister kinetochores are bound to microtubules, originating from the opposite spindle poles.

1.2 Spindle tension ensures bi-orientation of sister chromatids

Syntelic attachments occur in the cell with some probability during the normal cell division and are corrected. The first hint on the mechanism of how it happens came from the micromanipulation experiments with meiotic chromosomes of grasshopper *Melanoplus differentialis* spermatocytes. When the chromosomes were detached from the microtubules with a needle, they always managed to re-attach to the spindle. Importantly, anaphase was never observed until all chromosomes in the cell were attached to the spindle and lined up at the equator of the cell in a so called metaphase plate (Nicklas, 1967). Since the kinetochores are located at the ends of grasshopper acrocentric chromosomes, the bipolar-oriented bivalents had an X shape (stable “configuration”) and the maloriented monopolar bivalents were U-shaped (unstable “configuration”). Dietz suggested that the stability of chromosomal orientation might be determined by the spindle tension (Dietz, 1958). If the bipolar orientation is stabilized by spindle tension directed to opposite poles, mono-oriented bivalents would be stabilized by tension applied by micromanipulation. This prediction was experimentally verified by Nicklas. Under the normal conditions bivalent in monopolar orientation were re-oriented within 16 minutes. However, when the same bivalent was detached from one pole and artificial tension was applied with a micromanipulation needle, no reorientation was detected for the duration of the experiment (311.6 minutes). Interestingly, even after bivalent was released from the needle, no reorientation was observed within 54 min (Nicklas and Koch, 1969). Thus, spindle tension is necessary for the proper chromosomal bi-orientation.

1.3 Sister chromatid cohesion contributes to the formation of the spindle tension

But how is spindle tension generated in the cell? Two processes are equally important for the spindle tension generation: microtubules pull sister kinetochores to

the opposite spindle poles and cohesive forces between the sister chromatids resist the pulling.

Physical coupling of the two sister chromatids, which emerge as a result of the replication of parental chromosome is called sister chromatid cohesion (SCC). Ironically, even before the proteins involved in sister chromatid cohesion were identified it was first discovered how sister chromatid cohesion is broken in anaphase. Since sister chromatid cohesion is broken at metaphase to anaphase transition, a trigger of anaphase would perfectly fit the role of sister chromatid cohesion “remover”. A progression towards the anaphase is dependent on the activation of an E3 ubiquitin ligase APC/cyclosome. Certain APC mutants (such as *cdc23-1*) arrest at the onset of anaphase with condensed sister chromatids and fully formed spindle (Lamb et al., 1994). These mutants are defective in the proteolysis of cyclins, which happens in anaphase (Irniger et al., 1995). It was speculated that APC/cyclosome might ubiquitinate and target for degradation protein(s) mediating cohesion.

Budding yeast Pds1p was suspected to be one of the proteins directly involved in sister chromatid cohesion. Pds1p is an APC/cyclosome substrate, whose destruction just before anaphase onset is required for sister chromatid separation. Non-degradable mutants of Pds1 prevented sister chromatids separation. Inactivation of Pds1p in the absence of functional APC allowed cells to separate sister chromatids (Yamamoto et al., 1996a, b). But two facts about Pds1p challenged the idea that this protein was involved directly in building cohesion. First, *pds1* deletion is viable in budding yeast. Second, although Pds1p localizes to nuclei (Cohen-Fix et al., 1996), it is not detected on chromosomes (Ciosk et al., 1998). Later it was shown that although Pds1 is indeed involved in sister chromatid cohesion, it does not hold sister DNA molecules together.

1.3.1 Cohesin complex maintains sister chromatid cohesion

Michaelis and colleagues identified other candidates for sister chromatid cohesion factors, Smc1, Smc3, and Scc1, that were named “cohesins” (Michaelis et al., 1997). These proteins were found in an elegant genetic screen in budding yeast. Assuming that sister chromatid cohesion is destroyed at the onset of anaphase in an APC dependent manner, mutations that would cause sister chromatids to separate when the APC is inactivated by a conditional mutation, are expected to occur in genes that encode proteins involved in cohesion. Opposite to Pds1, Smc1, Smc3, and Scc1 proteins form a

complex that localizes to chromosomes. Interestingly, the amount of Scc1 in the cell varies during the cell cycle. Scc1 is non-detectable in early G1. It accumulates from S phase to metaphase, i.e. at the time when sister chromatids are cohesed, and is degraded after anaphase when cohesion is destroyed. Importantly, Scc1 co-localized with chromatin from S phase until early anaphase. It was proposed that a trimeric complex composed of Smc1, Smc3, and Scc1 physically holds sister chromatids together and the resolution of sister chromatid cohesion during the cell division is achieved by cohesin removal from DNA (Losada et al., 1998; Toth et al., 1999). Artificially induced removal of cohesins from chromatin in metaphase in budding yeast and fruit fly results in sister chromatid segregation to opposite poles with kinetics similar to segregation that normally occurs in the cell (Gruber et al., 2003; Pauli et al., 2008). During transition from metaphase to anaphase in a normal cell cycle cohesin is removed via Scc1 cleavage by the separase Esp1 (Uhlmann et al. 1999), which is set free from its chaperone/inhibitor Pds1. If TEV cleavage sites are introduced into Scc1, TEV protease is capable of breaking cohesion in vitro and in vivo (Uhlmann et al., 1999).

1.3.1.1 Structure of the cohesin complex

The core of the cohesin complex consists of a heterotrimer of Smc1, Smc3, and Scc1 proteins. Smc1 and Smc3 fold into a 50 nm long intramolecular anti-parallel coiled coil, which is flanked on one side by the globular “head” domain comprised of the N- and C-terminal protein sequences and the central “hinge” domain. The “head” domains possess the ATPase activity and belong to ABC family of ATPases (Figure 1.2) (Haering et al., 2002). ATP binding is required for cohesin assembly in vivo and ATP hydrolysis is necessary for cohesin loading on DNA (Arumugam et al., 2003).

Smc1 and Smc3 heterodimerize via their hinge domains and form V-shaped structures, that were observed by electron microscopy (Haering et al., 2002). Crystal structure of the mouse cohesin hinge revealed two U-shaped monomers that upon dimerization form a doughnut-like domain with a positively charged channel in the middle. Kurze and colleagues demonstrated that if the positive charge is eliminated by mutagenesis, cohesin complexes can be assembled and loaded on chromosomes but no cohesion is established (Kurze et al., 2011).

Scc1 belongs to the so called kleisin family of proteins. It is comprised of the globular N- and C-terminal domains that bind to the Smc3 and Smc1 heads, respectively and the unstructured middle portion, which contains the cleavage sites for

separate. Importantly, binding of N-terminal domain of Scc1 to Smc3 head can happen only when Scc1 C-terminal domain has already bound to Smc1 head. Mutations of three highly conserved amino acids in the C-terminal domain of Scc1 that are involved in its interaction with Smc1 head disrupt recruitment of Scc1 to Smc1/Smc3 heterodimer (Haering et al., 2004). Since Scc1 connects the heads of V-shaped Smc1/3 dimer the trimeric complex assumes the shape of a ring, which was directly observed by electron microscopy (Anderson et al., 2002).

Aside from *in vitro* analysis, the interactions between cohesin subunits were also tested in live budding yeast cells, employing fluorescence resonance energy transfer (FRET) (Mc Intyre et al., 2007). According to FRET analysis, which allows to assess the distances between the interacting proteins, in living cell Smc1 and Smc3 heads were found in close proximity to each other independently of Scc1 through S phase, G2, and M phase. This is unexpected, since recombinant heads interact with each other very weakly and cannot be co-immunoprecipitated even in the presence of non-hydrolysable ATP analogue and replacement of Smc1 dimerization domain with a linker abolishes Smc1/3 dimerization *in vitro* (Haering et al., 2002). Therefore it is likely that cohesin ring assembly is facilitated inside the cell by additional mechanisms that have not been yet re-constituted *in vitro*. FRET measurements support the model that Scc1 bridges the heads together, thus completing the cohesin ring as the distance between Scc1 and both heads was sufficiently small to allow the energy transfer (Mc Intyre et al., 2007).

To summarize, Smc1, Smc3, and Scc1 form a tripartite ring-shaped complex. It was demonstrated that cohesin forms a ring not only in soluble fraction, but also when bound to DNA. Gruber and colleagues showed that in budding yeast cleavage of Scc1 with TEV protease releases cohesin complex from chromatin *in vitro* and *in vivo*. Importantly the N-terminal fragment of Scc1 was still connected to its C-terminal fragment after Scc1 cleavage via Smc1/3 heterodimer and both Scc1 fragments could be co-immunoprecipitated. The experiment with TEV-induced Scc1 cleavage *in vivo* was reproduced in *Drosophila* embryo. In this organism, as in budding yeast, cleavage of Scc1 resulted in cohesin dissociation from chromosomes and sister chromatid separation (Pauli et al., 2008).

1.3.1.2 Additional proteins associate with cohesin complex

Cohesin ring was shown to be associated with three additional factors, whose functions are not completely understood: Scc3, Pds5, and Wpl1 (Figure 1.2).

All three factors share common features. These proteins are conserved among eukaryotes, localize to the nucleus and their association with chromosomes depends on cohesin complex (Hartman et al., 2000; Kueng et al., 2006; Losada et al., 2000; Panizza et al., 2000; Rowland et al., 2009; Sumara et al., 2000; Sutani et al., 2009; Tanaka et al., 2001; Toth et al., 1999; Warren et al., 2004). Scc3, Pds5, and Wpl1 are recruited to the chromosomes by Scc1 (Hartman et al., 2000; Kueng et al., 2006; Panizza et al., 2000; Toth et al., 1999). Scc3 binds to C -terminus of Scc1 subunit in vitro (Haering et al., 2002). Wpl1 interacts with Pds5 and Scc3, forming a tripartite complex (Rowland et al., 2009). Pds5 interaction with cohesin is less stable compared to Scc3 and was shown to be highly salt sensitive (Losada et al., 2000; Sumara et al., 2000).

Sequence analysis indicated that all three proteins contain evolutionarily related repeats, ARM (Wpl1) or HEAT (Scc3 and Pds5) (Dabrowska et al., 2004; Kueng et al., 2006; Neuwald and Hirano, 2000; Panizza et al., 2000). Both, ARM (Armadillo) and HEAT (Huntingtin/Elongation factor 3/Protein phosphatase 2A/Tor1), repeats consist of tandemly arranged α -helices. ARM repeats are built by three helices, whereas HEAT repeat consists of helical hairpins, formed by only two helices (Chook and Blobel, 1999; Cingolani et al., 1999; Groves et al., 1999; Kobe, 1999; Vetter et al., 1999). It is believed that ARM and HEAT repeats are able to mediate protein-protein interactions.

Pds5 contains 26 HEAT repeats and a highly charged C-terminal end domain. It was speculated that charged C-terminal domain could bind charged molecules, e.g. DNA, while HEAT repeats could mediate protein-protein interactions, possibly with other cohesin subunits (Panizza et al., 2000).

1.3.1.2.1 Scc3

Scc3p (sister chromatid cohesion) was identified in budding yeast as a factor essential for SCC in a screen for mutants that separate sister chromatids prematurely. Specific mutations in *SCC3* resulted in premature loss of sister chromatid cohesion and high levels of chromosome missegregation (Toth et al., 1999).

Scc3 homologues were identified in mammals, *Drosophila*, fission yeast, *C.elegance*, and *Xenopus*. For example, Scc3 from *S.cerevisiae* was shown to share homology with three mammalian proteins from stromal antigens (SA) family, namely SA1, SA2 and SA3. Two different cohesin complexes, containing either SA1 or SA2, are present in HeLa cells and in *Xenopus* egg extracts (Losada et al., 2000; Sumara et al., 2000). SA3 functions in chromosome cohesion during meiosis in human and mouse

(Pezzi et al., 2000). In human cells SA2 containing cohesin is a dominant form of cohesin, while in *Xenopus* egg extracts it is only a minor population. Interestingly, in human cells it was shown that SA1 and SA2 are essential for different types of cohesion. Thus, HeLa cells depleted of SA1 are not able to establish and maintain cohesion at the telomeres. The loss of telomeric cohesion consequently disrupted cohesion along the arms, altered chromosome morphology, abolished double strand break repair in G2 (see below) and finally, led to telomere loss. Contrary to SA1, SA2 depletion has no effect on telomeric cohesion, however centromeric cohesion is lost prematurely (Canudas and Smith, 2009). Unlike human cells, *Drosophila* cells depleted of SA were characterized by normal mitotic progression and no premature loss of cohesion was detected. Chromosomal alignment during metaphase and separation during anaphase in the absence of SA proceeded almost normally with very rare defects (Vass et al., 2003).

Apart from its role in SCC, Scc3 might be involved in cohesin recruitment to certain chromosomal sites (see below). Mammalian SA1 was shown to interact in vitro and in vivo with the CCTC-binding factor CTCF, and supposedly mediates interaction between CTCF and cohesin (Rubio et al., 2008). In vertebrates SA1 and SA2 subunits of cohesin are phosphorylated during mitosis in order to allow cohesin removal from chromosome arms in prophase pathway (Losada et al., 2000) (see below).

1.3.1.2.2 Pds5

Pds5 (precocious dissociation of sisters) was simultaneously and independently identified by several groups as a protein, which plays a role in SCC (Hartman et al., 2000; Losada et al., 2000; Panizza et al., 2000; Sumara et al., 2000). Pds5 homologues are found in *Aspergillus nidulans* (BimD6), *Sordaria* (Spo76), fission yeast (Pds5), and vertebrates (Pds5A and Pds5B) (Denison et al., 1993; Hartman et al., 2000; van Heemst et al., 1999; Wang et al., 2002b).

PDS5 is an essential gene in budding yeast and thus, in order to study Pds5 function thermo-sensitive mutants allowing conditional protein inactivation were generated. Pds5 inactivation resulted in precocious loss of sister chromatid cohesion at the centromeric regions as well as at the chromosomal arms and perturbed chromosome segregation. In order to determine whether Pds5 function is essential for SCC establishment or maintenance, Pds5 was inactivated before SCC establishment in S phase or after SCC was built in metaphase. Non-functional Pds5 in S phase resulted

only in 1.5 fold reduction of viability, when much more prominent effect, i.e. 40 folds reduction in viability and loss of SCC, was observed upon its inactivation in metaphase. Thus, it was proposed that Pds5 is a cohesion maintenance factor (Hartman et al., 2000; Panizza et al., 2000). In agreement with this proposal was the fact that amounts of Scc1 associated with arms and centromeres were significantly decreased in the cells with inactivated Pds5, suggesting that Pds5 is essential for cohesin stable association with chromosomes (Panizza et al., 2000). However, *Xenopus* egg extracts depleted of Pds5A and Pds5B assembled mitotic chromosomes almost normally, displaying only slightly loosened centromeric cohesion with unperturbed arm cohesion. In contrast to budding yeast, in *Xenopus* egg extracts no reduction in amount of cohesin complexes associated with chromatin was detected in extracts depleted of Pds5. It was concluded that neither Pds5A nor Pds5B is required for stable association of cohesin with chromatin in *Xenopus* (Losada et al., 2005). Phenotype caused by *PDS5* depletion in fission yeast differs from one observed in other organisms. Interestingly, no defects in cohesion were observed in exponentially growing fission yeast lacking Pds5. However, mutant cells arrested in G2 were characterized by precociously separated sister chromatids and were defective in chromosome segregation upon re-entry into the cell cycle after prolonged G2 arrest (Tanaka et al., 2001). Thus, different organisms are characterized by different requirements for Pds5 function in sister chromatid cohesion establishment and/or maintenance.

Pds5 function is regulated by various cell cycle stage-specific post-translational modifications. For example, in budding yeast Pds5 sumoylation, which commences before DNA replication and peaks at the anaphase onset, promotes cohesin removal from chromosomes. Stead and colleagues demonstrated that temperature sensitivity and precocious loss of SCC, caused by a mutant *pds5* allele, could be suppressed by overexpression of isopeptidase Smt4, able to remove SUMO (Stead et al., 2003). Inactivation of Smt4 results in premature loss of centromeric cohesion. Loss of SCC in *smt4* mutant coincides with increased levels of sumoylated Pds5 (Bachant et al., 2002). Regulation of cohesin via Pds5 sumoylation has not been yet detected in human cells or in *Xenopus* egg extracts (Losada et al., 2005). It was speculated that Pds5B mitosis-specific phosphorylation observed in *Xenopus* egg extracts, can facilitate cohesin dissociation from chromatin or prevent cohesin re-binding to chromatin after its removal during prophase (Losada et al., 2005).

1.3.1.2.3 Wapl

Wapl (wings apart-like) was first identified in *Drosophila* and was shown to be involved in heterochromatin structure maintenance, sister chromosome cohesion, meiotic chromosome segregation, tumorigenesis, and apoptosis (Oikawa et al., 2004; Verni et al., 2000). Wapl depletion resulted in decreased levels of cohesin associated with chromosomes and sister chromatid cohesion defect in vertebrate cells, as well as in budding yeast, although in yeast *WPL1* gene is non-essential (Kueng et al., 2006; Rowland et al., 2009; Sutani et al., 2009; Warren et al., 2004). These observations support the notion that like Pds5 and Scc3, Wpl1 ensures cohesin stable association with chromosomes. Surprisingly, at the same time, Wpl1 also possesses a cohesion destabilizing function, since in vertebrate cells it was shown to be involved in cohesin removal from chromosomal arms during prophase pathway in a subcomplex with Pds5 (see below) (Kueng et al., 2006).

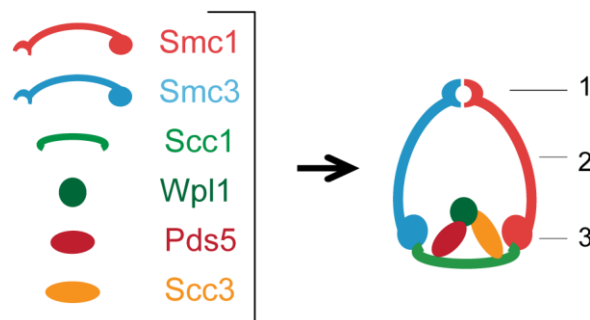


Figure 1.2 Structure of the cohesin complex associated with three additional factors.

Cohesin is a trimeric ring-shaped protein complex, formed by Smc1, Smc3, and Scc1. Smc1 and Smc3 proteins heterodimerize through their “hinge” domains (1), which are connected via two long coiled coils (2) with “head” domains (3). “Head” domains are bridged by Scc1, which recruits three additional factors, namely Pds5, Wpl1, and Scc3.

1.3.1.3 Models for sister chromatid cohesion

Early models for sister chromatid cohesion were based on an idea that V-shaped Smc1/Smc3 dimers bind DNA via the ATPase heads, i.e. one of the sister DNA molecules is bound to Smc1 head, while another is bound to Smc3 head (Figure 1.3A). Link between two sister chromatids is reinforced by Scc1, which connects Smc1 and Smc3 heads bound to DNA (Figure 1.3B) (Campbell and Cohen-Fix, 2002). However,

this model is not able to explain how Scc1 cleavage by separase can lead to sister chromatid separation.

Haering et al. proposed that cohesin associates with chromosomes by capturing sister chromatids inside the ring (Figure 1.3C). According to this so called “embrace” model, cohesin interaction with sister chromatids is strongly dependent on topology and much less on physical contacts between the proteins and DNA. Cohesin dissociation from chromatin can be triggered by ring opening, whether caused by proteolysis or subunit dissociation, but is expected to be insensitive to the treatments that will typically disrupt protein-DNA interaction, e.g., elevated salt concentrations or intercalating agents. These predictions were experimentally tested *in vivo* and *in vitro*. Indeed cohesin maintained association with DNA in 2 molar salt and in the presence of Ethidium Bromide. All mutations weakening interactions between cohesin subunits resulted in inability of cohesin rings to hold sister DNA molecules together, that argues for embrace model. The importance of the topological component in cohesin-DNA interaction can be evaluated if DNA is circular. In this case protein and DNA rings are expected to be intercatenated. They will maintain association with each other through various adverse treatments as long as the integrity of either of the rings is not broken. Cohesin rings, bound to circular minichromosomes could be immunoprecipitated from yeast lysates using antibodies against tags, fused to different subunits of tripartite cohesin ring. Linearization, but not nicking of the minichromosomes resulted in cohesin release from DNA presumably due to cohesin sliding off the DNA end. The strong dependence of protein-DNA interaction on whether DNA is circular or linear cannot be easily explained by classical protein-DNA binding. Cleavage of Scc1 with TEV protease also led to cohesin dissociation from minichromosomes (Ivanov and Nasmyth, 2005). Importantly, cohesin rings associated with minichromosomes were directly involved in holding two sisters. Cohesed and monomeric minichromosomes could be separated by native gel electrophoresis and cohesion was eliminated by either cleavage of Scc1 or linearization of DNA (Ivanov and Nasmyth, 2007).

The embrace model is compatible with a single ring embracing both sister DNAs or with cohesion being established via interaction between several cohesin rings. The models involving several rings appear attractive since a single ring is barely wide enough to accommodate two 10 nm chromatin fibers and certainly would not allow the passage of the replication fork. The hypothetical interaction between the rings can be mediated via ring intercatenation or via a separate protein (“handcuff” model) (Figure

1.3D). Alternatively, Scc1 might connect Smc1 and Smc3 heads not from the same Smc1/3 heterodimer, but from the different heterodimers. In this way Scc1 could generate a “super”-ring (Figure 1.3E) or multimeric filaments that wind around sister chromatids (“bracelet” model) (Figure 1.3F) (Huang et al., 2005; Nasmyth and Schleiffer, 2004). According to the “snap” model, the chromatid is trapped between Smc1 and Smc3 heads and Scc1 of one cohesin ring and sister chromatids tethering is caused by cohesin complexes oligomerisation (Figure 1.3G) (Huang et al., 2005). However, no oligomers of cohesin could be detected *in vivo* whether in soluble fraction or on DNA (Gruber et al., 2003). Experiments with Scc1 cleavage provide further arguments against dimeric “super” ring model. According to “super” ring model cleavage of one out of two Scc1 molecules would be sufficient to release dimers from sister chromatids. In experiments with heterozygous diploid yeast expressing TEV cleavable Scc1-HA and TEV non-cleavable Scc1-Myc cleavage of Scc1-HA did not result in the release of Scc1-Myc from minichromosomes (Ivanov and Nasmyth, 2005).

If cohesion is dependent on multimerization of cohesin rings via protein-protein contacts, it will not be able to withstand protein denaturation. To check this possibility Haering and colleagues constructed covalently closed cohesin rings. They substituted two residues on interacting surfaces of Smc1/Smc3 hinge and Scc1/Smc1 interface with cysteines and cross-linked their sulfhydryl groups with homobifunctional thiol-reactive chemicals. To lock Scc1/Smc3 interaction Scc1 N-terminus was fused via long flexible linker with 3 TEV sites to the C-terminus of Smc3 (Haering et al., 2008). When cohesed minichromosomes were isolated from strains that express mutated variants of cohesin subunits cross-linking of cysteines rendered minichromosome dimers resistant to protein denaturation with 1% SDS at 65°C. Minichromosome dimers lost their cohesion as a result of protease K digest or TEV cleavage of covalently locked cohesin, suggesting that they are indeed held together by the locked cohesin rings. These results exclude models in which sister chromatid cohesion is explained by non-topological interaction between cohesin and sister DNA molecules or involve protein-protein interactions beyond those that are required for the integrity of the ring.

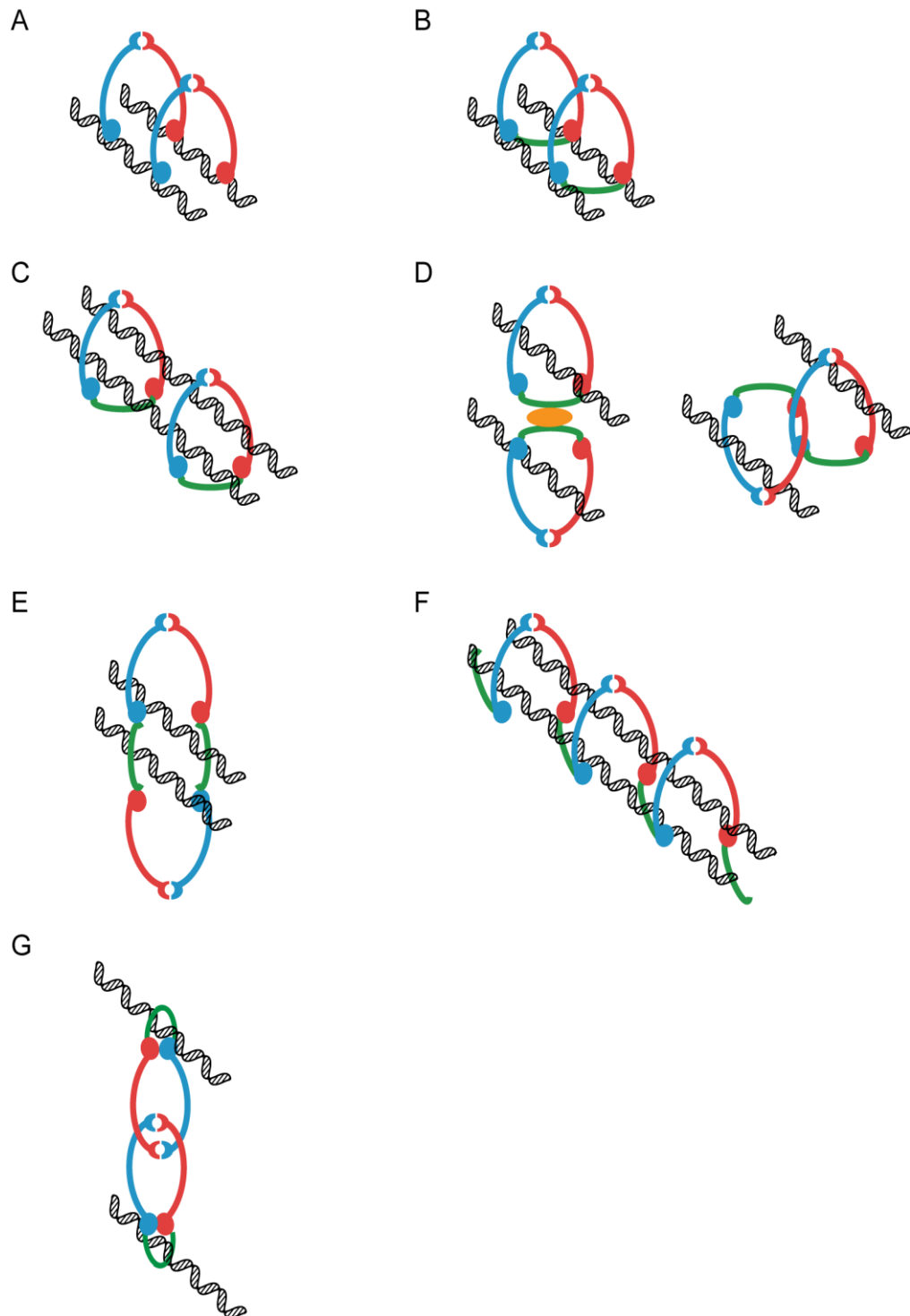


Figure 1.3 Models of how cohesin might hold sister chromatids together.

According to early models, cohesin complexes are able to bind sister chromatids via “head” domains (**A**) and Scc1 could re-enforce this binding (**B**). Embrace model postulates, that cohesion captures sister chromatids inside the ring (C, D, E, and F). Both sister chromatids could be trapped inside a single ring (“one ring embrace” model) (Gruber et al., 2003) (**C**) or each of the sister chromatids could be captured by separate cohesin rings, which then tightly associate with each other (“handcuff” model) (Zhang et al., 2008b) (**D**). This association might

be mediated by an additional hypothetical factor or by the intercatenation of two cohesin rings. According to “super-ring” model, sister chromatids are embraced by a ring, which is formed by two Smc1/Smc3 heterodimers and 2 molecules of Scc1, which connect head domains of different Smc1/Smc3 heterodimers **(E)**. Alternatively cohesin rings could form multimers, which wind around two sister chromatids (“bracelet” model) **(F)** (Huang et al., 2005; Nasmyth and Schleiffer, 2004). According to a “snap” model each of the two sister chromatids is trapped between Smc1/Smc3 “head” domains and Scc1 of two cohesin complexes, which are intercatenated (Huang et al., 2005) **(G)**.

1.3.2 Sister chromatid cohesion could be mediated by DNA

In principle sister chromatid cohesion can be mediated not only by the DNA-bound proteins but also by intertwining of the DNA molecules themselves. According to this model, two sister DNA molecules are held together via DNA catenation, which is a direct consequence of DNA replication (Murray and Szostak, 1985; Sundin and Varshavsky, 1980). This model invokes the function of topoisomerase II (Topo II), which is capable of resolving DNA catenations to promote sister chromatid separation. Since sister chromatids separate only after all chromosomes are bi-oriented, the activity of Topo II would have to be regulated very precisely, i.e., Topo II should be only activated after bi-orientation is achieved (Miyazaki and Orr-Weaver, 1994). There is no evidence of such strict regulation of Topo II activity. Experiments in vertebrates cells addressed the effect of Topo II inhibition on sister chromatid segregation. Inhibition of Topo II activity in cohesin-depleted HeLa and chicken DT40 cells resulted in a delay in early mitosis, which was nevertheless followed by anaphase (Vagnarelli et al., 2004; Wang et al., 2010). These experiments suggested that DNA catenation if not resolved until anaphase could compensate for the absence of cohesin on DNA. However, the observed compensation is incomplete, since cells, which undergo anaphase without cohesin, segregate chromatin very unevenly.

Even without Topo II inhibition ultrafine DNA bridges, which are connecting sister kinetochores are observed from metaphase till anaphase. They are presumably formed by the residual catenated DNA and their resolution requires Topo II, since observed bridges were especially prominent and persisted until cytokinesis in the cells with inhibited Topo II activity (Baumann et al., 2007; Chan et al., 2007). Topo II associated with chromosomes was shown to be active in metaphase, however, it did not succeed in completing DNA decatenation (Wang et al., 2010). It appears that centromeric cohesin has to be removed for DNA decatenation to be completed, supposedly because its presence creates physical obstacles for Topo II (Wang et al.,

2010). Topo II is able to resolve most catenation along chromosomes before metaphase, since cohesin is removed from chromosomal arms during prophase and prometaphase in vertebrate cells, while resolution of catenation within centromeric regions is postponed until the removal of centromeric cohesin, which happens during anaphase onset (Porter and Farr, 2004). It is plausible that under normal conditions the observed ultrafine DNA bridges are result of lagging or delayed decatenation, rather than structures holding sister chromatids together. Two helicases, which co-localize to the anaphase bridges, Plk1-interacting checkpoint helicase (PICH) and Bloom syndrome protein (BSP), were demonstrated to be required for the efficient decatenation. PICH and BSP form a complex, which removes nucleosomes from the centromeric DNA (Baumann et al., 2007; Chan et al., 2007; Ke et al., 2011). Helicase-mediated chromatin remodeling allows catenated threads to reel off between segregating chromosomes, and prevents DNA from being torn by spindle forces. It also provides more time and space for catenation resolution by Topo II.

Described DNA bridges could maintain inter-kinetochore tension, which may prevent undesirable reactivation of spindle assembly checkpoint (SAC) during early anaphase, caused by simultaneous removal of cohesin complexes and too abrupt loss of tension and thus prevent cell cycle arrest (Wang et al., 2010). SAC is a complex of processes in eukaryotic cell, which ensure proper chromosome segregation during cell division (for review see (Musacchio and Salmon, 2007)). SAC monitors the kinetochore binding to spindle microtubules and surveys the tension between sister kinetochores (Waters et al., 1996). Reduced tension at the kinetochore caused by inappropriate chromosome attachment, e.g. monotelic or syntelic, leads to phosphorylation of several kinetochore proteins by Aurora-B, which localizes to centromeres as a part of chromosome passenger complex (Cheeseman et al., 2002; King et al., 2007; Pinsky et al., 2003; Shang et al., 2003). Aurora-B kinase activity results in destabilization of microtubule-kinetochore attachments, thus, allowing kinetochore re-attachment (Hauf et al., 2003; Tanaka et al., 2002). In the case of attachment errors progression through the cell cycle should be paused to allow kinetochore re-attachment. Mitotic checkpoint complex (MCC) is formed during SAC activation in response to unattached kinetochores. MCC inhibits the activity of the key regulator of cell cycle progression, ubiquitin ligase APC/C, subsequently delaying degradation of securin and cyclin B, prolonging prometaphase stage and providing additional time for correction. As soon as all chromosomes are bi-oriented, SAC is

inactivated through several mechanisms and cell is allowed to progress further through the cell cycle (Howell et al., 2001; Qi and Yu, 2007).

1.4 Fate of cohesin during the cell cycle

1.4.1 Loading of cohesin on DNA

Cohesin is loaded on DNA with the help of the Scc2/Scc4 loading complex (Figure 1.5). Scc2/Scc4 homologues were identified in *S.cerevisiae*, *S.pombe*, *Xenopus* and mammals (Bernard et al., 2006; Ciosk et al., 2000; Takahashi et al., 2004; Watrin et al., 2006). Scc2/Scc4 complex is required for cohesin recruitment to DNA, but not for cohesion establishment and maintenance. In *scc2* or *scc4* mutants cohesin complexes assemble normally, but fail to associate with chromosomes at the centromere regions or along the arms (Ciosk et al., 2000). Scc2 can be co-immunoprecipitated with cohesin complex, but does not co-localize with it on the DNA (Arumugam et al., 2003). Scc2 and Scc4 are predicted to contain α -helical repeats. Similar to Pds5 and Scc3, Scc2 is composed of HEAT repeats, while Scc4 is composed of TPRs (tetratricopeptide repeats) (Neuwald and Hirano, 2000; Watrin et al., 2006). Since TPRs, as well as HEAT repeats are thought to mediate protein-protein interaction, it is possible that they facilitate Scc2/Scc4 interaction with cohesin, histones or other proteins.

In *Xenopus* Scc2/Scc4 recruitment to the chromatin in its turn depends on function of pre-replication complexes (pre-RCs) (Takahashi et al., 2004). Pre-replication complexes are composed of the initiation factors ORC, Cdc6, Cdt1, and MCM2-7, which are sequentially recruited to the origins of replication (Takahashi et al., 2004). The requirement of pre-RC for Scc2/Scc4 and cohesin loading on the DNA is likely to be specific to vertebrate, since for example in budding yeast pre-RCs are not found to interact with Scc2/Scc4 and cohesin complexes are able to associate with DNA even in G₂, when pre-RCs are already disassembled (Eckert et al., 2007; Uhlmann and Nasmyth, 1998).

Cohesin loading on DNA depends not only on Scc2/Scc4 complex, but also on ATPase activity of Smc head domains (Arumugam et al., 2003; Hu et al., 2011; Weitzer et al., 2003). The process of cohesin loading might proceed in two steps. The initial unstable interaction with DNA is converted into topological entrapment of the DNA by cohesin ring. While ATP binding to the heads is necessary for the assembly of

cohesin ring, ATP hydrolysis is required specifically for DNA topological entrapment. Mutations that abolish ATP hydrolysis, E1158Q in Smc1 and E1155Q in Smc3, lead to loss of chromatin localization as judged from the chromosome spreads, although the cohesin rings are assembled normally (Arumugam et al., 2003; Weitzer et al., 2003).

Since cohesin rings are pre-assembled prior to loading on DNA (Gruber et al., 2006; Haering et al., 2002), the rings have to be transiently opened for DNA to get inside. The ring can in principle be opened at three interfaces between cohesin subunits. Carabiner and bicycle lock models suggest that cohesin is opened due to transient dissociation of Scc1 from Smc1, or Smc3, or both of them at once. Clothes peg model suggests that Smc1 and Smc3 hinge domains transiently dissociate from each other. Gruber and colleagues tested these models by locking the interfaces between the cohesin's subunits (Gruber et al., 2006). Covalent fusions of Scc1 to Smc1, as well as Scc1 to Smc3, retained the ability to associate with chromosomes. To lock the hinge interface, Gruber et al. inserted into Smc1 and Smc3 hinges two mammalian protein domains, which form a tight dimer in the presence of a small molecule, rapamycin. These insertions had no effect on sister chromatid cohesion in the absence of rapamycin. However, when the drug was added to the growth media, cohesin was not able to associate with chromosomes although tripartite rings were formed and were able to localize to the nucleus and hydrolyze ATP (Gruber et al., 2006). It was concluded that the hinge serves as an entry gate for the DNA. Since ATP hydrolysis is a prerequisite for cohesin loading on the DNA, it is possible that the transient opening of Smc hinge domains is driven by the energy of ATP hydrolysis by the head domains.

ATP hydrolysis might, for example, trigger conformational changes within Smc1-Smc3 heads complex, which are further transmitted along the coiled coil arms to the hinge domains. Thus, torsion generated by conformational changes within heads could open hinge domains (Gruber et al., 2006). Process, similar to one proposed by this model was described for Rad50-Mre11 complex. Like Smc proteins, Rad50 possesses ABC ATPase heads connected via long coiled coils to the dimerization domains (Anderson et al., 2001; Chen et al., 2001; Connelly et al., 1998; de Jager et al., 2004; de Jager et al., 2001). It was shown that ATP hydrolysis results in the rotation of both heads up to 30° and in drastic conformational changes within coiled coils and dimerization domains (Carter et al., 2011; Lim et al., 2011; Moreno-Herrero et al., 2005). The integrity of coiled coils is expected to be of critical importance for the transmission of the conformational change from heads to the hinges. However, nicking

of either strand of the coiled coil within Smc3 does not lead to the loss of function (Gruber et al., 2003). Alternatively, conformational changes triggered by ATP hydrolysis could result in bending of the coiled coils, which would bring head domains in contact with the hinge domains and facilitate hinge opening (Gruber et al., 2006).

Cohesin complexes are found associated with chromosomes at certain sites termed cohesin associated regions (CARs). In budding yeast an average CAR site spans the length of 0,8-1 kb and they occur on chromosomal arms every 10,9 kb \pm 6,7 kb (Blat and Kleckner, 1999; Glynn et al., 2004; Laloraya et al., 2000). Cohesins are highly enriched 30-50 kb around centromere with 3-5 fold higher cohesin abundance compared to chromosomal arm sites. In budding yeast CARs are characterized by high AT-content (74 % of mapped CARs are AT-rich), however no consensus motif could be determined. CARs are correlated to the regions between convergent transcription units (70 % of CARs are located in the intergenic regions). Indeed, Glynn and colleagues showed that cohesin is expelled from highly transcribed loci, dependent not on binding of RNA Pol II per se, but rather on active transcription (Glynn et al., 2004; Lengronne et al., 2004). Therefore, cohesin preference for intergenic and non-transcribed regions is probably the result of cohesin displacement by transcriptional machinery (Tanaka et al., 1999). In addition to transcription, cohesin distribution along chromosomes is influenced by other factors, which contribute to the observed binding pattern. For example, cohesin accumulation at the centromeres and pericentric regions is at least partially dependent on the recruitment of kinetochore proteins and the assembly of a functional kinetochore (Eckert et al., 2007; Hu et al., 2011; Tanaka et al., 1999; Weber et al., 2004). Efficient recruitment of cohesin complexes to pericentromeric region depends on centromere-specific nucleosomes, Mif2p, CBF3 complex and specific regions within centromeric DNA: CDEIII is essential for cohesin's recruitment, when CDEII is needed for high efficiency of binding (Tanaka et al., 1999). Reduced tension across sister kinetochores in the absence of bipolar orientation results in increase of cohesin association with pericentromeric regions (Eckert et al., 2007). The mechanism of how kinetochores are able to recruit high levels of pericentromeric cohesin is not clear. It is possible that kinetochores recruit cohesin loading factors, such as Scc2/Scc4.

Centromeric heterochromatin is among other factors that ensure faithful chromosomal segregation during the cell division (Ekwall et al., 1995; Partridge et al., 2000; Takahashi et al., 1992). In fission yeast Swi6/HP1, a conserved component of

silent chromatin, was shown to recruit cohesin to the heterochromatic centromeres. Swi6 via its conserved chromo domain directly interacts with cohesin subunit Psc3 (homologue of Scc3) (Nonaka et al., 2002). Cohesin recruitment to the centromeres via Swi6/HP1 could be an evolutionary conserved mechanism in eukaryotes but not in budding yeast, which do not have centromeric heterochromatin or Swi6/HP1 orthologue. Deletion of Swi6 or inactivation of enzymes essential for Swi6 recruitment to heterochromatin, perturbed cohesin localization to centromeres, disrupted centromeric SCC and resulted in the defective chromosome segregation (Bernard et al., 2001b; Nonaka et al., 2002). However, deletion of *swi6* has no effect on cohesin localization to the chromosomal arms.

Additional factors facilitate cohesin loading on the chromosomal arms. For example, RSC-complex (Remodels the Structure of Chromatin), an ATP-dependent chromatin re-modeler from budding yeast, SWI/SNF nucleosome re-modeling complex, and SNF2h-containing chromatin re-modeling complex from human cells were shown to be involved in cohesin loading on the arms (Hakimi et al., 2002; Huang et al., 2004). RSC-complex was reported to localize to the cohesin binding sites shortly before cohesin complexes and to associate in vivo with cohesin subunit, Scc1, during S and G2/M phase (Huang et al., 2004). Mutations in RSC-complex subunits and SNF2h abolished cohesin binding to the sites at the chromosomal arms, but not to the centromeres (Hakimi et al., 2002; Huang et al., 2004). Subsequently, precocious sister chromatids separation was observed in the mutants. How chromatin remodeling complexes recruit cohesin to the chromosomal arm sites is not clear. According to one possible model, changes in nucleosome configuration brought about by RSC-complex facilitate stable cohesin binding to chromosomal arms.

Cohesin associated regions are distinct from the sites of cohesin loading on DNA. The initial sites of cohesin loading correspond to Scc2/Scc4 binding sites, which are located at the centromeres, adjacent to telomeres and along the chromosome arms. At many loci Scc2/Scc4 complex does not co-localize with cohesin (Hu et al., 2011; Lengronne et al., 2004). It is presumed that cohesin slides along the chromosomes from the loading sites to the CARs being pushed by transcription machinery and/or by hitherto unknown factors.

1.4.2 Establishment of sister chromatid cohesion

Sister chromatid cohesion is established in S phase, supposedly concomitant with the passage of the replication fork (Figure 1.5). If cohesin expression is blocked during DNA replication, subsequent expression cohesin in G2 does not result in cohesion establishment, i.e., it is not possible to capture sister chromatids once they separated from each other (Uhlmann and Nasmyth, 1998). Cohesin can associate with the DNA in a cohesive and a non-cohesive manner. Non-cohesive rings presumably embrace a single chromatin fiber, while cohesive rings capture both sister chromatids inside. The non-cohesive complexes were visualized cytologically in the studies of 3D cohesin distribution in the budding yeast cell (Yeh et al., 2008). In metaphase cells with assembled bipolar spindle cohesin subunits, Scc1 or Smc3, tagged with GFP form a cylindrical array between sister kinetochores (Yeh et al., 2008). This cylindrical structure in the transverse section resembles a ring, which encircles the microtubules connecting the opposite spindle poles, while in the sagittal section it appears as two lobes separated from each other by the microtubules, connecting spindle poles (Figure 1.4A). In order to be able to interpret the observed cohesin distribution in the cell, it is necessary to mention several special features of budding yeast mitotic spindle organization. Through most of the cell cycle the kinetochores of all 16 chromosomes, each attached to a single microtubule connecting it to the spindle pole, are organized in a cluster. Upon biorientation sister kinetochores split and appear as two clusters. It was shown that under the pulling forces exerted by the microtubules originating from opposite poles, SCC is lost 20 kb around the centromeres and they are separated by up to 800 nm. Separation of the centromeres by spindle forces was observed in several organisms, such as budding and fission yeast, diatoms and crustacean *Ulophysema öresundense* (Goshima and Yanagida, 2000; Nabeshima et al., 1998; Nasmyth et al., 2000; Tanaka et al., 2000). Despite the observed separation of centromeres, sister chromatids maintain their cohesion at the arm regions (Tanaka et al., 1999). Thus, in budding yeast cohesed sisters attached to the mitotic spindle adopt a cross-like shape, i.e. centromeric regions are stretched between the spindle poles and pericentromeric regions are intramolecularly paired (Figure 1.4B). The cohesin complexes in the cylindrical array localize mainly to the pericentromeric regions. Since the distance between the split sister centromeres greatly exceeds the dimensions of the cohesin ring, it was suggested that cohesin complexes in the cylindrical array are mainly non-

cohesive and embrace only one sister chromatid or even promote intramolecular pairing (Figure 1.4B). Interestingly, in budding yeast both cohesive and non-cohesive forms of cohesin were shown to bind chromatin stably, since no recovery of fluorescence was observed in FRAP experiments (Yeh et al., 2008).

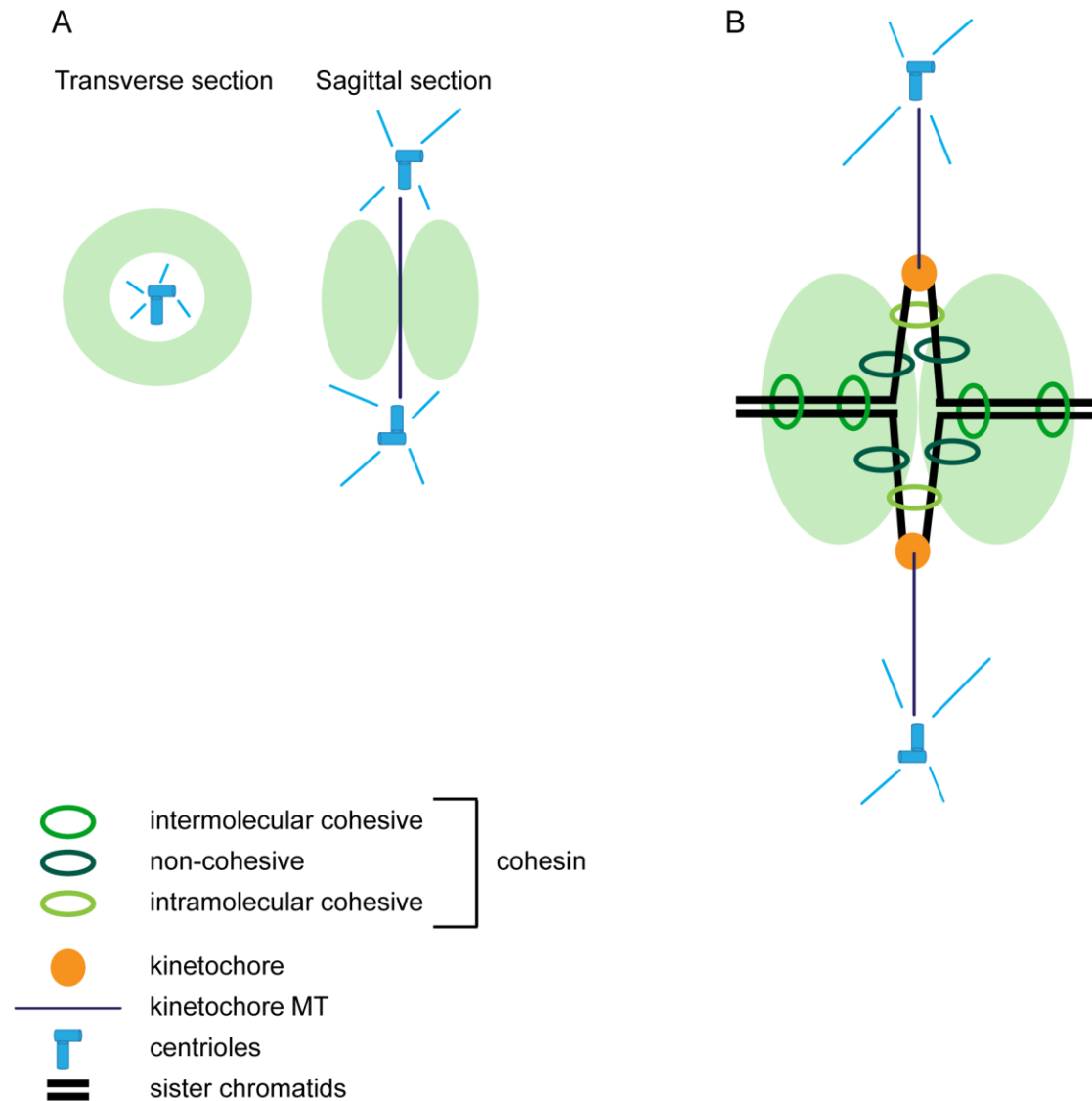


Figure 1.4 Cohesin complexes form a cylindrical array between sister kinetochores in metaphase.

A) Cohesin complexes, localized to pericentric chromatin of 16 chromosomes, form a cylindrical array, which in transverse section appears as a ring, encircling pole-to-pole microtubules, while in sagittal section it is represented by two lobes. **B)** According to a proposed model (Yeh et al., 2008), cylindrical array is formed of three types of cohesin rings: intermolecularly cohesive cohesin, which embraces sister chromatids at the arm regions (marked with green), intramolecularly cohesive cohesin, which embraces two regions of the same sister chromatid

(marked with light green) at the pericentromeric regions, and non-cohesive cohesin, which embraces only one of sister chromatids (marked with dark green).

The establishment of cohesion depends on the conversion of non-cohesive cohesin complexes to cohesive, which happens during DNA replication. Interestingly, in mammalian cells the cohesive complexes appear to be more stably bound to DNA than non-cohesive. This notion is supported by the fact that in mammalian cells two different pools of cohesin complexes with different half-lives on DNA can be detected starting from S phase. Cohesin in mammalian cells associates with chromatin already in telophase. This pool of cohesin is very dynamic with a half-life on chromatin of only 25 min. After S phase a very stably bound fraction of cohesin could be detected with the residence time on DNA of $6,3 \pm 3,7$ hours. This fraction comprised approximately 30 % of nuclear cohesin. This residence time is comparable with time from S phase to anaphase onset in proliferating mammalian cells, suggesting that there is no turn-over of cohesin complexes mediating sister chromatid cohesion (Gerlich et al., 2006). Unlike mammalian cells, in budding yeast cohesin is loaded on DNA only from the onset of S phase due to active separase in G1. While it was established that there is no detectable turn-over of the “cohesive” cohesins in budding yeast (Haering et al., 2004), it remains unclear whether cohesive and non-cohesive complexes have a different half-life on chromatin.

The establishment of cohesion correlates with the appearance of the stable cohesin on chromosomes and with the passage of the replication fork. Cohesion establishment is dependent on the activity of an acetyltransferase Eco1, which is recruited to the replication fork via PCNA (Figure 5) (Ben-Shahar et al., 2008; Ivanov et al., 2002; Lengronne et al., 2006; Moldovan et al., 2006; Unal et al., 2008; Xu et al., 2007). Eco1 is a highly conserved protein from yeast to vertebrates. It was initially identified in a genetic screen by a temperature-sensitive mutation resulting in a pronounced cohesion defect (Skibbens et al., 1999; Toth et al., 1999). Remarkably in an *eco1^{ts}* mutant cohesin is loaded on chromosomes normally, but is not able to hold sister chromatids together. Eco1 was shown to acetylate cohesin subunits in vitro (Ivanov et al., 2002; Toth et al., 1999). It was recently reported that the essential Eco1 target in vivo are two highly conserved lysines in the head domain of Smc3 (K112, K113) (Ben-Shahar et al., 2008; Unal et al., 2008; Zhang et al., 2008a). Mutation of lysines K112, 113 to non-acetylatable arginines prevented the establishment of cohesion, but did not affect

cohesin loading on the chromosomes (Unal et al., 2008). Recently, in fission yeast it was shown that deletion of *PDS5*, non-essential gene in this organism, resulted in abolished Smc3 acetylation by Eco1, necessary for cohesion establishment. This fact argues for Pds5 role in cohesion establishment, at least in fission yeast. Authors speculated that, since Pds5 was shown to interact with C-terminal domain of Eso1, an Eco1 homologue (Tanaka et al., 2001), lack of Pds5 could prevent Eco1 access to cohesin complexes resulting in abolished cohesin acetylation (Vaur et al., 2012).

Smc3 is acetylated starting from S phase coincident with cohesion establishment. The coupling between cohesion establishment and replication fork passage ensures that sister chromatids are captured within cohesin rings as soon as they are synthesized. Indeed, Eco1 was shown to associate with the replication forks (Lengronne et al., 2006) and to co-immunoprecipitate with the processivity factor of the DNA polymerase known as proliferating cell nuclear antigen (PCNA). Mutations in PCNA that abolish Eco1 binding resulted in a strong cohesion defect presumably due to the reduced amount of Eco1 associated with chromatin (Moldovan et al., 2006). Several nonessential proteins, which are associated with the replication fork, are involved in cohesion establishment. Among them are the subunit of DNA polymerase (Ctf4), the RFC complex, which loads PCNA and/or other DNA clamps on DNA (Ctf18, Ctf8, Dcc1), DNA helicase (Chl1) and proteins that coordinate helicase progression with DNA polymerase activity (Tof1 and Csm3) (Fernius and Marston, 2009; Mayer et al., 2004; Xu et al., 2007). The mechanism of how these activities are related to cohesion remains to be elucidated. It is possible that some of the replication fork proteins can alter the geometry of replisome facilitating its passage through the cohesin ring.

The passage of the replication fork through the ring will result in the entrapment of the nascent sister chromatids inside the ring. However, the replisome is presumed to be significantly bigger than cohesin and its geometry and/or composition would have to be modified for it to pass through the ring. Alternatively cohesin rings could be transiently opened to allow replication fork passage or removed altogether and reloaded after the fork. No cohesin reloading on chromatin during S phase could be detected, which argues against the latter model (Lengronne et al., 2006).

Eco1 is essential gene in yeast and its deletion is lethal. Strikingly, deletion of *PDS5* in fission yeast rescued the lethality of *Δeso1* mutant and restored sister chromatid cohesion ensuring proper chromosome segregation (Tanaka et al., 2001). Hence, Pds5, apart from its positive role in SCC, was proposed to possess cohesion

anti-establishment activity (Sutani et al., 2009; Tanaka et al., 2001). Interestingly, all three cohesin associated factors could possess anti-establishment activity, since in budding yeast specific mutations in *PDS5*, *RAD61/WPL1*, and *SCC3* were shown to suppress *eco1* ts mutations (Ben-Shahar et al., 2008; Rowland et al., 2009; Sutani et al., 2009). It was shown that the observed antiestablishment activity is caused by perturbed entrapment of sister DNAs inside the rings, since all identified suppressor mutations restore cohesion of minichromosomes in strains lacking *Eco1* (Rowland et al., 2009).

To sum up, *Scs3-Pds5-Wpl1* sub-complex inhibits the establishment of SCC, but at the same time is required for SCC establishment and/or maintenance. It remains unclear how the two opposite activities of *Scs3-Pds5-Wapl* sub-complex are mechanistically related to each other and regulated during the cell cycle. It was proposed that *Scs3-Pds5-Wapl* hinders cohesion establishment via direct interaction with *Smc3* head surface harboring non-acetylated K112 and K113. This anti-establishment activity is temporally counteracted by *Eco1* acetylation of *Smc3* K112, K113 residues, supposedly promoting *Scs3-Pds5-Wapl* dissociation (Rowland et al., 2009; Sutani et al., 2009). However, none of the three cohesin-associated factors binds to *Smc3* head in vitro regardless of *Smc3* acetylation status. Other cell cycle-specific modifications of cohesin or *Scs3-Pds5-Wpl1* sub-complex could switch on cohesion-stabilizing function.

In addition to cohesin, which plays an essential role in holding sister chromatids together and promoting their bi-orientation by resisting the splitting force of mitotic spindle, at least two other protein complexes were reported to maintain certain regions of sister chromatids in the immediate vicinity of each other. Whether this “cohesion without cohesin” is important for chromosomal segregation or indeed for any other aspects of chromosome biology remains to be established. Condensin, a cohesin-like complex, which in budding yeast comprises *Smc2*, *Smc4*, as well as non-*Smc* subunits *Ycs4*, *Ycg1*, and *Brn1* (Bhalla et al., 2002; Lavoie et al., 2002; Ouspenski et al., 2000; Strunnikov et al., 1995), links sister chromatids together at several loci at the chromosomal arms, but not at the centromeres or telomeres (Lam et al., 2006). Condensin-dependent cohesion is established during mitosis independently of DNA replication and can be re-established within one cell cycle (Lam et al., 2006).

An origin recognition complex (ORC), a conserved complex of 6 subunits, that in early G1 defines origins of DNA replication by recruiting pre-RC's components is implicated in cohesion of cohesin-free regions on chromosomal arms (Shimada and

Gasser, 2007). Depletion of ORC subunit, Orc2, after the formation of pre-RC, resulted in strong cohesion defect. ORC was shown to contribute to the sister chromatid cohesion independently of cohesin complexes, since Orc2 depletion did not affect cohesin association with DNA and additive cohesion defects were observed in *orc2 smc1* double mutants (Shimada and Gasser, 2007). It is important to note, that both pathways, condensin- and ORC-dependent cohesion, are not able to substitute for cohesin-mediated cohesion during the cell cycle.

1.4.3 Cohesin removal from chromosomal arms in vertebrate cells during prophase

Resolution of SCC via removal of cohesin complexes from chromosomes at the onset of anaphase, which leads to sister chromatid segregation to opposite spindle poles, is observed in all organisms. However, in vertebrate cells this event is preceded by massive cohesin dissociation from chromosomal arms already in prophase (Losada et al., 1998). The prophase pathway of cohesin removal does not depend on separase, since no detectable Scc1 cleavage fragments can be observed before the anaphase onset and cohesin with non-cleavable Scc1 dissociates from chromosomes in prophase (Hauf et al., 2001; Sumara et al., 2000; Waizenegger et al., 2000). Although a bulk of cohesin is removed during prophase, a small amount remains associated with chromosomes at the centromeres and is cleaved by separase in anaphase (Waizenegger et al., 2000).

Several factors were found to be essential for cohesin removal via prophase pathway. For example, inhibition of Aurora B protein kinase activity with hesperadin, led to high levels of cohesin remaining on chromosomal arms in prometaphase (Gimenez-Abian et al., 2004; Losada et al., 2002). Similar effect on cohesin dissociation from chromosomes during prophase was observed in *Xenopus* egg extracts depleted of Polo-like kinase (Plk1). Observed block of cohesin removal was relieved by the addition of recombinant Plk1, but not catalytically inactive mutant. Cohesin was shown to be phosphorylated by Plk1 in vitro, as well as in vivo during mitosis (Sumara et al., 2002). Numerous mitosis-specific phosphorylation sites were identified within Scc1 and SA2 cohesin subunits. Although Scc1 phosphorylation was shown to be dispensable for cohesin dissociation from chromosomes in prophase, SA2 phosphorylation plays an essential role in prophase pathway. In HeLa cells, carrying mutations in identified SA2 phosphorylation sites, which matched Polo box-binding

consensus sequence, cohesin stayed associated with arms and centromeres even after prophase was completed. Hence, sisters were tightly associated along all their length until anaphase onset, when all cohesin complexes were cleaved in separase-dependent manner (Gimenez-Abian et al., 2004). The phenotype observed in HeLa cells with mutated SA2 strongly resembles the phenotype caused by Plk1 depletion.

The mechanism by which Scc3 phosphorylation promotes cohesin unloading remains to be elucidated. It is possible, that Scc3 phosphorylation recruits cohesin unloading factors, which then enable dissociation of cohesin from chromosomes (Hauf et al., 2005). In addition, Plk1-dependent phosphorylation might prevent cohesin re-binding to chromosomes after it has been unloaded. Cohesin phosphorylation dramatically decreased its ability to bind to chromatin, while normal binding was restored by the phosphatase treatment (Sumara et al., 2002).

Cohesin complexes located to the centromeric regions should be protected from removal via prophase pathway in order to support sister chromatid cohesion until the onset of anaphase. Shugoshin associates with centromeres during prophase to shield centromeric cohesin from cleavage-independent removal, while its disappearance from centromeres at the onset of anaphase allows cohesin cleavage by separase. Cells depleted of shugoshin abruptly lose SCC before metaphase, because of simultaneous destruction of cohesion along the arms and at the centromere in prophase and prometaphase. It was speculated that shugoshin prevents cohesin removal from centromeres in prophase by preventing Scc3 phosphorylation. Indeed, expression of non-phosphorylatable Scc3 mutant rescued precocious loss of cohesion in shugoshin depleted cells. However, exact mechanism via which shugoshin abolishes removal of cohesin from centromeric regions is not known. It is possible that shugoshin prevents Scc3 phosphorylation or recruits phosphatase to the phosphorylated Scc3. Alternatively, shugoshin might make cohesin resistant to the destabilizing effects of Scc3 phosphorylation (McGuinness et al., 2005).

Wapl was suggested to be another regulator of sister chromatid resolution, since its depletion in HeLa cells resulted in transient accumulation of prometaphase-like cells characterized by chromosomes with poorly resolved sister chromatids harboring high levels of cohesin. However, the anaphase is only delayed and not blocked in Wapl-depleted cells and they are able to segregate chromosomes normally. Wapl overexpression led to premature sister chromatids separation (Gandhi et al., 2006; Kueng et al., 2006). Although depletion of either Sgo1 or Esco1 results in defective

SCC, no premature sister separation was observed after Sgo1 or Escal were co-depleted with Wapl. Interestingly, depletion of Wapl increased levels of cohesin bound to chromatin and prolonged its residence time on chromatin in interphase (Kueng et al., 2006). It is possible that the increase in chromosomal cohesin is caused by altered Sgo1 distribution, since Wapl depletion slightly increased amount of Sgo1 present on chromosomal arms (Kueng et al., 2006). It was proposed that Wapl could directly bind to cohesin and open the ring, thus releasing cohesin from chromatin (Gandhi et al., 2006). Indeed, it was demonstrated that Wapl is able to associate with soluble as well as with chromatin-bound fractions of cohesin throughout the cell cycle. Wapl forms a subcomplex with Pds5 (Kueng et al., 2006). Subcomplex formation and interaction with cohesin is mediated by Scc1-Scc3, since Scc1 depletion abolished Pds5 co-immunoprecipitation with Wapl and prevented Wapl localization to chromosomes in HeLa cells (Gandhi et al., 2006; Kueng et al., 2006). Wapl and Pds5 could indeed be the unloading factors that are recruited to cohesin upon Scc3 phosphorylation. Shintomi et al. proposed that Wapl-Pds5-Scc3 complex bends Scc1, and as a result Smc head domains are brought into close proximity to each other followed by ATP hydrolysis and subsequent opening of the ring (Shintomi and Hirano, 2009).

Depletion of a vertebrate-specific protein, called sororin, has an opposite effect on SCC compared to Wapl depletion. Sororin depletion in *Xenopus* egg extracts and in HeLa cells increases the distance between sister chromatids and decreases residence time of cohesin on chromatin, while depletion of Wapl results in tightly associated sister chromatids and increased residence time of cohesin on DNA (Kueng et al., 2006; Rankin et al., 2005). Sororin and Wapl overexpression also have opposite effects on SCC. Excessive amount of sororin in the HeLa cells results in failure to resolve SCC and segregate sister chromatids in mitosis and an elevated level of cohesin associated with metaphase chromosomes (Rankin et al., 2005), while Wapl overexpression leads to precocious sister chromatids separation. Thus, sororin and Wapl have antagonistic functions during the cell cycle. Simultaneous depletion of Wapl and sororin caused a phenotype similar to the one, observed in cells depleted of Wapl. Therefore, it was suggested that sororin antagonizes Wapl ability to dissociate cohesin from DNA and it is essential for SCC only in the presence of Wapl (Nishiyama et al., 2010; Rankin et al., 2005).

Sororin accumulates on chromatin in S- and G2-phases. During prophase, prometaphase, and metaphase only very small amount of sororin could be detected on

chromatin, mostly at the centromeres, and no sororin is bound to chromosomes in anaphase or telophase (Nishiyama et al., 2010; Rankin et al., 2005). Efficient sororin recruitment to chromosomes is dependent on DNA replication and Smc3 acetylation during cohesion establishment (Nishiyama et al., 2010; Rankin et al., 2005). Sororin directly interacts with cohesin via binding to Pds5 subunit and its association with chromosomes is dependent on cohesin and is abolished upon depletion of Scc1 or Pds5 (Nishiyama et al., 2010; Rankin et al., 2005). FRAP studies in HeLa cells revealed at least 2 fold reduction of cohesin stably associated with chromosomes in cells depleted of sororin. Thus, sororin promotes stable association of cohesin with chromatin (Schmitz et al., 2007).

Interestingly, sororin and Wapl share several FGF sites, which are required for their binding to Pds5 (Nishiyama et al., 2010; Shintomi and Hirano, 2009). It was proposed that sororin replaces Wapl in Wapl-Pds5 sub-complex, bound to the cohesin. Indeed, wild type (FGF), but not mutant (AGA) sororin is able to displace Wapl from Wapl-Pds5 heterodimer (Nishiyama et al., 2010). Cohesion defect caused by sororin depletion was rescued by addition of recombinant wild type FGF sororin, but not by mutant AGA sororin. In order to allow cohesin removal by Wapl during prophase pathway, sororin inhibitory activity is suppressed at the onset of mitosis by its phosphorylation in prophase, since phosphorylated form of sororin is not able to associate with chromosomes (Nishiyama et al., 2010; Rankin et al., 2005).

The function of prophase pathway remains unclear. It was speculated that prophase removal of cohesin from chromosomal arms enables rapid and synchronous separation of sister chromatids in anaphase.

1.4.4 Cohesin removal from chromosomes at the anaphase onset

Cohesin is removed from chromosomes at the time of metaphase to anaphase transition through the action of a specific protease, separase (Figure 1.5). The activation of separase is tightly regulated by several mechanisms. Separase cleaves Scc1 subunit of cohesin at two cleavage sites with a consensus sequence (SXEXGRR) (Uhlmann et al., 1999). Budding yeast separase, Esp1p, and its homologues from other organisms (for example, Cut1 from *S.pombe*, BimB from *E.nidulans*, separase from *H.sapiens*), contain a conserved C-terminal domain of about 300 amino acids (Uhlmann et al., 1999) with two short sequences of hydrophobic amino acids, that are predicted to form

β -sheets, each of them followed by two highly conserved amino acids, histidine and cysteine. Conserved histidine and cysteine are surrounded by amino acids with small side chains, serine and glycine. Based on these features it was suggested that separase belongs to a CD clan of cysteine endopeptidases (Uhlmann et al., 2000). This prediction was experimentally validated. Esp1 conserved catalytic dyad H1505 and C1531 was indeed found to be essential for proteolysis. Peptide based inhibitor that was able to bind covalently to the catalytic cysteine, as well as mutations of catalytic amino acids to alanines inhibited Scc1 cleavage by Esp1 (Uhlmann et al., 2000).

Activity of separase is regulated by a protein called securin, which performs a dual role of separase chaperone and inhibitor (Agarwal and Cohen-Fix, 2002; Jensen et al., 2001; Kumada et al., 1998; Uhlmann et al., 2000). Pds1p is normally present in the nucleus in excess over Esp1p. When Esp1p was overexpressed in the cells and all the available Pds1p was titrated, Esp1 molecules, that were left unbound, cleaved Scc1 resulting in a premature sister chromatid separation already in metaphase (Uhlmann et al., 2000). Securin protein stability is precisely regulated during cell cycle. In yeast securin is shown to be degraded shortly before or at the beginning of anaphase, and reappears in the cell in S phase (Cohen-Fix et al., 1996; Funabiki et al., 1996). Securin is degraded by 26S proteasome after its ubiquitination by APC-Cdc 20 ubiquitin ligase. Securin ubiquitination in its turn is controlled by mitotic spindle checkpoint, which allows sister chromatids separation only after successful assembly of spindle (Cohen-Fix et al., 1996). At the N-terminus securin contains a destruction box motif similar to the one found in B-cyclins, which are known to be ubiquitinated by the APC/cyclosome. Mutation in this N-terminal part of Pds1 prevented its degradation and blocked the progression to anaphase. Failure of nuclear localization of 26S proteasome subunits resulted in a prolonged delay in securin degradation, consistent with the key role of proteasome in securin degradation (Tatebe and Yanagida, 2000). Securin binding to separase also promotes separase nuclear localization necessary for its function. In the cells, lacking Pds1p, Esp1p fails to accumulate in the nucleus in G2 and remains distributed throughout the cell, unable to initiate anaphase (Jensen et al., 2001).

Some organisms possess additional mechanisms to regulate separase activity. Presence of this additional regulation explains why deletion of securin is not lethal in budding yeast. In budding yeast fraction of Scc1p during metaphase is phosphorylated by Polo-like kinase Cdc5 at sites adjacent to the sites of separase cleavage. While

unphosphorylated Scc1 is cleaved by separase only inefficiently, phosphorylated Scc1 is a much better separase substrate. Presumably phosphorylation increases the affinity of Scc1p cleavage sites binding to separase active site. When metaphase chromatin was treated with phosphatase no Scc1 cleavage by Esp1 was observed in vitro (Uhlmann et al., 2000). Inactivation of Cdc5 by a temperature-sensitive mutation inhibited the progression of sister chromatid separation along chromosome arms and Scc1 remained associated with chromatin after metaphase to anaphase transition (Alexandru et al., 2001).

Human separase is also regulated by phosphorylation and inhibitory complex formation, but the details of the regulation are different from yeast. Separase is phosphorylated by a cyclin dependent kinase 1, Cdk1. Subsequently Cdk1 stably binds to a phosphorylated separase via its regulatory subunit, cyclin B1 (Gorr et al., 2005; Stemmann et al., 2001). Complex formation results in mutual inhibition of both, the kinase and the protease. In mitotically arrested cells separase is fully phosphorylated. While cells undergo anaphase a considerable fraction of Esp1 is dephosphorylated (Stemmann et al., 2001). An elevated Cdk1 activity leads to anaphase inhibition in *Xenopus* egg extracts. While securin degradation was not affected, anaphase inhibition was rescued by mutating the separase phosphorylation site. It was initially proposed that separase phosphorylation might directly inhibit its activity. However, later it was established that phosphorylation itself is not inhibitory, but leads to recruitment of Cdk1 and it is Cdk1 binding, which inhibits separase, as well as kinase activities. Securin and Cdk1 bind separase in mutually exclusive manner, thus human separase is inhibited by formation of two different complexes (securin/separase and Cdk1-cyclinB1/separase) and stability of both complexes is under the control of APC/C-Cdc20 (Gorr et al., 2005).

1.4.5 Cohesin after anaphase

Scc1 cleavage by Esp1 opens the cohesin rings setting sister chromatids free to segregate to opposite spindle poles. The release of cohesin from chromosomes renders it accessible to the action of deacetylase Hos1, resulting in deacetylation of K112 and K113 of Smc3, which were acetylated during cohesion establishment (Figure 1.5). Smc3 deacetylation provides cells with a pool of non-acetylated Smc3 that could be reused during cohesion establishment in the next cell cycle (Borges et al., 2010).

Cohesin with pre-acetylated Smc3 appears to be less efficient in cohesion establishment, thus cells possess two ways to generate non-acetylated Smc3, namely de novo synthesis or deacetylation. Deletion of *HOS1* is characterized by elevated levels of acetylated Smc3 in G1, at which stage it is normally not detected, and by a cohesion defect, which was eliminated by induction of Smc3 expression in G1. Because of the crucial role of Smc3 acetylation in stable cohesion, Hos1 activity should be tightly regulated during the cell cycle. Hos1 does not localize to chromatin and cohesin dissociation from chromosomes is necessary for its action. Hence, deacetylation is regulated by accessibility of acetylated Smc3. On another hand, Scc1 cleavage per se is not required for Smc3 deacetylation, since it was shown that in crude yeast lysates of mitotically arrested cells micrococcal nuclease treatment, which releases intact cohesin ring from chromatin due to DNA fragmentation, resulted in Hos1 mediated Smc3 deacetylation (Borges et al., 2010).

Scc1 cleaved at the onset of anaphase, is degraded to release Smc1 and Smc3 (Figure 1.5). The C-terminal separase cleavage fragment of Scc1 is characterized by a very short half-life of about 2 minutes. It possesses at its N-terminus a destabilizing residue arginine, which serves as a degradation signal (degron), and targets Scc1 fragment for an ubiquitin/proteasome dependent N-end rule degradation pathway. Degron is recognized by ubiquitin E3 ligase Ubr1 (Rao et al., 2001). Destabilization of Scc1 cleavage fragment is important for cohesin recycling in the cell, since in *ubr1* deletion mutant Scc1 C-terminal fragment is stable and the rate of chromosomal missegregation is about 100 times higher than in wild type yeast. Furthermore, overexpression of stabilized forms of Scc1 fragment is lethal. It is possible that Scc1 C-terminal fragment may inhibit Esp1 activity via binding competition with full length Scc1. In addition, if Scc1 C-terminal fragment remains stably bound to Smc1, it will prevent Smc1 from binding to full length Scc1 in the next cell cycle (Rao et al., 2001).

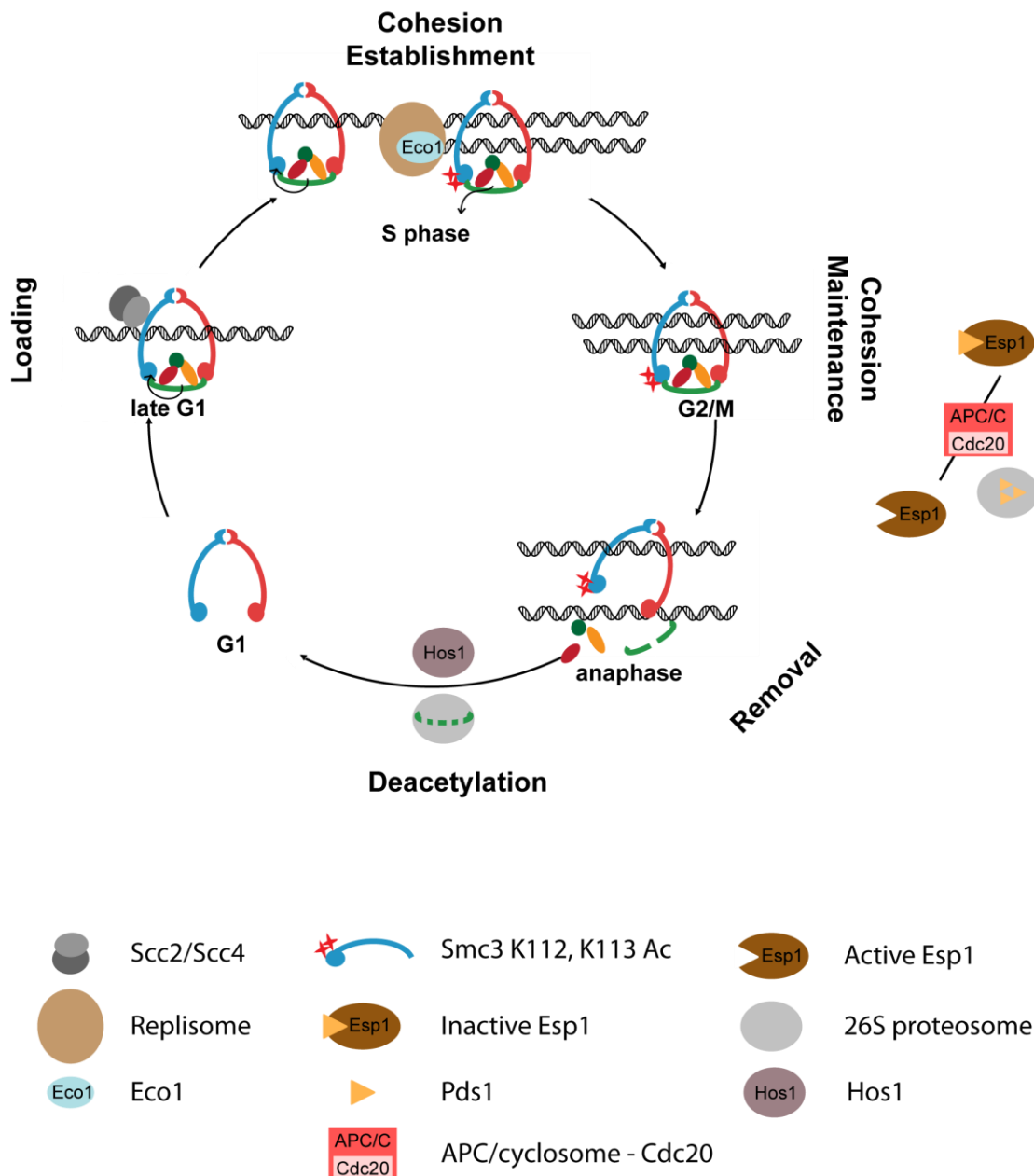


Figure 1.5 Fate of the cohesin ring during the cell cycle of budding yeast.

Pre-formed cohesin rings are loaded on DNA by Scc2/Scc4 loading complex during late G1. At this stage, a heterotrimeric protein complex Pds5-Wpl1-Scc3 is recruited by Scc1, destabilizes the interaction between the cohesin subunits and might release the ring from chromosomes. As soon as two sister chromatids are synthesized by the replisome in S phase, they are captured within the cohesin ring and destabilizing activity of Pds5-Wpl1-Scc3 subcomplex is relieved through Smc3 acetylation by Eco1. Established sister chromatid cohesion is maintained from S phase until the onset of anaphase, when separase inhibitor securin, Pds1, is destroyed and activated separase, Esp1, cleaves Scc1 cohesin subunit. This results in cohesin ring opening and allows sister chromatid segregation. Sister chromatids release is followed by Smc3 deacetylation by Hos1 and Scc1 cleavage fragments degradation by proteasome.

1.5 Non-mitotic functions of the cohesin ring

1.5.1 Cohesin role in DNA damage repair

Double strand breaks (DSBs), which spontaneously occur in the cell and are induced by DNA-damaging agents, could be repaired in eukaryotic cells through two different pathways. Homologous recombination (HR) pathway repairs DNA breaks using an intact DNA sequence of sister chromatid. Non-homologous end-joining (NHEJ) pathway directly ligates two ends of DNA, created by DSB. In budding yeast NHEJ is employed to repair DSB in G1 phase of the cell cycle. To repair DSB in post-replicative cells HR pathway is used preferentially. Cohesin facilitates DSB repair by HR and prevents less accurate NHEJ (Schar et al., 2004). In order to repair DSB via HR pathway, damaged DNA molecule should be in close proximity to an intact sister DNA. Therefore, sister chromatid cohesion is a requirement for DSB repair by HR. Cohesin is shown to be loaded at the regions around DSB further re-enforcing the link between the sisters (Figure 1.6A) (Strom et al., 2004; Unal et al., 2004). In the absence of double strand DNA breaks cohesin, loaded on the chromosomes in post-replicative cells does not establish cohesion, presumably because the ring embraces only one chromatid (Haering et al., 2004). While the expression of non-cleavable Scc1 in S phase blocks the subsequent cell division, its expression during metaphase arrest did not prevent the onset of the first anaphase, but blocked the anaphase of the following cell cycle. This result suggested that no new links between sister chromatids were formed in metaphase by cohesin complexes. However, the presence of even a single DSB activates a pathway that allows global establishment of cohesion throughout the cell (Strom et al., 2007). Strom and colleagues in an elegant experiment demonstrated that wild type cohesin complexes expressed in G2 in the presence of DSB were able to establish cohesion. Cells with two copies of *SMC1*, ts mutant *smc1* and wild type *SMC1* under the control of inducible promoter, underwent replication under permissive temperature and were arrested in G2/M. When cells were shifted to restrictive temperature, cohesion built by ts cohesin was destroyed. In agreement with previously obtained data, induction of wild type Smc1 expression in G2 was not able to rescue observed loss of SCC. Remarkably, when DSBs were induced by γ - irradiation, wild type Smc1, expressed in G2, rescued the cohesion defect caused by inactivation of the ts Smc1 (Strom et al., 2004). Later using the same approach it was shown that even a single DSB is able to trigger cohesion not only in the region adjacent to DSB, but also in a

genome-wide manner. Single DSB generated by HO endonuclease at the *MAT* locus on chromosome III in cells transiently expressing non-cleavable Scc1, resulted in separase-resistant cohesion between sister chromatids of damaged chromosome III, as well as undamaged chromosome V. Though during normal cell cycle cohesion establishment is directly connected to DNA replication, damage-induced cohesion is independent of DNA synthesis accompanying DNA repair. No defects in damage-induced cohesion were observed in cells lacking Rad52, a protein, which promotes a direct interaction between the broken DNA molecule and an intact template and is essential for DNA duplication at the break (Krejci et al., 2002; Strom et al., 2007; Sung, 1997).

It was shown that cohesin is enriched at least 5 fold in a region of about 100 kb around a single DSB, and this region was called “cohesin domain” (Unal et al., 2004). As in a normal cell cycle, Scc2/Scc4 complex is required for cohesin loading on DNA at the “cohesin domain”, since 5-7 fold cohesin enrichment around DSB was not observed in *scc2* mutant (Strom et al., 2004; Unal et al., 2004). Scc2 was also necessary for DSB induced genome-wide cohesion (Strom et al., 2007).

Cohesin complexes involved in genome-wide cohesion generated after DSB induction, localize to the same sites within undamaged regions of the genome as during the normal cell cycle (Strom et al., 2007). However, “cohesin domains” around DSBs are different from CARs and directly depend on localization of DSB itself. Cohesin association with DNA appears to be regulated by DNA damage repair pathway. Indeed, cohesin recruitment to “cohesin domain” depends on Mre11, which is one of the first proteins to localize to the DSB (Lisby et al., 2004). Mre11 together with two other proteins form MRN complex (Mre11/Rad50/Nbs1), which keeps the broken DNA ends together (van den Bosch et al., 2003). Deletion of *mre11* resulted in failure of “cohesin domain” formation and no damage-induced cohesion was observed (Strom et al., 2007; Unal et al., 2004; Unal et al., 2007).

A similar effect was caused by the deletion of two other components of DNA damage repair pathway, namely kinases Tel1 and Mec1. Tel1 and Mec1 were shown to phosphorylate histone H2AX in the vicinity of a DSB (Downs et al., 2000; Redon et al., 2003). It was speculated that, phosphorylation of H2AX induces cohesin enrichment within “cohesin domain”. Indeed, in cells with mutant H2AX, which could not be phosphorylated, no cohesin enrichment was detected around DSB. Interestingly, levels of phosphorylated histone H2AX were increased over the areas of 60 kb on either side of DSB, which correspond to the “cohesin domain”. Tel1 and Mec1 recruitment to the

DSB site is facilitated by the RSC remodeling complex. Thus, it was shown that RSC is necessary to maintain normal levels of DSB-induced H2A phosphorylation. Interestingly, deletion of Rsc2 subunit of RSC complex resulted in 2-4 fold decrease in cohesin enrichment around DSB. However, it is not clear whether RSC plays a role in cohesin recruitment to the DSB sites only via promoting histone phosphorylation or through yet unknown direct mechanisms (Liang et al., 2007). Thus, chromatin modification in the region around DSB could serve as a signal for cohesin loading.

DNA damage-induced cohesion is regulated by several other protein kinases. For example, DNA damage checkpoint kinase Rad63 phosphorylates Scc1 in response to DNA damage and promotes “cohesin domain” formation (Sidorova and Breeden, 2003). Chk1 kinase, known to act downstream of Rad50/Mre11 complex and Mec1 kinase in DNA damage response pathway, was shown to be essential for DSB-induced cohesion (Grenon et al., 2001; Heidinger-Pauli et al., 2008). Scc1 contains a consensus recognition site for Chk1 and is phosphorylated at the highly conserved serine 83 by Chk1 in vitro (Heidinger-Pauli et al., 2008; Wang et al., 2001). Mutation Ser83Ala does not affect the loading of cohesin around DSB, but leads to defective repair, which could be explained if Scc1 S83A were unable to establish cohesion after DSB induction. Further experiments showed that genome-wide cohesion induced by DSBs is abolished by deletion of *chk1*, but could be restored in Δ *chk1* cells by substitution of Scc1 serine 83 with aspartate, mimicking phosphorylated state. Since, constitutive phosphorylation of serine 83 allowed cohesion generation in G2/M independently of DSB induction, it was proposed that Chk1-dependent phosphorylation of Scc1 relieves the inhibition of cohesion establishment in G2/M. Based on described facts, Heidinger-Pauli and colleagues suggested a model, according to which Mec1 stimulates Chk1-dependent phosphorylation of Scc1 at serine 83, that specifically promotes transformation of chromatin-bound non-cohesive cohesin to cohesive in G2/M (Heidinger-Pauli et al., 2008). Further studies showed that Scc1 S83 phosphorylation induced by DSB promotes Eco1-dependent acetylation of Scc1 lysine 210 and lysine 84, which in its turn leads to cohesion generation in G2/M (Heidinger-Pauli et al., 2009). Therefore, different subunits of cohesin are acetylated by Eco1 during cohesion establishment in an unperturbed S phase and after DSBs induction. Accordingly, Scc1 acetylation-mimicking mutants could not compensate for the lack of Smc3 acetylation in an unperturbed S phase, and Smc3 acetylation is insufficient for DSB-induced cohesion in G2/M. However, cohesin acetylation by Eco1 allows cohesion establishment in S phase

and G2/M through the same mechanism, namely antagonizing Wpl1 activity (Ben-Shahar et al., 2008; Heidinger-Pauli et al., 2009; Sutani et al., 2009).

Accumulation of cohesin at the sites of DSBs apart from its direct role in DNA repair could be essential for activation of DNA damage checkpoint. The surveillance mechanism detects DNA damage and arrest cells until DSBs are repaired at three phases of the cell cycle, i.e., G1/S transition, S phase and G2/M transition. ATM kinase is activated by intramolecular auto phosphorylation in response to DNA damage and plays a role of a master switch initiating the checkpoint (Banin et al., 1998; Canman et al., 1998). Smc subunits of mammalian cohesin were shown to be phosphorylated by ATM in response to DNA damage.

Smc1 is phosphorylated at serines 957 and 966 (Kim et al., 2002; Yazdi et al., 2002). Cells expressing non-phosphorylatable Smc1 mutants, S957A or S966A, did not arrest in S phase in response to ionizing radiation and instead accumulated in G2, suggesting a defective intra-S phase checkpoint and an intact G2/M checkpoint.

Smc3 is phosphorylated *in vivo* at two residues, serines 1067 and 1083. Similar to non-phosphorylatable Smc1 mutants, Smc3 mutants S1067A and S1083A were defective in intra-S checkpoint and were unable to inhibit DNA synthesis in response to irradiation. Serine 1083 modification by ATM is induced by irradiation and depends on constitutive phosphorylation of serine 1067 by CK2 kinase (Luo et al., 2008). It was proposed that phosphorylation of serine 1067 might create a binding site for the Nbs1 component of the MRN complex, and Nbs1 in its turn recruits ATM kinase to phosphorylate Ser1087 (Luo et al., 2008).

Phosphorylation of Smc1 and Smc3 depends on functional Nbs1 and BRCA1, which co-localize with phosphorylated ATM and Smc1 at DSBs (Kim et al., 2002; Yazdi et al., 2002).

Mammalian Smc1 and Smc3 form a complex with DNA polymerase ϵ and DNA ligase III. This complex, called RC-1, was shown to repair the gaps and deletions through DNA recombination in a cell-free system (Jessberger et al., 1996). However, DNA polymerase ϵ or DNA ligase III could not be detected in cohesin preparation from irradiated HeLa cells in a separate study (Watrin and Peters, 2009).

Watrin and colleagues demonstrated that cohesin is essential not only for intra-S phase DNA damage checkpoint, but also for G2/M checkpoint. When DSBs are induced in HeLa cells in G2 most DSBs are repaired prior to the entry into mitosis and

very few mitotic cells display the foci of replication protein A, RPA, known to be accumulated at DNA breaks. Cells depleted of Scc1 or Smc3, enter mitosis with multiple RPA foci, indicating unfinished DSBs repair. The role of cohesin in G2/M checkpoint activation is apparently independent of the establishment of sister chromatid cohesion. Cells with depleted sororin are defective in cohesion and DSB repair, but remain arrested in G2 with unrepaired DSBs indicating an active checkpoint (Watrin and Peters, 2009).

At the moment there is very little mechanistic insight into cohesin role in the DNA damage checkpoint. The checkpoint effector kinase Chk2 is underphosphorylated at threonine 68 in cells depleted of Scc1 presumably due to impaired recruitment of 53BP1 to DSB sites. How cohesin influences 53BP1 recruitment remains to be investigated (Fernandez-Capetillo et al., 2002; Wang et al., 2002a; Watrin and Peters, 2009).

1.5.2 Cohesin role in apoptosis

Apoptosis is a process of a programmed cell death, which is initiated as a response to extrinsic inducers or during the process of development for selective cell elimination. Highly conserved cysteine proteases, called caspases (C), transduce programmed cell death signal (initiator caspases, C-8, 9, 10, 2) and execute apoptosis (effective caspases, C-3, 7, 6) by cleaving cellular proteins. Proteins involved in DNA repair are often caspase targets during apoptosis. Destruction of the cellular repair machinery and as a result absence of repair mechanism, allow DNA fragmentation by caspase-activated DNase, a hallmark of apoptosis. In human cells Scc1 homologue, Rad21, is cleaved upon induction of apoptosis and its cleavage is abolished by caspase inhibitors. Rad21, is cleaved *in vitro* by caspase-3 and caspase-7, which recognize the consensus DXXD and cleave hRad21 after D279 (Chen et al., 2002; Pati et al., 2002). However, since C-terminal Rad21 fragment was still generated in the cells lacking caspase-3 an additional protease is likely to play a role during apoptosis induction *in vivo*. Interestingly, caspase cleavage site is different from separase cleavage sites. A C-terminal fragment of Rad21 after cleavage by caspase partially dissociates from chromatin and is translocated from nucleus to the cytoplasm early in apoptosis, before chromatin condensation and fragmentation. It was speculated that, translocation of C-terminal

fragment of Rad21 to cytoplasm might act as a signal to initiate cytoplasmic events of apoptotic pathway (Chen et al., 2002; Pati et al., 2002).

In budding yeast, Scc1 is also cleaved upon apoptosis induction with hydrogen peroxide. C-terminal cleavage product of yeast Scc1 is further fragmented into smaller pieces, which are also translocated from nucleus. Fragment, containing 40 amino acids from C-terminus of Scc1 accumulates in mitochondria. Its accumulation results in decrease of mitochondrial membrane potential and cytochrome c release, which leads to amplification of apoptotic signal (Figure 1.6B) (Madeo et al., 2002; Yang et al., 2008).

Since caspase inhibitor abolished Scc1 fragmentation, it was speculated that the only caspase-like protease identified in yeast, Yca1, should be involved in Scc1 cleavage during apoptosis. However, in *yca1* deletion mutant, Scc1 was still cleaved after apoptosis induction. Since the amino acid sequence at the conserved catalytic site of *S.cerevisiae* separase homologue, Esp1, is similar to that of human caspase-1 (Uhlmann et al., 2000), it was speculated that the protease, which cleaves Scc1 upon apoptosis induction could indeed be separase. In accordance with this proposal, no Scc1 fragmentation and no accumulation of C-terminal fragment in mitochondria was observed when Esp1 was inactivated prior to the induction of apoptosis.

1.5.3 Cohesin role in meiosis

In meiosis one cycle of DNA replication is followed by two sequential chromosome segregations: during first division, meiosis I, homologous chromosomes are segregated to the opposite spindle poles, during second division, meiosis II, sister chromatids are segregated. In the course of meiosis of higher eukaryotes one diploid germ cell gives rise to four haploid gametes and in yeast a diploid vegetative cell produces four haploid spores.

Similar to mitosis, cohesion between pairs of sister chromatids is established during premeiotic replication and is mediated by meiosis-specific cohesin (Klein et al., 1999). In budding yeast in a meiotic cohesin Scc1 is replaced by a homologous protein, Rec8. In fission yeast in addition to Rec8, Scc3 homologue, Rec11, substitutes Scc3 on chromosomal arms, while at the centromere mitotic Scc3 is preserved (Kitajima et al., 2003). In mammalian cells there are meiosis-specific variants of Scc1 (Rec8), Smc1 (Smc1 β) (Revenkova et al., 2001), and Scc3 (SA3) (Pezzi et al., 2000). Similar to

mitosis, cohesin dissociation from chromosomes in meiosis depends on proteolysis by separase, since mutants with inactivated Esp1 fail to remove cohesin and segregate chromosomes. Proteolysis at either one of the 2 cleavage sites found within Rec8 releases cohesin from chromatin *in vivo* and was shown to be necessary for cohesin removal, since double non-cleavable mutant of Rec8 (E428R R431E R453E) completely blocked meiosis (Buonomo et al., 2000).

A key feature of meiosis is a reciprocal recombination between homologues, which happens in prophase I. Two homologous chromosomes during meiosis I are tightly paired along their length by a protein complex called synaptonemal complex (SC), which is built by two axial elements running along the length of sister chromatid pairs connected by central elements. Due to close vicinity of homologues, cell is able to repair DNA DSBs induced by the Spo11 endonuclease via recombination between sister chromatids. Structures called chiasmata are formed at the sites of recombination (Bergerat et al., 1997; Keeney et al., 1997). Efficient recombination between homologues was shown to require cohesin. In *rec8* or *smc3* mutants synaptonemal complex and axial elements were not formed, DSBs were produced normally, but not properly repaired resulting in deficient recombination (Klein et al., 1999).

In meiosis I sister kinetochores should be oriented in a monopolar manner, i.e., attached to microtubules originating from the same spindle pole. Monopolar attachment is achieved with the help of meiosis-specific kinetochore protein complex called monopolin (Mam1, Csm1, Lrs4, Hrr25) (Petronczki et al., 2006; Rabitsch et al., 2003; Toth et al., 2000). In budding yeast a pair of sister kinetochores in meiosis I was shown to be captured by a single microtubule (Winey et al., 2005). It is possible that in budding yeast meiosis I sister kinetochores act as if they were “fused” and thus, attach to the same pole. Alternatively one of the two sister kinetochores in a pair could be inactivated (Monje-Casas et al., 2007).

Cohesin complexes distal to chiasmata are embracing not sister chromatids, but chromatids of the two homologous chromosomes. Therefore, in meiosis I cohesin has to be removed from the chromosomal arms to allow the segregation of homologues. However, cohesin is retained at the centromeric regions until meiosis II, when it will be the time of sister chromatids to segregate (Figure 1.6C). Thus, cohesin complexes are removed from chromosomes in two steps during meiosis, corresponding to two sequential chromosome segregations. Pds1 is degraded at the onset of anaphase I, than is re-synthesized between divisions and it degraded again at the onset of anaphase II.

This cycle of Pds1 degradation and re-synthesis results in two peaks of separase proteolytic activity: it is transiently active in the first meiotic division and a second time in the second division (Salah and Nasmyth, 2000).

It was proposed that Rec8, located at the centromeres is protected from cleavage by separase at the onset of anaphase I, but loses this protection at the anaphase II (Klein et al., 1999). Indeed, centromeric cohesin is protected by a protein complex formed by pericentromeric protein called shugoshin and phosphatase 2A (PP2A) (Kitajima et al., 2004; Marston et al., 2004; Rabitsch et al., 2004). In fission yeast localization of Sgo1 to pericentromeric heterochromatin depends on a centromere-associated Bub1 kinase (Bernard et al., 2001a; Kitajima et al., 2004). In yeast Sgo1 is expressed exclusively in meiosis, localizes to pericentromeric chromosome regions in metaphase I, and disappears quickly during anaphase I in APC-dependent manner (Kitajima et al., 2004; Rabitsch et al., 2004). Deletion of *SGO1* resulted in complete dissociation of cohesin complexes from chromosomes during anaphase I and random chromosome segregation. Sgo1 function is to recruit phosphatase PP2A, which dephosphorylates Rec8 and inhibits its cleavage by separase (Kitajima et al., 2006; Riedel et al., 2006; Tang et al., 2006). Mutants with inactivated PP2A are characterized by a similar phenotype, i.e., failure to protect centromeric Rec8 during anaphase I and random segregation of sister chromatids during meiosis II. In vertebrate mitosis shugoshin fulfills similar role, namely it protects centromeric cohesin from removal by prophase pathway (McGuinness et al., 2005). Although the relevant targets in mitosis and meiosis are apparently different, it is likely that cohesin protection by shugoshin is in both cases dependent on cohesin subunit dephosphorylation by PP2A.

1.5.4 Cohesin role in centrosomes duplication and separation

Very recently it was discovered that apart from holding sister chromatids together cohesin performs several other important functions. One of them is the replication and segregation of the centrosome. Centrosome functions as a microtubules organizing center in animal cells. It influences all processes, which are dependent on microtubules and plays especially important role in spindle formation and chromosome segregation during the cell cycle. It is formed of two cylindrical centrioles, which are arranged perpendicularly to one another and are surrounded by pericentriolar proteinaceous material. Centrosome is duplicated only once during cell cycle, in S phase, ensuring

that each daughter cell harbors only one centrosome (for review see (Meraldi and Nigg, 2002)). Centrosome could be duplicated only after the licensing step, which occurs in late mitosis or early G1 phase and depends on centriole disengagement (Wong and Stearns, 2003). Centriole disengagement in its turn was shown to be regulated by separase, since inhibition of its proteolytic activity blocked centriole separation (Schockel et al., 2011; Stemmann et al., 2001; Thein et al., 2007; Tsou and Stearns, 2006; Zou et al., 1999). Interestingly, cohesin localizes to centrosomes in vertebrate cells (Guan et al., 2008; Kong et al., 2009; Wong and Blobel, 2008) and later was shown to be important for centriolar engagement (Schockel et al., 2011). Several observations argue for cohesin role in centriolar cohesion, for example, expression of non-cleavable Scc1 led to complete block of centriole disjunction, while centriole disengagement was triggered by the proteolytic cleavage of Scc1 or Smc3 cohesin subunits, which disrupted the cohesin ring integrity. It was speculated that cohesin might topologically embrace the two centrioles, similar to its function in sister chromatid cohesion (Schockel et al., 2011) (Figure 1.6D). Thus, cohesin is involved in the regulation of centrosome duplication at the replication licensing step of the centriole cycle in animal cells (Schockel et al., 2011). Although, cohesin was implicated in centriolar function in budding yeast as well, EM-immunostaining experiments failed to detect cohesin at the yeast spindle pole bodies (SPBs), which are yeast equivalents of animal centrosomes (Jin et al., 2012). Jin and colleagues speculated that in budding yeast cohesin might play an indirect role in SPB cohesion.

1.5.5 Cohesin role in interphase genome organization, regulation of gene expression and development

In vertebrate cells cohesin binds to chromosomes already in telophase, long before the S phase when cohesion is established. It is also expressed in non-dividing postmitotic cells suggesting that cohesin might be required for the other processes in addition to sister chromatid cohesion. Indeed, cohesin was shown to regulate transcription in vertebrate cells and *Drosophila*, and to be involved in silencing and transcription termination in yeast.

Gene expression is regulated by transcription factors bound to the enhancer DNA sequences, which are located at a significant distance from the promoters, occupied by the transcription initiation factors. In order to activate gene expression, enhancer and

promoter-bound factors should come into contact, which would require DNA looping. Indeed, the chromosome conformation capture (3C) experiments demonstrated, that during active transcription enhancers co-localize with the promoters, supposedly as a result of DNA loop formation (Jiang and Peterlin, 2008; Miele and Dekker, 2008; Vakoc et al., 2005). Recruitment of co-activators by enhancer-bound transcription factors leads to the subsequent recruitment of RNA polymerase II to the core promoter, allowing coordinated gene regulation (Bulger and Groudine, 2010; Conaway et al., 2005; Graf and Enver, 2009; Kornberg, 2005; Malik and Roeder, 2005; Panne, 2008; Taatjes, 2010). Mediator protein complex functions as a co-activator and was shown to occupy enhancers and core promoters of more than 60% of actively transcribed genes in the embryonic stem cells (EC). Interestingly, the mediator sites were co-occupied by cohesin and cohesin loader, Nipbl (homologue of yeast Scc2), suggesting their role in transcriptional control (Kagey et al., 2010). Mediator, cohesin, and Nipbl were shown to form a complex in vivo. In embryonic stem cells decreased levels of cohesin subunit, Scc1, or mediator complex subunit, Med12, result in reduced enhancer-promoter interactions and decreased mRNA expression from genes required for ES cell pluripotency (Kagey et al., 2010). Based on these observations Kagey and colleagues proposed that loop formation is facilitated by the mediator, which bridges the enhancer-bound transcription factors and RNA polymerase II bound to the promoters. The loop is stabilized by the subsequent recruitment of Nipbl and cohesin (Kagey et al., 2010) (Figure 1.6E left). It remains to be established whether the DNA loop is threaded through a single cohesin ring or whether it is stabilized by an interaction between two cohesin rings at the base of the loop.

More than 70% of cohesin-associated sites mapped in human and mouse cells are shared with CTCF-binding factor, CTCF. CTCF is a transcription factor, harboring 11 zinc-finger domains, which supposedly function in different combinations and are able to mediate binding to different DNA sequences (Filippova et al., 1996). CTCF has so far been identified only in vertebrates and *Drosophila*. It functions as a barrier, preventing transcriptional inactivation of genes located in the vicinity of heterochromatic regions, as well as preventing inappropriate gene activation by distant enhancers. For example, CTCF bound to 5'HS4 chicken β -globin insulator was demonstrated to possess both of these activities (Chung et al., 1997).

CTCF was shown to be essential for cohesin enrichment at several specific sites, but not for cohesin loading on DNA. In HeLa cells depleted of CTCF or cohesin subunit, Scc1, upregulation of 194 genes and downregulation of about 90 genes were observed, suggesting that both proteins could regulate gene expression in a similar way. It was proposed that cohesin itself and not cohesion is essential for CTCF insulator function (Wendt et al., 2008). Precise mechanism of cohesin function in gene regulation is unclear. It is possible, that cohesin ring could stabilize the loop created by CTCF or other transcription factors via connecting two DNA sites at the base of the loop and in this way help to establish the boundaries of actively transcribed and silenced regions (Kurukuti et al., 2006; Splinter et al., 2006; Wendt and Peters, 2009). Alternatively, DNA bound cohesin complexes might pose an obstacle to spreading of transcription factors or movement of RNA polymerase along the DNA (Wendt and Peters, 2009; Wendt et al., 2008).

Schmidt and colleagues demonstrated that apart from CTCF, cohesin co-localized with tissue-specific master regulators of transcription. For example, in human breast cancer cells cohesin co-localizes with estrogen receptor α (ER) independently of CTCF at several sites along DNA and displays a remarkable enrichment within estrogen-regulated genes (Schmidt et al., 2010). It was shown that ER association with DNA results in the establishment of specific chromatin three-dimensional structures (Fullwood et al., 2009), which could be stabilized by cohesin (Schmidt et al., 2010). In hepatocellular carcinoma cells HepG2 cohesin is found at several sites occupied by the transcription factors specific for this cell type, HNF4A and CEBPA. Interestingly, depletion of these transcription factors led to reduced cohesin binding at the identified sites. Thus, cohesin binding at some of the chromosomal loci is highly specific for different cell types and depends on binding of tissue-specific transcription factors.

Cohesin binding sites in the vicinity of silent mating type cassettes in budding yeast overlap with boundary elements, which restrict silent chromatin to these loci. In budding yeast two silent mating type loci, HMR and HML, are flanked by silencers E and I, which recruit silencing factors, namely, a conserved NAD-dependent histone deacetylase Sir2 and histone-binding proteins Sir3 and Sir4 (Brand et al., 1985; Loo and Rine, 1994; Sauve et al., 2006). Histone deacetylation promotes the binding of Sir protein complexes to DNA, resulting in the formation of chromatin domains, which are inaccessible to enzymes and are transcriptionally repressed (Rusche et al., 2003).

Deletion of either one of the two boundary elements led to spreading of the silenced chromatin (Donze et al., 1999). Similar spreading of silent chromatin was observed in cells with inactivated cohesin subunits, *Smc1*, *Scc1* or *Smc3*, uncovering the important role of cohesin in boundary elements function (Donze et al., 1999; Lau et al., 2002). Cohesin binding to the boundary elements was shown to be Sir2 dependent (Kobayashi et al., 2004). It is possible, that boundary elements promote the establishment of DNA loops, which could be further stabilized by cohesin (Donze et al., 1999) (Figure 1.6E right). Apart from its function at the boundary elements, cohesin is essential for cohesion of the silent chromatin and ensures genomic stability by preventing uneven recombination of highly repetitive sequences, such as rDNA array. According to the existing model, cohesin complexes keep sister rDNA repeats aligned to each other, thus ensuring equal sister chromatids recombination (Gartenberg, 2009). Chang and colleagues demonstrated that cohesion is not required for silencing maintenance, but rather that silencing is required for the maintenance of cohesion, since relieve of transcriptional inhibition disturbs pre-existing cohesion at the HMR (Chang et al., 2005). Interestingly, cohesin, which is bound topologically to the DNA at the silenced HMR locus, does not embrace both sister chromatids, but only one. In this case cohesion is expected to be mediated by the interaction between two cohesin complexes bound to the silenced regions of sister chromatids (Chang et al., 2005; Gartenberg, 2009; Huang and Moazed, 2006). It was proposed, that this mode of cohesion is a specific characteristic of silenced chromatin and might have evolved as a response to the increase in chromatin fiber diameter, caused by binding of silencing factors (Chang et al., 2005; Gartenberg, 2009; Huang and Moazed, 2006).

Yeast genome is characterized by a high density of genes, which are often arranged in a convergent orientation. Transcription of neighboring genes should be carefully regulated to prevent transcriptional interference or collision of elongating RNA polymerase II (Pol II) complexes (Hongay et al., 2006; Martin et al., 2004; Prescott and Proudfoot, 2002). Cohesin is one of the factors, which can block a read-through transcription from an upstream gene into a downstream gene. Gullerova et al. demonstrated that in fission yeast cohesin directly facilitates the release of RNA 3'-end and transcriptional termination, since ts *scc1* mutants were characterized by a read-through transcription at several tested loci at the restrictive temperature (Gullerova and Proudfoot, 2008). It was suggested that DNA-bound cohesin creates a physical

hindrance for PolIII causing it to terminate transcription (Gullerova and Proudfoot, 2008).

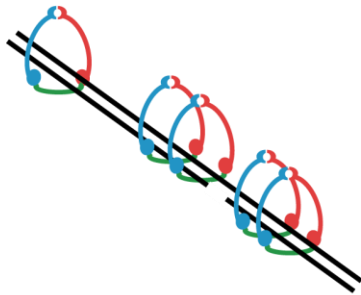
Thus, cohesin was shown to be involved in both positive and negative transcriptional regulation. Therefore, it is only to be expected that defects in cohesin function would result in perturbed genes expression and would lead to developmental abnormalities (Wendt et al., 2008). Indeed, in zebrafish reduction in the expression levels of cohesin subunits Scc1 or Smc3, impairs *runx1* gene expression and consequently compromises hematopoiesis and nervous system development (Horsfield et al., 2007).

In *Drosophila* loss-of-function mutations in SMC1 and SA blocked γ neuron axon pruning (Schuldiner et al., 2008). Supposedly, these mutations disrupted cohesin regulation of the ecdysone receptor gene (*ECR*) expression in the mushroom body γ neurons, which is required for neuron axon pruning (Lee et al., 2000; Pauli et al., 2008; Schuldiner et al., 2008). Indeed, cohesin and cohesin loader Nipped-B (homologue of yeast Scc2) were shown to bind to the active *ECR* gene and receptor levels were decreased in SMC1 mutant γ neurons (Schuldiner et al., 2008). Interestingly, Nipped-B was first identified in a screen for genes controlling long-range activation of another *Drosophila* gene, namely *cut* (Rollins et al., 1999), which is located 80 kb away from its transcriptional activator (Jack et al., 1991). *Cut* gene product, a homeobox protein, regulates many processes during *Drosophila* embryonic development (Nepveu, 2001). It was proposed that Nipped-B facilitates interaction between *cut* promoter and enhancer, since mutations within Nipped-B reduce *cut* expression (Rollins et al., 1999). In contrast to Nipped-B, cohesin inhibits communication between *cut* promoter and enhancer, since decrease in the levels of Rad21, SA, and Smc1 cohesin subunits leads to an increase in the expression of *cut* (Dorsett, 2004; Dorsett et al., 2005; Rollins et al., 2004). Nipped-B and cohesin were also shown to control the expression of Bithorax homeobox genes, which control limb and organ development in *Drosophila* (Gause et al., 2008; Hallson et al., 2008; Maeda and Karch, 2006; Rollins et al., 1999). Interestingly, unlike *cut* gene regulation, both Nipped-B and cohesin positively affect the expression of Bithorax genes. Apart from these roles, cohesin was also shown to be required for normal development of salivary glands in *Drosophila* (Pauli et al., 2008).

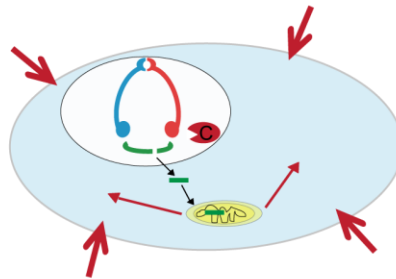
In humans certain mutations in cohesin subunits or cohesin-associated factors cause severe developmental abnormalities without dramatic cohesion defects. Cornelia

de Lange syndrome (CdLS) is a dominantly inherited developmental disorder, termed cohesinopathy, which is characterized by mental and growth retardation and is caused by diverse heterozygous mutations in *NIPBL* (Krantz et al., 2004), as well as in *SMC1* and *SMC3* (Deardorff et al., 2007; Musio et al., 2006). It is presumed that mutations in both cohesin and NIPBL could perturb cohesin binding to DNA and subsequently alter the expression of cohesin-regulated genes during embryonic development that is the cause of the phenotype observed in patients. CdLS-like phenotype without sister chromatid cohesion defect was observed in mice homozygous for *PDS5B* knockout, demonstrating that also Pds5 could be involved in gene regulation during development in mice (Zhang et al., 2007). Interestingly, around 40 % of patients with CdLS do not harbor mutations in any of the known cohesin genes. Thus, mutations in other proteins could also contribute to CdLS (Liu and Krantz, 2008). Other cohesinopathies, Roberts syndrome and SC phocomelia, are caused by truncations or loss-of-function mutations in *ESCO2* (homologue of yeast *ECO1*) (Schule et al., 2005; Vega et al., 2005). However, only patients with Robert syndrome are characterized by the presence of cohesion defects, termed heterochromatin repulsion (heterochromatic regions of sister chromatids are not associated with each other during the cell division) (German, 1979; Louie and German, 1981; Tomkins et al., 1979). It remains unclear whether the disease is caused by the cohesion defect or transcriptional deregulation. It is possible, that changes in cohesin binding to heterochromatin result in altered expression levels of heterochromatic genes. Alternatively, uncontrolled heterochromatin spreading could reduce or abolish expression of genes, located in the vicinity of the heterochromatin (Dorsett, 2007).

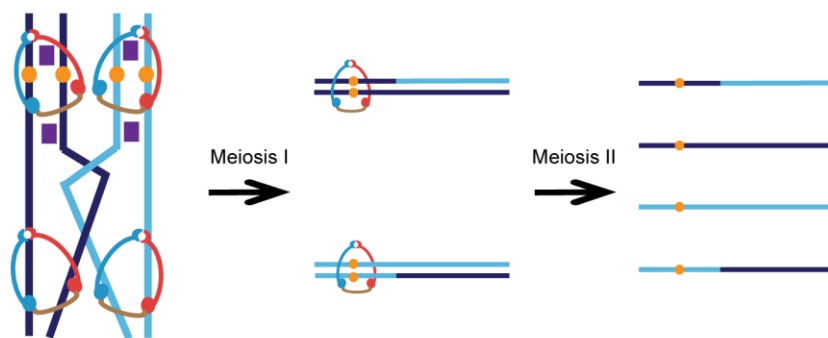
A DSBs repair



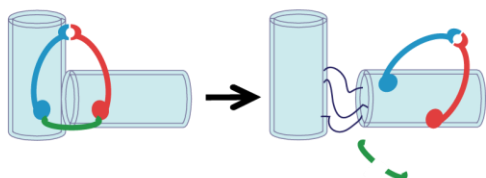
B Signaling during apoptosis



C Meiosis



D Centriolar cohesion



E Gene regulation

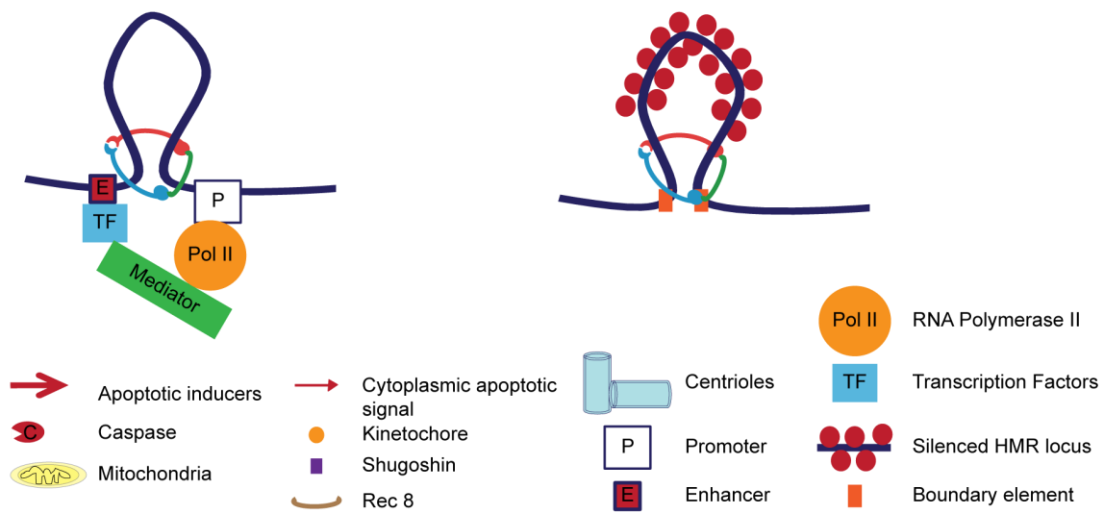


Figure 1.6 Multiple functions of cohesin

A) Cohesin complexes are required for double strand break repair via homologous recombination and activation of DNA damage checkpoint. Complexes are loaded in the vicinity of DSB and hold sister chromatids together, allowing recombination. **B)** Cohesin is involved in apoptosis signalling pathway. Scc1 subunit of cohesin is cleaved by caspase under the apoptosis-inducing conditions. Scc1 cleavage fragment is translocated from the nucleus into the cytoplasm and is accumulated in the mitochondria, leading to a decrease in the mitochondrial membrane potential, followed by the subsequent release of cytochrome c and the amplification of the cytoplasmic apoptotic signal. **C)** Cohesin in meiosis. During meiosis I after recombination between homologous chromosomes has taken place, cohesin complexes are removed from chromosomal arms, allowing recombined pairs of chromosomes to segregate. Centromeric cohesin, protected from removal during meiosis I by shugoshin, persists till meiosis II ensuring proper segregation of sister chromatids. **D)** Cohesin mediates centriolar cohesion. **E)** Cohesin in gene expression regulation. Cohesin stabilizes the base of a chromatin loop, which brings a gene enhancer associated with the transcription factors in the vicinity of the gene promoter occupied by RNA polymerase II, thus controlling the gene expression (left). Cohesin prevents spreading of silenced chromatin from silenced loci through stabilization of DNA loop at the boundary elements (right).

1.6 Aim of this study

The trimeric cohesin ring, which holds sister chromatids together is associated with three additional factors, namely Pds5, Scc3, and Wpl1 whose function remains a mystery. Since inactivation of Pds5 and Scc3 by conditional mutations resulted in reduced amount of cohesin on chromosomes and cohesion defects, it was proposed, that in budding yeast these factors might be required for maintenance of cohesin association with DNA and maintenance of sister chromatid cohesion. However, the temperature-sensitive mutants employed in these studies contained multiple amino acid substitutions and required the shift to an elevated temperature. Since the molecular mechanism of protein inactivation was unknown and unnatural growth condition had to be used, the obtained results did not go beyond confirming the role of Pds5 and Scc3 in sister chromatid cohesion without providing further insight into their action. More recently Scc3 was proposed to mediate cohesin association with CTCF transcription factor in human cells and might be potentially involved in defining the chromosomal addresses of cohesin complex.

We decided to investigate the role of cohesin factors employing degron tagging in budding yeast. Degron, a specific sequence, which targets the protein for degradation, when fused to the protein of interest is capable of dramatically reducing its amount in the cell. Degrons are reputedly highly specific and are capable of extracting the protein of interest out of the protein complex, leaving other components intact. In this regard, they pose certain advantages over the temperature-sensitive mutants that might have

unwanted properties and affect other components of the protein complex, e.g., unfolding at the restrictive temperature. We used two different degrons to deplete Pds5 and Scc3, namely a previously described DHFR-based N-terminal degron and a novel Eco1-derived C-terminal degron discovered in our laboratory. Surprisingly, Scc3 and Pds5 depletion with Eco1-derived C-terminal degron did not affect stability of cohesin binding to the DNA, which was tested in FRAP experiments *in vivo* and minichromosome immunoprecipitation experiments *in vitro*. No changes were detected in cohesin distribution throughout yeast genome, which was monitored in ChIP Seq experiments. However, Scc3 or Pds5 depletion resulted in sister chromatid cohesion defects. Similar results were obtained in experiments with Pds5, tagged with DHFR N-terminal degron. Unfortunately, Scc3 depletion employing DHFR N-terminal degron led to Scc1 co-depletion, making the results difficult to interpret.

We conclude, that contrary to the previous suggestions, Pds5 and Scc3 do not function to lock cohesin ring on the DNA or to restrict cohesin to certain sites on chromosomes, but are rather required for the entrapment of both sister chromatids inside the cohesin ring during cohesion establishment.

2 Results

2.1 Contributions

The design of described experiments as well as the analysis of data was performed together with my direct supervisor Dr. Dmitri Ivanov.

Vipin T Sreedharan and Dr. Gunnar Rättsch analyzed the CHIP-Seq data presented in Figures 2.10-2.13. Dr. Dmitri Ivanov performed the experiment shown in Figure 2.3. Vikash Verma purified recombinant Pds5-HA and Scc3-HA proteins used to estimate efficiencies of Pds5 and Scc3 depletion with Eco1-derived degron in the experiment shown in Figure 2.4. I performed all other experiments shown. A great part of the presented results here was published in (Kulemzina et al., 2012). See appendix for further information.

2.2 Approaches for Pds5 and Scc3 depletion

Since both proteins, Pds5 and Scc3, are essential for budding yeast viability we established the methods for their efficient depletion from yeast cells in order to address their functions during cohesion establishment and/or maintenance in vivo. Thus, *SCC3* and *PDS5* were fused to N-terminal or C-terminal ‘degron’ sequences, targeting the tagged proteins for degradation. As opposed to Pds5 and Scc3, Wpl1 in budding yeast is dispensable for viability, therefore to obtain an insight into its function we studied the consequences of *WPL1* gene deletion.

2.2.1 N-terminal DHFR-based degron

The endogenous genes encoding Pds5 or Scc3 were N-terminally tagged with DHFR-based degron cassette in yeast strains expressing an E3 ubiquitin ligase Ubr1 from the Gal promoter. The degron cassette encodes ubiquitin, followed by N-terminal domain of the thermo-sensitive version of dihydrofolate reductase (DHFR), 18 Myc tags and a flexible linker. Ubiquitin is cleaved after translation, and exposed N-terminal arginine is recognized by Ubr1. Ubr1 binding to the protein fusion leads to ubiquitylation of the lysines within DHFR domain by ubiquitin-conjugating enzyme Ubc2. DHFR ubiquitylation is facilitated by the partial DHFR unfolding upon

temperature increase, which exposes the lysine residues. DHFR ubiquitylation in turn targets the fusion protein for degradation (Dohmen et al., 1994; Kanemaki et al., 2003; Labib et al., 2000; Sanchez-Diaz et al., 2004) (Figure 2.1).

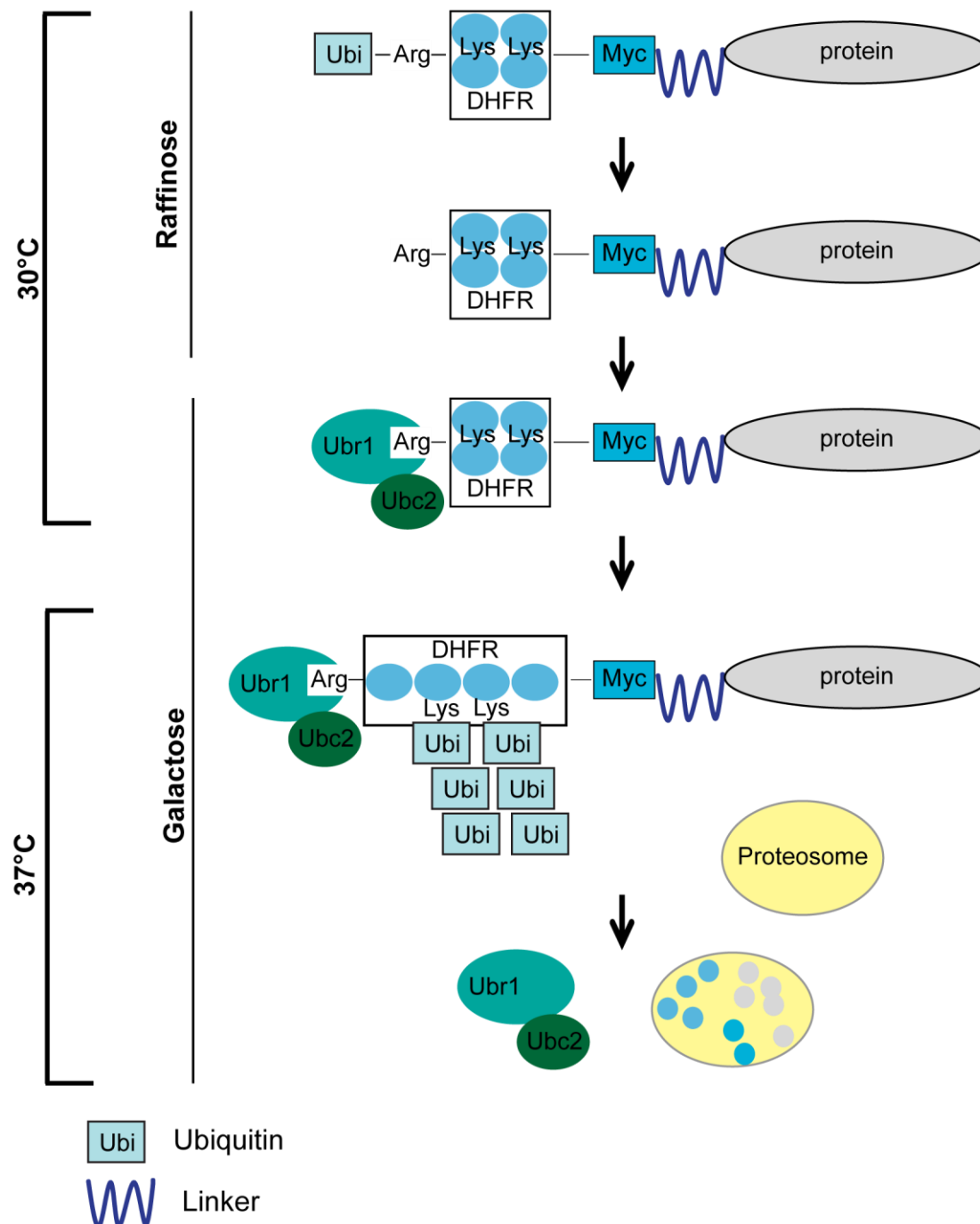


Figure 2.1 Mechanism of the heat-inducible degradation of a DHFR-based degron-protein fusion.

Yeast growing in raffinose-containing media at the permissive temperature, express protein of interest fused to a degron cassette, which includes ubiquitin, DHFR, Myc-epitope, and a flexible linker. N-terminal ubiquitin is removed immediately after translation, exposing the N-terminal arginine residue. Ubr1, whose expression is induced by transferring yeast to galactose-containing media, recognizes the N-terminal arginine and binds to the fusion protein, recruiting Ubc2. Upon increase in the ambient temperature, DHFR partially unfolds. As a result, the exposed lysine residues are ubiquitylated by Ubc2. This polyubiquitylation of the DHFR domain marks the fusion protein for degradation by 26S proteasome.

In order to achieve even stronger depletion of proteins of interest, corresponding genes were placed under the control of the *CUP1* promoter, which is inactive in the absence of CuSO_4 in the growth media. Thus, upon degron induction by temperature shift in media containing no CuSO_4 , Pds5 and Scc3 already present in the cell are degraded, and transcription of *PDS5* and *SCC3* genes is switched off. However, Pds5 and Scc3 depletion employing described approach resulted only in a moderate decrease in their abundance in the cell in such a way that constructed strains were able to grow at 37°C on galactose-containing media without CuSO_4 (data not shown). Even in the absence of CuSO_4 in the growth media, silencing of *PDS5* and *SCC3* genes was likely to be inefficient. Therefore, an alternative approach was applied, namely *CUP1* promoter was substituted with the tetO2 promoter, allowing doxycycline-dependent gene repression (Yen et al., 2003).

In this system transactivator (tTA) binds to the bacterial tetO promoter and allows gene expression in the absence of doxycycline. In the presence of doxycycline a tet repressor fused to the *S.cerevisiae* Ssn6 repressor (tetR'-SSN6) replaces tTA at the promoter and silences transcription (Belli et al., 1998). Upon degron induction using this system, Pds5 and Scc3 were efficiently depleted and constructed strains were unable to grow at 37°C on galactose-containing medium with doxycycline (data not shown). In order to test whether Pds5 and Scc3 have redundant functions, we constructed a strain harbouring Pds5 and Scc3 degron fusions simultaneously. All constructed fusions are fully functional in the absence of degron induction, since fusion proteins and cohesin complexes are loaded on chromatin in a way indistinguishable from wild type strain as could be judged from chromosomal spreads (data not shown). Importantly, Pds5 and Scc3 degradation was complete as judged by Western blot analysis. No fragments that would indicate incomplete protein degradation were detected after degron induction in strains, harboring Pds5 and Scc3 N-terminally tagged with degron cassette and C-terminally tagged with HA epitope (Figure 2.2). As induction of the degron may result in the degradation not only of the protein of interest,

but of the entire cohesin complex as well, we examined the abundance of the Scc1 subunit of cohesin after degradation of Pds5 and Scc3. Indeed, upon the induction of Scc3 degron Scc1 levels were noticeably reduced (data not shown), which precluded further use of DHFR-based degron for Scc3 depletion. Interestingly, Pds5 degradation employing the same DHFR-based degron did not affect Scc1 levels in the cell and Scc1 association with chromatin (data not shown). The observed difference could be due to the tight Scc3 binding to Scc1, while Pds5 associates with Scc1 in a very salt-sensitive and therefore, presumably less stable manner.

The experiments with the N-terminal DHFR-based degron prompted us to develop a novel degron system, which would be more selective in protein elimination.

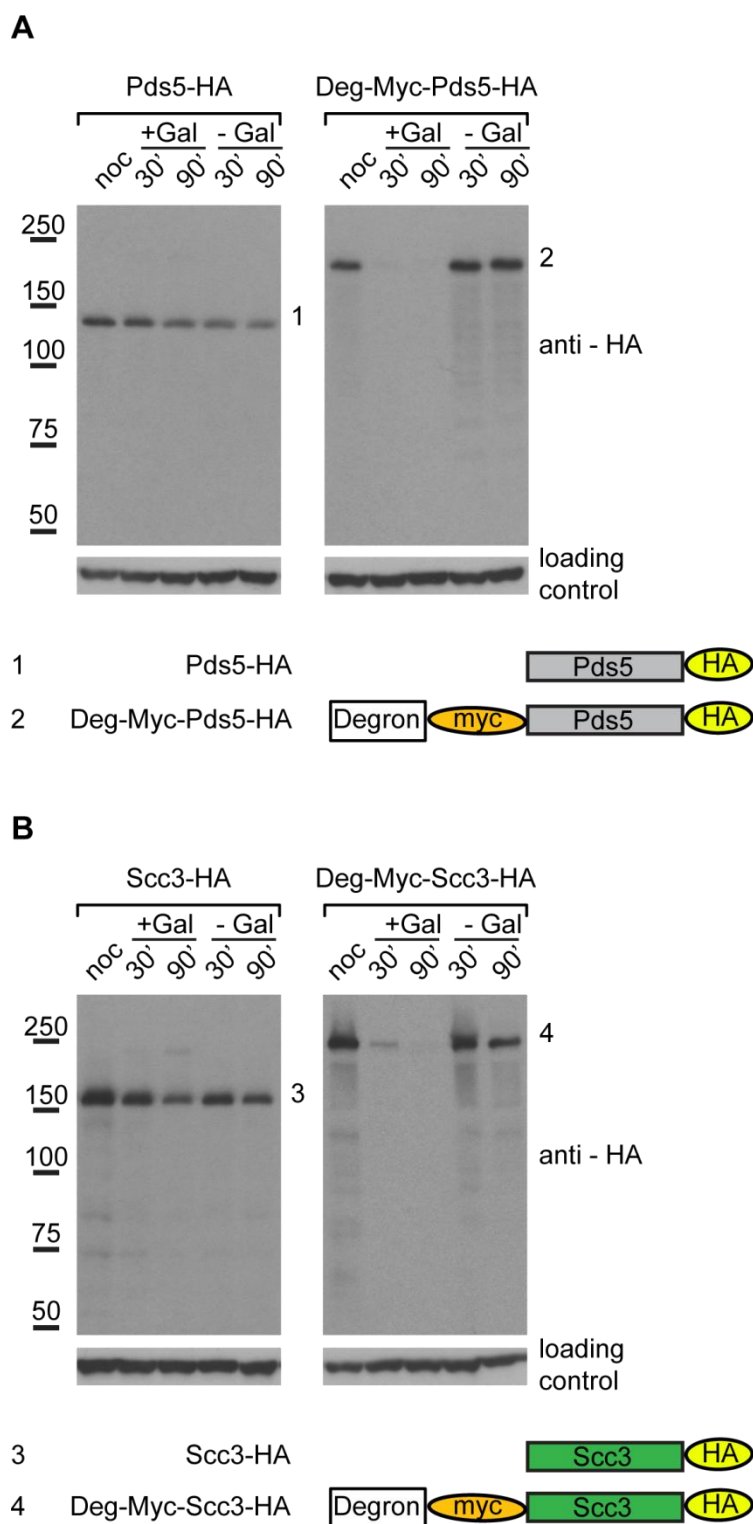


Figure 2.2 An induction of the N-terminal DHFR-based degron results in efficient and complete degradation of Pds5 and Scs3.

Strains 2576 (Pds5-HA6) and 2577 (Deg-Myc18-Pds5-HA6) (**A**), 2578 (Scs3-HA6) and 2579 (Deg-Myc18-Scs3-HA6) (**B**) were arrested with nocodazole in YPRaff at 30°C for 2 hours. Half of the cells were resuspended in YPGal containing nocodazole and incubated for 45 minutes at

30°C to induce Ubr1 expression and then shifted to 37°C in YPGal containing nocodazole and doxycycline to deplete Pds5 and/or Scc3 for 90 minutes. Another half of the cells were resuspended in YPRaff containing nocodazole and doxycycline and incubated at 30°C for 90 minutes. Aliquots were collected at the indicated time points and TCA protein extracts were prepared. Western blots probed with anti-HA (16B12) antibody and anti-Cdc28 (sc-28550, Santa Cruz) as a loading control are shown. No fragments of Scc3 and Pds5 could be detected after degnon induction (Kulemzina et al., 2012).

2.2.2 C-terminal Eco1-derived degnon

It was discovered in our laboratory that the amount of Eco1 acetyltransferase fluctuates dramatically during the cell cycle. The level of Eco1 decreases upon exit from S-phase and Eco1 is almost non-detectable in the G2 arrested cells (data not shown). Presence of a cyclin-dependent kinase-induced degnon within Eco1, which targets it for degradation was recently proposed (Lyons and Morgan, 2011). In our laboratory it was shown that two separate domains of Eco1, namely an unstructured S/P-rich middle domain and a C-terminal acetyltransferase domain, target heterologous proteins for degradation, when artificially fused to them. We employed the ability of the middle domain of Eco1 to deplete Pds5 or Scc3 from the yeast cells by creating Pds5 and Scc3 C-terminal fusions with a degnon cassette, which contained HA-epitope followed by a middle fragment of Eco1 (63-109 aa), which is predicted to be unstructured and does not possess the acetyltransferase activity. Levels of fusion proteins, Pds5-HA-Deg and Scc3-HA-Deg, were monitored at different stages of the cell cycle by Western Blot analysis. We found that the abundance of fusion proteins was dramatically decreased throughout the cell cycle compared to the wild type proteins (Figure 2.3). Thus, Eco1-derived degnon reduces the stability of the heterologous proteins throughout the cell cycle, rather than specifically inducing their degradation after S-phase.

Importantly for our experiments, Scc3 depletion with Eco1-derived degnon, does not result in decreased levels of Scc1 (data not shown). Scc1 levels were only slightly reduced in the cell expressing Pds5-HA-Deg, when compared to the wild type (data not shown).

In order to be able to use this approach for Pds5 and Scc3 depletion, it was important to assess the amount of protein-degnon fusions that remain undegraded in the cell. We were able to estimate the absolute numbers of nondegraded Pds5-HA-Deg and Scc3-HA-Deg molecules left in the cell by comparing serial dilutions of purified

recombinant Pds5-HA and Scc3-HA proteins with known concentration to serial dilutions of lysates prepared from known numbers of yeast cells, expressing Pds5-HA-Deg, Pds5-HA, Scc3-HA-Deg, or Scc3-HA (Figure 2.4). Our estimation of the amount of Pds5 and Scc3 present per cell in wild type budding yeast arrested in nocodazole is approximately 10000 molecules of Pds5 and 4500 molecules of Scc3, which is in good agreement with the numbers provided in the yeast database (approximately 7720 molecules of Pds5 and 4090 molecules of Scc3) (Ghaemmaghami et al., 2003). According to our estimation obtained for degron strains, there are only 250 molecules of Scc3 and Pds5 each left undegraded per cell. Assuming that all molecules of Scc3 and Pds5 are bound to the cohesin complexes that are loaded on DNA in the degron fusion strains (presumably an overestimate), only 15 molecules or less of Scc3 and Pds5 per chromosome are present in degron yeast strains. A similar quantity analysis performed with cohesin subunit, Scc1, resulted in an estimate of 4000 Scc1 molecules per haploid yeast genome (Weitzer et al., 2003). Thus, only 6 % or less of cohesin complexes in degron strains can be associated with Pds5 or Scc3.

Another important aspect of Pds5 and Scc3 depletion, namely completeness of their degradation, was also addressed. An addition of N-terminal Myc tag to the Pds5 and Scc3 fusions with the C-terminal degron cassette allowed us to confirm that degradation of fusions was complete and no stable fragments are generated (Figure 2.5). We were not able to construct a strain expressing both Pds5- and Scc3-degron fusions, or to delete *WPL1* in either of the degron strains.

Of the two degron systems that we tested each offers certain advantages over another. The Eco1-derived degron allows highly selective depletion of the protein of interest and, since no induction is required, the phenotype of the cells can be examined under normal growth conditions. The DHFR-based degron, on another hand, makes it possible to achieve a conditional depletion of Pds5 at a certain stage of the cell cycle.

In our further experiments, addressing Pds5 and Scc3 role in cohesin association with chromosomes, cohesion establishment, and maintenance, we employed Eco1-derived degrons to deplete Pds5 and Scc3 or DHFR-based degron to conditionally degrade Pds5.

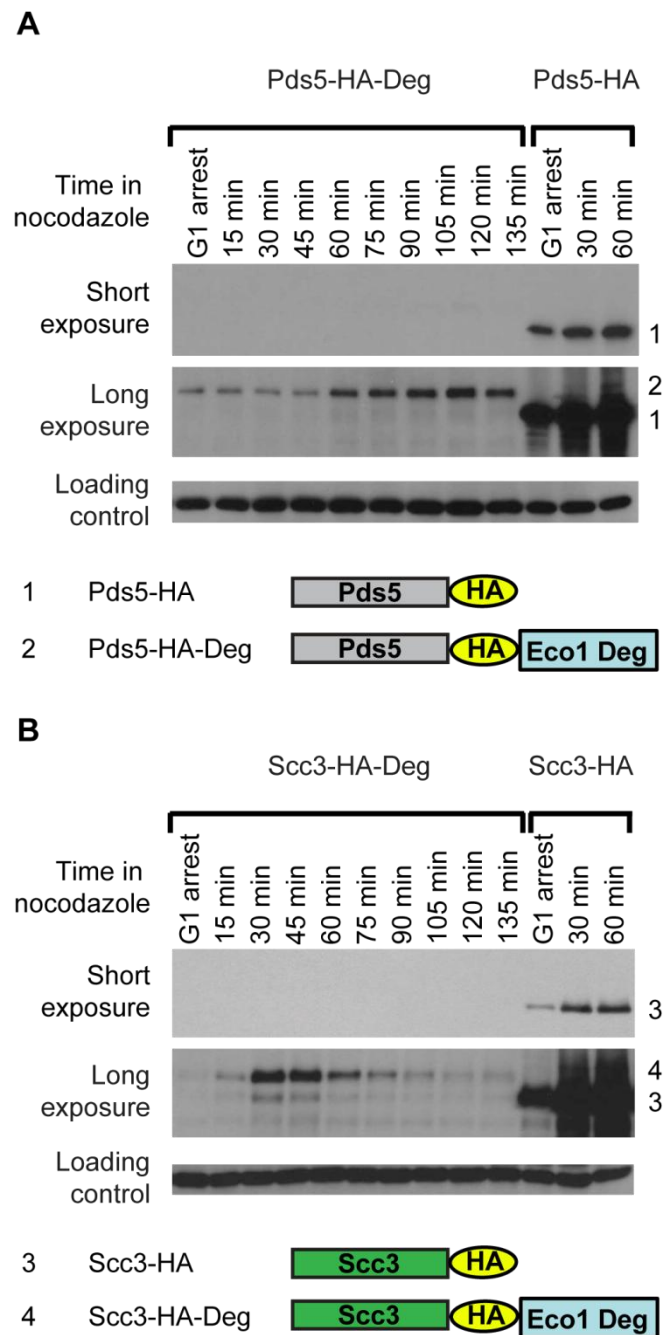


Figure 2.3 Pds5 and Scc3 are efficiently depleted with a C-terminal Eco1-derived degron.

Strains 1677 (*PDS5-HA6*) and 1675 (*PDS5-HA6-degron*) (**A**), 12544 (*SCC3-HA6*) and 1323 (*SCC3-HA6-degron*) (**B**) were arrested in G1 and then released into full media with nocodazole. Aliquots were collected at the indicated time points and TCA protein extracts were prepared. Western blots were probed with anti-HA (16B12) antibody. For loading control blots were probed with anti-Cdc28 antibody (sc-28550, Santa Cruz). This figure was adapted from (Kulemzina et al., 2012).

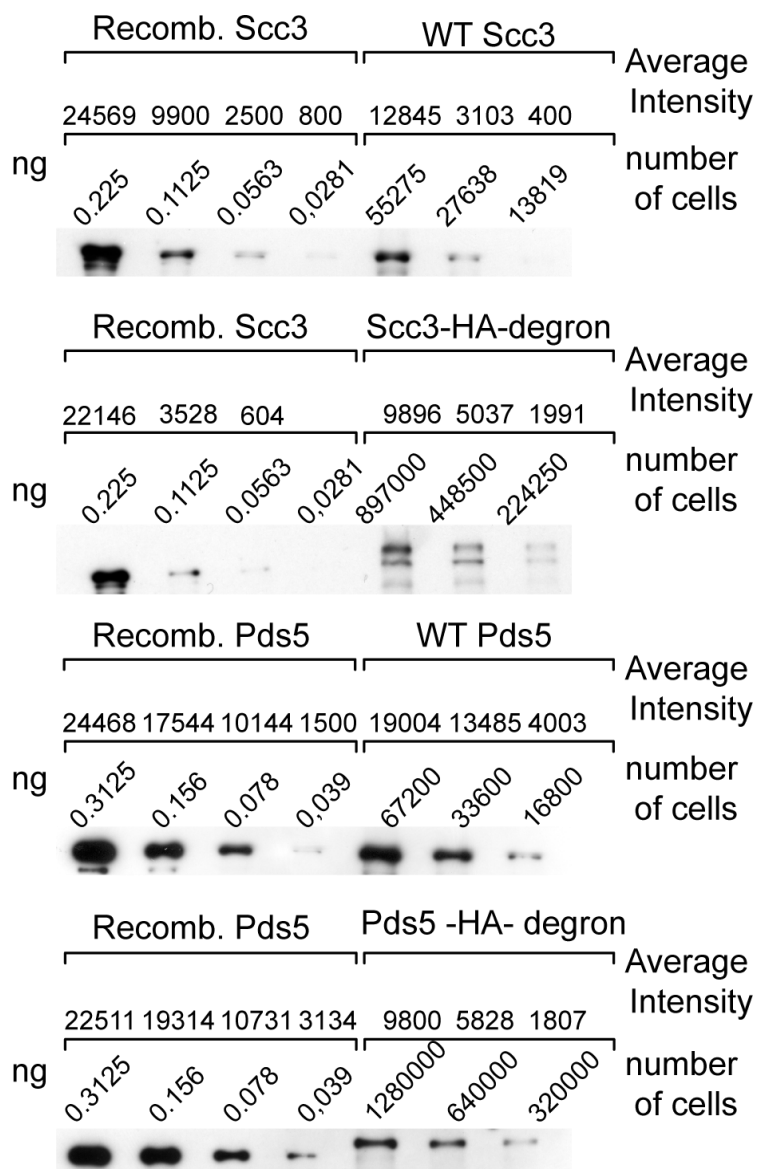


Figure 2.4 Efficiency of Pds5 and Scc3 depletion with a C-terminal Eco1-derived degron. Strains 1479 (*SCC3-HA6*), 1323 (*SCC3-HA6-degron*), 1677 (*PDS5-HA6*), and 1675 (*PDS5-HA6-degron*) were arrested in nocodazole and used for TCA protein extracts preparation. Extracts from indicated number of cells and known quantities of recombinant Scc3-HA6 and Pds5-HA6 were used for Western Blot analysis. Bands intensities were quantified with MetaMorph software and corresponding Average intensity is indicated. Western blots probed with anti-HA (16B12) antibody are shown (Kulemzina et al., 2012).

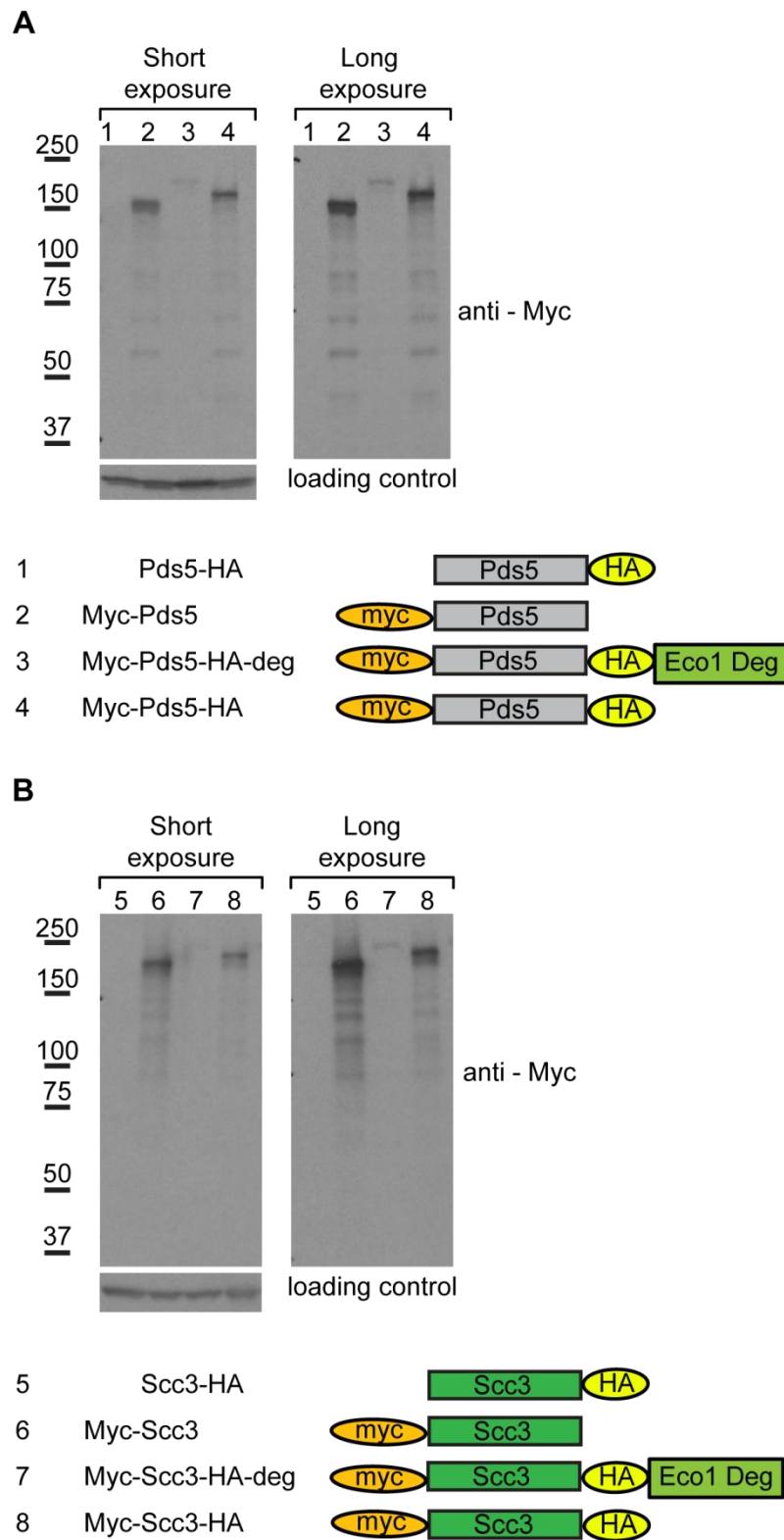


Figure 2.5 Pds5 and Scc3 depletion with a C-terminal Eco1-derived degron is complete.

Strains 2523 (Pds5-HA6), 2587 (Myc9-Pds5), 2601 (Myc9-Pds5-HA6-degtron), and 2590 (Myc9-Pds5-HA6) **(A)**, 1479 (Scc3-HA6), 2584 (Myc9-Scc3), 2608 (Myc9-Scc3-HA6-degtron), and 2603 (Myc9-Scc3-HA6) **(B)** were arrested in G2/M with nocodazole for 3 hours and TCA protein extracts were prepared. Western blots probed with anti-Myc (71D10) antibody are shown. For loading control blots were probed with anti-Cdc28 antibody (sc-28550, Santa Cruz). No fragments of Pds5 and Scc3 fused to an Eco1-derived C-terminal degtron could be detected (Kulemzina et al., 2012).

2.3 Stoichiometric amounts of Pds5, Scc3, and Wpl1 are not required to maintain the stable association of cohesin with chromosomes

2.3.1 Cohesin complexes devoid of Pds5 and Scc3 maintain their association with DNA

Since both proteins, Pds5 and Scc3 were proposed to be cohesin maintenance factors, we expected that their depletion would result in a dramatic decrease in the amount of cohesin complexes associated with chromosomes, since, according to our estimates, in degtron strains more than 94% of cohesin complexes are devoid of these factors. To check this prediction we examined the levels of cohesin in chromatin pellets, which are commonly used to evaluate protein-chromatin binding (Liang and Stillman, 1997). Yeast strains expressing Pds5-HA, Pds5-HA-Deg, Scc3-HA, and Scc3-HA-Deg fusions from endogenous loci were arrested with nocodazole in G2/M, treated with lyticase to remove the cell wall (spheroplasted), and lysed by addition of detergent. Cell lysates were fractionated via low speed centrifugation through a sucrose cushion to yield a chromatin pellet, containing chromatin with bound proteins, and a supernatant, harboring soluble proteins.

Western blot analysis confirmed that Scc3 and Pds5 fused to Eco1 degtron were efficiently depleted not only from cell lysates, but also from chromatin compared to wild type (Figure 2.6, upper row). Unexpectedly, the remarkable reduction in the amounts of Scc3 or Pds5 did not lead to a decrease in the amount of Scc1 bound to the chromatin or to a relative increase of Scc1 level in the soluble supernatant (Figure 2.6, second row from the top). Interestingly, deletion of *WPL1* also did not affect the levels of Scc1 associated with chromatin. These results were further supported by the analysis of cohesin on chromosomal spreads performed in the laboratory by Martin Schumacher.

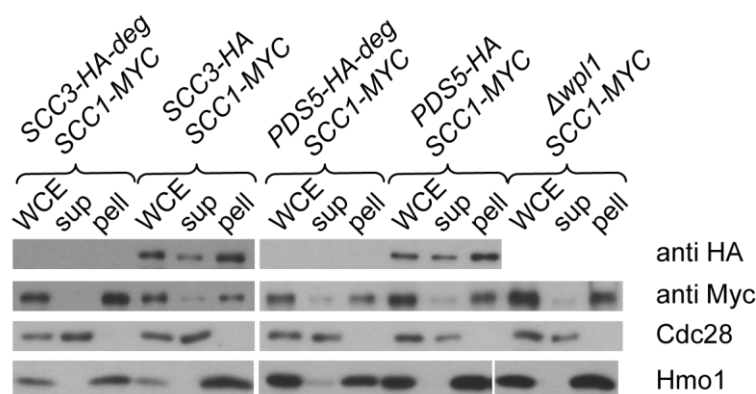


Figure 2.6 Chromatin-associated fraction of cohesin is not affected by the depletion of Scc3, Pds5 or Wpl1.

Strains 1625 (*SCC1-Myc18*, *SCC3-HA6-deg*), 1813 (*SCC1-Myc18*, *SCC3-HA6*), 1818 (*SCC1-Myc18*, *PDS5-HA6-deg*), 2525 (*SCC1-Myc18*, *PDS5-HA6*), and 1906 (*SCC1-Myc18*, $\Delta wpl1$) were arrested with nocodazole in G2/M phase and whole cell extracts (WCE) were prepared. WCE was further fractionated into soluble supernatant (sup) and chromatin pellet (pell). Comparable amounts of protein samples were separated on SDS-PAGE. Western Blots probed with anti-HA (16B12) and anti-Myc (71D10) antibodies are shown. Blots were also probed with anti-Cdc28 (sc-28550, Santa Cruz) and anti-Hmo1 antibodies as loading controls for the soluble supernatant and chromatin pellet, respectively (Kulemzina et al., 2012).

Since both chromatin pellets and chromosomal spreads are capable of measuring only the bulk amounts of cohesin on DNA, more precise analysis of the cohesin association with specific chromosomal loci was performed by chromatin immunoprecipitation followed by quantitative polymerase chain reaction (ChIP-qPCR) method. The same strains that were used in chromatin pellets experiments were arrested in G2/M, DNA was cross-linked to associated proteins, and then fragmented via sonication. DNA fragments bound to Scc1 were purified via Scc1 immunoprecipitation (IP) and were used as a template for quantitative PCR. In a parallel experiment using the same cell lysates we immunoprecipitated DNA fragments cross-linked to histone H3 as a control. The efficiencies of Scc1 chromatin immunoprecipitation (ChIP) at the centromere-adjacent region and at the arm sites, which are known to be cohesin positive or negative, were calculated and normalized to the efficiencies of the histone H3 ChIP at the same loci (Figure 2.7B) as described in (Sutani et al., 2009). The amount of cohesin bound to the centromere-adjacent or chromosomal arm sites in the Scc3-HA-deg strain was unchanged compared to wild type (Figure 2.7B). Consistent with previous results obtained for *pds5* ts and $\Delta wpl1$ mutants (Sutani et al., 2009), we detected 2-3 fold decrease in the amount of cohesin associated with

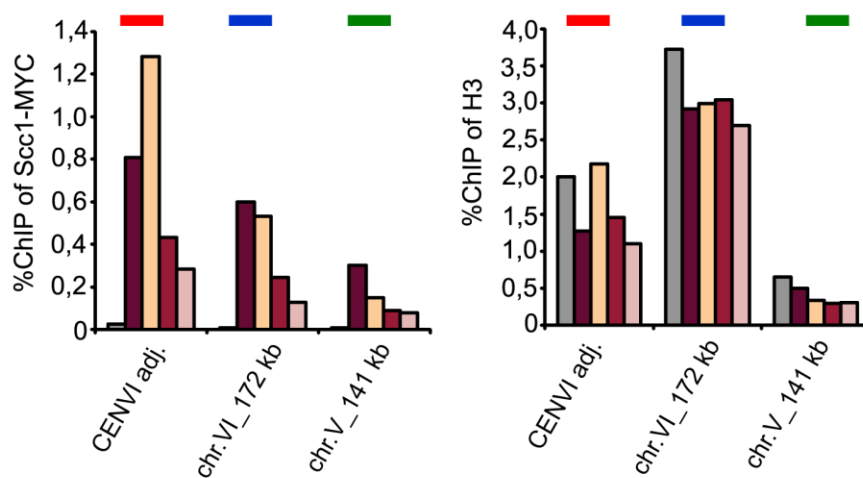
chromosomes at the indicated sites in Pds5-HA-degrom and $\Delta wpl1$ strains (Figure 2.7B). Interestingly, deletion of *WPL1*, which is a non-essential gene in budding yeast, has the strongest effect on the amount of the Scc1 associated with analyzed chromosomal loci. It is possible, that the observed phenotype in the cells depleted of Pds5 could be explained by the inability to recruit Wpl1 to cohesin in the absence of Pds5.

2.3.2 Depletion of Pds5, Scc3 or Wpl1 does not affect the stability of cohesin association with the chromosomes

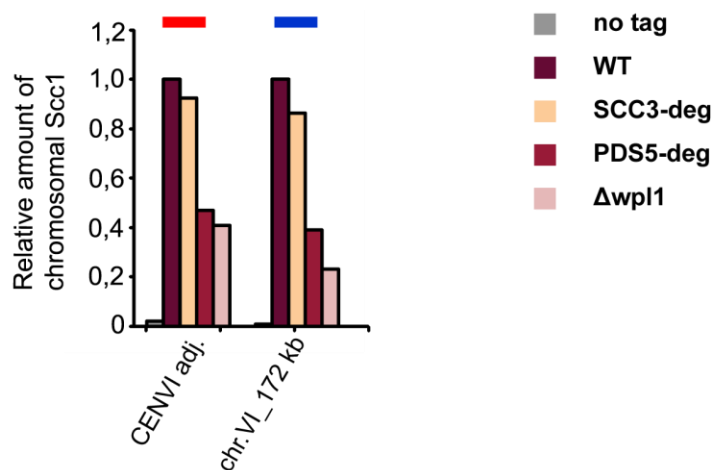
Although the amounts of cohesin on chromosomes remain unchanged after Scc3 and Pds5 depletion, it is conceivable that the stability of cohesin association with the DNA is affected and the observed association of cohesin complexes with the chromosomes is a result of a continuous cycle of cohesin unloading and re-loading. In order to check this possibility, we tagged endogenous *SMC3* with GFP in *Scc3*-degrom and *PDS5*-degrom strains, as well as $\Delta wpl1$ and wild type strains and performed a fluorescence recovery after photobleaching (FRAP) experiment. As discussed earlier (see Introduction) in metaphase cohesin complexes localize between the separated spindle poles and form a cylindrical array, which in sagittal section appears as a two lobes (Yeh et al., 2008). When one of these lobes was bleached, no recovery of fluorescent signal was observed, suggesting that cohesin is stably bound to the DNA in vivo with no detectable turnover (Rowland et al., 2009; Yeh et al., 2008). In contrast to the wild type cohesin, a mutant version of Smc3-GFP defective in ATP hydrolysis is unstably bound to the chromosomes at several foci and rapidly recovers fluorescence in the similar FRAP experiments (Hu et al., 2011). In our experiments after a portion of the GFP fluorescence was photobleached in metaphase cells fluorescence signal did not recover for the duration of the experiment (5 minutes) in either the wild type, *SCC3*-degrom, *PDS5*-degrom or $\Delta wpl1$ strains, indicating that there is little or no turnover of Smc3 on DNA (Figure 2.8A). In order to confirm that not only Smc3, but the entire cohesin complex is stably bound to the chromosomes when Scc3 and Pds5 are depleted, we repeated the FRAP experiments with the strains harboring another cohesin subunit, *SCC1*, tagged with GFP. No fluorescence recovery was detected after portion of Scc1-GFP was bleached in *SCC3*-degrom, *PDS5*-degrom, wild type or $\Delta wpl1$ strains, indicating that there is no turnover of Scc1 on the DNA (Figure 2.8B). On another

hand, when histone H2B tagged with GFP was used in the in the parallel FRAP experiment, it readily recovered the fluorescence (Figure 2.8B), consistent with the

A



B



C

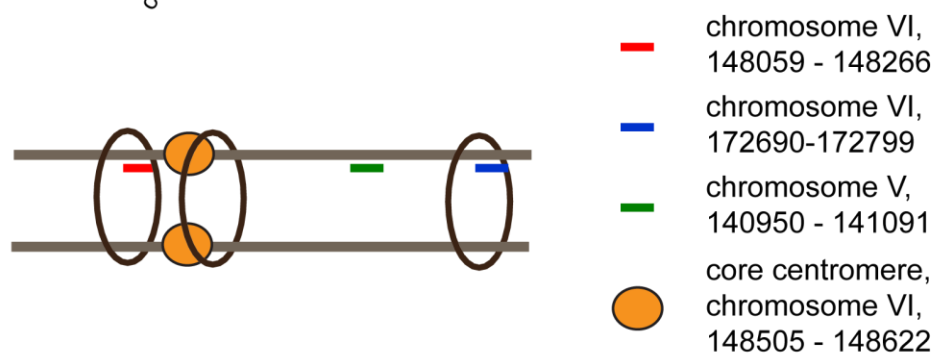


Figure 2.7 ChIP-qPCR assay of Scc1.

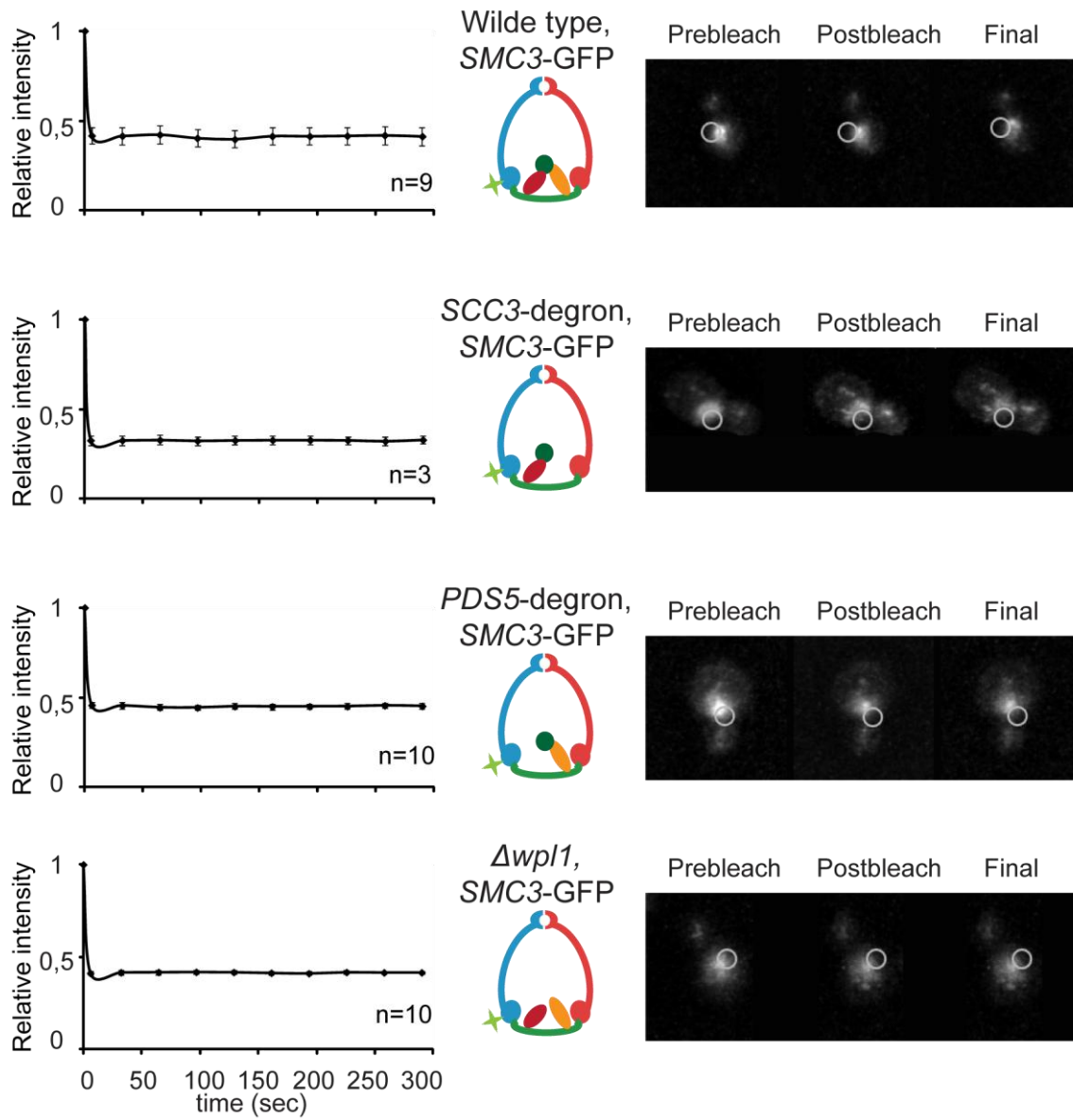
A) Strains 10589 (wild type), 1625 (*SCC3*-degron), 1818 (*PDS5*-degron), and 1906 ($\Delta wpl1$) with endogenous *SCC1* tagged with Myc18, and untagged strain (1021) were arrested with nocodazole in G2/M, incubated with formaldehyde to cross-link proteins to DNA and lysed. Prepared lysates were used for chromatin immunoprecipitation with anti-Myc (9E11) and anti-

histone H3 (ab1791, abcam) antibodies. ChIP DNA was quantified by quantitative PCR employing three pairs of primers specific to a centromere adjacent region of chromosome VI, to a site on the arm of the chromosome VI (172 kb), which is known to be cohesin-rich, and to the site on the arm of the chromosome V (141 kb), which is known to be cohesin-poor. **B)** The immunoprecipitation/input ratios from Scc1 ChIP were normalized between the strains using the control immunoprecipitation/input ratios from H3 ChIP and divided by the resultant immunoprecipitation/input ratio obtained for the wild type strain. **C)** Schematic of the analyzed chromosomal regions. Centromere adjacent site, cohesin-rich and cohesin-low sites at the chromosomal arms are marked with red, blue, and green, respectively (Kulemzina et al., 2012).

previously published data (Yeh et al. 2008). We conclude, that cohesin is stably bound to the DNA in the absence of Wpl1, as well as when the levels of Pds5 or Scc3 in the cell are dramatically reduced.

Since cohesin complexes devoid of Pds5, Scc3, and Wpl1 are capable of stable binding to chromosomes with no detectable turnover, it is highly unlikely that these proteins serve as locks of cohesin rings on DNA as was previously proposed in the literature. However, at this moment we cannot exclude the possibility, that Pds5 and Scc3 play a catalytic role to promote stable binding of cohesin to chromosomes. In this case even the small amounts of Pds5 and Scc3 remaining in our strains would be able to fulfil their role in cohesin maintenance. The important corollary is that grossly substoichiometric quantities of Scc3 and Pds5 would be able to “stabilize” multiple cohesin rings implying the turnover of Scc3 and Pds5 subunits between cohesin complexes.

A



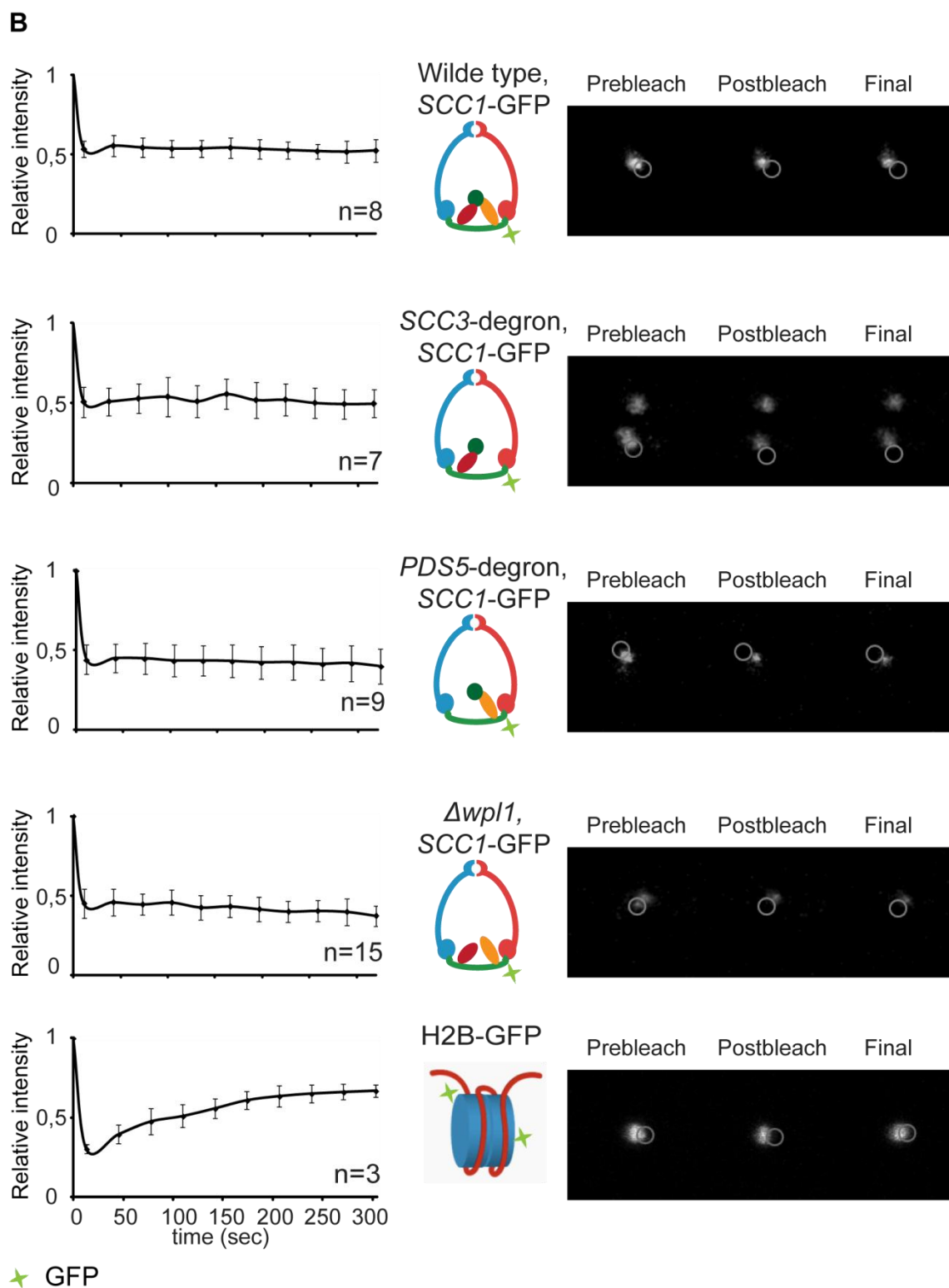


Figure 2.8 Depletion of Scc3, Pds5 or Wpl1 does not induce cohesin turnover on chromosomes.

Mitotic cells of strains 2003 (wild type), 2040 (*SCC3*-degron), 2004 (*PDS5*-degron), and 2034 ($\Delta wpl1$) with endogenous *SMC3* tagged with GFP (**A**) or mitotic cells of 2353 (wild type), 2390

(*SCC3-HA6-degron*), 2389 (*PDS5-HA6-degron*), and 2391 (Δ *wpl1*) with endogenous *SCC1* tagged with GFP (**B**) were used for fluorescence recovery after photobleaching experiment (FRAP). Histone H2B-GFP strain (1904) was used as a control. No recovery of bleached pericentromeric *Scs1*-GFP or *Smc3*-GFP was observed during this experiment in contrast with the H2B-GFP control. The mean and standard deviation are calculated from independent experiments (numbers of analyzed cells for each strain are indicated on the graphs) (Kulemzina et al., 2012).

2.4 *Pds5* and *Scs3* are stable subunits of the cohesin ring in vivo

While *Scs3* is presumed to be stably associated with cohesin, *Pds5* interaction with cohesin is salt-sensitive and recoveries of *Pds5* and *Wpl1* in cohesin preparations from cells are low. In order to address the question whether *Pds5*, *Scs3*, and *Wpl1* are stable cohesin subunits in vivo we tagged these proteins C-terminally with GFP and performed FRAP experiments. In metaphase cells, *Pds5* and *Scs3* visualized with GFP form a cylindrical array lying between separated spindle poles similar to the one formed by the cohesin complex. However, no cylindrical array was observed in the metaphase cells expressing *Wpl1*-GFP fusion, instead we observed a diffuse fluorescent signal, which precluded further FRAP experiments. When a portion of *Pds5*-GFP or *Scs3*-GFP was bleached, no recovery of the fluorescent signal was detected (Figure 2.9). Since it is known from the literature and from the experiments performed in our laboratory that *Scs3* and *Pds5* association with DNA is strictly dependent on cohesin, the results of the FRAP experiment suggest that *Pds5* and *Scs3* are stable subunits of cohesin complexes associated with DNA in the cell under physiological conditions. The reported salt-sensitivity of *Pds5* association with cohesin is therefore, likely an in vitro phenomenon. Our results suggest that *Wpl1* is not stably associated with cohesin in the cell. Alternatively, *Wpl1* could bind to only a small fraction of cohesin complexes.

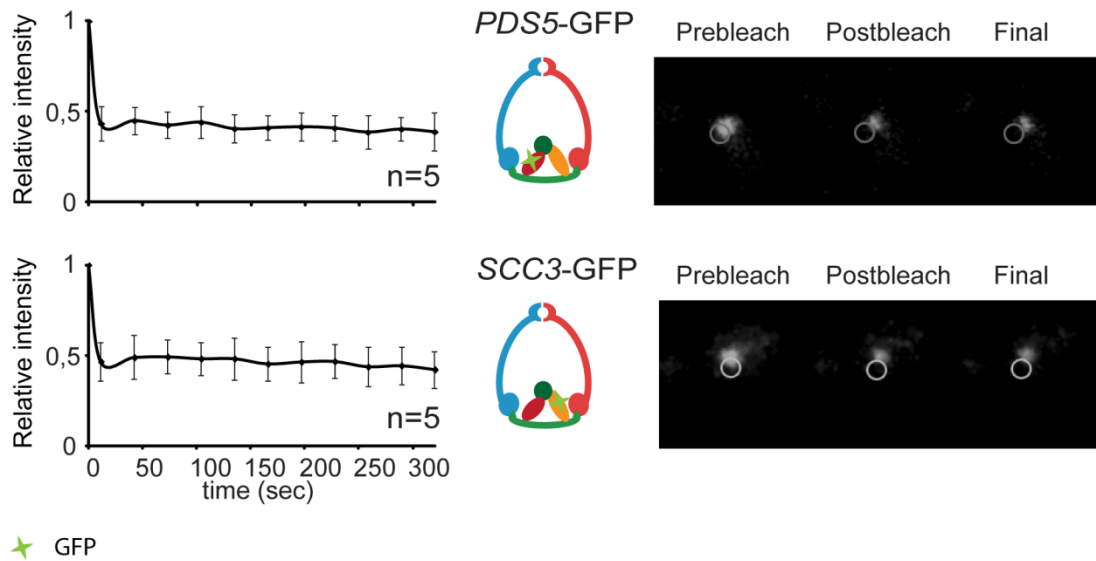


Figure 2.9 Pds5 and Scc3 stably bind to the chromatin in vivo.

Mitotic cells of the strains 2417 (*PDS5-GFP*) and 2281 (*SCC3-GFP*) were used for FRAP experiments. The mean and standard deviation are calculated from independent experiments (numbers of analyzed cells for each strain are indicated on the graphs). No recovery of bleached Pds5 and Scc3 could be detected during experiment (Kulemzina et al., 2012).

2.5 Depletion of Pds5, Scc3 or Wpl1 does not affect the genome-wide distribution of the cohesin

Although Pds5 and Scc3 are not required for the stable maintenance of cohesin on the chromosomes, it is possible that these factors function to target cohesin to the distinct loci on the chromosomes. In order to address this possibility, we analysed cohesin distribution along the chromosomes using ChIP-Seq. DNA fragments recovered from Scc1 ChIP as described above were ligated to adaptors and sequenced. The pattern of genome-wide distribution of Scc1 in *PDS5*-degron, *SCC3*-degron, and $\Delta wpl1$ strains highly resembles the one observed in the wild type strain (Figure 2.10A) and the calculated correlation coefficients of Scc1 distribution in *PDS5*-degron, *SCC3*-degron, and $\Delta wpl1$ strains and wild type are 0.80, 0.88, and 0.83, respectively (Figure 2.10B). We observe the relative enrichment of cohesin in the vicinity of the centromere and distinct peaks along the chromosomal arms.

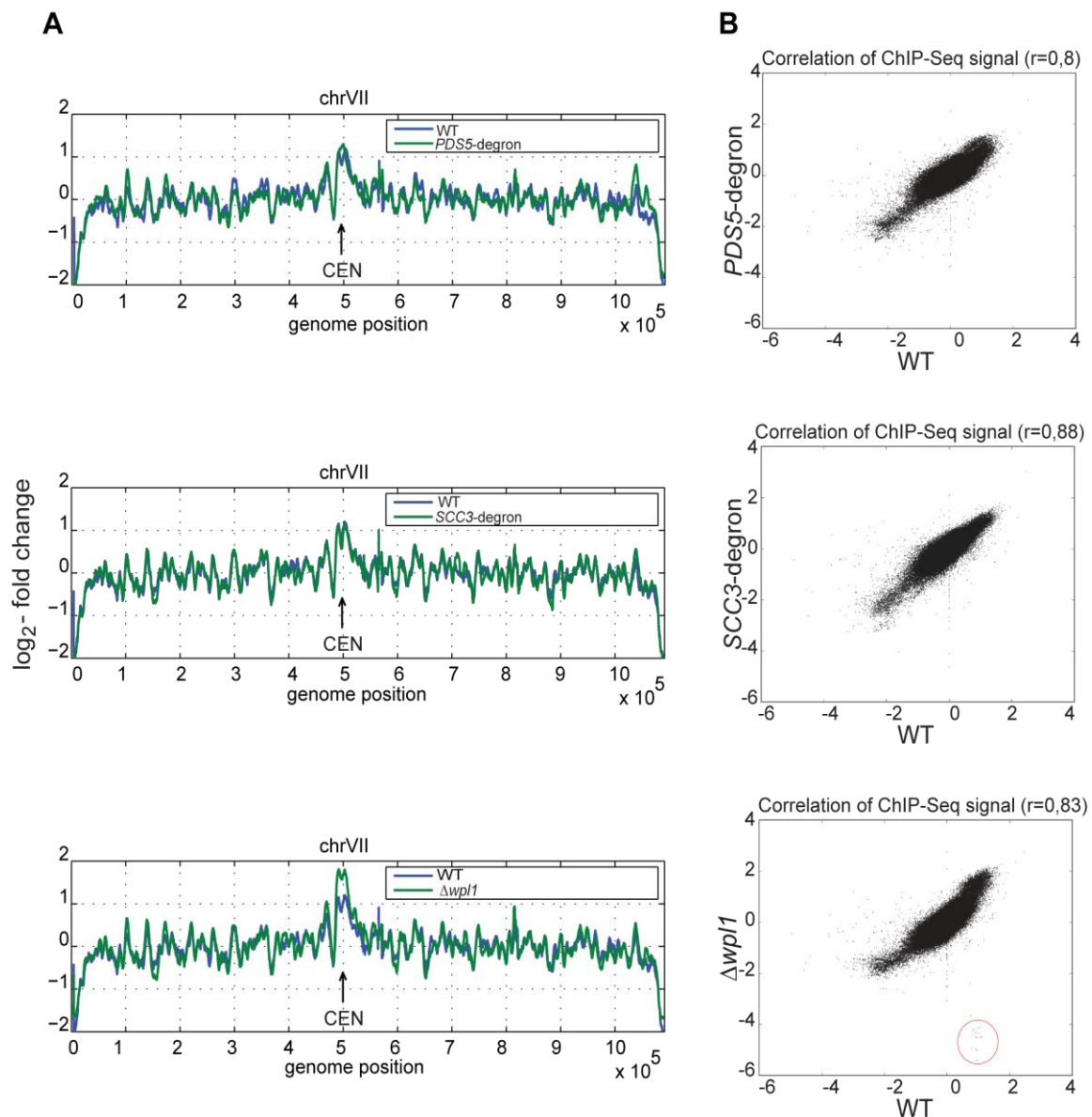


Figure 2.10 Depletion of Pds5, Scc3 or Wpl1 does not affect cohesin genome-wide distribution.

Strains 10589 (wild type), 1818 (*PDS5-HA6*-degron), 1625 (*SCC3-HA6*-degron), and 1906 ($\Delta wpl1$) with endogenous *SCC1* tagged with Myc18 were used for Scc1-Myc18 ChIP with anti-Myc (9E11) antibodies. ChIP DNA was sequenced. Untagged strain (1021) was used as a control to determine signal log ratio. **(A)** Scc1 distribution on chromosome VII is presented. The data sets for the wild type and one of the degron strains are plotted on the same graph to facilitate comparison. A window of 5.000 bps (i.e., 2.500 bps in each direction) was used for smoothing. **(B)** Scatter plot between chromosomal Scc1 distributions in wild type versus *PDS5*-degron, *SCC3*-degron, and $\Delta wpl1$ strains are shown. Reads, which correspond to *WPL1* gene that are absent in $\Delta wpl1$ strain are marked in red (Kulemzina et al., 2012).

To obtain a close-up view of cohesin distribution at the distinct loci, we used a smaller window to analyse the ChIP-Seq data, but still were not able to detect any reproducible differences in Scc1 distribution. For example, similar to global pattern,

cohesin binding within centromere region is comparable between *PDS5*-degron, *SCC3*-degron, $\Delta wpl1$, and wild type strains (Figure 2.11). Interestingly, we observed a dip in the amount of DNA-bound cohesin corresponding to the core centromeric sequences as reported previously based on the chromosomal walk with conventional ChIP (Warren et al., 2004). Although the extent of cohesin depletion at the core centromere was variable among different samples, no reproducible strain-dependent differences could be confirmed in independent experiments (Figure 2.12).

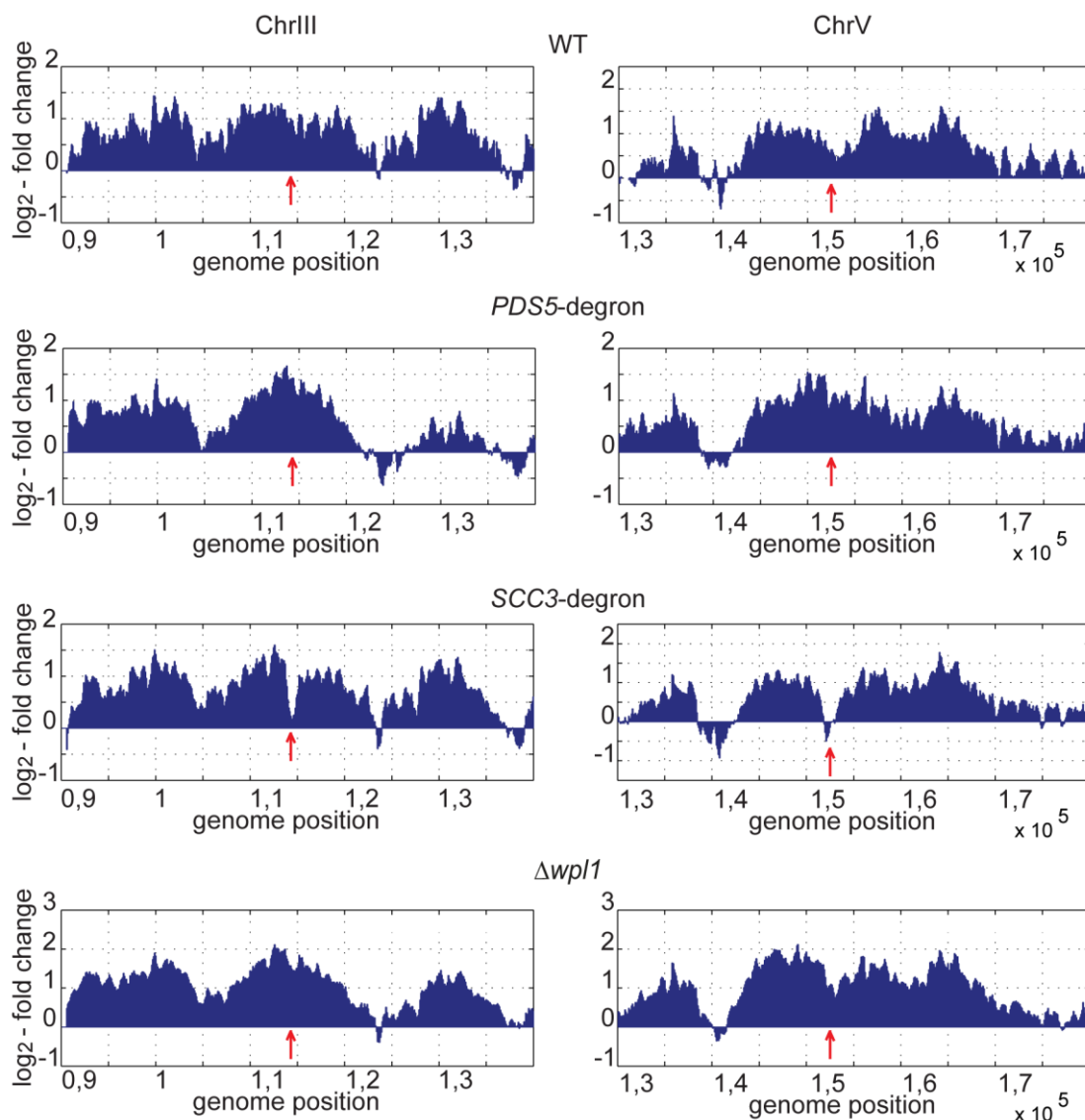


Figure 2.11 Cohesin distribution in the pericentromeric regions of chromosome III and V in the strains depleted of Pds5, Scc3 or Wpl1.

Position of the centromere is marked with red arrow. A window of 500 bp with a 50 bp step was used (Kulemzina et al., 2012).

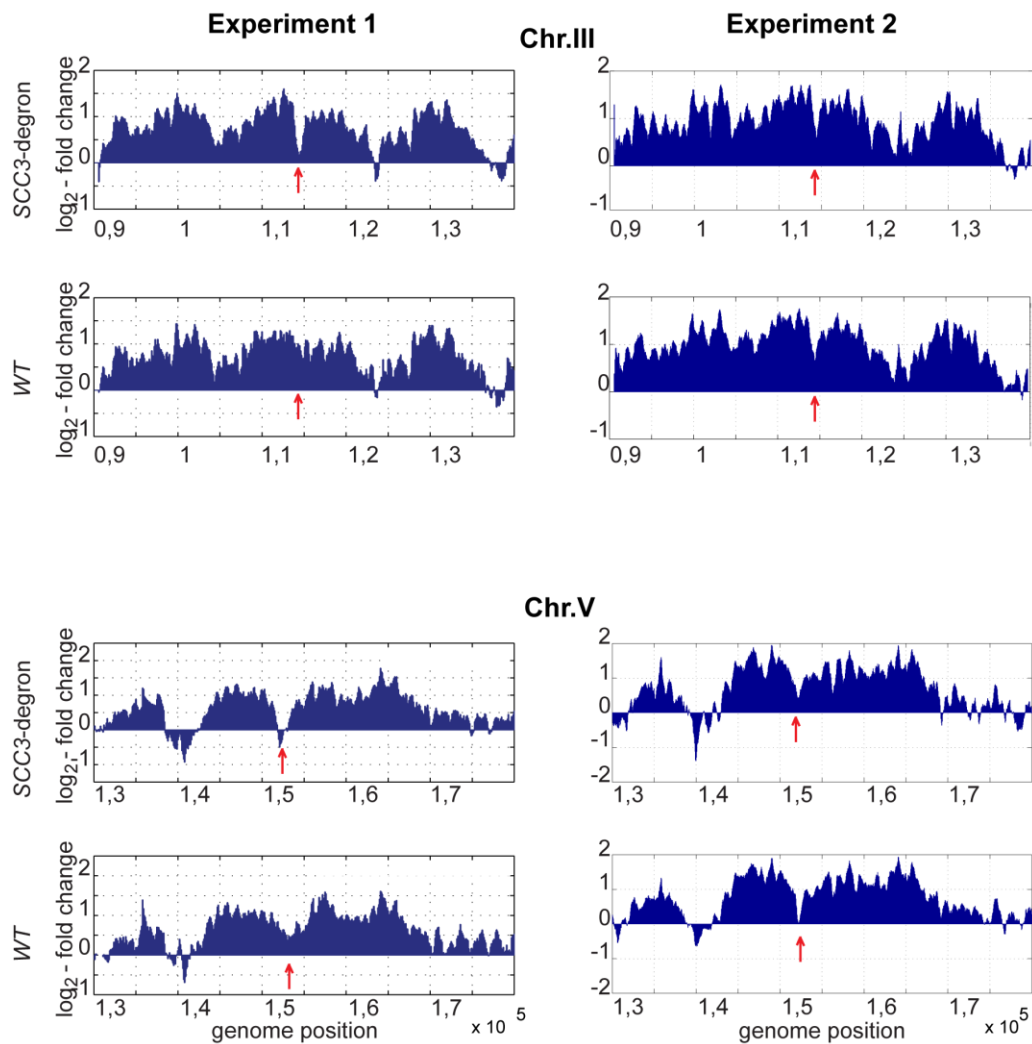


Figure 2.12 Reproducibility of ChIP-Seq experiments.

Cohesin distribution in the pericentromeric regions of chromosome III and V in wild type and in the strain depleted of Scc3 in two independent ChIP-Seq experiments are presented. Overall pattern of cohesin distribution at the pericentromeric region is remarkably similar. Position of the centromere is marked with a red arrow. A window of 500 bp with a 50 bp step was used.

Similar results were obtained at the other cohesin loading sites, e.g. for two tDNA genes on chromosome VII, which were previously reported to be associated with Scc2/Scc4 cohesin loading complex (Hu et al., 2011) (Figure 2.13).

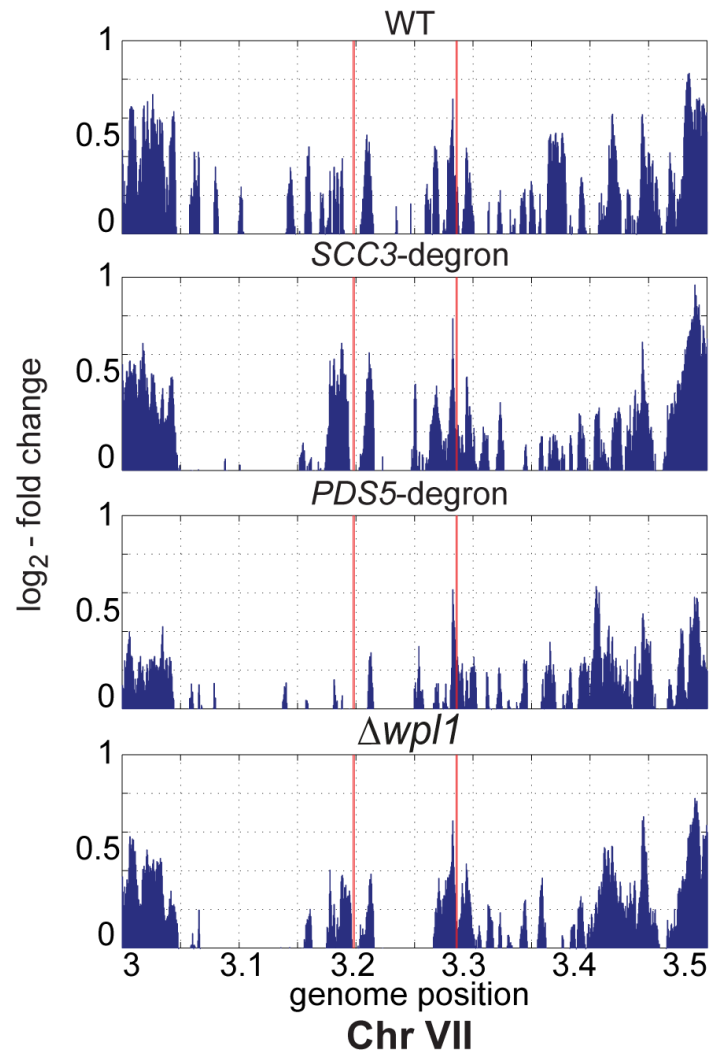


Figure 2.13 Cohesin distribution at the tDNA loci of chromosome VII in the strains depleted of Pds5, Scc3 or Wpl1.

Positions of the tDNA genes are marked with red lines. A window of 500 bp with a 50 bp step was used (Kulemzina et al., 2012).

We conclude that Pds5, Scc3, and Wpl1 do not target cohesin to the specific loci, since no remarkable changes in cohesin distribution along the chromosomes were detected in *PDS5-deg*, *SCC3-deg*, and $\Delta wpl1$ strains when compared to wild type strain.

2.6 Cohesin rings devoid of Scc3 and Pds5 topologically embrace DNA

A distinctive feature of cohesin association with DNA is the ability of cohesin rings to trap DNA inside them. If DNA is circular, e.g., a plasmid or a minichromosome, the protein and DNA rings are intercatenated and remain stably associated with each other unless one of the two is opened as a result of proteolysis or restriction digest. The stability of most other protein-DNA complexes is not expected to be strongly influenced by the changes in the DNA topology. A circular minichromosome-based assay for the topological association of cohesin with the DNA was developed by (Ivanov and Nasmyth 2005).

Minichromosome is a circular plasmid containing a centromeric region of chromosome IV, which is known to recruit cohesin (Figure 2.14A). Hence, the immunoprecipitation of cohesin complex from the yeast cell lysates via Scc1 subunit results in co-immunoprecipitation of the minichromosome (Figure 2.14B -BglII). If the minichromosome is linearized by restriction digest cohesin slides off the end of the linear DNA and no minichromosome can be detected in the cohesin IP (Figure 2.14B +BglII).

We assayed the cohesin binding to the minichromosome in the strains depleted of Scc3 and Pds5 with the help of Eco1-derived degrons. We were able to co-immunoprecipitate circular, but not linearized minichromosomes with Scc1 subunit of cohesin from the wild type, *SCC3*-degron, and *PDS5*-degron strains as judged from the Southern blot analysis of Scc1 immunoprecipitates (Figure 2.14C). Therefore, we conclude that cohesin rings topologically embrace DNA in the strains depleted of Scc3 and Pds5.

Additional co-immunoprecipitation experiments were performed to confirm the absence of Pds5 or Scc3 from the cohesin complexes, associated with the minichromosomes in *SCC3*-degron and *PDS5*-degron strains. We reasoned that upon efficient depletion it would be impossible to co-immunoprecipitate minichromosome with the Pds5- and Scc3-degron fusions. Indeed, we were able to co-immunoprecipitate circular minichromosome with Scc3, but not with Scc3-degron fusion (Figure 2.14D). However, the minichromosome could not be co-immunoprecipitated with either Pds5 or Pds5-degron fusion (Figure 2.14D) in agreement with the previous report, that Pds5 association with cohesin complex is very salt sensitive (Sumara et al., 2000).

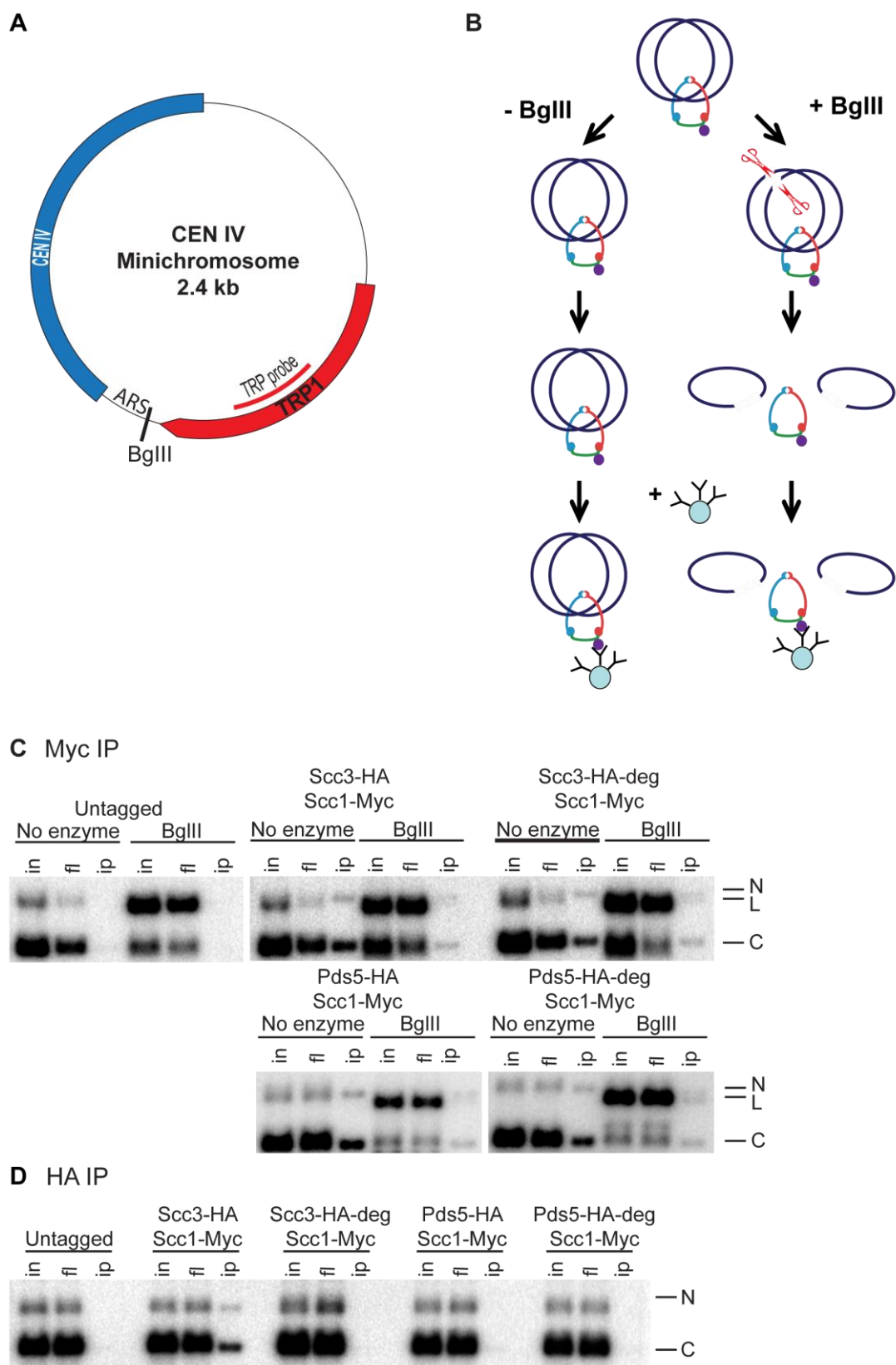


Figure 2.14 Cohesin complexes devoid of Scc3 or Pds5 topologically embrace minichromosomes.

A) Map of minichromosome. Minichromosome contains sequences of the core centromere and pericentromeric region of chromosome IV (marked in blue), selective marker (marked in red) and *ARS1*. **B)** Scheme of an experimental assay of the topological interaction between cohesin and a circular minichromosome (Ivanov and Nasmyth, 2005). Minichromosome recruits cohesin via its centromeric sequence. If the binding between cohesin and a minichromosome is topological, it would be possible to co-immunoprecipitate cohesin with the circular minichromosome. However, minichromosomal cleavage with *BglIII* will lead to plasmid linearization, subsequent cohesin sliding and absence of minichromosomes in cohesin immunoprecipitates. Amount of minichromosomes, which co-precipitate with cohesin, is analyzed by Southern blot. **C)** Strains 1021 (untagged), 1813 (*SCC3-HA6*, *SCC1-Myc18*), 1625 (*SCC3-HA6-degron*, *SCC1-Myc18*), 2525 (*PDS5-HA6*, *SCC1-Myc18*), and 1818 (*PDS5-HA6-degron*, *SCC1-Myc18*) carried the minichromosome and were used for an experiment described in (B). Yeast lysates were incubated with *BglIII* as indicated. Minichromosomes were co-immunoprecipitated with *Scc1-Myc18*. DNA was purified from proteins by phenol/chloroform extraction and separated on a 1% agarose gel with ethidium bromide. Southern blot probed with a *TRP1*-specific probe is shown. Nicked (N), linear (L), and closed circular (C) forms of the minichromosome are indicated. **D)** Minichromosome plasmids were immunoprecipitated with anti-HA antibody from the cell lysates same as in (C). Minichromosomes from *SCC3-HA6*, but not *SCC3-HA6-degron* strain could be co-immunoprecipitated with *Scc3*. Thus, *Scc3* is efficiently depleted from the minichromosomes in the *SCC3-HA6-degron* strain. Since *Pds5* association with cohesin complexes is very salt-sensitive, it is not possible to co-immunoprecipitate minichromosomes with *Pds5-HA6* in either the wild type or *PDS5-HA6-degron* strains under our experimental conditions. Southern blot probed with a *TRP1*-specific probe is shown. Nicked (N), linear (L), and closed circular (C) forms of the minichromosome are indicated (Kulemzina et al., 2012).

Thus, under our immunoprecipitation conditions cohesin complexes on the minichromosomes are devoid of *Pds5*, yet remain stably and topologically associated with the DNA throughout the experiment. This observation further strengthens our conclusion, that *Pds5* is not required for the maintenance of the stable association of cohesin with DNA.

2.7 *Pds5* and *Scc3* depletion affects sister chromatid cohesion

Since budding yeast chromosomes are too small to be observed with light microscopy, to detect sister chromatid cohesion in the cell it is necessary to mark the specific loci on the chromosomes with the fluorescent marker. For this purpose, a repetitive array of bacterial DNA sequences capable of recruiting fluorescent protein fusions, is integrated at a specific site (Michaelis et al., 1997; Straight et al., 1996). This site can be visualized as a fluorescent dot within the nucleus. Lac operators in combination with Lac repressors fused to GFP (Straight et al., 1996) or Tet operators combined with Tet repressors fused to GFP (Michaelis et al., 1997) are commonly used to assay sister chromatid cohesion. Two tightly cohesed sister chromatids in G2/M arrested cells will be observed as a single fluorescent dot and two separate dots will be visible if cohesion is defective (Figure 2.15A).

2.7.1 Pds5 and Scc3 depletion via Eco1-derived degron results in cohesion defect

In order to examine the effect of Pds5, Scc3 or Wpl1 depletion on sister chromatid cohesion, we used the *PDS5*⁻, *SCC3*-degron, *Δwpl1*, and wild type strains with 200 Tet operators integrated in the *URA3* locus, which is located 35 kb from the centromere of chromosome V. In addition, the strains expressed TetR-GFP fusion. Strains were arrested with nocodazole in G2/M and examined for the cohesion defect. More than 20% of the cells of *PDS5*-degron or *SCC3*-degron strains contained prematurely separated sister chromatids compared to 3% in the wild type (Figure 2.15B). In agreement with the previously published data (Sutani et al., 2009) sister chromatid cohesion defect in *Δwpl1* strain was less prominent than in the strains depleted of Pds5 or Scc3 and was only 13%. We conclude that although depletion of Pds5 or Scc3 did not affect cohesin association with DNA, it remarkably weakened sister chromatid cohesion. We can speculate that cohesin rings devoid of Scc3 and Pds5 frequently capture only one of the two sister chromatids and are therefore defective in cohesion establishment.

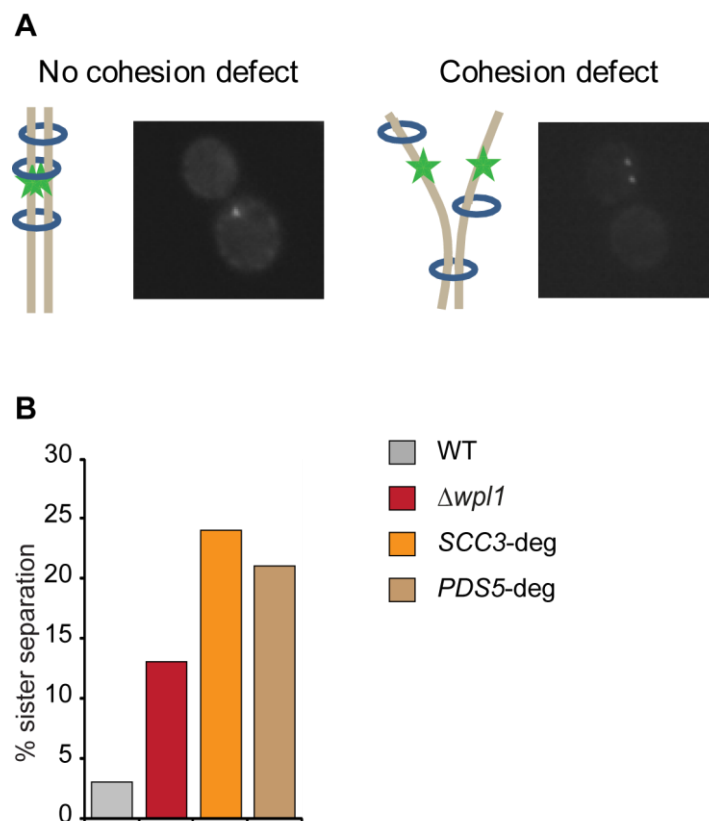


Figure 2.15 Sister chromatid cohesion defect in yeast depleted of Scc3 and Pds5 with the Eco1-derived degron.

A) Scheme of the experimental assay for sister chromatid cohesion in budding yeast. Budding yeast cells, which harbor an array of 200 Tet operators, integrated into *URA3* locus 35 kb from the centromere on chromosome V and express TetR fused to GFP are synchronized with α -factor and released into media with nocodazole. Tet operators bound by TetR-GFP could be detected as a single fluorescent dot in G2/M arrested cells if sister chromatids are cohesed or as two dots if cohesion is lost or defective (Michaelis et al., 1997). **B)** Strains 1417 (wild type), 2190 ($\Delta wpl1$), 1621 (*SCC3*-degron), and 1678 (*PDS5*-degron), harboring 200 Tet operators integrated in *URA3* locus and expressing TetR-GFP were used for the experiment described in (A). Dots separation was scored in 300 cells per strain.

2.7.2 *Pds5* and *Scs3* depletion with DHFR-degron in a single cell cycle experiment results in a modest cohesion defect

Since the depletion of *Pds5* and *Scs3* from the cell does not affect cohesin association with the DNA, but results in a cohesion defect, we hypothesize that *Pds5* and *Scs3* are required for cohesion establishment, rather than for the maintenance of cohesin on the chromosomes. In this case depletion of *Pds5* or *Scs3* in G1 prior to cohesion establishment would lead to sister chromatid cohesion defect later in the cell cycle, while depletion of *Pds5* or *Scs3* in G2 will have no effect on cohesion. Conditional depletion of *Pds5* or *Scs3* using an inducible DHFR-based degron should make it possible to test this prediction.

We integrated an array of Lac operators at the *URA3* locus in the strains with endogenous *PDS5* and/or *SCC3* genes fused with DHFR-based degron. The strains also expressed LacI-GFP from a transgene. Strains were arrested in G1 with α -factor, *Pds5* and/or *Scs3* degradation was induced and strains were released in media with nocodazole. Cells arrested in G2/M were examined for defect in sister chromatid cohesion. Surprisingly, cells depleted of *Pds5* in G1 developed a very modest cohesion defect in G2 if at all (only 5% of cells separated sister chromatids prematurely) (Figure 2.16A). More prominent cohesion defects were observed in cells depleted of *Scs3* or both *Scs3* and *Pds5* (13% and 11% respectively), presumably due to the concomitant degradation of *Scs1* upon induction of *Scs3* degron.

When *Pds5* and/or *Scs3* depletion was induced in G2/M arrested cells after cohesion was already established, very modest effect on sister chromatid cohesion was detected compared to wild type cells treated in the same manner (Figure 2.16A). Cohesion defect observed in cells depleted of *Pds5* and *Scs3* simultaneously either in G1 arrest or in G2/M arrest appears indistinguishable from the one observed in cells depleted of *Scs3* only. Hence, there is no indication that *Scs3* and *Pds5* function redundantly.

We confirmed that Pds5 and Scc3 were efficiently depleted upon degron induction by Western blot analysis (Figure 2.16C). However, it is possible that a small amount of Pds5 fused to DHFR-based degron remains in the cells after degron induction and is sufficient to establish cohesion. When we monitored the cells under the conditions of degron induction over an extended time period (more than 10 hours), we observed a progressive development of the cohesion defect (data not shown). Therefore we conclude that either grossly sub-stoichiometric amounts of Pds5 are sufficient for cohesion establishment or the cell is capable of establishing cohesion without Pds5 for at least one cell cycle.

Our results underscore the importance of using several independent methods of protein depletion and/or inactivation *in vivo*. The use of a single approach, e.g., only the temperature sensitive mutant or the conventional degron, might lead to distorted data due to, e.g. concomitant degradation and/or inactivation of other proteins in the same protein complex. Multi-method approach is instrumental in obtaining more reliable interpretation of the observed phenotypes.

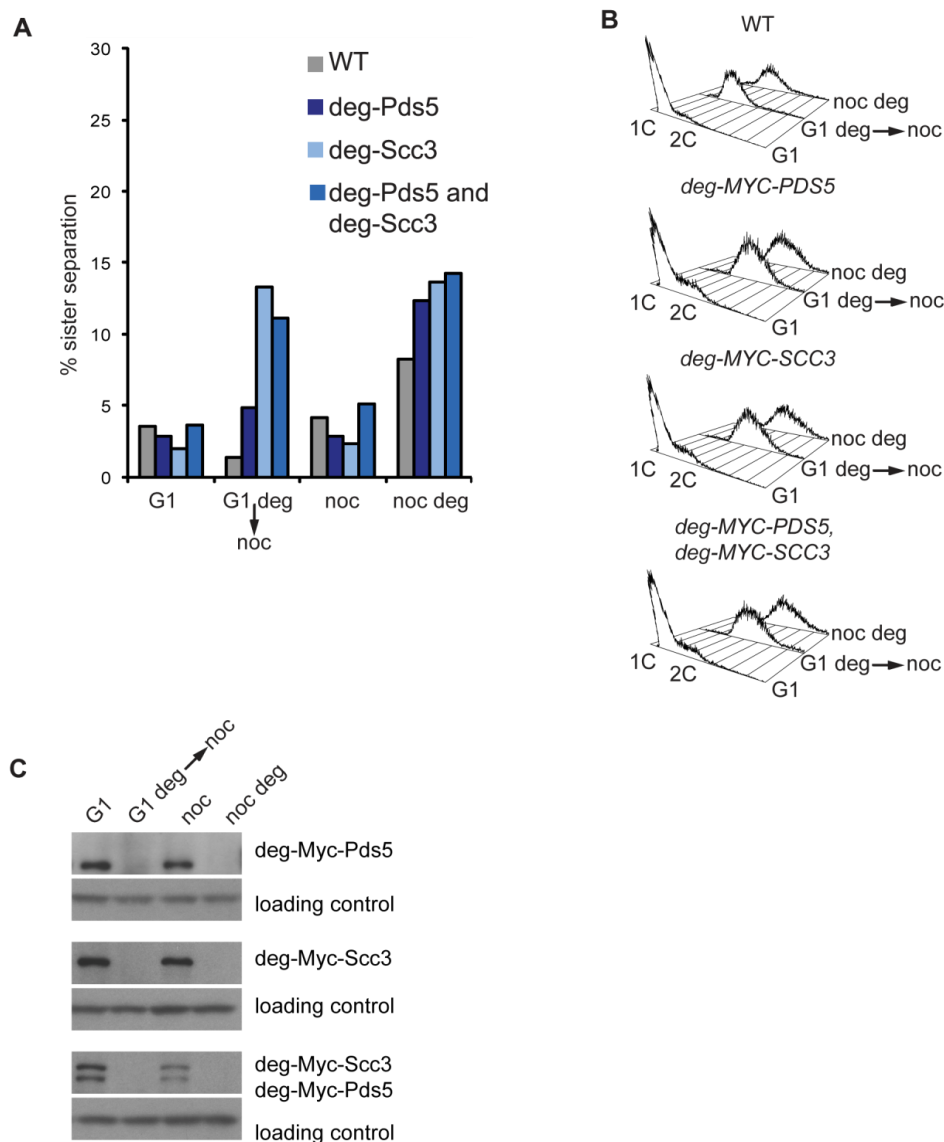


Figure 2.16 Sister chromatid cohesion in yeast depleted of Scc3 and Pds5 with the DHFR-based degron.

A) Strains 2418 (wild type), 2419 (degron-*PDS5*), 2420 (degron-*SCC3*), and 2449 (degron-*PDS5* and degron-*SCC3*) have an array of Lac operators integrated into *URA3* locus 35 kb from the centromere on chromosome V and express LacI-GFP (Straight et al., 1996).

In order to induce the degron in G1, strains were staged with α -factor in YPRaff and Ubr1 expression was induced by shifting cells into the media containing galactose and α -factor for 45 minutes at 30°C. Cells were then incubated for additional 90 minutes at 37°C in YPGal containing α -factor and doxycycline for efficient Pds5 and/or Scc3 degradation. After degradation was complete, cells were released from α -factor arrest into YPGal containing nocodazole and doxycycline at 25°C for 3 hours.

In order to induce degron in G2/M, strains were synchronized with α -factor and released into nocodazole containing YPRaff media for 2 hours, Ubr1 expression was induced by shifting cells into the media containing galactose and nocodazole for 45 minutes at 30°C. Cells were then incubated for additional 90 minutes at 37°C in YPGal containing nocodazole and doxycycline for efficient Pds5 and/or Scc3 degradation. After degradation was complete, cells were chased in YPGal containing nocodazole and doxycycline at 25°C for 3 hours.

Additional incubation at 25°C was found necessary, since the GFP signal was weakened under the conditions of degron induction. Dots separation was scored in 300 cells per strain. **B)** FACS analysis of cellular DNA content of cells used for the experiment in (A). **C)** Western blot demonstrating the depletion of Pds5 and Scc3 in the cells used for the experiment in (A). TCA protein extracts were prepared at indicated time points. Blots were probed with anti-Myc antibody (71D10) and anti-Cdc28 (sc-28550, Santa Cruz) for loading control (Kulemzina et al., 2012).

3 Discussion

In order to be able to assure the bi-orientation and proper segregation of sister chromatids, cohesin rings, which have captured the sister DNA molecules during DNA replication, must retain their integrity throughout G2 until cell division. The duration of the G2 phase of the cell cycle is highly variable depending on the organism, cell type and growth conditions. The multi-subunit nature of the cohesin complex suggests the existence of the maintenance factors, which would keep cohesin ring locked when on DNA. Three proteins, which associate with cohesin, Pds5, Scc3, and Wpl1, might fulfil this function, since their mutational inactivation resulted in a cohesion defect and, in case of Pds5, also reduced the amount of cohesin loaded on chromosomes (Hartman et al., 2000; Panizza et al., 2000; Toth et al., 1999). On another hand, these proteins were reported to possess the cohesion anti-establishment activity, since certain amino acid substitutions in them allowed cohesion establishment in the absence of an establishment factor, Eco1 (Rowland et al., 2009; Sutani et al., 2009). This apparent paradox formed the basis of this study.

The main aim of this Thesis was to address the requirements of Pds5, Scc3, and Wpl1 for cohesin association with DNA and for the establishment and maintenance of sister chromatid cohesion. Rather than studying the pathology of the temperature-sensitive mutants, we employed the degron-mediated depletion of Pds5 and Scc3, which are the essential proteins in budding yeast. We were able to efficiently deplete Pds5, Scc3, and Wpl1 from the cells and analyse the effects of their depletion on sister chromatid cohesion. Remarkably, Pds5, Scc3, and Wpl1 depletion did not result in any obvious changes in cohesin association with DNA, since cohesin quantity, stability and distribution along the chromosomes remained unaffected, but led to the defects in sister chromatid cohesion. Thus, our results call for the revision of the proposed function of Pds5 and Scc3 as maintenance factors and suggest a role for Pds5 and Scc3 in the cohesion establishment, rather than in its maintenance.

3.1 Are Pds5 and Scc3 cohesin maintenance factors?

If Pds5 and Scc3 function as a cohesin lock, they would be expected to possess the following properties: 1) they should be stably associated with cohesin *in vivo*, 2) in their absence cohesin complexes should be released from chromosomes, which should

be possible to detect with the available methods measuring the stability, amounts and distribution of proteins on the DNA.

3.1.1 Pds5 and Scc3 are stably bound to the cohesin ring in vivo

The results of several in vitro experiments in budding yeast argue for the stable association of Scc3 with the cohesin complex. Thus, it was possible to co-immunoprecipitate cohesin and Scc3 from yeast cell lysates, indicating stable association of Scc3 with soluble cohesin (Toth et al., 1999). Furthermore, while Scc3 association with DNA is strictly dependent on Scc1 and therefore on cohesin ring, Scc3 can be readily co-immunoprecipitated with the minichromosomes in the absence of any cross-link demonstrating its stable association with cohesin complexes bound to DNA ((Ivanov and Nasmyth, 2005) and Figure 2.14D). In an in vivo study measuring the stability of cohesin association with the chromosomes throughout the cell cycle in human cells, Scc3 interaction with the chromosomes was indistinguishable from Scc1. Both proteins were dynamically bound to chromosomes until S phase, when a more stably bound fraction was detected and persisted until mitosis (Gerlich et al., 2006). It is hypothesized that the stable fraction represents cohesin rings holding the sister chromatids together. According to our results, Scc3 distribution in metaphase cells closely resembles the pattern observed for Scc1 and Smc3, which form a stable barrel-like structure and no recovery of fluorescent signal could be detected in FRAP experiments (Figure 2.9). Therefore at least in metaphase there is no exchange of Scc3 between the chromatin-bound rings.

On the contrary, Pds5 association with cohesin rings was reported to be less stable. It is possible to co-immunoprecipitate cohesin complex with Pds5, but only a small fraction of Pds5 co-sedimented with cohesin in sucrose gradient centrifugation experiments (Sumara et al., 2000). We were unable to co-immunoprecipitate circular minichromosomes with Pds5 ((Ivanov and Nasmyth, 2005) and Figure 2.14D). However, our in vivo data demonstrated that Pds5 is stably bound to the cohesin ring under physiological conditions, since no recovery of the fluorescent signal was registered in the FRAP experiment with metaphase cells (Figure 2.9). Observed differences in the stability of Pds5 association with cohesin in vitro and in vivo could be explained by the extreme salt-sensitivity of this interaction, which is arguably an in vitro phenomenon (Sumara et al., 2000).

It was demonstrated that Scc3 binds close to the C-terminus of Scc1 (Haering et al., 2002; Hu et al., 2011). According to the recent results from our laboratory (Kulemzina et al., 2012), Pds5 interacts with the N-terminal part of Scc1. Thus, Scc3 and Pds5 bind in the proximity of the two protein-protein interfaces within the cohesin ring, Smc1/Scc1 and Smc3/Scc1, respectively, and it is possible that they reinforce the interactions between Scc1 and the Smc heads and thereby help to maintain the integrity of cohesin ring. However, a covalent fusion of Smc3 C-terminus to Scc1 N-terminus, which was able to rescue *scc1* mutants with the weakened Smc3-Scc1 interaction (Gruber et al., 2006), did not suppress the lethality of *pds5* deletion (data not shown). Therefore, the maintenance of Smc3/Scc1 interaction cannot be the essential function of Pds5.

3.1.2 Does the depletion of Pds5 and Scc3 release cohesin from DNA?

Previous experiments demonstrated that temperature-sensitive *pds5* mutants prematurely separate sister chromatids upon temperature shift in G2 phase of the cell cycle. This cohesion defect is accompanied by the remarkable decrease in the amount of cohesin rings bound to DNA, suggesting the role of Pds5 in cohesion maintenance (Panizza et al., 2000). However, in *Xenopus* Pds5 is not required for the stable association of cohesin with the chromosomes, since no reduction in the amount of cohesin bound to DNA was observed in egg extracts depleted of Pds5 (Losada et al., 2005). The question of whether the observed differences reflect differences in Pds5 function in various organisms or are the consequence of different methods that were employed (depletion versus mutational inactivation), remains unresolved. The mechanism of Scc3 function was studied less extensively and the consequences of its inactivation in G2 were never reported to our knowledge. Depletion of Scc3 employing dsRNAi in *Drosophila* cells resulted in a dramatic decrease in Scc3 protein levels, but no obvious defects in sister chromatid cohesion were detected (Vass et al., 2003).

We decided to re-investigate how depletion of Pds5 and Scc3 affects the stability of cohesin association with DNA in budding yeast. We employed an Eco1-derived degron sequence to specifically destabilize Pds5 and Scc3 and carefully analysed the effects caused by their depletion in the cell. We confirmed that in our experiments the majority of cohesin complexes in *SCC3*- and *PDS5*-degron strains are no longer associated with Scc3 or Pds5 (Figure 2.4). Surprisingly, we observed that the reduced

cellular levels of Pds5 and Scc3 result in little or no decrease in the amount of Scc1 bound to chromosomes, when examined by chromosomal spreads and in chromatin pellets (Figure 2.6). Furthermore, cohesin complexes devoid of Scc3 and Pds5 remained stably bound to the chromosomes (Figure 2.8) and localized at usual cohesin sites (Figure 2.10 and 2.11). However, Eco1-derived degron decreased the amount of the proteins throughout the cell cycle, making it difficult to assess the requirement of the protein function at the specific stages of the cell cycle. Therefore, we used a DHFR-based degron to induce Pds5 and Scc3 depletion in synchronized cultures in G1 versus G2 phases of the cell cycle. Pds5 depletion in G2 arrested cells had no remarkable effect on cohesin association with the chromosomes or on sister chromatid cohesion (Figure 2.16). Even though Scc3 degradation was accompanied by the concomitant destruction of Scc1, an unfortunate “side effect”, very modest sister chromatid cohesion defect was detected upon protein depletion in G2 in agreement with the recent report, according to which an 8-fold decrease in the Scc1 abundance does not cause premature sister chromatid separation (Heidinger-Pauli et al., 2010). Our results are inconsistent with the previously proposed function of Pds5 and Scc3 in the maintenance of cohesin rings on the DNA.

It is unlikely that Pds5 and Scc3 function redundantly, i.e., either one is sufficient to lock the cohesin rings on DNA. Although it was not possible to combine the *SCC3*-degron and *PDS5*-degron when Eco1-derived degrons were used, we were able to construct the “double degron” strain using DHFR-based degrons. Depletion of Pds5 alone with the DHFR-based degron had no effect on cohesin association with DNA, while depletion of Scc3 resulted in a decreased amount of cohesin bound to DNA, supposedly due to the concomitant degradation of Scc1. Simultaneous depletion of both, Pds5 and Scc3, resulted in a phenotype very similar to the depletion of Scc3 alone. Therefore no synergistic effect of the double depletion was observed arguing against the redundant mode of function.

Based on our results we conclude that Pds5 and Scc3 do not lock cohesin rings on DNA. However, it is still possible that Pds5 and Scc3 are important for the maintenance of cohesion, i.e. preventing one of the two sister DNAs from escaping from the ring. In principle, this function could be fulfilled by a much smaller number of molecules than normally present in the cell, especially if only very few cohesin complexes per chromosome are sufficient to ensure cohesion. Recently it was shown that the reduction of Scc1 levels to 13% of the normal amount of protein in the cell, resulted in a decrease

in *Scc1* bound to the chromosomes as detected by the chromosomal spreads, as well as ChIP experiments at the different chromosomal sites (Heidinger-Pauli et al., 2010), but did not lead to a detectable cohesion defect or chromosomal mis-segregation. Therefore, it appears that sister chromatid cohesion could be mediated even by a small number of cohesin complexes. Hence, it is possible that in our degron strains the bulk of cohesin complexes are devoid of Pds5 and Scc3 and stably bound to the chromosomes without embracing both sister chromatids. At the same time very few cohesin rings per chromosome remain associated with Pds5 and Scc3, which were left undegraded and these rings hold sister chromatids together. If this is indeed the case, in the *SCC3*- and *PDS5*-degron strains with Eco1-derived degron less than 15 cohesin complexes per chromosome are associated with Scc3 and Pds5 and, according to this model, are capable of providing cohesion. Another scenario that we cannot exclude is that Pds5 and Scc3 possess a catalytic function in cohesion maintenance. However, the absence of a detectable turn-over of Scc3 and Pds5 associated with DNA-bound cohesins makes it difficult to envision the catalytic role of these proteins. Alternatively, Scc3 and Pds5 are required only transiently, which points towards their involvement in cohesion establishment rather than maintenance.

3.2 What is the function of Pds5 and Scc3 in sister chromatid cohesion?

3.2.1 Are Pds5 and Scc3 cohesion establishment factors?

Based on our results we conclude, that Pds5 and Scc3 are unlikely to function in cohesion maintenance, instead we speculate that they are involved in cohesion establishment. In agreement with this hypothesis, continuous depletion of Scc3 or Pds5 with Eco1-derived degron leads to a cohesion defect (Figure 2.15), which might stem from a partial failure to capture both sister-chromatids inside the ring (Figure 3.1).

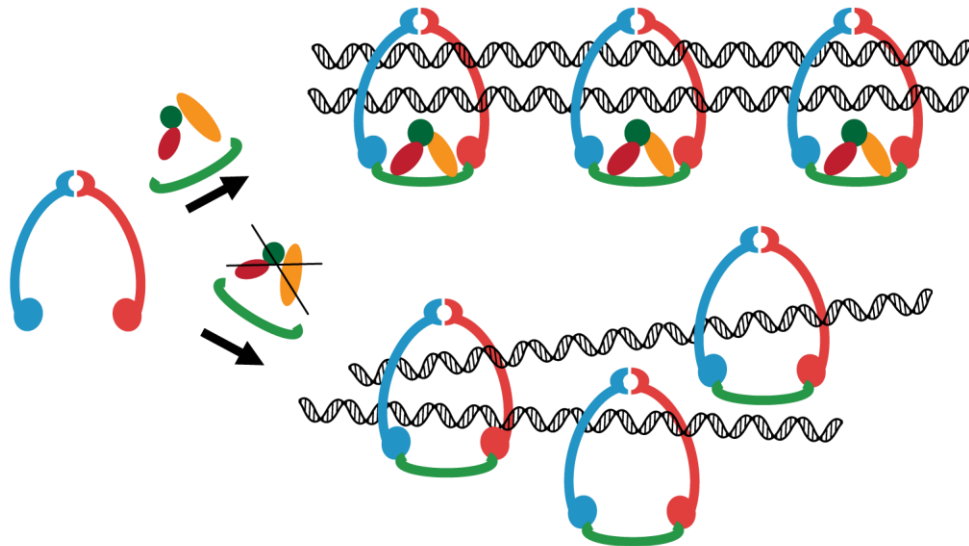


Figure 3.1 Cohesin rings depleted of Pds5, Scc3 or Wpl1 are defective in embracing both sister chromatids.

During the unperturbed cell cycle of budding yeast, Scc1 subunit is synthesized in the late G1 or early S phase, binds to Smc1/Smc3 heterodimer and completes the cohesin ring. Scc3 and Pds5 are recruited via Scc1 and stably associate with the cohesin complex. Two sister chromatids, generated during DNA replication, are captured inside a single cohesin ring in a process, which remains poorly understood. It is possible that both, Pds5 and Scc3, are required to assure sister chromatids entrapment inside the cohesin ring. Thus, in the absence of these factors, cohesin complexes are loaded and stably associate with the DNA, but fail to embrace both of the sister chromatids resulting in defective cohesion (Kulemzina et al., 2012).

How could Pds5 and Scc3 facilitate the entrapment of both sister chromatids inside the cohesin ring? At the moment very little is known about the processes that take place during the passage of the replication fork and ensure the capture of the two emerging sister chromatids inside cohesin rings. The major question is whether the replication fork passes through the cohesin ring, or whether the ring opens transiently, allows the replication fork passage and then closes again, or whether cohesin is loaded in the wake of the replication fork. We can hypothesize, that Pds5 and Scc3 might ensure the stability of cohesin rings during the passage of the replisome, thereby allowing cohesin to capture sister chromatids immediately after their synthesis (Figure 3.2A). Another possibility is that each of the sister chromatids could be first transiently anchored by Scc3 and Pds5, bound to the cohesin, and are subsequently guided inside the ring during the cohesion establishment (Figure 3.2B). Alternatively, each of the sister chromatids might be initially embraced by separate cohesin rings, which then dimerize via Scc3-Scc3 interaction as proposed by (Zhang et al., 2008b) (Figure 3.2C). The

“dimeric rings” intermediates are then converted into two individual rings, each embracing both sister chromatids inside.

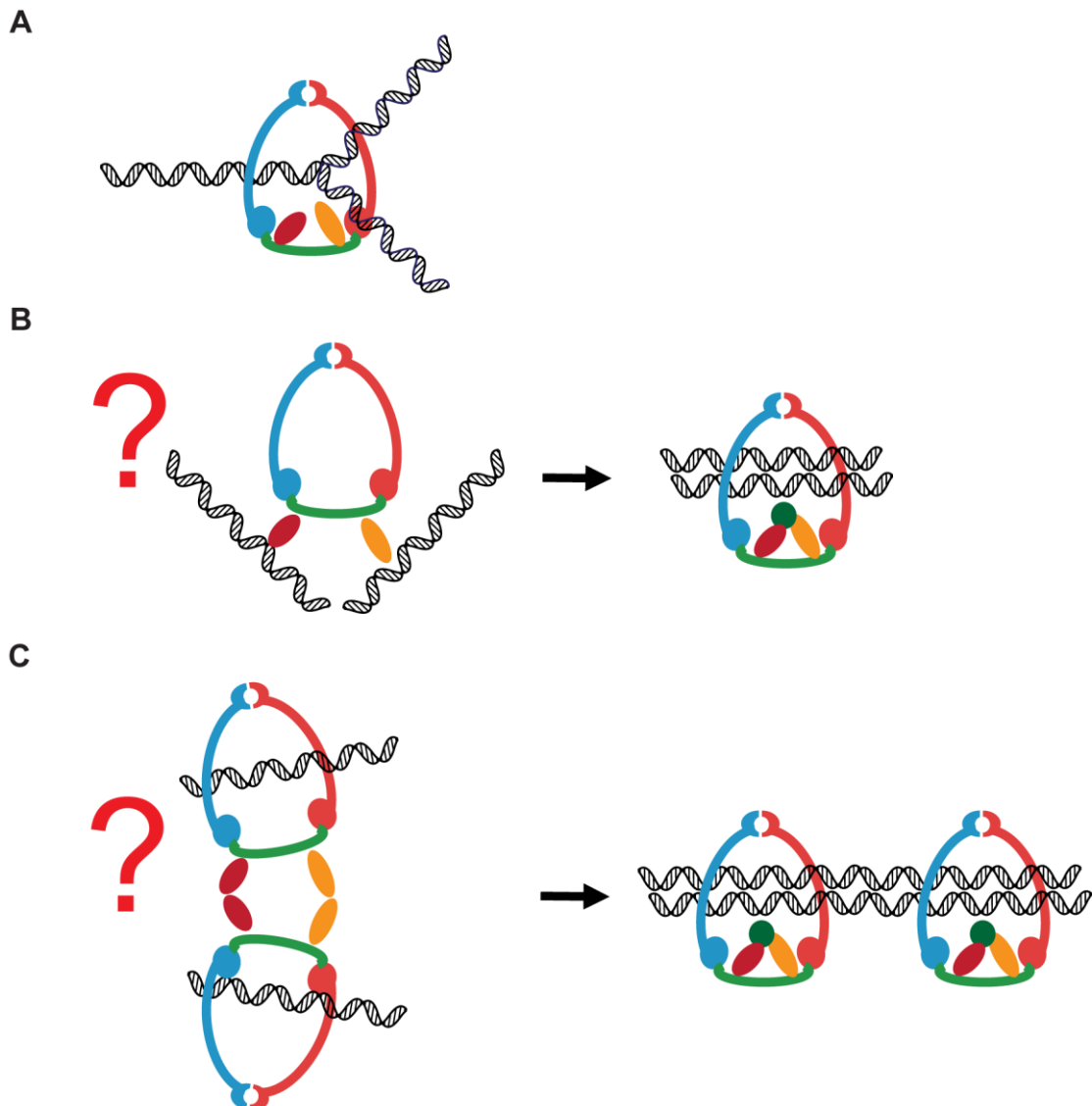


Figure 3.2 Scc3 and Pds5 function to ensure that two sister chromatids are captured inside a single cohesin ring during the cohesion establishment.

A) Pds5 and Scc3 could stabilize cohesin rings specifically during the replication fork passage.
B) Pds5 and Scc3 could transiently bind sister chromatids during the cohesion establishment.
C) Alternatively, they could mediate a transient interaction between two cohesin rings as proposed by (Zhang et al., 2008b) (Kulemzina et al., 2012).

The phenotype observed in the cells depleted of Pds5 or Scc3, namely premature sister separation without obvious defects in cohesin association with DNA, resembles the phenotype observed in *ecol* mutant strains. Eco1 is associated with PCNA and acts

during DNA replication to acetylate two adjacent lysine residues in the Smc3 head domain. In our laboratory it was shown that the level of Smc3 head acetylation was reduced in strains, depleted of Pds5, Scc3 or Wpl1 (Kulemzina et al., 2012). Thus, it is possible that Smc3 head acetylation during cohesion establishment happens preferentially in cohesins associated with Pds5, Scc3, and Wpl1, if, for example, these factors contribute to Eco1 recruitment to the cohesin in vivo (Figure 3.3).

However, the observed reduction in Smc3 acetylation in cells, depleted of Pds5 and Scc3 is unlikely to be the only reason for the observed cohesion defects in *SCC3*-degron and *PDS5*-degron strains, since cells, depleted of Wpl1, are characterized by a similar reduction in acetylation and have only a very modest defect in sister chromatid cohesion.

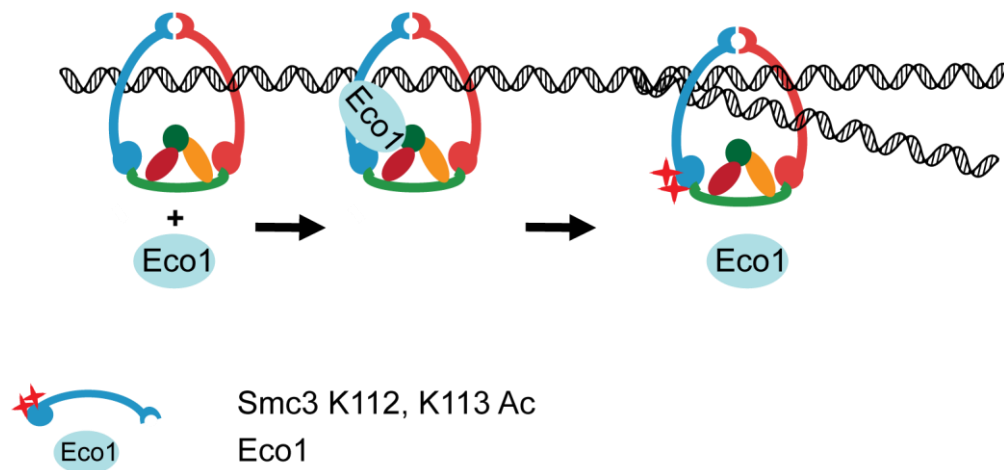


Figure 3.3 Pds5, Scc3, and Wpl1 might facilitate Eco1 recruitment to the cohesin complex.

According to this hypothesis, Pds5, Scc3 and/or Wpl1 recruit Eco1 to the cohesin complex and promote Smc3 head acetylation during cohesion establishment.

Recently it was reported that in fission yeast depletion of Pds5 results in a more pronounced defect in the acetylation of Smc3 head than in budding yeast and the deletion of the non-essential *PDS5* gene in fission yeast completely abolished Smc3 acetylation by Eco1 (Vaur et al., 2012). The authors speculated that, since Pds5 was shown in a two-hybrid assay to interact with the C-terminal domain of Eco1, a fission yeast Eco1 homologue (Tanaka et al., 2001), in the absence of Pds5, Eco1 is not recruited to the cohesin complex and is unable to acetylate cohesin. These results

further support our hypothesis about the role of Pds5 in cohesion establishment. It is important to note, that in the *PDS5*-degron strain Smc3 acetylation is decreased, but not abolished, which might be due to the incomplete degradation of Pds5. The attempts in our laboratory to demonstrate in vitro interaction of recombinant budding yeast Scc3, Pds5 or Wpl1 with Eco1 were unsuccessful; however, it is possible that Pds5 interaction with Eco1 is dependent on post-translational modifications or happens only in the context of cohesin complex and, therefore could not be reconstituted in an in vitro assay.

If Scc3 and Pds5 are functioning during cohesion establishment, it is possible that they might influence the dynamics of the replication fork. However, in our laboratory we could not detect any alterations in the duration of the S phase when wild type, *SCC3*-degron, and *PDS5*-degron strains were released from the G1 arrest and the cellular DNA content was measured by FACS every 15 minutes (data not shown). Since FACS measurements provide only very rough estimates of the rate of the DNA synthesis, a single molecule analysis of the replication fork progression (Terret et al. 2009) might be required to study the S phase kinetics in strains depleted of Pds5 and Scc3.

3.2.2 Are Pds5 and Scc3 cohesin recruitment factors?

It was shown that Scc3 homologues are involved in the cohesin recruitment to the heterochromatic loci in fission yeast (Nonaka et al., 2002), as well as to CTCF binding sites in mammalian cells (Rubio et al., 2008). Budding yeast lacks the pericentromeric heterochromatin and the identified CTCF homologues. We wanted to test whether Scc3 and/or other cohesin associated factors are required for the cohesin localization to specific loci in this organism as well. In order to address this possibility, we analysed the distribution of cohesin along the chromosomes in the strains depleted of Pds5, Scc3 or Wpl1 employing a ChIP-Seq approach. Pds5, Scc3, and Wpl1 depletion affected the chromosomal addresses of the cohesin complex only modestly if at all (Figure 2.10). Upon more detailed examination of ChIP Seq data our attention was drawn to the fact, that cohesin bound to the core centromeres of all 16 chromosomes in the strain depleted of Scc3 was reduced when compared to the wild type, suggesting the role of Scc3 in the retention of cohesin at the core centromere (Figure 2.11). However, in an independent ChIP experiment the difference between *SCC3*-degron and wild type strains was not

reproduced (Figure 2.12). We reasoned that the observed variation could be caused by ChIP-Seq resolution differences stemming from the different extent of DNA shearing prior to immunoprecipitation. In our experiment we employed a protocol, which minimizes potential differences in the DNA fragments size, namely immunoprecipitated DNA fragments were gel fractionated (150-500 bp) and the adaptor-ligated PCR-amplified libraries were analyzed on High Sensitivity DNA Chips with Bioanalyzer 2100. However, the importance of multiple replicates of ChIP cannot be underestimated. It is worth noting that even in the wild type strain cohesin is low at the core centromere compared to the pericentromeric sequences as was observed earlier (Warren et al., 2004). We conclude that in budding yeast cohesin associated factors, namely Pds5, Scc3, and Wpl1 are not involved in recruitment of the cohesin at specific loci.

3.3 What is the function of Wpl1 in budding yeast?

In budding yeast the function of Wpl1 remains a mystery. In vertebrate cells the Wpl1 homologue, Wapl, is required for cohesin removal from chromosomal arms during prophase and prometaphase (Gandhi et al., 2006; Kueng et al., 2006; Shintomi and Hirano, 2009) (see Introduction). The prophase pathway of cohesin removal from the chromosomes is absent in budding yeast. It was recently proposed that Wapl might have evolved its “unloading” function together with the acquisition of an N-terminal extension, which is absent in yeast and is implicated in the binding of Wpl1 to cohesin in vertebrates (Shintomi and Hirano, 2009). In fission yeast Wpl1 destabilizes cohesin binding to chromosomes in G1 (Bernard et al., 2008). However, this function of Wpl1 cannot be relevant in budding yeast, since in this organism Scc1 is synthesized only at the beginning of the S phase and there is no cohesin on G1 chromosomes. While one previous report concluded that *wpl1* deletion leads to an increased association of cohesin with DNA (Rolef Ben-Shahar et al., 2008), two other studies reported a modest reduction in the amount of cohesin bound to DNA in the absence of Wpl1 (Rowland et al., 2009; Sutani et al., 2009). In analogous experiments in our laboratory, no remarkable changes in the amount of cohesin bound to the chromatin were detected in $\Delta wpl1$ strain using chromatin pellets (Figure 2.6). The absolute amount of the chromosomal cohesin was found modestly reduced in $\Delta wpl1$ strain at several tested

sites using ChIP-qPCR (Figure 2.7). It is likely that, even in budding yeast, Wpl1 acts as a negative regulator of cohesin binding. We speculate that Wpl1 might act as a “quality” control mechanism selectively removing non-acetylated cohesions, that are not engaged in holding sisters and thus enriching for cohesin rings that do embrace both sister chromatids. Interestingly, it was found in our laboratory that, similar to *WPL1* deletion, a covalent fusion between Smc3 and Scc1 rescues the non-acetylatable Smc3 mutant and renders Eco1 acetyltransferase dispensable for viability. Therefore, it is highly likely that Wpl1 “opens” the non-acetylated cohesin rings at the Smc3/Scc1 interface, thus releasing them from the DNA.

3.4 Methods employed to address Scc3 and Pds5 function in budding yeast: advantages and limitations

Early studies, which addressed the role of Scc3 and Pds5 in budding yeast, relied on the use of temperature-sensitive alleles, causing protein inactivation upon increase in the ambient temperature (Hartman et al., 2000; Panizza et al., 2000; Stead et al., 2003; Toth et al., 1999). The ability to inactivate proteins at a specific cell cycle stage is an obvious advantage of this approach, however, alleles used in these experiments were multiple amino acid substitutions and the mechanism of their inactivation at the restrictive temperature is not characterized. Mutant proteins might unfold and block other proteins from interacting with the complex or alternatively, they might recruit protein degradation machinery and affect the stability of the other protein components of cohesin ring. Although temperature-sensitive alleles were instrumental in identifying the essential players in sister chromatid cohesion, they should be used with caution in studying molecular details, since the phenotypes observed at the restrictive temperature could be difficult to interpret.

Another approach to study the function of essential proteins is based on the use of a short degron sequence, which, when fused to the protein of interest, will target it for degradation. During the last ten years several degron systems were characterized and established, for example, auxin-based degron system can be used for protein depletion in nonplant cells (Nishimura et al., 2009). In this case, the protein-degron fusion is recognised by a specific E3 ubiquitin ligase in the presence of a small molecule, auxin, followed by the recruitment of E2 ligase and the subsequent degron polyubiquitylation

and degradation of the protein by the proteasome. TEV protease-mediated induction of protein instability (TIPI) is an alternative approach, which employs dormant N-degron fused to the protein of interest that could be conditionally de-protected by TEV protease cleavage (Taxis et al. 2009), resulting in the rapid proteasomal degradation through the N-end rule pathway (for review see (Varshavsky, 2011)). However, in budding yeast the most popular system to-date is the heat-inducible DHFR-based degron, which induces the fusion protein degradation through the N-rule pathway (see Results, Figure 2.1) (Dohmen et al., 1994; Kanemaki et al., 2003; Labib et al., 2000; Sanchez-Diaz et al., 2004). In this study we employed for the first time an Eco1-derived degron, which was independently discovered in our laboratory and the laboratory of David Morgan (Lyons and Morgan, 2011) for the depletion of heterologous proteins. Although all degron systems allow conditional elimination of the protein of interest, they do not provide 100% depletion, leaving the cell with minute amounts of undegraded protein.

In our study we employed two different degron systems, the DHFR-based degron and the Eco1-derived degron, to deplete Pds5 and Scc3. It was important to rule out the possibility of an incomplete degradation of Scc3 and Pds5 polypeptide chains and the generation of stable functional fragments during protein destruction. By tagging the proteins at both N- and C-termini at the same time, we confirmed that Pds5 and Scc3 are completely degraded when targeted for destruction by either of the two degron sequences (Figure 2.2 and 2.4). The degradation of Pds5 and Scc3 DHFR-based degron fusions was induced in G1 arrest or G2/M arrest, in order to examine their roles in the cohesion establishment or maintenance, respectively. However, Scc3-degron destruction induced a concomitant degradation of another cohesin subunit, Scc1, to which it is tightly bound. This precluded further use of DHFR-degron for Scc3 depletion. Remarkably, Pds5 degradation employing the same DHFR-based degron did not lead to Scc1 degradation and had no effect on cohesin binding to DNA or cohesion when depleted in G2, ruling out a ‘maintenance function’ of Pds5 (Figure 2.16). However, depletion of Pds5 prior to cohesion establishment, in G1 arrest also had only modest effect on cohesin binding to DNA and sister chromatid cohesion (Figure 2.16). Thus, Pds5 quantity in the cell can be reduced dramatically at least within a single cell cycle without compromising cohesin function, whether it is the stability of cohesin association with DNA or its ability to hold sister chromatids together. If Pds5 is indeed involved in cohesion maintenance, this function can be accomplished by a very small number of molecules. Applying the Eco1-derived degron, we were able to efficiently

deplete Pds5 and Scc3 without causing Scc1 co-degradation. However, the Eco1-derived degron constitutively reduces Pds5 and Scc3 levels throughout the entire cell cycle making it difficult to ablate the proteins specifically in G2 to address their roles in cohesion maintenance independently of an S phase. Our study illustrates the importance of a multi-method approach to protein inactivation *in vivo* as each of the available methods suffers from certain drawbacks.

Our most important finding is the demonstration that cohesin complexes devoid of Scc3 or Pds5 remain stably associated with chromosomes that contradicts the existing hypothesis, according to which Pds5 and Scc3 are cohesin maintenance factors. Importantly, in our experiments cells depleted of Pds5 and Scc3 display a prominent cohesion defect, suggesting their role in cohesion establishment.

4 Materials and Methods

4.1 Molecular biology techniques

4.1.1 Polymerase chain reaction (PCR)

PCR reactions were performed according to the manufacturer's protocols employing Fermentas enzymes and buffers in a BioRad DNA Engine PTC-200.

4.1.2 Transformation of competent *E.coli* cells

Plasmid DNA (1-2 ng) was added to the 100 µl aliquot of chemically competent *E.coli* XL1-Blue cells and cells were incubated on ice for 30 minutes. Subsequently, cells were heat-shocked for 45 sec at 42°C, cooled on ice for 2-5 minutes and added to 1 ml of LB media (1 % W/v Bacto-Tryptone, 0.5 % w/v yeast extract, 0.5 % w/v NaCl). After growing for 1 hour at 37°C, transformed cells were plated on LB agar plates (LB plus 1.5 % w/v agar) supplemented with the appropriate antibiotic (100 µg/ml ampicillin or 50 µg/ml kanamycin) and plates were incubated overnight at 37°C. To miniprep plasmid DNA, colonies obtained on selective media were inoculated into 3 ml LB containing appropriate antibiotic and incubated overnight at 37°C with shaking. Cells were harvested by centrifugation in Eppendorf centrifuge 5810 R 4°C.

The transformation of MAX Efficiency Stbl2 competent cells (Invitrogen) with plasmid 1494 (Rohner et al., 2008) was performed according to the manufacturer's protocol.

4.1.3 Isolation of plasmid DNA from *E.coli*

Plasmid DNA was purified from bacterial pellets using QIAprep Spin Miniprep Kit (Qiagen) according to the manufacturer's protocol. The concentration of DNA, eluted from the spin column with water, was measured with the spectrophotometer NanoDrop ND1000 (PeqLab). Plasmids used in this study are listed in **Table 4.1**.

Table 4.1 List of plasmids

| Name | Origin | Description |
|------|--------------------------------------|--|
| 1098 | Ivanov laboratory (Jochen Reiter) | Vector for C-terminal tagging with Eco1-derived degen |

| | | |
|---------------|---|---|
| 1174 | Nasmyth laboratory (Ivanov and Nasmyth, 2007) | Sal I/Sal I <i>TRPIARS1</i> circle with <i>CEN4</i> (850nt); BglII site in the ARS1. |
| 1320 (pYM25) | Euroscarf (Janke et al., 2004) | yeGFP tagging vector |
| 1343 (pYM27) | Euroscarf (Janke et al., 2004) | EGFP tagging vector |
| 1399 (pKL187) | Euroscarf (Kanemaki et al., 2003; Sanchez-Diaz et al., 2004) | DHFR-degron tagging vector with 1 Myc tag and <i>CUP1</i> promoter |
| 1434 (pCM324) | Euroscarf (Yen et al., 2003) | Promoter substitution cassette for one step PCR integration of tetracycline repressible expression under the control of tetO2 |
| 1493 | This study | YIplac211-lacO repeats |
| 1494 (pRS7) | Gasser laboratory (Rohner et al., 2008) | lacO repeats |
| 1497 | This study | DHFR-degron tagging vector with 1 Myc tag and tetO2 promoter |
| 1498 | This study | DHFR-degron tagging vector with 18 Myc tag and tetO2 promoter |
| pOM20 | Spang laboratory (Gauss et al., 2005) | Vector for N-terminal tagging with 9Myc |
| pSH47 | Hegemann laboratory (Guldener et al., 1996) | Vector, encoding Cre recombinase under the control of <i>GAL</i> promoter |
| YIplac211 | Sugino laboratory (Gietz and Sugino, 1988) | Integrative vector |

| | | |
|---------|-----------|---------------------------------|
| pJet1.2 | Fermentas | Cloning vector for PCR products |
|---------|-----------|---------------------------------|

4.1.4 Restriction digest of plasmid DNA

Restriction digest of purified plasmid DNA was performed with commercial restriction enzymes from Fermentas and New England Biolabs according to the manufacturer's protocol.

4.1.5 Analysis of DNA by agarose gel electrophoresis

DNA samples were supplemented with 6 x DNA loading buffer (10 mM Tris-HCl pH 7.6, 0.03 % bromophenol blue, 0.035 xylene cyanol FF, 60 % glycerol, 60 mM EDTA) (Fermentas) and loaded on an agarose gel. Gene Ruler™ 1 kb ladder (Fermentas) was used as a marker. DNA was separated by the size on the agarose gels, containing 0.8 – 2 % w/v agarose (UltraPure Agarose, Invitrogen), 1 x TAE buffer (40mM Tris base, 1 mM EDTA, 20 mM acetic acid, pH 8.5) and 0.5 µg/ml ethidium bromide. Agarose gels were run for at least 30 minutes at 100 or 120 V in electrophoresis chambers (HE33 or HE99X, Amersham). The DNA fragments were visualized with Multi Light Cabinet (AlphaInnotec) using AlphaEaseFC software (AlphaImager).

4.1.6 Extraction of DNA fragments from agarose gels

Excised DNA fragments were extracted from the agarose gel slab employing QIAquick Gel Extraction Kit (Qiagen) according to the manufacturer's protocol. The concentration of DNA eluted from the spin column with water was measured with the spectrophotometer NanoDrop ND1000 (PeqLab).

4.1.7 DNA Ligation

DNA fragments (vector and insert) were ligated using the Rapid Ligation Kit (Fermentas) according to the manufacturer's protocol. In order to avoid vector re-ligation and increase efficiency of vector-insert ligation, the vector was dephosphorylated with shrimp alkaline phosphatase (SAP, Fermentas) according to the manufacturer's protocol.

4.1.8 DNA sequencing

DNA sequencing was performed using the ABI 3730xl DNA analyzer by the sequencing facility of the Max Planck Campus, Tübingen.

4.2 Yeast techniques

4.2.1 Budding yeast cultivation and storage of yeast strains

Yeast cells were grown in liquid media (see 4.2.2.1) at 25°C, 30°C or 37 °C with shaking (200 rpm) or on solid media plates (see 4.2.2.2) at 25°C, 30°C or 37 °C. Yeast strains were stored in 1 ml of 15 % glycerol at -80°C. Strains were freshly plated from frozen stocks on the appropriate plates and grown at 25°C or 30°C.

4.2.2 Budding yeast media

4.2.2.1 Liquid media

| | |
|---------------------------|---|
| YPD: | 1.1 % w/v yeast extract, 2.2 % w/v bacto-peptone, 0.0055 % w/v adenine-HCL, 2 % w/v glucose |
| YPDCu: | YPD, 0.1 mM CuSO ₄ |
| YPGal: | 1.1 % w/v yeast extract, 2.2 % w/v bacto-peptone, 0.0055 % w/v adenine-HCL, 2 % w/v galactose |
| YPGalCu: | YPGal, 0.1 mM CuSO ₄ |
| YPGal doxycycline: | YPGal, 20 µg/m doxycycline |
| YPRaff: | 1.1 % w/v yeast extract, 2.2 % w/v bacto-peptone, 0.0055 % w/v adenine-HCL., 2 % w/v raffinose |
| YPRaffCu | YPRaff, 0.1 mM CuSO ₄ |
| -trp: | 0.8 % w/v difco yeast nitrogen base w/o amino acids, 0.0055 % w/v tyrosine, 0.0055 % w/v adenine, 0.0055 % w/v uracil, 1.1 % w/v CAA vitamin assay (bacto casamino acids), 0.01 % leucine, 2 % glucose |

4.2.2.2 Solid media

| | |
|---------------------------------|--|
| YPD-NAT: | YPD supplemented with 0.1 mg/l clonNAT (nourseothricin) |
| YPD-KAN: | YPD supplemented with 0.2 mg/l G148 (kanamycin) |
| YPD-KAN Cu | YPD-KAN, 0.1 mM CuSO ₄ |
| YPD-HPH: | YPD supplemented with 0.3 mg/l hygromycin |
| SPO (sporulation media): | 0.25 % w/v yeast extract, 1.5 % w/v potassium acetate, 0.1 % glucose, 2.2 % w/v agar |
| MIN (minimal media) | 0.8 % difco yeast nitrogen base w/o amino acids, 2.2 % w/v agar |
| -ura: | 0.8 % w/v difco yeast nitrogen base w/o amino acids, 0.0055 % w/v tyrosine, 0.0055 % w/v adenine, 1.1 % w/v CAA vitamin assay (bacto casamino acids), 0.005 % leucine, 0.005 % tryptophan, 2 % glucose, 2.2 % w/v agar |

-leu: 0.8 % w/v difco yeast nitrogen base w/o amino acids, 0.0055 % w/v tyrosine, 0.0055 % w/v adenine, 0.0055 % w/v uracil, 1 % v/v -leu drop out solution (100x), 2% glucose, 2.2 % w/v agar

-his: 0.8 % w/v difco yeast nitrogen base w/o amino acids, 0.0055 % w/v tyrosine, 0.0055 % w/v adenine, 0.0055 % w/v uracil, 1 % v/v -his drop out solution (100x), 2% glucose, 2.2 % w/v agar

4.2.2.3 Drop out solutions

-leu drop out solution (100x): 0.1 % w/v histidine, 0.6 % w/v iso-leucine, 0.4 % w/v lysine, 0.1 % w/v methionine, 0.6 % w/v phenylalanine, 0.5 % w/v threonine, 0.4 % w/v tryptophan, 0.2 % w/v arginine

-his drop out solution (100x): 0.2 % w/v arginine, 0.6 % w/v iso-leucine, 0.6 % w/v leucine, 0.4 % w/v lysine, 0.1 % w/v methionine, 0.6 % w/v phenylalanine, 0.5 % w/v threonine, 0.4 % w/v tryptophan

To prepare solid YPD, YPDCu, YPGal, YPGalCu, YPGal doxycycline, YPRaff, YPRaff doxycycline, or –trp media, corresponding liquid media was supplemented with 2.2 % agar before autoclaving.

4.2.3 Cell cycle arrest

4.2.3.1 Arrest in G1 with pheromone α -factor

MATa cells were inoculated from the o/n cultures to a final OD₆₀₀ 0.05 and grown until OD₆₀₀ reached 0.2. Subsequently, α -factor (5 mg/ml stock solution in 100% methanol) was added to the culture to a final concentration of 2 μ g/ml and cells were incubated for 1 hour. Since α -factor is quickly metabolized, an additional 1.5 μ g/ml of α -factor was added and cells were incubated for an extra 1 h.

To release cells from α -factor arrest they were centrifuged for 3 minutes 3000 rpm in Eppendorf centrifuge 5810 R at 4°C, washed at least three times with ice-cold media, and subsequently, resuspended in a pre-warmed media for further growth.

4.2.3.2 Arrest in G2/M with nocodazole and benomyl

Cells were inoculated from o/n cultures in fresh media to a final OD₆₀₀ 0.2 and grown until OD₆₀₀ reached 0.65. Subsequently, nocodazole (1 mg/ml stock solution in DMSO) and benomyl (10 mg/ml stock solution in DMSO) were added to the culture to final concentrations of 15 µg/ml and 10 µg/ml, respectively. Cells were incubated with nocodazole and benomyl for 2-3 hours.

4.2.4 Flow cytometry analysis of DNA content in arrested yeast cells

Cell culture aliquot (1 ml) was centrifuged for 1 minutes at 4000 rpm in Eppendorf centrifuge 5415R at 4°C. Obtained pellet was resuspended in 1ml of ice cold 70 % ethanol and incubated for at least 2 hours at -20°C. Subsequently, cells were centrifuged, re-suspended in 1 ml of 50 mM Tris buffer pH 7.5 supplemented with 0.2 mg/ml RNase A (Fermentas) and incubated o/n at 37°. The next day cells were pelleted, resuspended in 0.5 ml of propidium iodide buffer (200 mM Tris pH 7.5, 211 mM NaCl, 78 mM MgCl₂, 54 µg/ml propidium iodide) and sonicated (Sonifier S-450 analogue, Branson Danbury USA) for 5 sec (output control 2.5, duty cycle 100%). For measurements sonicated cells were diluted 1:20 with sheath fluid (Partec) and DNA content of at least 10,000 cells was examined using CyFlow SL and FloMax software (Partec). The FACS graphs were created with the WIN MDI Software.

4.2.5 Transformation of budding yeast

Yeast cells from overnight culture in YPD were inoculated in 50 ml of fresh YPD to a final OD₆₀₀ of 0.2 and grown till OD₆₀₀ reached 0.8. Cells were harvested by centrifuging at 3000 rpm for 3 minutes in Eppendorf 5810R and washed twice in 1 ml of 1 M lithium acetate, centrifuged at RT for 1 minute at 4000 rpm in an Eppendorf centrifuge 5415R and resuspended in a 1:1 volume of 1 M lithium acetate. 8 µl of salmon sperm DNA (Fermentas), 90 µl 50 % PEG 3350, and 8 µl of DNA (200 ng of PCR product or plasmid DNA) were added to 24 µl aliquot of cell suspension, briefly vortexed and incubated at RT for 30 minutes. Then 12 µl of 60% glycerol were added to the suspension and incubated for the additional 30 minutes at RT. After heat shock for 10 minutes at 42°C, cells were plated on a selective media without antibiotic or incubated in YPD for 3 hours at 25°C or 30°C and plated on a selective media, containing antibiotics. The plates were incubated for 2-3 days at 25°C or 30°C. The transformants were checked for the correct integration or plasmid presence by PCR, stability assay, Western blot analysis and fluorescent microscopy.

4.2.6 Stability assay for strains transformed with the minichromosome

Transformants carrying the minichromosomal plasmid 1174 were plated on YPD plate and grown o/n. The next day cells were streaked for singles on YPD and incubated o/n before replica plating the colonies on –trp plates and incubating both plates o/n. The colonies grown on YPD plates were compared to the colonies, which grew on –trp replica plate. The transformation of a strain with the minichromosome was considered successful, when the minichromosomal marker displayed unstable inheritance. In this case, a transformant will produce colonies that lost the ability to grow on the –trp plate due to the loss of the plasmid during the non-selective growth on YPD plates.

4.2.7 Isolation of genomic DNA

Yeast cells from the fresh patch on an agar plate were resuspended in 180 µl SCE buffer (1 M sorbitol, 0.1 M sodium citrate, 60 mM EDTA, pH 7), 20 µl zymolyase T100 (10 mg/ml stock solution in 20% glucose), and 1.5 µl β-mercaptoethanol and incubated for 1 hour at 37°C in an Eppendorf Thermomixer Compact at 900 rpm to digest the cell walls. Cells were lysed by the addition of 200 µl of lysis buffer (0.1 M Tris pH 9.0, 2 % SDS, 0.05 M EDTA) and incubation for 5 minutes at 65°C. The suspension was cooled down before adding 200 µl of 5 M potassium acetate and vortexed. The sample was centrifuged at maximum speed for 5 minutes in Eppendorf 5415R at 4°C and an aliquot of the supernatant (350 µl) was transferred into a fresh tube with 800 µl of 100% ethanol (Roth), mixed and centrifuged at max speed for 10 minutes in Eppendorf 5415R at 4°C. After the supernatant was removed, the pellet was dried at 65°C for 10 minutes and resuspended in 300 µl of MQ. 1 µl of isolated genomic DNA were used as a template in a PCR reaction.

4.2.8 Crossing of budding yeast

A small amount of *MATa* or *MATα* haploid parental yeast strain from the fresh patch was resuspended in 25 µl of sterile MQ. Two suspensions were combined together in a fresh Eppendorf-tube and mixed. 15 µl of the resulting suspension were pipetted on a pre-warmed YPD plate and incubated for 5 hours at 25°C. Subsequently, a small portion of the cells was resuspended in 90 µl of 1 M Sorbitol and pipetted on a fresh pre-warmed YPD plate. The zygotes were pulled with a micromanipulator MSM System 300 TSA microscope (Singer Instruments) and grown for 2 days at 25°C.

4.2.9 Tetrad dissection and analysis

Diploid yeast cells from the fresh patch on YPD plate were streaked on SPO plate and incubated for 2-3 days at 25°C for sporulation. A small amount of cells was re-suspended in 90 µl of 1 M sorbitol supplemented with 10 µl of zymolyase T100 (10 mg/ml stock in 20 % glucose) and incubated for 30 minutes at 30°C with shaking (750 rpm). Subsequently, 20 µl of the suspension were transferred to the YPD plate. The tetrads were dissected using a MSM System 300 TSA microscope (Singer Instruments) and the dissection plates were incubated for 2-3 days at 25°C. The colonies, obtained from single spores, were analysed by streaking on an YPD plate and replica plating to the plates with appropriate selective media. To examine mating type the YPD plate was replica plated onto a YPD plate with a suspension of the mating tester strains, namely 216 (*MATa*) or 217 (*MATα*), and incubated for 5 hours at 25°C before replica plating on MIN plates.

4.2.10 Budding yeast strain construction

4.2.10.1 Construction of strains with endogenous genes tagged C-terminally

Endogenous *SMC3*, *SCC1*, *PDS5*, *SCC3*, and *WPL1* were C-terminally tagged with yGFP and EGFP using plasmids 1320 and 1343 according to (Janke et al., 2004). *PDS5* and *SCC3* were tagged with Eco1-derived degron using plasmid 1098.

PCR-amplified *yGFP-kanMX*, *EGFP-kanMX* or *HA-degron-nat1* cassettes were transformed into yeast strains as described in 4.2.5. The cassettes were targeted for an insertion via homologous recombination at the endogenous locus due to the overhangs on the amplification primers, which were complementary to the sequences at the end of the ORF and at the 3'UTR of the gene of interest. Genomic DNA was isolated from obtained transformants as described in 4.2.7, and used as a template for checking PCR and sequencing. Expression of GFP- and HA-degron fusions was confirmed with Western Blot analysis.

4.2.10.2 Construction of strains with endogenous genes tagged N-terminally

N-terminal tagging of *PDS5* and *SCC3* with 9 Myc epitopes was performed as described in (Gauss et al., 2005). Briefly, *9Myc-kanMX* cassette was amplified by PCR from pOM20 plasmid and transformed into a diploid yeast strain. The cassette was targeted for an insertion at the endogenous locus via homologous recombination due to

overhangs on the primers that were complementary to the promoter and the beginning of the ORF. Transformants were checked for correct insertion by PCR. The marker cassette, disrupting the promoter, was then excised as described in (Gueldener et al., 2002). For this, yeast clones were transformed with a plasmid encoding Cre recombinase under the control of Gal promoter, pSH47, and enzyme expression was induced. As a result, the marker cassette, flanked by two loxP sites was removed via recombination and expression of the tagged gene was restored. Absence of the marker cassette was confirmed by PCR. In order to obtain a haploid yeast strain with the N-terminally tagged protein of interest, diploids were sporulated and tetrads were dissected as described in **4.2.9**.

N-terminal tagging of *PDS5* and *SCC3* with DHFR-based degron was performed as described in (Sanchez-Diaz et al., 2004). *kanMX-CUP1-degron-Myc1* or *kanMX-tetO2-degron-Myc18* cassettes were amplified by PCR from plasmids 1399 or 1498 and transformed into yeast strain, expressing Ubr1 under the control of *GAL* promoter as described in **4.2.5**. After transformation cells were incubated for 3 hours at 25°C in 1 ml media (YPD Cu or YPD) and plated on YPD-KAN Cu or YPD-KAN plates. After 3 days of incubation at 25°C transformants were tested by PCR.

4.2.10.3 Constructing strains with array of LacO repeats in URA3 locus

LacO repeats, originating from plasmid 1494 (generous gift of Susanne Gasser), were cloned into a yeast integrative vector YIplac211. Yeast strains, expressing LacI-GFP fusion, were transformed with a vector linearized via restriction digest at a unique cleavage site in *URA3* gene, StuI. LacO repeats (along with the rest of the vector) were inserted in the endogenous *URA3* locus via homologous recombination. Transformants were examined for the presence of GFP dots by fluorescent microscopy.

4.2.10.4 List of strains

^aAll strains are isogenic in the W303 background unless indicated otherwise and have the genotype *MATa ade2-1 trp1-1 can1-100 leu2-3,112, his3-11,15 ura3 GAL psi⁺*

Table 4.2 List of yeast strains used in this study

| Strain number | Source | Genotype^a |
|----------------------|------------------------------|---|
| 216 | Nasmyth lab | <i>MATa, his1</i> , DC14a background |
| 217 | Nasmyth lab | <i>MATalpha, his1</i> , DC14a background |
| 1021 | Ivanov lab | <i>MATa</i> Wild type |
| 1016 | Ivanov lab | <i>MATa/MATα</i> WT diploid |
| 1323 | Ivanov lab (J.Reiter) | <i>scc3::SCC3-HA6-ECO1(aa63-109)::NAT</i> |
| 1417 | Ivanov lab (J.Reiter) | <i>TetO200::URA3 TetR-GFP::LEU2</i> |
| 1457 | Nasmyth lab | <i>spc42::SPC42-4mCherry::natMX</i> |
| 1479 | Ivanov lab (D.Ivanov) | <i>scc3::SCC3-HA6::HIS3</i> |
| 1621 | Ivanov lab (B.Lochmann) | <i>TetR-GFP::LEU2 TetO200::URA3, scc3::SCC3-HA6-ECO1(aa63-109)::NAT</i> |
| 1625 | Ivanov lab (J.Reiter) | <i>scc3::SCC3-HA6-ECO1(aa63-109)::NAT, scc1::SCC1-Myc18::HIS3</i> |
| 1675 | Ivanov lab (D.Ivanov) | <i>pds5::PDS5-HA6-ECO1(aa63-109) :: NAT</i> |
| 1677 | Ivanov lab (B.Lochmann) | <i>pds5::PDS5-HA6::TRP1</i> |
| 1678 | Ivanov lab (D.Ivanov) | <i>TetO200::URA3, TetR-GFP::LEU2 pds5::PDS5-HA6-ECO1(aa63-109)::NAT</i> |
| 1813 | Ivanov lab (D.Ivanov) | <i>scc3::SCC3-HA6::HIS3, scc1::SCC1-Myc18::HIS3</i> |
| 1815 | Ivanov lab (D.Ivanov) | <i>scc1::SCC1-Myc18::HIS3, pds5::PDS5-HA6::TRP1</i> |
| 1818 | Ivanov lab (D.Ivanov) | <i>pds5::PDS5-HA6-ECO1(aa63-109)::NAT, scc1::SCC1-Myc18::HIS3</i> |
| 1904 | Bloom lab (Yeh et al., 2008) | <i>MATa trp1Δ63 leu2Δ1 ura3-52 his3Δ200 lys2-801 HTB2-GFP::KAN SPC29-RFP::HPH</i> |

4 Materials and Methods

| | | |
|------|---|--|
| | | YEF473 background, |
| 1906 | Ivanov lab (J.Metzler) | <i>scc1::SCC1-Myc18::HIS3, wpl1::HPH</i> |
| 2003 | This study | <i>MATa/α</i> diploid homozygous for <i>SPC42-mCherry::NAT</i> and <i>SMC3-EGFP::KAN</i> |
| 2004 | This study | <i>MATa/α</i> diploid homozygous for <i>SPC42-mCherry::NAT</i> , <i>SMC3-EGFP::KAN</i> and <i>PDS5-HA6-ECO1(aa63-109)::NAT</i> |
| 2034 | This study | <i>MATa/α</i> diploid homozygous for <i>SPC42-mCherry::NAT</i> , <i>SMC3-EGFP::KAN</i> and <i>wpl1::HPH</i> |
| 2040 | This study | <i>MATa/α</i> diploid <i>SPC42-mCherry::NAT/SPC42wt</i> <i>SMC3-yEGFP::HYGRO/Smc3-EGFP::KAN</i> homozygous for <i>SCC3-HA6-ECO1(aa66-109)::NAT</i> |
| 2086 | Euroscarf (Sanchez-Diaz <i>et al.</i> , 2004) | <i>MATa</i> <i>ubr1::GAL-HA-UBR1 (HIS3)</i> |
| 2172 | This study | <i>ubr1:: GAL-HA-UBR1 (HIS3)</i> <i>pds5::CUP1-Myc1-DHFR-PDS5::KAN</i> |
| 2173 | This study | <i>ubr1::GAL-HA-UBR1 (HIS3)</i> <i>scc3::CUP1-Myc1-DHFR-SCC3::KAN</i> |
| 2190 | Ivanov lab (D.Ivanov) | <i>wpl1::HPH TetO200::URA3 TetR-GFP::LEU2</i> |
| 2281 | This study | <i>MATa/α</i> diploid homozygous for <i>SPC42-mCherry::NAT</i> and <i>SCC3-EGFP::KAN</i> |
| 2312 | This study | <i>MAT a/ MAT alpha</i> diploid heterozygous for <i>SPC42-4mCherry::NAT</i> and <i>WPL1-EGFP::KAN</i> |
| 2353 | This study | <i>MATa/α</i> diploid homozygous for <i>SPC42-4mCherry::NAT</i> and <i>SCC1-EGFP::KAN</i> |
| 2389 | This study | <i>MATa/α</i> diploid homozygous for <i>PDS5-HA6-EcoI(aa63-109) :: NAT</i> , <i>SPC42-mCherry::NAT</i> , and <i>SCC1-EGFP::KAN</i> |
| 2390 | This study | <i>MATa/α</i> diploid homozygous for |

| | | |
|------|------------|--|
| | | <i>SCC3-HA6-ECO1(aa63-109)::NAT</i> and <i>SCC1-EGFP::KAN</i> |
| 2391 | This study | <i>MATa/a</i> diploid homozygous for <i>wpl1::HPH</i> , <i>SPC42-mCherry::NAT</i> , and <i>SCC1-EGFP::KAN</i> |
| 2395 | This study | <i>MAT a</i> <i>ubr1::GAL-HA-UBR1 (HIS3)</i> , <i>CMVp (tetR'-SSN6)::LEU2</i> , <i>trp1::tTA</i> , <i>scc1::SCC1-HA6::TRP1</i> |
| 2417 | This study | <i>MATa/a</i> diploid homozygous for <i>SPC42-mCherry::NAT</i> and <i>PDS5-EGFP::KAN</i> |
| 2418 | This study | <i>MATa</i> <i>ubr1::GAL-HA-UBR1(HIS3)</i> , <i>CMVp(tetR'-SSN6)::LEU2</i> , <i>trp1::tTA</i> , <i>lacO repeat::URA</i> , <i>GFP-LacI::HIS3</i> |
| 2419 | This study | <i>MAT a</i> <i>ubr1::GAL-HA-UBR1 (HIS3)</i> , <i>CMVp (tetR'-SSN6)::LEU2</i> , <i>trp1::tTA</i> , <i>pds5::tet02-DHFR-Myc1-PDS5::KANN</i> , <i>lacO repeat::URA</i> , <i>GFP-LacI::HIS3</i> |
| 2420 | This study | <i>MAT a</i> <i>ubr1::GAL-HA-UBR1 (HIS3)</i> , <i>CMVp (tetR'-SSN6)::LEU2</i> , <i>trp1::tTA</i> , <i>scc3::tetO2-DHFR-Myc1-SCC3 ::KAN</i> , <i>lacO repeat::URA</i> , <i>GFP-LacI::HIS3</i> |
| 2449 | This study | <i>MATa</i> <i>ubr1::GAL-HA-UBR1 (HIS3)</i> , <i>CMVp (tetR'-SSN6)::LEU2</i> , <i>trp1::tTA</i> , <i>scc3::tetO2-DHFR-Myc1-SCC3 ::KAN</i> , <i>pds5::tetO2-DHFR-Myc1-PDS5::KAN</i> , <i>lacO repeat::URA</i> , <i>GFP-LacI::HIS3</i> |
| 2452 | This study | <i>ubr1::GAL-HA-UBR1 (HIS3)</i> <i>CMVp (tetR'-SSN6)::LEU2</i> , <i>trp1::tTA</i> , |

| | | |
|------|------------|--|
| | | <i>scc1::SCC1-HA6::TRP1</i> , <i>pds5::tet02-DHFR-Myc18-PDS5::KAN</i> |
| 2455 | This study | <i>ubr1::GAL-HA-UBR1 (HIS3), CMVp (tetR⁻-SSN6)::LEU2</i> , <i>trp1::tTA, scc1::SCC1-HA6::TRP1</i> , <i>scc3::tet02-DHFR-Myc18-SCC3::KAN</i> |
| 2456 | This study | <i>ubr1::GAL-HA-UBR1 (HIS3), CMVp (tetR⁻-SSN6)::LEU2</i> <i>trp1::tTA, scc1::SCC1-HA6::TRP1</i> , <i>scc3::tet02-DHFR-Myc18-SCC3::KAN</i> , <i>pds5::tet02-DHFR-Myc18-PDS5::KANN</i> |
| 2517 | This study | <i>MATa</i> WT carrying plasmid 1174 |
| 2518 | This study | <i>MAT a</i> <i>scc3::SCC3-HA6-Eco1 (aa63-109)::NAT</i> , <i>scc1::SCC1-Myc18::HIS3</i> , carrying plasmid 1174 |
| 2519 | This study | <i>MATa</i> <i>scc3::SCC3-HA6::HIS3</i> , <i>scc1::SCC1-Myc18::HIS3</i> , carrying plasmid 1174 |
| 2520 | This study | <i>MATa</i> <i>pds5::PDS5-HA6-ECO1(aa63-109)::NAT</i> , <i>scc1::SCC1-Myc18::HIS3</i> , carrying plasmid 1174 |
| 2523 | This study | <i>pds5::PDS5-HA6::HIS</i> |
| 2525 | This study | <i>pds5::PDS5-HA6::HIS3, scc1::SCC1-Myc18::HIS3</i> |
| 2530 | This study | <i>MAT a</i> <i>pds5::PDS5-HA6::HIS3, scc1::SCC1-Myc18::HIS3</i> , carrying plasmid 1174 |
| 2576 | This study | <i>ubr1::GAL-HA-UBR1 (HIS3), CMVp (tetR⁻-SSN6)::Leu2</i> , <i>trp1::tTA, pds5::PDS5-HA6::TRP</i> |
| 2577 | This study | <i>ubr1::GAL-HA-UBR1 (HIS3), CMVp (tetR⁻-SSN6)::LEU2</i> , <i>trp1::tTA, pds5::KAN::tetO2-DHFR-Myc18-PDS5-</i> |

| | | |
|-------|-------------|--|
| | | <i>HA6::TRP</i> |
| 2578 | This study | <i>ubr1::GAL-HA-UBR1 (HIS3), CMVp (tetR'-SSN6)::Leu2, trp1::tTA, scc3::SCC3-HA6::TRP</i> |
| 2579 | This study | <i>ubr1::GAL-HA-UBR1 (HIS3), CMVp (tetR'-SSN6)::LEU2, trp1::tTA, scc3::KAN::tetO2-DHFR-Myc18-SCC3-HA6::TRP</i> |
| 2584 | This study | <i>scc3::Myc9-SCC3</i> |
| 2587 | This study | <i>pds5::Myc9-PDS5</i> |
| 2590 | This study | <i>pds5::Myc9-PDS5-HA6::TRP1</i> |
| 2601 | This study | <i>pds5::Myc9-PDS5-HA6-ECO1(aa63-109)::NAT</i> |
| 2603 | This study | <i>scc3::Myc9-SCC3-HA6::HIS</i> |
| 2608 | This study | <i>scc3::Myc9-SCC3-HA6-ECO1(aa63-109)::NAT</i> |
| 10589 | Nasmyth lab | <i>scc1::SCC1-Myc18::HIS3</i> |
| 12544 | Nasmyth lab | <i>SCC3-HA6::HIS3 TetR-GFP-TAP::LEU2</i> |

4.2.11 Induction of DHFR-based degron

4.2.11.1 In strains with tetO2 promoter

In order to induce protein degradation in G2/M, yeast cells were grown o/n in YPRaff media, the next day cells were inoculated in fresh YPRaff media to final OD₆₀₀ 0.2 and grown till OD₆₀₀ reached 0.65. After cells were arrested for 4 hours with nocodazole as described in 4.2.3.2, an aliquot of culture was pelleted and used for TCA protein isolation as described in 4.4.6, while the rest of the culture was harvested by centrifugation in Eppendorf centrifuge 5810 R. Cells were resuspended in YPGal media supplemented with 15 µg/ml nocodazole and grown for 35 minutes at 30°C to induce Ubr1 expression. After Ubr1 expression was induced, an aliquot of culture was pelleted and used for TCA protein isolation. The rest of the culture was centrifuged and obtained pellet was resuspended in the pre-warmed to 37°C YPGal media supplemented with 20 µg/ml doxycycline. Cells were grown for 2 hours at 37°C to induce the degradation of Pds5 and Scc3 fusions to the DHFR-based degron. To monitor the destruction of proteins fused to degrons, aliquots of culture were taken every 30 minutes and used for TCA protein isolation followed by Western Blot analysis.

In order to induce protein degradation in G1, cells were arrested with pheromone α -factor as described in **4.2.3.1** and degnon was induced as described above.

4.2.11.2 In strains with CUP1 promoter

Induction of DHFR-based degnon under the control of *CUP1* promoter was performed as described in (Sanchez-Diaz et al., 2004) with some modifications. Yeast cells were grown o/n in YPRaffCu media and inoculated in fresh YPRaffCu media to final OD₆₀₀ 0.2 and grown till OD₆₀₀ reached 0.65. After cells were arrested for 3 hours with nocodazole as described in **4.2.3.2** an aliquot of culture was pelleted and used for TCA protein isolation, while the rest of the culture was harvested by centrifugation in Eppendorf centrifuge 5810R. Cells were resuspended in YPGalCu supplemented with 15 μ g/ml nocodazole and grown for 35 minutes at 30°C to induce Ubr1 expression. After Ubr1 expression was induced, an aliquot of culture was pelleted and used for TCA protein isolation and the rest of the culture was centrifuged and obtained pellet was resuspended in the pre-warmed to 37°C YPGal supplemented with 15 μ g/ml nocodazole. Cells were grown for 2 hours at 37°C to induce the degradation of Pds5 and Scc3 fusions to the DHFR-based degnon. To monitor the destruction of proteins fused to degnons, aliquots of culture were taken every 30 minutes and used for TCA protein isolation followed by Western Blot analysis.

4.3 Fluorescence microscopy

4.3.1 Fixation of *S.cerevisiae* cells for microscopy

An aliquot of cell culture (1 ml) was centrifuged, supernatant was removed completely and the cells were resuspended in 1 ml of cold (-20°C) 100% methanol (ROTH) and incubated for at least 2 hours at -80°C. Subsequently, cells were washed once with 1:1 methanol (100%)/PEM buffer (100 mM PIPES, 1 mM EGTA, 1 mM MgSO₄, adjusted to pH 6.8 with KOH), and once with PEM buffer. Fixed cells were subjected to fluorescent microscopy analysis using an Axio Imager fluorescence microscope (Zeiss) with a 63X or a 100X objective.

4.3.2 Assay for sister chromatid cohesion employing strains with Eco1-derived degron

Yeast cells, harboring Tet operators in *URA3* locus and expressing tetR-GFP fusion were arrested with α -factor as described in 4.2.3.1 and released in media supplemented with 15 $\mu\text{g/ml}$ nocodazole. After cells were arrested for 3 hours with nocodazole, an aliquot of culture was pelleted, washed with 1M sorbitol and subjected to the fluorescent microscopy analysis using an Axio Imager fluorescence microscope (Zeiss) with a 100X objective. Dots separation (1 dot versus 2 dots) was scored in 300 cells per strain.

4.3.3 Assay for sister chromatid cohesion employing strains with DHFR-based degron

DHFR-based degron was induced either in G2/M or in G1 arrested yeast cells, harboring an array of Lac operators integrated in *URA3* locus and expressing LacI-GFP fusion, as described in 4.2.11.1. After degron induction in G2/M was complete, cells were chased in YPGal media supplemented with 15 $\mu\text{g/ml}$ nocodazole and 20 $\mu\text{g/ml}$ doxycycline for 3 hours at 25°C. In case of degron induction in G1, cells were released from α -factor arrest into YPGal media supplemented with 15 $\mu\text{g/ml}$ nocodazole and 20 $\mu\text{g/ml}$ doxycycline for 3 hours at 25°C. An additional incubation at 25°C was found necessary, since the GFP signal was weakened under the conditions of degron induction. Dots separation (1 dot versus 2 dots) was scored in 300 fixed cells per strain.

4.3.4 Fluorescence recovery after photobleaching (FRAP)

Fluorescence microscopy and photobleaching were performed according to the protocol described in (Yeh et al., 2008) with modifications. Cells were immobilized in a slab of media supplemented with 10% low melting point agarose (NuSieve GTG Agarose, Lonza) and imaged at the RT (20°C) with Olympus fv1000 laser scan confocal microscope with standard eGFP band pass filter (500-550 nm) and argon laser (488 nm excitation line). Seven z sections were acquired in 750 nm steps and analyzed with Imaris software. The mean and the standard deviation of the acquired intensity were calculated using MatLAB (Mathworks Inc., Natick, MA).

4.4 Biochemical techniques

4.4.1 Chromatin immunoprecipitation experiments

Chromatin immunoprecipitation (ChIP) was performed as described in (Tanaka et al., 1999) using strains with Myc-tagged Scc1 subunit of cohesin, anti-Myc 9E11 antibody and protein A Dynabeads (Invitrogen) (for ChIP qPCR) or rat anti-mouse IgG2a Dynabeads M-450 (Dyna) (for ChIP Seq), as well as anti-H3 antibody (ab-1791, abcam) and protein A Dynabeads (Invitrogen) (for ChIP qPCR).

Yeast strains, grown overnight in YPD at 30°C, were inoculated into 50 ml of fresh YPD media to a final OD₆₀₀ 0.2, and grown until the OD₆₀₀ reached 0.8. After the addition of formaldehyde (solution for molecular biology, SIGMA) to a final concentration of 1 %, cell cultures were incubated for 30 minutes at 25°C in order to cross-link DNA-associated proteins to DNA. After 5 minutes incubation with 125 mM glycine at 25°C, cells were harvested by centrifugation for 5 minutes 3500 rpm in Eppendorf centrifuge 5810 R at 4°C. Obtained cell pellets were washed 4 times with 40 ml ice-cold TBS buffer (20 mM Tris pH 7.5, 150 mM NaCl) and resuspended in 200 µl of lysis buffer (50 mM HEPES pH 7.5, 140 mM NaCl, 1 mM EDTA, 1 % TritonX-100, 0.1 % Na-deoxycholate, 1 mM PMSF, 1 mM benzamidine, 1X complete EDTA-free inhibitors (Roche)). Cells were transferred in Vetter tube (Roland Vetter Laborbedarf OHG, Ammerbuch) containing 1.2 ml of acid washed glass beads (Sigma-Aldrich) and disrupted by beads beating in FastPrepTM machine (Qbiogen, MPBiomedicals, Heidelberg) 5 times for 10 sec at speed 6.5 at 4°C. After disruption Vetter tubes were punctured at the bottom and spun down in an empty 2 ml Eppendorf-tubes for 3 minutes 1200 rpm in Eppendorf centrifuge 5415R at 4°C. DNA in obtained cell lysates was fragmented by sonication (Sonifier S-450 analogue, Branson Danbury USA) 3 times for 15 sec (output control 3.5, duty cycle 90%) at 4°C. After sonication cell lysates were centrifugated for 5 minutes at 12000 rpm in Eppendorf centrifuge 5415 R at 4°C. 200 µl of supernatant (whole cell extract, WCE) was transferred in a new tube and split in 3 aliquots: 7 µl were mixed with 143 µl of TE-SDS buffer (10 mM TrisCl pH 7.5, 1 mM EDTA, 1 % SDS) for reversion of cross-links (WCE sample for qPCR), 13 µl were added to equal volume of 2x SDS loading dye (125 mM Tris, 20 % glycerol, 2 % SDS, 1 % bromphenol blue, w/ 350 mM β-mercaptoethanol) (WCE sample for Western Blot analysis), 180µl of lysate were added to the Dynabeads coupled to the antibodies, 9E11 or anti-H3. Lysates were incubated with Dynabeads at 4°C for 2 hours

(for ChIP Seq) or o/n (for ChIP qPCR). Beads were washed 2 times for 5 minutes with 1 ml of pre-cooled lysis buffer, 1 ml of pre-cooled lysis buffer with 360 mM NaCl, 1 ml of pre-cooled washing buffer (10 mM Tris pH 8.0, 0.5 % NP-40, 250 mM LiCl, 1 mM EDTA, 0.5 % Na-deoxycholate) and 1 time with 1 ml of TE buffer (10 mM TrisCl pH7.5, 1 mM EDTA), spun down for 3 minutes 5000 rpm in the Eppendorf centrifuge 5415R and supernatant was completely removed. Immunoprecipitated DNA with cross-linked Scc1 or histone H3 was eluted off the beads in 50 µl of elution buffer (50 mM Tris pH 8.0, 10 mM EDTA, 1 % SDS) for 10 minutes at 65°C. 20 µl of eluate were added to equal volume of 2x SDS loading dye (IP sample for Western Blot analysis), 30 µl were added to 120 µl of TE-SDS buffer for reversion of cross-links. Reversion of crosslink of WCE and IP samples were performed o/n at 65°C.

Decross-linked WCE and IP samples were incubated with proteinase K (Roche) for 2 hours at 37°C and DNA was extracted with phenol/chloroform/isoamyl alcohol (25:24:1), ethanol precipitated overnight at -20°C in the presence of 20 µg glycogen (Roche) and dissolved in 30 µl TE with 10 µg of RNase (Fermentas) for 1 hour at 37°C. Obtained DNA samples were used for qPCR analysis (WCE and IP samples) or ChIP-Seq analysis (IP samples), while WCE and IP protein samples were used for Western Blot analysis.

4.4.2 ChIP qPCR analysis

ChIP DNA, immunoprecipitated as described in 4.4.1 (WCE and IP samples), was quantified by quantitative PCR employing the LightCycler® 480 SYBR Green I Master Mix according to the manufacturer's protocol and LightCycler® 480 Instrument II (Roche). One PCR reaction mixture with total volume of 20 µl contained 3.6 µl PCR grade water, 0.7 µl of sense and anti-sense primers (10 µM), 10 µl of SYBR Green I Master Mix and 5 µl of serial dilutions of DNA template. DNA fragments were amplified in 40 cycles employing standard PCR program (pre-incubation step: 95°C 5 minutes; amplification step: 95°C 10 sec, 60°C 30 sec, 72°C 20 sec; calculation of melting curve: 95°C 5 sec, 65°C 1 min). Primers GCGGCCTTAAGTTCGTAGT (sense) and AAGTGCCGGAAATTGTCTTG (anti-sense) were used for amplification of the centromere adjacent region of chromosome VI, ACGGTTTCAGTTCCTCCATTG (sense) and TGCAAAAGCTTTGCTGGTTA (anti-sense) - for a cohesin site on the arm of chromosome VI (172 kb) as described in (Hu et al., 2011). Primers for a

cohesin-low site on the arm of chromosome V (141 kb) were GCTGGGTCTCACGATCCATATCAG (sense) and TCTTGTTTCGGTGAGTTGGACAGATC (anti-sense) as described in (Sutani et al., 2009). PCR product amplified with each pair of primers were cloned in pJet 1.2 vector (Fermentas) and serial dilutions with known DNA concentration were used to create standard curves for absolute quantification of immunoprecipitated DNA. Obtained data was analysed using the LightCycler® 480 SW 1.5.0 software.

4.4.3 ChIP Seq

Chromatin immunoprecipitation was performed as described in 4.4.1. Immunoprecipitated DNA was used to create DNA libraries according to the manufacturer's protocol employing ChIP-Seq Sample Prep Kit, Illumina. DNA fragments were ligated to the adaptors, size fractionated (150 – 500 bp) on 2 % agarose (Certified Low Range Ultra Agarose, Bio-Rad) gel supplemented with ethidium bromide, excised from the gel and extracted from the gel using the QIAGEN Gel Extraction Kit (Qiagen). Gel-extracted DNA libraries were amplified by PCR and analysed on High Sensitivity DNA Chips with Bioanalyzer 2100 (Agilent Technologies). Cluster generation and sequencing analysis were performed on Illumina Genome Analyzer II with the help of Standard Cluster Generation V4-GA II and 36 cycle Sequencing v4 kits (Illumina).

Obtained reads were aligned against the *Saccharomyces cerevisiae* reference genome employing Palmapper v0.5 (Ossowski et al., 2008) reporting all alignments with at most three mismatches and one gap. To minimize the effect of possible contamination with human DNA, we also aligned the reads against the human genome and used for further analysis only reads that were uniquely mapped to the yeast genome. The multimapper resolution tool (<http://bioweb.me/mmr>) was used to identify the best location of reads mapping to multiple sites and only reads, mapping to the chromosomal DNA of *Saccharomyces cerevisiae* were considered for further analysis. The summary of counts of aligned reads is presented in **Table 6.1**. The log₂-ratios between the samples' read coverage and the negative control (untagged strain) at equi-spaced genomic locations were computed and plotted using Matlab.

4.4.4 Minichromosome immunoprecipitation

Minichromosome immunoprecipitation was performed as described in (Ivanov and Nasmyth, 2005). Yeast strains transformed with a plasmid 1174 (Ivanov and Nasmyth, 2007) containing an 850 bp long *CEN4* sequence from YCplac22 and *TRPIARS1* sequence were grown overnight in -trp media at 30°C. Overnight cultures were inoculated into 400 ml YPD to the final OD₆₀₀ 0.2 and grown at 30°C till OD₆₀₀ reached 0.65. Cells were arrested with 10 µg/ml nocodazole for 90 minutes. Spheroplasting was carried out as described in (Deshaies and Kirschner, 1995) with modifications. After cells were arrested in G2/M, they were pelleted, washed twice with cold MQ, resuspended in pre-spheroplasting buffer (0.1 M Tris pH 9.4, 10 mM DTT, 10 µg/ml nocodazole) and incubated at RT for 15 minutes. Subsequently, cells were centrifuged for 3 minutes 3500 rpm in Eppendorf centrifuge 5810R at 4°C. Obtained pellet was washed with cold water, resuspended in pre-warmed to 30°C spheroplasting buffer (1 M sorbitol, 50 mM Tris pH 7.5, 1 mM CaCl₂, 1 mM MgCl₂, 10 µg/ml nocodazole, 400 U/ml lyticase (Sigma)) and incubated for 30 minutes at 30°C in the water bath with shaking. Spheroplasts were washed with 1 M sorbitol and lysed in 4.5 ml of lysis buffer (25 mM HEPES/KOH pH 8.0, 50 mM KCl, 10 mM MgSO₄, 10 mM Na citrate, 25 mM Na sulfite, 0.25 % TritonX-100, 1 mM PMSF, 3 mM DTT, and 1X complete EDTA-free inhibitors (Roche)) supplemented with 100 µg/ml RNase A (Fermentas) for 30 minutes on ice. The lysate was cleared by centrifugation at 10,000 rpm for 5 minutes in an Eppendorf centrifuge 5810R at 4°C. DNA digest was performed with 1000 units of BglII (NEB) per 1 ml of lysate for 2 hours at 4°C. The reaction was stopped by the addition of 5 M NaCl to a final concentration of 200 mM. To immunoprecipitate minichromosomes, pre-cleared lysates (1 ml) were incubated with 12.5 µg/ml of anti-HA (12CA5, Roche) or anti-Myc (9E11, Santa Cruz) antibodies and 0.25 ml suspension of protein A Dynabeads (Invitrogen) in cold room o/n. Beads were washed 3 times with 1.5 ml of the lysis buffer with 300 mM NaCl. Subsequently, minichromosomes were eluted off the beads twice with 0.25 ml of elution buffer (50 mM Tris pH 8.0, 10 mM EDTA, 1 % SDS) at 65°C, extracted with phenol/chloroform/isoamyl alcohol (25:24:1) and ethanol precipitated. Samples were dissolved in 40 µl of TE and subjected for Southern blot analysis.

4.4.5 Southern blot analysis: capillary transfer and radioactive detection

To analyse the efficiency of minichromosome immunoprecipitation described in 4.4.4, purified circular and linear minichromosomes were separated on 1 % agarose gel supplemented with 0.5 µg/ml ethidium bromide for 2.5 hours at 120 V and transferred to Hybond-XL (GE Healthcare) under denaturing conditions according to the manufacturer's protocol. After the capillary transfer, DNA was cross-linked to the membrane in a UV Stratlinker 2400 (Auto Cross Link setting), membrane was rinsed with 2x SSC (34.2 mM tri-sodium citrate, 0.3 M sodium chloride, pH 7-8). The blot was hybridized with a radioactive probe for the *TRP1* gene in the hybridization buffer (7 ml of Dextran buffer (200 g/l Dextran, 2 % SLS, 12 x SSC), 6 ml of MQ water, 60 µl salmon sperm DNA (Invitrogen)) o/n at 65°C. The probe was labelled with [α -³²P]dCTP (Hartmann Analytic) employing a Prime-It II Random Primer Labeling Kit (Stratagene), according to the manufacturer's protocol and purified from unincorporated [α -³²P]dCTP on a Nick Column G50 Sepharose DNA grade (GE Healthcare). After the hybridization the blot was washed three times with washing buffer (2x SSC, 1 % SDS) for 30 minutes at 65°C. Subsequently, blots were exposed to storage phosphor screen (Molecular Dynamics) for two days, scanned on a Storm 840 (Molecular Dynamics) and bands were quantified with QuantityOne 4.6.7.

4.4.6 Isolation of proteins from *S. cerevisiae* with Trichloroacetic acid

25 ml of liquid culture with OD₆₀₀ 0.6 or an equivalent amount of a culture with different OD₆₀₀ were spun down for 3 minutes 3000 rpm in Eppendorf centrifuge 5810R at 4°C. Cells were washed with 1 ml of ice cold 10 % Trichloroacetic acid (TCA) and re-suspended in 200 µl of ice cold 10 % TCA and transferred to the Vetter tube (Roland Vetter Laborbedarf OHG, Ammerbuch) containing 1.2 ml of acid washed glass beads (Sigma-Aldrich). Yeast cells were disrupted by beads beating in a FastPrep™ machine (Qbiogen, MPBiomedicals, Heidelberg) for 40 sec at speed 6.5 at 4 °C. After disruption, tubes were cooled for 10 minutes on ice. In order to harvest yeast cell lysates Vetter tubes were punctured at the bottom and lysates were spun down in an empty 1.5 ml Eppendorf-tubes for 3 minutes 1200 rpm in the Eppendorf centrifuge 5415R at 4°C. Additional 200 µl of ice cold 10 % TCA were added to the glass beads and re-centrifuged. Obtained cell lysates were centrifuged at maximal speed for 10 minutes at RT, the supernatant was removed and the pellets, containing precipitated proteins, were resuspended in 100 µl of 2x SDS loading buffer and 25 µl of

2 M Tris base were added to neutralize acidic pH. Samples were vortexed briefly, boiled for 10 minutes, centrifuged for 10 minutes at the maximal speed at RT in Eppendorf centrifuge 5415R and protein-containing supernatant was transferred to a new Eppendorf-tube.

Sample concentrations were adjusted according to the Bradford measurements prior to Western blot analysis.

4.4.7 Western blot analysis

Protein samples were added to equal volume of 2x SDS loading dye (125 mM Tris, 20 % glycerol, 2 % SDS, 1 % bromphenol blue, w/ 350 mM β -mercaptoethanol) and boiled for 5 minutes. Denaturated proteins together with Precision Plus Protein Standard (BioRad), used as a marker, were separated according to their molecular masses on a SDS-PAGE gel with the appropriate polyacrylamide percentage for 90 minutes at 110 V in 1x SDS running buffer (118 mM Tris-base, 40 mM glycine, 0.1 % SDS).

For Western blot analysis a SDS-PAGE gel, a methanol activated PVDF membrane (0.45 μ m, BioRad), and an extra thick blotting paper (BioRad) were pre-equilibrated in 1x Transfer buffer (48 mM Tris-base, 39 mM glycine, 0.0375 % SDS, 20 % methanol) for 15 minutes at RT. Then Western blot was assembled and transferred either in a SemiDry Transfer Cell (BioRad) (15 minutes at 15 V) or in an ECL SemiDry Transfer Unit (Amersham Bioscience) (1 hour at 30 mA). After transfer, PVDF membrane was blocked for 45 minutes in blocking buffer (1x PBS, 0.05 % Tween 20, 5 % powdered milk (Roth)) and probed with primary and then secondary (anti-primary HRP conjugated) antibody diluted to the appropriate concentration in 1:10 diluted blocking buffer. PVDF membrane was washed three times with PBS-T buffer (1x PBS, 0.05 % Tween 20) for 15 minutes after incubation with primary and secondary antibodies. The Western blot was analysed with ECL Western detection system (Amersham) according to the manufacturer's protocol and exposed to the Hyperfilm ECL (Amersham) or BioMax MR Film, High Resolution (Kodak).

Table 4.3 Primary and secondary antibodies used in this study for Western blot analysis.

| Anti- | Source | Host | Dilution |
|-------|--------|------|----------|
|-------|--------|------|----------|

| | | | |
|------------------|--|---------------------------|--------------------|
| Cdc28 (sc-28550) | Santa Cruz | Rabbit | 1:5000 |
| GFP | Santa Cruz | Mouse | 1:3000-1:5000 |
| HA (16B12) | Covance | Mouse | 1:1000- 1:10000 |
| HA (12CA5) | Cell signalling Technology | Mouse | 1:3000-1:5000 |
| Hmo1 | Brill laboratory, (Lu et al., 1996) | Rabbit | 1:3000-1:5000 |
| Myc (71D10) | Cell signalling Technology | Rabbit | 1:1000- 1:10000 |
| mouse IgG | GE Healthcare | Sheep, HRP- conjugated | 1:5000 |
| rabbit IgG | GE Healthcare | Goat, HRP- conjugated | 1:5000 |

4.4.8 Preparation of yeast chromatin pellets

Chromatin pellets were prepared as described in (Ben-Shahar et al., 2008) with several modifications. Yeast strains, grown overnight in YPD at 30°C, were inoculated into 50 ml of fresh YPD media to a final OD₆₀₀ 0.2. When OD₆₀₀ reached 0.65, cells were arrested in G2/M as described in 4.2.3.2. Amount of cells equal to 50 ml OD₆₀₀ 0.8 was pelleted by centrifugation in Eppendorf centrifuge 5180R for 5 min 3000 rpm, re-suspended in 3 ml of pre-spheroplasting buffer (100 mM Tris pH 9.4, 10 mM DTT, 15 µg/ml nocodazole) and incubated for 10 minutes at RT. Cells were pelleted, resuspended in 2 ml of spheroplasting buffer (0.6 M Sorbitol, 50 mM KPi pH 7.4, 10 mM DTT, 40 µg/ml zymolase T100) and incubated for 10 minutes in water bath at 37°C. Subsequently, cells were centrifuged for 1 minute 4000 rpm in Eppendorf centrifuge 5415R and washed with washing buffer (50 mM HEPES/KOH pH 7.5, 100 mM KCl, 2.5 mM MgCl₂, 0.4 M sorbitol). Spheroplasts were resuspended in equal volume of EB buffer (50 mM HEPES/KOH pH 7.5, 100 mM KCl, 2.5 mM MgCl₂, 1 mM DTT, 2 mM benzamidine, 1 mM PMSF) and lysed for 3 minutes on ice by addition of Triton X-100 to the final concentration of 0.25 %. An aliquot of obtained whole cell extract (WCE) was added to the equal volume of 2x SDS loading buffer and

boiled for 5 minutes (WCE sample). To separate chromatin from soluble proteins, 100 μ l aliquot of WCE was applied onto 100 μ l of EBX-S buffer (50 mM HEPES/KOH pH 7.5, 100 mM KCl, 2.5 mM MgCl₂, 1 mM DTT, 2 mM benzamidine, 1 mM PMSF, 0.25 % TritonX-100, 30 % sucrose) and spun down for 10 minutes 12000 rpm in the Eppendorf centrifuge 5415R at 4°C. An aliquot of supernatant fraction was added to the equal volume of 2x SDS loading dye and boiled (sup sample). Rest of supernatant and sucrose buffer were removed and chromatin pellet was washed once with 100 μ l of EBX buffer (50 mM HEPES/KOH pH 7.5, 100 mM KCl, 2.5 mM MgCl₂, 1 mM DTT, 2 mM benzamidine, 1 mM PMSF, 0.25 % TritonX-100) and then resuspended in 100 μ l of EBX buffer and boiled with equal volume of 2x SDS loading buffer (pell sample). WCE, sup and pell protein samples were subjected to Western Blot analysis as described in **4.4.7**.

5 References

- Agarwal, R., and Cohen-Fix, O. (2002). Phosphorylation of the mitotic regulator Pds1/securin by Cdc28 is required for efficient nuclear localization of Esp1/separase. *Genes Dev* 16, 1371-1382.
- Alexandru, G., Uhlmann, F., Mechtler, K., Poupart, M.A., and Nasmyth, K. (2001). Phosphorylation of the cohesin subunit Scc1 by Polo/Cdc5 kinase regulates sister chromatid separation in yeast. *Cell* 105, 459-472.
- Alushin, G.M., Ramey, V.H., Pasqualato, S., Ball, D.A., Grigorieff, N., Musacchio, A., and Nogales, E. (2010). The Ndc80 kinetochore complex forms oligomeric arrays along microtubules. *Nature* 467, 805-810.
- Anderson, D.E., Losada, A., Erickson, H.P., and Hirano, T. (2002). Condensin and cohesin display different arm conformations with characteristic hinge angles. *J Cell Biol* 156, 419-424.
- Anderson, D.E., Trujillo, K.M., Sung, P., and Erickson, H.P. (2001). Structure of the Rad50 x Mre11 DNA repair complex from *Saccharomyces cerevisiae* by electron microscopy. *J Biol Chem* 276, 37027-37033.
- Arumugam, P., Gruber, S., Tanaka, K., Haering, C.H., Mechtler, K., and Nasmyth, K. (2003). ATP hydrolysis is required for cohesin's association with chromosomes. *Curr Biol* 13, 1941-1953.
- Bachant, J., Alcasabas, A., Blat, Y., Kleckner, N., and Elledge, S.J. (2002). The SUMO-1 isopeptidase Smt4 is linked to centromeric cohesion through SUMO-1 modification of DNA topoisomerase II. *Mol Cell* 9, 1169-1182.
- Banin, S., Moyal, L., Shieh, S., Taya, Y., Anderson, C.W., Chessa, L., Smorodinsky, N.I., Prives, C., Reiss, Y., Shiloh, Y., *et al.* (1998). Enhanced phosphorylation of p53 by ATM in response to DNA damage. *Science* 281, 1674-1677.
- Baumann, C., Korner, R., Hofmann, K., and Nigg, E.A. (2007). PICH, a centromere-associated SNF2 family ATPase, is regulated by Plk1 and required for the spindle checkpoint. *Cell* 128, 101-114.
- Belli, G., Gari, E., Aldea, M., and Herrero, E. (1998). Functional analysis of yeast essential genes using a promoter-substitution cassette and the tetracycline-regulatable dual expression system. *Yeast* 14, 1127-1138.
- Ben-Shahar, T.R., Heeger, S., Lehane, C., East, P., Flynn, H., Skehel, M., and Uhlmann, F. (2008). Eco1-dependent cohesin acetylation during establishment of sister chromatid cohesion. *Science* 321, 563-566.
- Bergerat, A., de Massy, B., Gabelle, D., Varoutas, P.C., Nicolas, A., and Forterre, P. (1997). An atypical topoisomerase II from Archaea with implications for meiotic recombination. *Nature* 386, 414-417.

- Bernard, P., Drogat, J., Maure, J.F., Dheur, S., Vaur, S., Genier, S., and Javerzat, J.P. (2006). A screen for cohesion mutants uncovers Ssl3, the fission yeast counterpart of the cohesin loading factor Scc4. *Curr Biol* 16, 875-881.
- Bernard, P., Maure, J.F., and Javerzat, J.P. (2001a). Fission yeast Bub1 is essential in setting up the meiotic pattern of chromosome segregation. *Nat Cell Biol* 3, 522-526.
- Bernard, P., Maure, J.F., Partridge, J.F., Genier, S., Javerzat, J.P., and Allshire, R.C. (2001b). Requirement of heterochromatin for cohesion at centromeres. *Science* 294, 2539-2542.
- Bernard, P., Schmidt, C.K., Vaur, S., Dheur, S., Drogat, J., Genier, S., Ekwall, K., Uhlmann, F., and Javerzat, J.P. (2008). Cell-cycle regulation of cohesin stability along fission yeast chromosomes. *Embo J* 27, 111-121.
- Bhalla, N., Biggins, S., and Murray, A.W. (2002). Mutation of YCS4, a budding yeast condensin subunit, affects mitotic and nonmitotic chromosome behavior. *Mol Biol Cell* 13, 632-645.
- Blat, Y., and Kleckner, N. (1999). Cohesins bind to preferential sites along yeast chromosome III, with differential regulation along arms versus the centric region. *Cell* 98, 249-259.
- Borges, V., Lehane, C., Lopez-Serra, L., Flynn, H., Skehel, M., Rolef Ben-Shahar, T., and Uhlmann, F. (2010). Hos1 deacetylates Smc3 to close the cohesin acetylation cycle. *Mol Cell* 39, 677-688.
- Brand, A.H., Breeden, L., Abraham, J., Sternglanz, R., and Nasmyth, K. (1985). Characterization of a "silencer" in yeast: a DNA sequence with properties opposite to those of a transcriptional enhancer. *Cell* 41, 41-48.
- Brinkley, B.R., and Stubblefield, E. (1966). The fine structure of the kinetochore of a mammalian cell in vitro. *Chromosoma* 19, 28-43.
- Bulger, M., and Groudine, M. (2010). Enhancers: the abundance and function of regulatory sequences beyond promoters. *Developmental biology* 339, 250-257.
- Buonomo, S.B., Clyne, R.K., Fuchs, J., Loidl, J., Uhlmann, F., and Nasmyth, K. (2000). Disjunction of homologous chromosomes in meiosis I depends on proteolytic cleavage of the meiotic cohesin Rec8 by separin. *Cell* 103, 387-398.
- Campbell, J.L., and Cohen-Fix, O. (2002). Chromosome cohesion: ring around the sisters? *Trends in biochemical sciences* 27, 492-495.
- Canman, C.E., Lim, D.S., Cimprich, K.A., Taya, Y., Tamai, K., Sakaguchi, K., Appella, E., Kastan, M.B., and Siliciano, J.D. (1998). Activation of the ATM kinase by ionizing radiation and phosphorylation of p53. *Science* 281, 1677-1679.
- Canudas, S., and Smith, S. (2009). Differential regulation of telomere and centromere cohesion by the Scc3 homologues SA1 and SA2, respectively, in human cells. *J Cell Biol* 187, 165-173.

- Carter, A.P., Cho, C., Jin, L., and Vale, R.D. (2011). Crystal structure of the dynein motor domain. *Science* 331, 1159-1165.
- Chan, K.L., North, P.S., and Hickson, I.D. (2007). BLM is required for faithful chromosome segregation and its localization defines a class of ultrafine anaphase bridges. *Embo J* 26, 3397-3409.
- Chang, C.R., Wu, C.S., Hom, Y., and Gartenberg, M.R. (2005). Targeting of cohesin by transcriptionally silent chromatin. *Genes Dev* 19, 3031-3042.
- Cheeseman, I.M., Anderson, S., Jwa, M., Green, E.M., Kang, J., Yates, J.R., 3rd, Chan, C.S., Drubin, D.G., and Barnes, G. (2002). Phospho-regulation of kinetochore-microtubule attachments by the Aurora kinase Ipl1p. *Cell* 111, 163-172.
- Cheeseman, I.M., and Desai, A. (2008). Molecular architecture of the kinetochore-microtubule interface. *Nature reviews* 9, 33-46.
- Chen, F., Kamradt, M., Mulcahy, M., Byun, Y., Xu, H., McKay, M.J., and Cryns, V.L. (2002). Caspase proteolysis of the cohesin component RAD21 promotes apoptosis. *J Biol Chem* 277, 16775-16781.
- Chen, L., Trujillo, K., Ramos, W., Sung, P., and Tomkinson, A.E. (2001). Promotion of Dnl4-catalyzed DNA end-joining by the Rad50/Mre11/Xrs2 and Hdf1/Hdf2 complexes. *Mol Cell* 8, 1105-1115.
- Chook, Y.M., and Blobel, G. (1999). Structure of the nuclear transport complex karyopherin-beta2-Ran x GppNHp. *Nature* 399, 230-237.
- Chung, J.H., Bell, A.C., and Felsenfeld, G. (1997). Characterization of the chicken beta-globin insulator. *Proc Natl Acad Sci U S A* 94, 575-580.
- Cingolani, G., Petosa, C., Weis, K., and Muller, C.W. (1999). Structure of importin-beta bound to the IBB domain of importin-alpha. *Nature* 399, 221-229.
- Ciosk, R., Shirayama, M., Shevchenko, A., Tanaka, T., Toth, A., and Nasmyth, K. (2000). Cohesin's binding to chromosomes depends on a separate complex consisting of Scc2 and Scc4 proteins. *Mol Cell* 5, 243-254.
- Ciosk, R., Zachariae, W., Michaelis, C., Shevchenko, A., Mann, M., and Nasmyth, K. (1998). An ESP1/PDS1 complex regulates loss of sister chromatid cohesion at the metaphase to anaphase transition in yeast. *Cell* 93, 1067-1076.
- Clarke, L., and Carbon, J. (1980). Isolation of a yeast centromere and construction of functional small circular chromosomes. *Nature* 287, 504-509.
- Clarke, L., and Carbon, J. (1983). Genomic substitutions of centromeres in *Saccharomyces cerevisiae*. *Nature* 305, 23-28.
- Cohen-Fix, O., Peters, J.M., Kirschner, M.W., and Koshland, D. (1996). Anaphase initiation in *Saccharomyces cerevisiae* is controlled by the APC-dependent degradation of the anaphase inhibitor Pds1p. *Genes Dev* 10, 3081-3093.

- Conaway, R.C., Sato, S., Tomomori-Sato, C., Yao, T., and Conaway, J.W. (2005). The mammalian Mediator complex and its role in transcriptional regulation. *Trends in biochemical sciences* 30, 250-255.
- Connelly, J.C., Kirkham, L.A., and Leach, D.R. (1998). The SbcCD nuclease of *Escherichia coli* is a structural maintenance of chromosomes (SMC) family protein that cleaves hairpin DNA. *Proc Natl Acad Sci U S A* 95, 7969-7974.
- Dabrowska, M., Jagielska, E., Ciesla, J., Plucienniczak, A., Kwiatowski, J., Wranicz, M., Boireau, P., and Rode, W. (2004). *Trichinella spiralis* thymidylate synthase: cDNA cloning and sequencing, and developmental pattern of mRNA expression. *Parasitology* 128, 209-221.
- de Jager, M., Trujillo, K.M., Sung, P., Hopfner, K.P., Carney, J.P., Tainer, J.A., Connelly, J.C., Leach, D.R., Kanaar, R., and Wyman, C. (2004). Differential arrangements of conserved building blocks among homologs of the Rad50/Mre11 DNA repair protein complex. *J Mol Biol* 339, 937-949.
- de Jager, M., van Noort, J., van Gent, D.C., Dekker, C., Kanaar, R., and Wyman, C. (2001). Human Rad50/Mre11 is a flexible complex that can tether DNA ends. *Mol Cell* 8, 1129-1135.
- Deardorff, M.A., Kaur, M., Yaeger, D., Rampuria, A., Korolev, S., Pie, J., Gil-Rodriguez, C., Arnedo, M., Loeys, B., Kline, A.D., *et al.* (2007). Mutations in cohesin complex members SMC3 and SMC1A cause a mild variant of cornelia de Lange syndrome with predominant mental retardation. *American journal of human genetics* 80, 485-494.
- Denison, S.H., Kafer, E., and May, G.S. (1993). Mutation in the bimD gene of *Aspergillus nidulans* confers a conditional mitotic block and sensitivity to DNA damaging agents. *Genetics* 134, 1085-1096.
- Deshaies, R.J., and Kirschner, M. (1995). G1 cyclin-dependent activation of p34^{CDC28} (Cdc28p) in vitro. *Proc Natl Acad Sci U S A* 92, 1182-1186.
- Dietz, R. (1958). [Multiple sex chromosomes in Ostracoda cypria, their evolution and division characteristics]. *Chromosoma* 9, 359-440.
- Dohmen, R.J., Wu, P., and Varshavsky, A. (1994). Heat-inducible degron: a method for constructing temperature-sensitive mutants. *Science* 263, 1273-1276.
- Donze, D., Adams, C.R., Rine, J., and Kamakaka, R.T. (1999). The boundaries of the silenced HMR domain in *Saccharomyces cerevisiae*. *Genes Dev* 13, 698-708.
- Dorsett, D. (2004). Adherin: key to the cohesin ring and cornelia de Lange syndrome. *Curr Biol* 14, R834-836.
- Dorsett, D. (2007). Roles of the sister chromatid cohesion apparatus in gene expression, development, and human syndromes. *Chromosoma* 116, 1-13.

- Dorsett, D., Eissenberg, J.C., Misulovin, Z., Martens, A., Redding, B., and McKim, K. (2005). Effects of sister chromatid cohesion proteins on cut gene expression during wing development in *Drosophila*. *Development (Cambridge, England)* *132*, 4743-4753.
- Downs, J.A., Lowndes, N.F., and Jackson, S.P. (2000). A role for *Saccharomyces cerevisiae* histone H2A in DNA repair. *Nature* *408*, 1001-1004.
- Eckert, C.A., Gravdahl, D.J., and Megee, P.C. (2007). The enhancement of pericentromeric cohesin association by conserved kinetochore components promotes high-fidelity chromosome segregation and is sensitive to microtubule-based tension. *Genes Dev* *21*, 278-291.
- Ekwall, K., Javerzat, J.P., Lorentz, A., Schmidt, H., Cranston, G., and Allshire, R. (1995). The chromodomain protein Swi6: a key component at fission yeast centromeres. *Science* *269*, 1429-1431.
- Fernandez-Capetillo, O., Chen, H.T., Celeste, A., Ward, I., Romanienko, P.J., Morales, J.C., Naka, K., Xia, Z., Camerini-Otero, R.D., Motoyama, N., *et al.* (2002). DNA damage-induced G2-M checkpoint activation by histone H2AX and 53BP1. *Nat Cell Biol* *4*, 993-997.
- Fernius, J., and Marston, A.L. (2009). Establishment of cohesion at the pericentromere by the Ctf19 kinetochore subcomplex and the replication fork-associated factor, Csm3. *PLoS Genet* *5*, e1000629.
- Filippova, G.N., Fagerlie, S., Klenova, E.M., Myers, C., Dehner, Y., Goodwin, G., Neiman, P.E., Collins, S.J., and Lobanenkov, V.V. (1996). An exceptionally conserved transcriptional repressor, CTCF, employs different combinations of zinc fingers to bind diverged promoter sequences of avian and mammalian c-myc oncogenes. *Mol Cell Biol* *16*, 2802-2813.
- Fitzgerald-Hayes, M., Clarke, L., and Carbon, J. (1982). Nucleotide sequence comparisons and functional analysis of yeast centromere DNAs. *Cell* *29*, 235-244.
- Fullwood, M.J., Liu, M.H., Pan, Y.F., Liu, J., Xu, H., Mohamed, Y.B., Orlov, Y.L., Velkov, S., Ho, A., Mei, P.H., *et al.* (2009). An oestrogen-receptor-alpha-bound human chromatin interactome. *Nature* *462*, 58-64.
- Funabiki, H., Yamano, H., Kumada, K., Nagao, K., Hunt, T., and Yanagida, M. (1996). Cut2 proteolysis required for sister-chromatid separation in fission yeast. *Nature* *381*, 438-441.
- Gandhi, R., Gillespie, P.J., and Hirano, T. (2006). Human Wapl is a cohesin-binding protein that promotes sister-chromatid resolution in mitotic prophase. *Curr Biol* *16*, 2406-2417.
- Gartenberg, M. (2009). Heterochromatin and the cohesion of sister chromatids. *Chromosome Res* *17*, 229-238.
- Gause, M., Webber, H.A., Misulovin, Z., Haller, G., Rollins, R.A., Eissenberg, J.C., Bickel, S.E., and Dorsett, D. (2008). Functional links between *Drosophila* Nipped-B and cohesin in somatic and meiotic cells. *Chromosoma* *117*, 51-66.

- Gauss, R., Trautwein, M., Sommer, T., and Spang, A. (2005). New modules for the repeated internal and N-terminal epitope tagging of genes in *Saccharomyces cerevisiae*. *Yeast* 22, 1-12.
- Gerlich, D., Koch, B., Dupeux, F., Peters, J.M., and Ellenberg, J. (2006). Live-cell imaging reveals a stable cohesin-chromatin interaction after but not before DNA replication. *Curr Biol* 16, 1571-1578.
- German, J. (1979). Roberts' syndrome. I. Cytological evidence for a disturbance in chromatid pairing. *Clinical genetics* 16, 441-447.
- Ghaemmaghami, S., Huh, W.K., Bower, K., Howson, R.W., Belle, A., Dephoure, N., O'Shea, E.K., and Weissman, J.S. (2003). Global analysis of protein expression in yeast. *Nature* 425, 737-741.
- Gietz, R.D., and Sugino, A. (1988). New yeast-*Escherichia coli* shuttle vectors constructed with in vitro mutagenized yeast genes lacking six-base pair restriction sites. *Gene* 74, 527-534.
- Gimenez-Abian, J.F., Sumara, I., Hirota, T., Hauf, S., Gerlich, D., de la Torre, C., Ellenberg, J., and Peters, J.M. (2004). Regulation of sister chromatid cohesion between chromosome arms. *Curr Biol* 14, 1187-1193.
- Glynn, E.F., Megee, P.C., Yu, H.G., Mistrot, C., Unal, E., Koshland, D.E., DeRisi, J.L., and Gerton, J.L. (2004). Genome-wide mapping of the cohesin complex in the yeast *Saccharomyces cerevisiae*. *PLoS Biol* 2, E259.
- Gorr, I.H., Boos, D., and Stemmann, O. (2005). Mutual inhibition of separase and Cdk1 by two-step complex formation. *Mol Cell* 19, 135-141.
- Goshima, G., and Yanagida, M. (2000). Establishing biorientation occurs with precocious separation of the sister kinetochores, but not the arms, in the early spindle of budding yeast. *Cell* 100, 619-633.
- Graf, T., and Enver, T. (2009). Forcing cells to change lineages. *Nature* 462, 587-594.
- Grenon, M., Gilbert, C., and Lowndes, N.F. (2001). Checkpoint activation in response to double-strand breaks requires the Mre11/Rad50/Xrs2 complex. *Nat Cell Biol* 3, 844-847.
- Groves, M.R., Hanlon, N., Turowski, P., Hemmings, B.A., and Barford, D. (1999). The structure of the protein phosphatase 2A PR65/A subunit reveals the conformation of its 15 tandemly repeated HEAT motifs. *Cell* 96, 99-110.
- Gruber, S., Arumugam, P., Katou, Y., Kuglitsch, D., Helmhart, W., Shirahige, K., and Nasmyth, K. (2006). Evidence that Loading of Cohesin Onto Chromosomes Involves Opening of Its SMC Hinge. *Cell* 127, 523-537.
- Gruber, S., Haering, C.H., and Nasmyth, K. (2003). Chromosomal cohesin forms a ring. *Cell* 112, 765-777.

- Guan, J., Ekwurtzel, E., Kvist, U., and Yuan, L. (2008). Cohesin protein SMC1 is a centrosomal protein. *Biochem Biophys Res Commun* 372, 761-764.
- Gueldener, U., Heinisch, J., Koehler, G.J., Voss, D., and Hegemann, J.H. (2002). A second set of loxP marker cassettes for Cre-mediated multiple gene knockouts in budding yeast. *Nucleic Acids Res* 30, e23.
- Guldener, U., Heck, S., Fielder, T., Beinhauer, J., and Hegemann, J.H. (1996). A new efficient gene disruption cassette for repeated use in budding yeast. *Nucleic Acids Res* 24, 2519-2524.
- Gullerova, M., and Proudfoot, N.J. (2008). Cohesin complex promotes transcriptional termination between convergent genes in *S. pombe*. *Cell* 132, 983-995.
- Haering, C.H., Farcas, A.M., Arumugam, P., Metson, J., and Nasmyth, K. (2008). The cohesin ring concatenates sister DNA molecules. *Nature* 454, 297-301.
- Haering, C.H., Lowe, J., Hochwagen, A., and Nasmyth, K. (2002). Molecular architecture of SMC proteins and the yeast cohesin complex. *Mol Cell* 9, 773-788.
- Haering, C.H., Schoffnegger, D., Nishino, T., Helmhart, W., Nasmyth, K., and Lowe, J. (2004). Structure and Stability of Cohesin's SMC1-Kleisin Interaction. *Mol Cell* 15, 951-964.
- Hakimi, M.A., Bochar, D.A., Schmiesing, J.A., Dong, Y., Barak, O.G., Speicher, D.W., Yokomori, K., and Shiekhata, R. (2002). A chromatin remodelling complex that loads cohesin onto human chromosomes. *Nature* 418, 994-998.
- Hallson, G., Syrzycka, M., Beck, S.A., Kennison, J.A., Dorsett, D., Page, S.L., Hunter, S.M., Keall, R., Warren, W.D., Brock, H.W., *et al.* (2008). The *Drosophila* cohesin subunit Rad21 is a trithorax group (trxG) protein. *Proc Natl Acad Sci U S A* 105, 12405-12410.
- Hartman, T., Stead, K., Koshland, D., and Guacci, V. (2000). Pds5p is an essential chromosomal protein required for both sister chromatid cohesion and condensation in *Saccharomyces cerevisiae*. *J Cell Biol* 151, 613-626.
- Hauf, S., Cole, R.W., LaTerra, S., Zimmer, C., Schnapp, G., Walter, R., Heckel, A., van Meel, J., Rieder, C.L., and Peters, J.M. (2003). The small molecule Hesperadin reveals a role for Aurora B in correcting kinetochore-microtubule attachment and in maintaining the spindle assembly checkpoint. *J Cell Biol* 161, 281-294.
- Hauf, S., Roitinger, E., Koch, B., Dittrich, C.M., Mechtler, K., and Peters, J.M. (2005). Dissociation of cohesin from chromosome arms and loss of arm cohesion during early mitosis depends on phosphorylation of SA2. *PLoS Biol* 3, e69.
- Hauf, S., Waizenegger, I.C., and Peters, J.M. (2001). Cohesin cleavage by separase required for anaphase and cytokinesis in human cells. *Science* 293, 1320-1323.
- Hayden, J.H., Bowser, S.S., and Rieder, C.L. (1990). Kinetochores capture astral microtubules during chromosome attachment to the mitotic spindle: direct visualization in live newt lung cells. *J Cell Biol* 111, 1039-1045.

- Heidinger-Pauli, J.M., Mert, O., Davenport, C., Guacci, V., and Koshland, D. (2010). Systematic reduction of cohesin differentially affects chromosome segregation, condensation, and DNA repair. *Curr Biol* 20, 957-963.
- Heidinger-Pauli, J.M., Unal, E., Guacci, V., and Koshland, D. (2008). The kleisin subunit of cohesin dictates damage-induced cohesion. *Mol Cell* 31, 47-56.
- Heidinger-Pauli, J.M., Unal, E., and Koshland, D. (2009). Distinct targets of the Eco1 acetyltransferase modulate cohesion in S phase and in response to DNA damage. *Mol Cell* 34, 311-321.
- Hieter, P., Pridmore, D., Hegemann, J.H., Thomas, M., Davis, R.W., and Philippsen, P. (1985). Functional selection and analysis of yeast centromeric DNA. *Cell* 42, 913-921.
- Hongay, C.F., Grisafi, P.L., Galitski, T., and Fink, G.R. (2006). Antisense transcription controls cell fate in *Saccharomyces cerevisiae*. *Cell* 127, 735-745.
- Horsfield, J.A., Anagnostou, S.H., Hu, J.K., Cho, K.H., Geisler, R., Lieschke, G., Crosier, K.E., and Crosier, P.S. (2007). Cohesin-dependent regulation of Runx genes. *Development (Cambridge, England)* 134, 2639-2649.
- Howell, B.J., McEwen, B.F., Canman, J.C., Hoffman, D.B., Farrar, E.M., Rieder, C.L., and Salmon, E.D. (2001). Cytoplasmic dynein/dynactin drives kinetochore protein transport to the spindle poles and has a role in mitotic spindle checkpoint inactivation. *J Cell Biol* 155, 1159-1172.
- Hu, B., Itoh, T., Mishra, A., Katoh, Y., Chan, K.L., Upcher, W., Godlee, C., Roig, M.B., Shirahige, K., and Nasmyth, K. (2011). ATP hydrolysis is required for relocating cohesin from sites occupied by its Scc2/4 loading complex. *Curr Biol* 21, 12-24.
- Huang, C.E., Milutinovich, M., and Koshland, D. (2005). Rings, bracelet or snaps: fashionable alternatives for Smc complexes. *Philos Trans R Soc Lond B Biol Sci* 360, 537-542.
- Huang, J., Hsu, J.M., and Laurent, B.C. (2004). The RSC nucleosome-remodeling complex is required for Cohesin's association with chromosome arms. *Mol Cell* 13, 739-750.
- Huang, J., and Moazed, D. (2006). Sister chromatid cohesion in silent chromatin: each sister to her own ring. *Genes Dev* 20, 132-137.
- Irniger, S., Piatti, S., Michaelis, C., and Nasmyth, K. (1995). Genes involved in sister chromatid separation are needed for B-type cyclin proteolysis in budding yeast. *Cell* 81, 269-278.
- Ivanov, D., and Nasmyth, K. (2005). A topological interaction between cohesin rings and a circular minichromosome. *Cell* 122, 849-860.
- Ivanov, D., and Nasmyth, K. (2007). A physical assay for sister chromatid cohesion in vitro. *Mol Cell* 27, 300-310.

- Ivanov, D., Schleiffer, A., Eisenhaber, F., Mechtler, K., Haering, C.H., and Nasmyth, K. (2002). Eco1 is a novel acetyltransferase that can acetylate proteins involved in cohesion. *Curr Biol* 12, 323-328.
- Jack, J., Dorsett, D., Delotto, Y., and Liu, S. (1991). Expression of the cut locus in the *Drosophila* wing margin is required for cell type specification and is regulated by a distant enhancer. *Development (Cambridge, England)* 113, 735-747.
- Janke, C., Magiera, M.M., Rathfelder, N., Taxis, C., Reber, S., Maekawa, H., Moreno-Borchart, A., Doenges, G., Schwob, E., Schiebel, E., *et al.* (2004). A versatile toolbox for PCR-based tagging of yeast genes: new fluorescent proteins, more markers and promoter substitution cassettes. *Yeast* 21, 947-962.
- Jensen, S., Segal, M., Clarke, D.J., and Reed, S.I. (2001). A novel role of the budding yeast separin Esp1 in anaphase spindle elongation: evidence that proper spindle association of Esp1 is regulated by Pds1. *J Cell Biol* 152, 27-40.
- Jessberger, R., Riwar, B., Baechtold, H., and Akhmedov, A.T. (1996). SMC proteins constitute two subunits of the mammalian recombination complex RC-1. *Embo J* 15, 4061-4068.
- Jiang, H., and Peterlin, B.M. (2008). Differential chromatin looping regulates CD4 expression in immature thymocytes. *Mol Cell Biol* 28, 907-912.
- Jin, H., Avey, M., and Yu, H.G. (2012). Is cohesin required for spindle-pole-body/centrosome cohesion? *Communicative & integrative biology* 5, 26-29.
- Jokelainen, P.T. (1967). The ultrastructure and spatial organization of the metaphase kinetochore in mitotic rat cells. *Journal of ultrastructure research* 19, 19-44.
- Kagey, M.H., Newman, J.J., Bilodeau, S., Zhan, Y., Orlando, D.A., van Berkum, N.L., Ebmeier, C.C., Goossens, J., Rahl, P.B., Levine, S.S., *et al.* (2010). Mediator and cohesin connect gene expression and chromatin architecture. *Nature* 467, 430-435.
- Kanemaki, M., Sanchez-Diaz, A., Gambus, A., and Labib, K. (2003). Functional proteomic identification of DNA replication proteins by induced proteolysis in vivo. *Nature* 423, 720-724.
- Ke, Y., Huh, J.W., Warrington, R., Li, B., Wu, N., Leng, M., Zhang, J., Ball, H.L., Li, B., and Yu, H. (2011). PICH and BLM limit histone association with anaphase centromeric DNA threads and promote their resolution. *Embo J* 30, 3309-3321.
- Keeney, S., Giroux, C.N., and Kleckner, N. (1997). Meiosis-specific DNA double-strand breaks are catalyzed by Spo11, a member of a widely conserved protein family. *Cell* 88, 375-384.
- Khodjakov, A., Rieder, C.L., Sluder, G., Cassels, G., Sibon, O., and Wang, C.L. (2002). De novo formation of centrosomes in vertebrate cells arrested during S phase. *J Cell Biol* 158, 1171-1181.

- Kim, S.T., Xu, B., and Kastan, M.B. (2002). Involvement of the cohesin protein, Smc1, in Atm-dependent and independent responses to DNA damage. *Genes Dev* *16*, 560-570.
- King, E.M., Rachidi, N., Morrice, N., Hardwick, K.G., and Stark, M.J. (2007). Ipl1p-dependent phosphorylation of Mad3p is required for the spindle checkpoint response to lack of tension at kinetochores. *Genes Dev* *21*, 1163-1168.
- Kirschner, M., and Mitchison, T. (1986). Beyond self-assembly: from microtubules to morphogenesis. *Cell* *45*, 329-342.
- Kitajima, T.S., Kawashima, S.A., and Watanabe, Y. (2004). The conserved kinetochore protein shugoshin protects centromeric cohesion during meiosis. *Nature* *427*, 510-517.
- Kitajima, T.S., Sakuno, T., Ishiguro, K., Iemura, S., Natsume, T., Kawashima, S.A., and Watanabe, Y. (2006). Shugoshin collaborates with protein phosphatase 2A to protect cohesin. *Nature* *441*, 46-52.
- Kitajima, T.S., Yokobayashi, S., Yamamoto, M., and Watanabe, Y. (2003). Distinct cohesin complexes organize meiotic chromosome domains. *Science* *300*, 1152-1155.
- Klein, F., Mahr, P., Galova, M., Buonomo, S.B., Michaelis, C., Nairz, K., and Nasmyth, K. (1999). A central role for cohesins in sister chromatid cohesion, formation of axial elements, and recombination during yeast meiosis. *Cell* *98*, 91-103.
- Kobayashi, T., Horiuchi, T., Tongaonkar, P., Vu, L., and Nomura, M. (2004). SIR2 regulates recombination between different rDNA repeats, but not recombination within individual rRNA genes in yeast. *Cell* *117*, 441-453.
- Kobe, B. (1999). Autoinhibition by an internal nuclear localization signal revealed by the crystal structure of mammalian importin alpha. *Nature structural biology* *6*, 388-397.
- Kong, X., Ball, A.R., Jr., Sonoda, E., Feng, J., Takeda, S., Fukagawa, T., Yen, T.J., and Yokomori, K. (2009). Cohesin associates with spindle poles in a mitosis-specific manner and functions in spindle assembly in vertebrate cells. *Mol Biol Cell* *20*, 1289-1301.
- Kornberg, R.D. (2005). Mediator and the mechanism of transcriptional activation. *Trends in biochemical sciences* *30*, 235-239.
- Krantz, I.D., McCallum, J., DeScipio, C., Kaur, M., Gillis, L.A., Yaeger, D., Jukofsky, L., Wasserman, N., Bottani, A., Morris, C.A., *et al.* (2004). Cornelia de Lange syndrome is caused by mutations in NIPBL, the human homolog of *Drosophila melanogaster* Nipped-B. *Nat Genet* *36*, 631-635.
- Krejci, L., Song, B., Bussen, W., Rothstein, R., Mortensen, U.H., and Sung, P. (2002). Interaction with Rad51 is indispensable for recombination mediator function of Rad52. *J Biol Chem* *277*, 40132-40141.

- Kueng, S., Hegemann, B., Peters, B.H., Lipp, J.J., Schleiffer, A., Mechtler, K., and Peters, J.M. (2006). Wapl controls the dynamic association of cohesin with chromatin. *Cell* 127, 955-967.
- Kulemzina, I., Schumacher, M.R., Verma, V., Reiter, J., J., M., Failla, A.V., Lanz, C., Sreedharan, V., Rättsch, G., and Ivanov, D. (2012). Cohesin Rings Devoid of Scc3 and Pds5 Maintain Their Stable Association with the DNA. *PLoS Genet* 8, e1002856.
- Kumada, K., Nakamura, T., Nagao, K., Funabiki, H., Nakagawa, T., and Yanagida, M. (1998). Cut1 is loaded onto the spindle by binding to Cut2 and promotes anaphase spindle movement upon Cut2 proteolysis. *Curr Biol* 8, 633-641.
- Kurukuti, S., Tiwari, V.K., Tavoosidana, G., Pugacheva, E., Murrell, A., Zhao, Z., Lobanenkova, V., Reik, W., and Ohlsson, R. (2006). CTCF binding at the H19 imprinting control region mediates maternally inherited higher-order chromatin conformation to restrict enhancer access to Igf2. *Proc Natl Acad Sci U S A* 103, 10684-10689.
- Kurze, A., Michie, K.A., Dixon, S.E., Mishra, A., Itoh, T., Khalid, S., Strmecki, L., Shirahige, K., Haering, C.H., Lowe, J., *et al.* (2011). A positively charged channel within the Smc1/Smc3 hinge required for sister chromatid cohesion. *Embo J* 30, 364-378.
- Labib, K., Tercero, J.A., and Diffley, J.F. (2000). Uninterrupted MCM2-7 function required for DNA replication fork progression. *Science* 288, 1643-1647.
- Laloraya, S., Guacci, V., and Koshland, D. (2000). Chromosomal addresses of the cohesin component Mcd1p. *J Cell Biol* 151, 1047-1056.
- Lam, W.W., Peterson, E.A., Yeung, M., and Lavoie, B.D. (2006). Condensin is required for chromosome arm cohesion during mitosis. *Genes Dev* 20, 2973-2984.
- Lamb, J.R., Michaud, W.A., Sikorski, R.S., and Hieter, P.A. (1994). Cdc16p, Cdc23p and Cdc27p form a complex essential for mitosis. *Embo J* 13, 4321-4328.
- Lau, A., Blitzblau, H., and Bell, S.P. (2002). Cell-cycle control of the establishment of mating-type silencing in *S. cerevisiae*. *Genes Dev* 16, 2935-2945.
- Lavoie, B.D., Hogan, E., and Koshland, D. (2002). In vivo dissection of the chromosome condensation machinery: reversibility of condensation distinguishes contributions of condensin and cohesin. *J Cell Biol* 156, 805-815.
- Lee, T., Marticke, S., Sung, C., Robinow, S., and Luo, L. (2000). Cell-autonomous requirement of the USP/EcR-B ecdysone receptor for mushroom body neuronal remodeling in *Drosophila*. *Neuron* 28, 807-818.
- Lengronne, A., Katou, Y., Mori, S., Yokobayashi, S., Kelly, G.P., Itoh, T., Watanabe, Y., Shirahige, K., and Uhlmann, F. (2004). Cohesin relocation from sites of chromosomal loading to places of convergent transcription. *Nature*.

- Lengronne, A., McIntyre, J., Katou, Y., Kanoh, Y., Hopfner, K.P., Shirahige, K., and Uhlmann, F. (2006). Establishment of sister chromatid cohesion at the *S. cerevisiae* replication fork. *Mol Cell* *23*, 787-799.
- Liang, B., Qiu, J., Ratnakumar, K., and Laurent, B.C. (2007). RSC functions as an early double-strand-break sensor in the cell's response to DNA damage. *Curr Biol* *17*, 1432-1437.
- Liang, C., and Stillman, B. (1997). Persistent initiation of DNA replication and chromatin-bound MCM proteins during the cell cycle in *cdc6* mutants. *Genes Dev* *11*, 3375-3386.
- Lim, H.S., Kim, J.S., Park, Y.B., Gwon, G.H., and Cho, Y. (2011). Crystal structure of the Mre11-Rad50-ATPgammaS complex: understanding the interplay between Mre11 and Rad50. *Genes Dev* *25*, 1091-1104.
- Lisby, M., Barlow, J.H., Burgess, R.C., and Rothstein, R. (2004). Choreography of the DNA damage response: spatiotemporal relationships among checkpoint and repair proteins. *Cell* *118*, 699-713.
- Liu, J., and Krantz, I.D. (2008). Cohesin and human disease. *Annual review of genomics and human genetics* *9*, 303-320.
- Loo, S., and Rine, J. (1994). Silencers and domains of generalized repression. *Science* *264*, 1768-1771.
- Losada, A., Hirano, M., and Hirano, T. (1998). Identification of *Xenopus* SMC protein complexes required for sister chromatid cohesion. *Genes Dev* *12*, 1986-1997.
- Losada, A., Hirano, M., and Hirano, T. (2002). Cohesin release is required for sister chromatid resolution, but not for condensin-mediated compaction, at the onset of mitosis. *Genes Dev* *16*, 3004-3016.
- Losada, A., Yokochi, T., and Hirano, T. (2005). Functional contribution of Pds5 to cohesin-mediated cohesion in human cells and *Xenopus* egg extracts. *J Cell Sci* *118*, 2133-2141.
- Losada, A., Yokochi, T., Kobayashi, R., and Hirano, T. (2000). Identification and characterization of SA/Scc3p subunits in the *Xenopus* and human cohesin complexes. *J Cell Biol* *150*, 405-416.
- Louie, E., and German, J. (1981). Roberts's syndrome. II. Aberrant Y-chromosome behavior. *Clinical genetics* *19*, 71-74.
- Lu, J., Kobayashi, R., and Brill, S.J. (1996). Characterization of a high mobility group 1/2 homolog in yeast. *J Biol Chem* *271*, 33678-33685.
- Luo, H., Li, Y., Mu, J.J., Zhang, J., Tonaka, T., Hamamori, Y., Jung, S.Y., Wang, Y., and Qin, J. (2008). Regulation of intra-S phase checkpoint by ionizing radiation (IR)-dependent and IR-independent phosphorylation of SMC3. *J Biol Chem* *283*, 19176-19183.

- Lyons, N.A., and Morgan, D.O. (2011). Cdk1-dependent destruction of Eco1 prevents cohesion establishment after S phase. *Mol Cell* *42*, 378-389.
- Madeo, F., Herker, E., Maldener, C., Wissing, S., Lachelt, S., Herlan, M., Fehr, M., Lauber, K., Sigrist, S.J., Wesselborg, S., *et al.* (2002). A caspase-related protease regulates apoptosis in yeast. *Mol Cell* *9*, 911-917.
- Maeda, R.K., and Karch, F. (2006). The ABC of the BX-C: the bithorax complex explained. *Development (Cambridge, England)* *133*, 1413-1422.
- Maiato, H., Rieder, C.L., and Khodjakov, A. (2004). Kinetochores-driven formation of kinetochore fibers contributes to spindle assembly during animal mitosis. *J Cell Biol* *167*, 831-840.
- Malik, S., and Roeder, R.G. (2005). Dynamic regulation of pol II transcription by the mammalian Mediator complex. *Trends in biochemical sciences* *30*, 256-263.
- Marston, A.L., Tham, W.H., Shah, H., and Amon, A. (2004). A genome-wide screen identifies genes required for centromeric cohesion. *Science* *303*, 1367-1370.
- Martin, A.M., Pouchnik, D.J., Walker, J.L., and Wyrick, J.J. (2004). Redundant roles for histone H3 N-terminal lysine residues in subtelomeric gene repression in *Saccharomyces cerevisiae*. *Genetics* *167*, 1123-1132.
- Mayer, M.L., Pot, I., Chang, M., Xu, H., Aneliunas, V., Kwok, T., Newitt, R., Aebersold, R., Boone, C., Brown, G.W., *et al.* (2004). Identification of protein complexes required for efficient sister chromatid cohesion. *Mol Biol Cell* *15*, 1736-1745.
- Mc Intyre, J., Muller, E.G., Weitzer, S., Snyderman, B.E., Davis, T.N., and Uhlmann, F. (2007). In vivo analysis of cohesin architecture using FRET in the budding yeast *Saccharomyces cerevisiae*. *Embo J* *26*, 3783-3793.
- McGrew, J., Diehl, B., and Fitzgerald-Hayes, M. (1986). Single base-pair mutations in centromere element III cause aberrant chromosome segregation in *Saccharomyces cerevisiae*. *Mol Cell Biol* *6*, 530-538.
- McGuinness, B.E., Hirota, T., Kudo, N.R., Peters, J.M., and Nasmyth, K. (2005). Shugoshin prevents dissociation of cohesin from centromeres during mitosis in vertebrate cells. *PLoS Biol* *3*, e86.
- McIntosh, J.R., Grishchuk, E.L., and West, R.R. (2002). Chromosome-microtubule interactions during mitosis. *Annu Rev Cell Dev Biol* *18*, 193-219.
- Meraldi, P., and Nigg, E.A. (2002). The centrosome cycle. *FEBS letters* *521*, 9-13.
- Michaelis, C., Ciosk, R., and Nasmyth, K. (1997). Cohesins: chromosomal proteins that prevent premature separation of sister chromatids. *Cell* *91*, 35-45.
- Miele, A., and Dekker, J. (2008). Long-range chromosomal interactions and gene regulation. *Molecular bioSystems* *4*, 1046-1057.

- Miyazaki, W.Y., and Orr-Weaver, T.L. (1994). Sister-chromatid cohesion in mitosis and meiosis. *Annu Rev Genet* 28, 167-187.
- Moldovan, G.L., Pfander, B., and Jentsch, S. (2006). PCNA controls establishment of sister chromatid cohesion during S phase. *Mol Cell* 23, 723-732.
- Monje-Casas, F., Prabhu, V.R., Lee, B.H., Boselli, M., and Amon, A. (2007). Kinetochore orientation during meiosis is controlled by Aurora B and the monopolin complex. *Cell* 128, 477-490.
- Moreno-Herrero, F., de Jager, M., Dekker, N.H., Kanaar, R., Wyman, C., and Dekker, C. (2005). Mesoscale conformational changes in the DNA-repair complex Rad50/Mre11/Nbs1 upon binding DNA. *Nature* 437, 440-443.
- Murray, A.W., and Szostak, J.W. (1985). Chromosome segregation in mitosis and meiosis. *Annual review of cell biology* 1, 289-315.
- Musacchio, A., and Salmon, E.D. (2007). The spindle-assembly checkpoint in space and time. *Nature reviews* 8, 379-393.
- Musio, A., Selicorni, A., Focarelli, M.L., Gervasini, C., Milani, D., Russo, S., Vezzoni, P., and Larizza, L. (2006). X-linked Cornelia de Lange syndrome owing to SMC1L1 mutations. *Nat Genet* 38, 528-530.
- Nabeshima, K., Nakagawa, T., Straight, A.F., Murray, A., Chikashige, Y., Yamashita, Y.M., Hiraoka, Y., and Yanagida, M. (1998). Dynamics of centromeres during metaphase-anaphase transition in fission yeast: Dis1 is implicated in force balance in metaphase bipolar spindle. *Mol Biol Cell* 9, 3211-3225.
- Nasmyth, K., Peters, J.M., and Uhlmann, F. (2000). Splitting the chromosome: cutting the ties that bind sister chromatids. *Science* 288, 1379-1385.
- Nasmyth, K., and Schleiffer, A. (2004). From a single double helix to paired double helices and back. *Philos Trans R Soc Lond B Biol Sci* 359, 99-108.
- Nepveu, A. (2001). Role of the multifunctional CDP/Cut/Cux homeodomain transcription factor in regulating differentiation, cell growth and development. *Gene* 270, 1-15.
- Neuwald, A.F., and Hirano, T. (2000). HEAT repeats associated with condensins, cohesins, and other complexes involved in chromosome-related functions. *Genome Res* 10, 1445-1452.
- Nicklas, R.B. (1967). Chromosome micromanipulation. II. Induced reorientation and the experimental control of segregation in meiosis. *Chromosoma* 21, 17-50.
- Nicklas, R.B., and Koch, C.A. (1969). Chromosome micromanipulation. 3. Spindle fiber tension and the reorientation of mal-oriented chromosomes. *J Cell Biol* 43, 40-50.
- Nishimura, K., Fukagawa, T., Takisawa, H., Kakimoto, T., and Kanemaki, M. (2009). An auxin-based degron system for the rapid depletion of proteins in nonplant cells. *Nature methods* 6, 917-922.

- Nishiyama, T., Ladurner, R., Schmitz, J., Kreidl, E., Schleiffer, A., Bhaskara, V., Bando, M., Shirahige, K., Hyman, A.A., Mechtler, K., *et al.* (2010). Sororin mediates sister chromatid cohesion by antagonizing Wapl. *Cell* *143*, 737-749.
- Nonaka, N., Kitajima, T., Yokobayashi, S., Xiao, G., Yamamoto, M., Grewal, S.I., and Watanabe, Y. (2002). Recruitment of cohesin to heterochromatic regions by Swi6/HP1 in fission yeast. *Nat Cell Biol* *4*, 89-93.
- Oikawa, K., Ohbayashi, T., Kiyono, T., Nishi, H., Isaka, K., Umezawa, A., Kuroda, M., and Mukai, K. (2004). Expression of a novel human gene, human wings apart-like (hWAPL), is associated with cervical carcinogenesis and tumor progression. *Cancer research* *64*, 3545-3549.
- Ossowski, S., Schneeberger, K., Clark, R.M., Lanz, C., Warthmann, N., and Weigel, D. (2008). Sequencing of natural strains of *Arabidopsis thaliana* with short reads. *Genome Res* *18*, 2024-2033.
- Ouspenski, II, Cabello, O.A., and Brinkley, B.R. (2000). Chromosome condensation factor Brn1p is required for chromatid separation in mitosis. *Mol Biol Cell* *11*, 1305-1313.
- Panizza, S., Tanaka, T., Hochwagen, A., Eisenhaber, F., and Nasmyth, K. (2000). Pds5 cooperates with cohesin in maintaining sister chromatid cohesion. *Curr Biol* *10*, 1557-1564.
- Panne, D. (2008). The enhanceosome. *Current opinion in structural biology* *18*, 236-242.
- Partridge, J.F., Borgstrom, B., and Allshire, R.C. (2000). Distinct protein interaction domains and protein spreading in a complex centromere. *Genes Dev* *14*, 783-791.
- Pati, D., Zhang, N., and Plon, S.E. (2002). Linking sister chromatid cohesion and apoptosis: role of Rad21. *Mol Cell Biol* *22*, 8267-8277.
- Pauli, A., Althoff, F., Oliveira, R.A., Heidmann, S., Schuldiner, O., Lehner, C.F., Dickson, B.J., and Nasmyth, K. (2008). Cell-type-specific TEV protease cleavage reveals cohesin functions in *Drosophila* neurons. *Dev Cell* *14*, 239-251.
- Petronczki, M., Matos, J., Mori, S., Gregan, J., Bogdanova, A., Schwickart, M., Mechtler, K., Shirahige, K., Zachariae, W., and Nasmyth, K. (2006). Monopolar attachment of sister kinetochores at meiosis I requires casein kinase 1. *Cell* *126*, 1049-1064.
- Pezzi, N., Prieto, I., Kremer, L., Perez Jurado, L.A., Valero, C., Del Mazo, J., Martinez, A.C., and Barbero, J.L. (2000). STAG3, a novel gene encoding a protein involved in meiotic chromosome pairing and location of STAG3-related genes flanking the Williams-Beuren syndrome deletion. *Faseb J* *14*, 581-592.
- Pfarr, C.M., Coue, M., Grissom, P.M., Hays, T.S., Porter, M.E., and McIntosh, J.R. (1990). Cytoplasmic dynein is localized to kinetochores during mitosis. *Nature* *345*, 263-265.

- Pinsky, B.A., Tatsutani, S.Y., Collins, K.A., and Biggins, S. (2003). An Mtw1 complex promotes kinetochore biorientation that is monitored by the Ipl1/Aurora protein kinase. *Dev Cell* 5, 735-745.
- Porter, A.C., and Farr, C.J. (2004). Topoisomerase II: untangling its contribution at the centromere. *Chromosome Res* 12, 569-583.
- Prescott, E.M., and Proudfoot, N.J. (2002). Transcriptional collision between convergent genes in budding yeast. *Proc Natl Acad Sci U S A* 99, 8796-8801.
- Qi, W., and Yu, H. (2007). KEN-box-dependent degradation of the Bub1 spindle checkpoint kinase by the anaphase-promoting complex/cyclosome. *J Biol Chem* 282, 3672-3679.
- Rabitsch, K.P., Gregan, J., Schleiffer, A., Javerzat, J.P., Eisenhaber, F., and Nasmyth, K. (2004). Two fission yeast homologs of *Drosophila* Mei-S332 are required for chromosome segregation during meiosis I and II. *Curr Biol* 14, 287-301.
- Rabitsch, K.P., Petronczki, M., Javerzat, J.P., Genier, S., Chwalla, B., Schleiffer, A., Tanaka, T.U., and Nasmyth, K. (2003). Kinetochore recruitment of two nucleolar proteins is required for homolog segregation in meiosis I. *Dev Cell* 4, 535-548.
- Rankin, S., Ayad, N.G., and Kirschner, M.W. (2005). Sororin, a substrate of the anaphase-promoting complex, is required for sister chromatid cohesion in vertebrates. *Mol Cell* 18, 185-200.
- Rao, H., Uhlmann, F., Nasmyth, K., and Varshavsky, A. (2001). Degradation of a cohesin subunit by the N-end rule pathway is essential for chromosome stability. *Nature* 410, 955-959.
- Redon, C., Pilch, D.R., Rogakou, E.P., Orr, A.H., Lowndes, N.F., and Bonner, W.M. (2003). Yeast histone 2A serine 129 is essential for the efficient repair of checkpoint-blind DNA damage. *EMBO Rep* 4, 678-684.
- Revenkova, E., Eijpe, M., Heyting, C., Gross, B., and Jessberger, R. (2001). Novel meiosis-specific isoform of mammalian SMC1. *Mol Cell Biol* 21, 6984-6998.
- Riedel, C.G., Katis, V.L., Katou, Y., Mori, S., Itoh, T., Helmhart, W., Galova, M., Petronczki, M., Gregan, J., Cetin, B., *et al.* (2006). Protein phosphatase 2A protects centromeric sister chromatid cohesion during meiosis I. *Nature* 441, 53-61.
- Rieder, C.L., and Alexander, S.P. (1990). Kinetochores are transported poleward along a single astral microtubule during chromosome attachment to the spindle in newt lung cells. *J Cell Biol* 110, 81-95.
- Rohner, S., Gasser, S.M., and Meister, P. (2008). Modules for cloning-free chromatin tagging in *Saccharomyces cerevisiae*. *Yeast* 25, 235-239.
- Rolef Ben-Shahar, T., Heeger, S., Lehane, C., East, P., Flynn, H., Skehel, M., and Uhlmann, F. (2008). Eco1-dependent cohesin acetylation during establishment of sister chromatid cohesion. *Science* 321, 563-566.

- Rollins, R.A., Korom, M., Aulner, N., Martens, A., and Dorsett, D. (2004). *Drosophila* nipped-B protein supports sister chromatid cohesion and opposes the stromalin/Scc3 cohesion factor to facilitate long-range activation of the cut gene. *Mol Cell Biol* *24*, 3100-3111.
- Rollins, R.A., Morcillo, P., and Dorsett, D. (1999). Nipped-B, a *Drosophila* homologue of chromosomal adherins, participates in activation by remote enhancers in the cut and Ultrabithorax genes. *Genetics* *152*, 577-593.
- Rowland, B.D., Roig, M.B., Nishino, T., Kurze, A., Uluocak, P., Mishra, A., Beckouet, F., Underwood, P., Metson, J., Imre, R., *et al.* (2009). Building sister chromatid cohesion: smc3 acetylation counteracts an antiestablishment activity. *Mol Cell* *33*, 763-774.
- Rubio, E.D., Reiss, D.J., Welch, P.L., Distèche, C.M., Filippova, G.N., Baliga, N.S., Aebersold, R., Ranish, J.A., and Krumm, A. (2008). CTCF physically links cohesin to chromatin. *Proc Natl Acad Sci U S A* *105*, 8309-8314.
- Rusche, L.N., Kirchmaier, A.L., and Rine, J. (2003). The establishment, inheritance, and function of silenced chromatin in *Saccharomyces cerevisiae*. *Annu Rev Biochem* *72*, 481-516.
- Salah, S.M., and Nasmyth, K. (2000). Destruction of the securin Pds1p occurs at the onset of anaphase during both meiotic divisions in yeast. *Chromosoma* *109*, 27-34.
- Sanchez-Diaz, A., Kanemaki, M., Marchesi, V., and Labib, K. (2004). Rapid depletion of budding yeast proteins by fusion to a heat-inducible degron. *Sci STKE* *2004*, PL8.
- Santaguida, S., and Musacchio, A. (2009). The life and miracles of kinetochores. *Embo J* *28*, 2511-2531.
- Sauve, A.A., Wolberger, C., Schramm, V.L., and Boeke, J.D. (2006). The biochemistry of sirtuins. *Annu Rev Biochem* *75*, 435-465.
- Schar, P., Fasi, M., and Jessberger, R. (2004). SMC1 coordinates DNA double-strand break repair pathways. *Nucleic Acids Res* *32*, 3921-3929.
- Schmidt, D., Schwalie, P.C., Ross-Innes, C.S., Hurtado, A., Brown, G.D., Carroll, J.S., Flicek, P., and Odom, D.T. (2010). A CTCF-independent role for cohesin in tissue-specific transcription. *Genome Res* *20*, 578-588.
- Schmitz, J., Watrin, E., Lenart, P., Mechtler, K., and Peters, J.M. (2007). Sororin is required for stable binding of cohesin to chromatin and for sister chromatid cohesion in interphase. *Curr Biol* *17*, 630-636.
- Schockel, L., Mockel, M., Mayer, B., Boos, D., and Stemmann, O. (2011). Cleavage of cohesin rings coordinates the separation of centrioles and chromatids. *Nat Cell Biol* *13*, 966-972.
- Schuldiner, O., Berdnik, D., Levy, J.M., Wu, J.S., Luginbuhl, D., Gontang, A.C., and Luo, L. (2008). piggyBac-based mosaic screen identifies a postmitotic function for cohesin in regulating developmental axon pruning. *Dev Cell* *14*, 227-238.

- Schule, B., Oviedo, A., Johnston, K., Pai, S., and Francke, U. (2005). Inactivating mutations in ESCO2 cause SC phocomelia and Roberts syndrome: no phenotype-genotype correlation. *American journal of human genetics* 77, 1117-1128.
- Shang, C., Hazbun, T.R., Cheeseman, I.M., Aranda, J., Fields, S., Drubin, D.G., and Barnes, G. (2003). Kinetochore protein interactions and their regulation by the Aurora kinase Ipl1p. *Mol Biol Cell* 14, 3342-3355.
- Shimada, K., and Gasser, S.M. (2007). The origin recognition complex functions in sister-chromatid cohesion in *Saccharomyces cerevisiae*. *Cell* 128, 85-99.
- Shintomi, K., and Hirano, T. (2009). Releasing cohesin from chromosome arms in early mitosis: opposing actions of Wapl-Pds5 and Sgo1. *Genes Dev* 23, 2224-2236.
- Sidorova, J.M., and Breeden, L.L. (2003). Rad53 checkpoint kinase phosphorylation site preference identified in the Swi6 protein of *Saccharomyces cerevisiae*. *Mol Cell Biol* 23, 3405-3416.
- Skibbens, R.V., Corson, L.B., Koshland, D., and Hieter, P. (1999). Ctf7p is essential for sister chromatid cohesion and links mitotic chromosome structure to the DNA replication machinery. *Genes Dev* 13, 307-319.
- Splinter, E., Heath, H., Kooren, J., Palstra, R.J., Klous, P., Grosveld, F., Galjart, N., and de Laat, W. (2006). CTCF mediates long-range chromatin looping and local histone modification in the beta-globin locus. *Genes Dev* 20, 2349-2354.
- Stead, K., Aguilar, C., Hartman, T., Drexel, M., Meluh, P., and Guacci, V. (2003). Pds5p regulates the maintenance of sister chromatid cohesion and is sumoylated to promote the dissolution of cohesion. *J Cell Biol* 163, 729-741.
- Stemmann, O., Zou, H., Gerber, S.A., Gygi, S.P., and Kirschner, M.W. (2001). Dual inhibition of sister chromatid separation at metaphase. *Cell* 107, 715-726.
- Steuer, E.R., Wordeman, L., Schroer, T.A., and Sheetz, M.P. (1990). Localization of cytoplasmic dynein to mitotic spindles and kinetochores. *Nature* 345, 266-268.
- Straight, A.F., Belmont, A.S., Robinett, C.C., and Murray, A.W. (1996). GFP tagging of budding yeast chromosomes reveals that protein-protein interactions can mediate sister chromatid cohesion. *Curr Biol* 6, 1599-1608.
- Strom, L., Karlsson, C., Lindroos, H.B., Wedahl, S., Katou, Y., Shirahige, K., and Sjogren, C. (2007). Postreplicative formation of cohesion is required for repair and induced by a single DNA break. *Science* 317, 242-245.
- Strom, L., Lindroos, H.B., Shirahige, K., and Sjogren, C. (2004). Postreplicative recruitment of cohesin to double-strand breaks is required for DNA repair. *Mol Cell* 16, 1003-1015.
- Strunnikov, A.V., Hogan, E., and Koshland, D. (1995). SMC2, a *Saccharomyces cerevisiae* gene essential for chromosome segregation and condensation, defines a subgroup within the SMC family. *Genes Dev* 9, 587-599.

- Sumara, I., Vorlaufer, E., Gieffers, C., Peters, B.H., and Peters, J.M. (2000). Characterization of vertebrate cohesin complexes and their regulation in prophase. *J Cell Biol* 151, 749-762.
- Sumara, I., Vorlaufer, E., Stukenberg, P.T., Kelm, O., Redemann, N., Nigg, E.A., and Peters, J.M. (2002). The dissociation of cohesin from chromosomes in prophase is regulated by Polo-like kinase. *Mol Cell* 9, 515-525.
- Sundin, L.J., Guimaraes, G.J., and Deluca, J.G. (2011). The NDC80 complex proteins Nuf2 and Hec1 make distinct contributions to kinetochore-microtubule attachment in mitosis. *Mol Biol Cell* 22, 759-768.
- Sundin, O., and Varshavsky, A. (1980). Terminal stages of SV40 DNA replication proceed via multiply intertwined catenated dimers. *Cell* 21, 103-114.
- Sung, P. (1997). Function of yeast Rad52 protein as a mediator between replication protein A and the Rad51 recombinase. *J Biol Chem* 272, 28194-28197.
- Sutani, T., Kawaguchi, T., Kanno, R., Itoh, T., and Shirahige, K. (2009). Budding yeast Wpl1(Rad61)-Pds5 complex counteracts sister chromatid cohesion-establishing reaction. *Curr Biol* 19, 492-497.
- Taatjes, D.J. (2010). The human Mediator complex: a versatile, genome-wide regulator of transcription. *Trends in biochemical sciences* 35, 315-322.
- Takahashi, K., Murakami, S., Chikashige, Y., Funabiki, H., Niwa, O., and Yanagida, M. (1992). A low copy number central sequence with strict symmetry and unusual chromatin structure in fission yeast centromere. *Mol Biol Cell* 3, 819-835.
- Takahashi, T.S., Yiu, P., Chou, M.F., Gygi, S., and Walter, J.C. (2004). Recruitment of *Xenopus* Scc2 and cohesin to chromatin requires the pre-replication complex. *Nat Cell Biol* 6, 991-996.
- Tanaka, K., Hao, Z., Kai, M., and Okayama, H. (2001). Establishment and maintenance of sister chromatid cohesion in fission yeast by a unique mechanism. *Embo J* 20, 5779-5790.
- Tanaka, T., Cosma, M.P., Wirth, K., and Nasmyth, K. (1999). Identification of cohesin association sites at centromeres and along chromosome arms. *Cell* 98, 847-858.
- Tanaka, T., Fuchs, J., Loidl, J., and Nasmyth, K. (2000). Cohesin ensures bipolar attachment of microtubules to sister centromeres and resists their precocious separation. *Nat Cell Biol* 2, 492-499.
- Tanaka, T.U., Rachidi, N., Janke, C., Pereira, G., Galova, M., Schiebel, E., Stark, M.J., and Nasmyth, K. (2002). Evidence that the Ipl1-Sli15 (Aurora kinase-INCENP) complex promotes chromosome bi-orientation by altering kinetochore-spindle pole connections. *Cell* 108, 317-329.
- Tang, Z., Shu, H., Qi, W., Mahmood, N.A., Mumby, M.C., and Yu, H. (2006). PP2A is required for centromeric localization of Sgo1 and proper chromosome segregation. *Dev Cell* 10, 575-585.

- Tatebe, H., and Yanagida, M. (2000). Cut8, essential for anaphase, controls localization of 26S proteasome, facilitating destruction of cyclin and Cut2. *Curr Biol* *10*, 1329-1338.
- Thein, K.H., Kleylein-Sohn, J., Nigg, E.A., and Gruneberg, U. (2007). Astrin is required for the maintenance of sister chromatid cohesion and centrosome integrity. *J Cell Biol* *178*, 345-354.
- Tomkins, D., Hunter, A., and Roberts, M. (1979). Cytogenetic findings in Roberts-SC phocomelia syndrome(s). *American journal of medical genetics* *4*, 17-26.
- Tooley, J.G., Miller, S.A., and Stukenberg, P.T. (2011). The Ndc80 complex uses a tripartite attachment point to couple microtubule depolymerization to chromosome movement. *Mol Biol Cell* *22*, 1217-1226.
- Toth, A., Ciosk, R., Uhlmann, F., Galova, M., Schleiffer, A., and Nasmyth, K. (1999). Yeast cohesin complex requires a conserved protein, Eco1p(Ctf7), to establish cohesion between sister chromatids during DNA replication. *Genes Dev* *13*, 320-333.
- Toth, A., Rabitsch, K.P., Galova, M., Schleiffer, A., Buonomo, S.B., and Nasmyth, K. (2000). Functional genomics identifies monopolin: a kinetochore protein required for segregation of homologs during meiosis I. *Cell* *103*, 1155-1168.
- Tsou, M.F., and Stearns, T. (2006). Mechanism limiting centrosome duplication to once per cell cycle. *Nature* *442*, 947-951.
- Uhlmann, F., Lottspeich, F., and Nasmyth, K. (1999). Sister-chromatid separation at anaphase onset is promoted by cleavage of the cohesin subunit Scc1. *Nature* *400*, 37-42.
- Uhlmann, F., and Nasmyth, K. (1998). Cohesion between sister chromatids must be established during DNA replication. *Curr Biol* *8*, 1095-1101.
- Uhlmann, F., Wernic, D., Poupard, M.A., Koonin, E.V., and Nasmyth, K. (2000). Cleavage of cohesin by the CD clan protease separin triggers anaphase in yeast. *Cell* *103*, 375-386.
- Unal, E., Arbel-Eden, A., Sattler, U., Shroff, R., Lichten, M., Haber, J.E., and Koshland, D. (2004). DNA damage response pathway uses histone modification to assemble a double-strand break-specific cohesin domain. *Mol Cell* *16*, 991-1002.
- Unal, E., Heidinger-Pauli, J.M., Kim, W., Guacci, V., Onn, I., Gygi, S.P., and Koshland, D.E. (2008). A molecular determinant for the establishment of sister chromatid cohesion. *Science* *321*, 566-569.
- Unal, E., Heidinger-Pauli, J.M., and Koshland, D. (2007). DNA double-strand breaks trigger genome-wide sister-chromatid cohesion through Eco1 (Ctf7). *Science* *317*, 245-248.
- Vagnarelli, P., Morrison, C., Dodson, H., Sonoda, E., Takeda, S., and Earnshaw, W.C. (2004). Analysis of Scc1-deficient cells defines a key metaphase role of vertebrate cohesin in linking sister kinetochores. *EMBO Rep* *5*, 167-171.

- Vakoc, C.R., Mandat, S.A., Olenchock, B.A., and Blobel, G.A. (2005). Histone H3 lysine 9 methylation and HP1gamma are associated with transcription elongation through mammalian chromatin. *Mol Cell* *19*, 381-391.
- van den Bosch, M., Bree, R.T., and Lowndes, N.F. (2003). The MRN complex: coordinating and mediating the response to broken chromosomes. *EMBO Rep* *4*, 844-849.
- van Heemst, D., James, F., Poggeler, S., Berteaux-Lecellier, V., and Zickler, D. (1999). Spo76p is a conserved chromosome morphogenesis protein that links the mitotic and meiotic programs. *Cell* *98*, 261-271.
- Varshavsky, A. (2011). The N-end rule pathway and regulation by proteolysis. *Protein Sci.*
- Vass, S., Cotterill, S., Valdeolmillos, A.M., Barbero, J.L., Lin, E., Warren, W.D., and Heck, M.M. (2003). Depletion of Drad21/Sccl in *Drosophila* cells leads to instability of the cohesin complex and disruption of mitotic progression. *Curr Biol* *13*, 208-218.
- Vaur, S., Feytout, A., Vazquez, S., and Javerzat, J.P. (2012). Pds5 promotes cohesin acetylation and stable cohesin-chromosome interaction. *EMBO Rep* *13*, 645-652.
- Vega, H., Waisfisz, Q., Gordillo, M., Sakai, N., Yanagihara, I., Yamada, M., van Gosliga, D., Kayserili, H., Xu, C., Ozono, K., *et al.* (2005). Roberts syndrome is caused by mutations in ESCO2, a human homolog of yeast ECO1 that is essential for the establishment of sister chromatid cohesion. *Nat Genet* *37*, 468-470.
- Verdaasdonk, J.S., and Bloom, K. (2011). Centromeres: unique chromatin structures that drive chromosome segregation. *Nature reviews* *12*, 320-332.
- Verni, F., Gandhi, R., Goldberg, M.L., and Gatti, M. (2000). Genetic and molecular analysis of wings apart-like (*wapl*), a gene controlling heterochromatin organization in *Drosophila melanogaster*. *Genetics* *154*, 1693-1710.
- Vetter, I.R., Arndt, A., Kutay, U., Gorlich, D., and Wittinghofer, A. (1999). Structural view of the Ran-Importin beta interaction at 2.3 Å resolution. *Cell* *97*, 635-646.
- Waizenegger, I.C., Hauf, S., Meinke, A., and Peters, J.M. (2000). Two distinct pathways remove mammalian cohesin from chromosome arms in prophase and from centromeres in anaphase. *Cell* *103*, 399-410.
- Wang, B., Matsuoka, S., Carpenter, P.B., and Elledge, S.J. (2002a). 53BP1, a mediator of the DNA damage checkpoint. *Science* *298*, 1435-1438.
- Wang, H., Liu, D., Wang, Y., Qin, J., and Elledge, S.J. (2001). Pds1 phosphorylation in response to DNA damage is essential for its DNA damage checkpoint function. *Genes Dev* *15*, 1361-1372.
- Wang, L.H., Mayer, B., Stemmann, O., and Nigg, E.A. (2010). Centromere DNA decatenation depends on cohesin removal and is required for mammalian cell division. *J Cell Sci* *123*, 806-813.

- Wang, S.W., Read, R.L., and Norbury, C.J. (2002b). Fission yeast Pds5 is required for accurate chromosome segregation and for survival after DNA damage or metaphase arrest. *J Cell Sci* *115*, 587-598.
- Warren, C.D., Eckley, D.M., Lee, M.S., Hanna, J.S., Hughes, A., Peyser, B., Jie, C., Irizarry, R., and Spencer, F.A. (2004). S-phase checkpoint genes safeguard high-fidelity sister chromatid cohesion. *Mol Biol Cell* *15*, 1724-1735.
- Waters, J.C., Skibbens, R.V., and Salmon, E.D. (1996). Oscillating mitotic newt lung cell kinetochores are, on average, under tension and rarely push. *J Cell Sci* *109* (Pt 12), 2823-2831.
- Watrin, E., and Peters, J.M. (2009). The cohesin complex is required for the DNA damage-induced G2/M checkpoint in mammalian cells. *Embo J* *28*, 2625-2635.
- Watrin, E., Schleiffer, A., Tanaka, K., Eisenhaber, F., Nasmyth, K., and Peters, J.M. (2006). Human Scc4 is required for cohesin binding to chromatin, sister-chromatid cohesion, and mitotic progression. *Curr Biol* *16*, 863-874.
- Weber, S.A., Gerton, J.L., Polancic, J.E., DeRisi, J.L., Koshland, D., and Megee, P.C. (2004). The kinetochore is an enhancer of pericentric cohesin binding. *PLoS Biol* *2*, E260.
- Weitzer, S., Lehane, C., and Uhlmann, F. (2003). A model for ATP hydrolysis-dependent binding of cohesin to DNA. *Curr Biol* *13*, 1930-1940.
- Wendt, K.S., and Peters, J.M. (2009). How cohesin and CTCF cooperate in regulating gene expression. *Chromosome Res* *17*, 201-214.
- Wendt, K.S., Yoshida, K., Itoh, T., Bando, M., Koch, B., Schirghuber, E., Tsutsumi, S., Nagae, G., Ishihara, K., Mishiro, T., *et al.* (2008). Cohesin mediates transcriptional insulation by CCCTC-binding factor. *Nature* *451*, 796-801.
- Westermann, S., Drubin, D.G., and Barnes, G. (2007). Structures and functions of yeast kinetochore complexes. *Annu Rev Biochem* *76*, 563-591.
- Winey, M., Morgan, G.P., Straight, P.D., Giddings, T.H., Jr., and Mastronarde, D.N. (2005). Three-dimensional ultrastructure of *Saccharomyces cerevisiae* meiotic spindles. *Mol Biol Cell* *16*, 1178-1188.
- Wong, C., and Stearns, T. (2003). Centrosome number is controlled by a centrosome-intrinsic block to reduplication. *Nat Cell Biol* *5*, 539-544.
- Wong, R.W., and Blobel, G. (2008). Cohesin subunit SMC1 associates with mitotic microtubules at the spindle pole. *Proc Natl Acad Sci U S A* *105*, 15441-15445.
- Xu, H., Boone, C., and Brown, G.W. (2007). Genetic dissection of parallel sister-chromatid cohesion pathways. *Genetics* *176*, 1417-1429.
- Yamamoto, A., Guacci, V., and Koshland, D. (1996a). Pds1p is required for faithful execution of anaphase in the yeast, *Saccharomyces cerevisiae*. *J Cell Biol* *133*, 85-97.

- Yamamoto, A., Guacci, V., and Koshland, D. (1996b). Pds1p, an inhibitor of anaphase in budding yeast, plays a critical role in the APC and checkpoint pathway(s). *J Cell Biol* *133*, 99-110.
- Yang, H., Ren, Q., and Zhang, Z. (2008). Cleavage of Mcd1 by caspase-like protease Esp1 promotes apoptosis in budding yeast. *Mol Biol Cell* *19*, 2127-2134.
- Yazdi, P.T., Wang, Y., Zhao, S., Patel, N., Lee, E.Y., and Qin, J. (2002). SMC1 is a downstream effector in the ATM/NBS1 branch of the human S-phase checkpoint. *Genes Dev* *16*, 571-582.
- Yeh, E., Haase, J., Paliulis, L.V., Joglekar, A., Bond, L., Bouck, D., Salmon, E.D., and Bloom, K.S. (2008). Pericentric chromatin is organized into an intramolecular loop in mitosis. *Curr Biol* *18*, 81-90.
- Yen, K., Gitsham, P., Wishart, J., Oliver, S.G., and Zhang, N. (2003). An improved tetO promoter replacement system for regulating the expression of yeast genes. *Yeast* *20*, 1255-1262.
- Yen, T.J., Li, G., Schaar, B.T., Szilak, I., and Cleveland, D.W. (1992). CENP-E is a putative kinetochore motor that accumulates just before mitosis. *Nature* *359*, 536-539.
- Zhang, B., Jain, S., Song, H., Fu, M., Heuckeroth, R.O., Erlich, J.M., Jay, P.Y., and Milbrandt, J. (2007). Mice lacking sister chromatid cohesion protein PDS5B exhibit developmental abnormalities reminiscent of Cornelia de Lange syndrome. *Development (Cambridge, England)* *134*, 3191-3201.
- Zhang, J., Shi, X., Li, Y., Kim, B.J., Jia, J., Huang, Z., Yang, T., Fu, X., Jung, S.Y., Wang, Y., *et al.* (2008a). Acetylation of Smc3 by Eco1 is required for S phase sister chromatid cohesion in both human and yeast. *Mol Cell* *31*, 143-151.
- Zhang, N., Kuznetsov, S.G., Sharan, S.K., Li, K., Rao, P.H., and Pati, D. (2008b). A handcuff model for the cohesin complex. *J Cell Biol* *183*, 1019-1031.
- Zou, H., McGarry, T.J., Bernal, T., and Kirschner, M.W. (1999). Identification of a vertebrate sister-chromatid separation inhibitor involved in transformation and tumorigenesis. *Science* *285*, 418-422.

6 Supplemental data

Table 6.1 Summary of ChIP-Seq reads alignment against the *Saccharomyces cerevisiae* genome.

| | | Untagged | WT | <i>PDS5</i> - degron | <i>SCC3</i> - degron | <i>Δwpl1</i> |
|--|---------------------------|----------------|----------------|-------------------------|-------------------------|----------------|
| Number of reads from ChIP-Seq experiment | | 33,753,63 3 | 31,232,86 4 | 36,054,82 1 | 33,880,10 1 | 32,914,38 8 |
| Reads mapped to Yeast genome | Number | 13,780,13 1 | 17,312,70 1 | 20,785,52 8 | 29,531,33 9 | 20,245,83 7 |
| | mapped ratio (%) | 40.83 | 55.43 | 57.65 | 87.16 | 61.51 |
| Reads uniquely mapped to Yeast genome | Number | 13,436,40 1 | 17,156,95 7 | 29,428,46 7 | 20,096,50 7 | 20,639,51 5 |
| | mapped ratio (%) | 39.8 | 54.93 | 57.24 | 86.86 | 61.06 |
| Reads uniquely mapped to Yeast chromosomal genome | Number | 13,171,59 5 | 16,806,81 4 | 20,198,72 2 | 29,039,73 5 | 20,066,86 5 |
| | mapped ratio (%) | 39.02 | 53.81 | 56.02 | 85.71 | 60.97 |
| | Average coverage | 46.21 | 59.41 | 101.49 | 71.04 | 69.14 |
| | covered region (%) | 95.62 | 94.97 | 95.36 | 95.54 | 95.59 |

Shown are the numbers of sequenced reads for five ChIP-Seq libraries. Between 40-87% of the reads could be aligned to the *Saccharomyces cerevisiae* genome. To

reduce the effect of contamination with human DNA, we also aligned the reads to the human genome and determined the reads uniquely mapping to the yeast genome. For analysis we only used the reads mapping to the chromosomal DNA (in particular, excluding the mitochondrial genome). The average reads coverage for the five libraries ranged from 46-101, covering 95-96% of the chromosomal part of the *Saccharomyces cerevisiae* genome.

7 Appendix

A great part of the presented results in the thesis was published in (Kulemzina et al., 2012)

Cohesin Rings Devoid of Scc3 and Pds5 Maintain Their Stable Association with the DNA

Irina Kulemzina¹, Martin R. Schumacher¹, Vikash Verma¹, Jochen Reiter^{1,2a}, Janina Metzler¹, Antonio Virgilio Failla^{1,2b}, Christa Lanz², Vipin T. Sreedharan^{1,2c}, Gunnar Rättsch^{1,2c}, Dmitri Ivanov^{1*}

1 Friedrich Miescher Laboratory of the Max Planck Society, Tübingen, Germany, **2** Max Planck Institute for Developmental Biology, Tübingen, Germany

Abstract

Cohesin is a protein complex that forms a ring around sister chromatids thus holding them together. The ring is composed of three proteins: Smc1, Smc3 and Scc1. The roles of three additional proteins that associate with the ring, Scc3, Pds5 and Wpl1, are not well understood. It has been proposed that these three factors form a complex that stabilizes the ring and prevents it from opening. This activity promotes sister chromatid cohesion but at the same time poses an obstacle for the initial entrapment of sister DNAs. This hindrance to cohesion establishment is overcome during DNA replication via acetylation of the Smc3 subunit by the Eco1 acetyltransferase. However, the full mechanistic consequences of Smc3 acetylation remain unknown. In the current work, we test the requirement of Scc3 and Pds5 for the stable association of cohesin with DNA. We investigated the consequences of Scc3 and Pds5 depletion *in vivo* using degron tagging in budding yeast. The previously described DHFR-based N-terminal degron as well as a novel Eco1-derived C-terminal degron were employed in our study. Scc3 and Pds5 associate with cohesin complexes independently of each other and require the Scc1 “core” subunit for their association with chromosomes. Contrary to previous data for Scc1 downregulation, depletion of either Scc3 or Pds5 had a strong effect on sister chromatid cohesion but not on cohesin binding to DNA. Quantity, stability and genome-wide distribution of cohesin complexes remained mostly unchanged after the depletion of Scc3 and Pds5. Our findings are inconsistent with a previously proposed model that Scc3 and Pds5 are cohesin maintenance factors required for cohesin ring stability or for maintaining its association with DNA. We propose that Scc3 and Pds5 specifically function during cohesion establishment in S phase.

Citation: Kulemzina I, Schumacher MR, Verma V, Reiter J, Metzler J, et al. (2012) Cohesin Rings Devoid of Scc3 and Pds5 Maintain Their Stable Association with the DNA. *PLoS Genet* 8(8): e1002856. doi:10.1371/journal.pgen.1002856

Editor: Beth A. Sullivan, Duke University, United States of America

Received: November 24, 2011; **Accepted:** June 11, 2012; **Published:** August 9, 2012

Copyright: © 2012 Kulemzina et al. This is an open-access article distributed under the terms of the Creative Commons Attribution License, which permits unrestricted use, distribution, and reproduction in any medium, provided the original author and source are credited.

Funding: The funding was provided by Max Planck Society. The funders had no role in study design, data collection and analysis, decision to publish, or preparation of the manuscript.

Competing Interests: The authors have declared that no competing interests exist.

* E-mail: dmitri.ivanov@tuebingen.mpg.de

2a Current address: Lehrstuhl für Chemie Biogener Rohstoffe, Technische Universität München, Straubing, Germany

2b Current address: Universitätsklinikum Hamburg-Eppendorf, Hamburg, Germany

2c Current address: Computational Biology Center, Memorial Sloan-Kettering Cancer Center, New York, New York, United States of America

Introduction

Cohesin is a ring-shaped protein complex whose major function is to hold sister chromatids together from the onset of DNA replication until their separation to daughter cells in anaphase of mitosis (for review see [1]). The cohesin ring is composed of Smc1, Smc3 and Scc1. At least three additional proteins, Scc3, Pds5, and Wpl1, associate with the ring. Smc1 and Smc3 both contain a 50 nm long intramolecular anti-parallel coiled coil flanked by a central hinge domain on one side and, on the other, by an ATPase head domain formed from the N and C-terminal regions of the protein. The hinge domain of Smc1 associates with the hinge domain of Smc3. Connecting the two head domains is Scc1, thus completing the ring.

Cohesin was recently demonstrated to function by capturing two sister DNAs inside a single ring [2] although alternative models have also been proposed [3]. However, the ring is also capable of embracing a single sister, which does not lead to the establishment of sister chromatid cohesion [4]. Stable capture of both sisters is ensured via the action of an acetyltransferase, Eco1 [5–7]. Eco1 acetylates two adjacent lysine residues in the ATPase

head domain of Smc3, which in budding yeast correspond to lysines 112 and 113 [8–10]. Mutation of both lysines to non-acetylatable arginines is lethal while their mutation to acetylation-mimicking asparagines or glutamines makes Eco1 dispensable for cohesion establishment. The relevant target of Eco1 acetylation in S phase differs from acetylation in response to double-stranded DNA breaks when two lysine residues of Scc1, K84 and K210, are proposed to be critical [11]. Acetylation of cohesin is initiated during S phase after it is loaded onto DNA and persists through G2 until cell division. Acetylated cohesin can only inefficiently establish cohesion, necessitating either *de novo* synthesis of non-acetylated Smc3 or deacetylation of the Smc3 that was released from DNA in the previous mitotic cycle. A deacetylase, Hos1 was recently discovered to be critical for Smc3 deacetylation [12–14].

The mechanistic role of cohesin acetylation remains unclear. It is reported to counteract the function of Wpl1, also known in budding yeast as Rad61 [9,15]. While Wpl1 function in yeast remains to be established, the vertebrate Wpl1 orthologue is required for the removal of cohesin from DNA in prophase of mitosis [16,17]. Wpl1 forms a complex with Scc3 and Pds5 *in vitro* and mutations in *WPL1*, *SCC3* and *PDS5* genes were found to

Author Summary

When a cell divides, each daughter cell receives one, and only one, of each sister DNA molecule from the mother. These identical DNA molecules, called chromatids, result from the replication of a single DNA molecule and are held together by a ring-shaped protein complex termed cohesin. As a cell's genetic information is divided into several distinct chromosomes, this arrangement, termed sister chromatid cohesion, makes it possible to distinguish sister and non-sister chromatids and is a prerequisite for the faithful division of genetic information. Cohesin rings, consisting of three subunits, trap two sister DNA molecules inside them. Additional proteins are required to load the rings onto DNA and to ensure that they capture both sister DNA molecules. We have investigated the roles of Scc3 and Pds5, two proteins that associate with cohesin rings, and were previously proposed to keep them stably locked once loaded onto DNA. Surprisingly, when we depleted Scc3 and Pds5 from yeast, the rings remained stably associated with the DNA; however, cohesion between the sisters was severely compromised. We conclude that Scc3 and Pds5 function to capture the two sister DNA molecules together inside the cohesin ring.

suppress lethality caused by *eco1* deletion [18]. *SCC3* [6] and *PDS5* [19,20] were discovered in yeast as genes that when mutated result in cohesion defects. Both proteins are conserved in evolution from yeast to humans [21–23]. In budding yeast both *SCC3* and *PDS5* are essential. However, in fission yeast *PDS5* can be deleted [24], reflecting different requirements for Pds5 function in different organisms. In budding yeast, Pds5 is comprised of 26 HEAT repeats and a highly charged C-terminal domain [19]. Scc3 was also predicted to contain HEAT repeats [25], although they appear too divergent to be predicted with statistical confidence. The phosphorylation of Scc3 in mammalian mitosis leads to the Wpl1-dependent removal of cohesin from chromosomes [26]. Therefore it appears that all three proteins are, at least in some organisms, involved in destabilizing the association of cohesin with DNA. On the other hand, Scc3 and Pds5 have been proposed to be cohesin maintenance factors because temperature-sensitive mutations in the respective genes result in reduced association of cohesin with DNA [6,19]. Importantly, Eco1 mediated cohesin acetylation is implicated in the stabilization of cohesin binding to DNA during S phase [27] and at the same time it is thought to counteract the function of Scc3, Pds5 and Wpl1 [18].

Early studies of Scc3 and Pds5 function *in vivo* relied on conditional mutations that inactivate the proteins at the restrictive temperature of 37°C. These mutants frequently contain multiple amino acid substitutions and the mechanism by which they affect protein function is therefore difficult to elucidate. We decided to deplete Scc3 and Pds5 from the cell by fusing the genes to degon sequences. A “conventional” DHFR-based temperature-induced degon fused to Scc3 caused the degradation of Scc1, a “core” subunit of cohesin complex precluding the specific analysis of the role of Scc3. However, using a novel and efficient degon derived from the Eco1 protein we were able to specifically deplete Scc3 and Pds5 in the cell while leaving the “core” cohesin subunits intact. Our results demonstrate that in the absence of Scc3 and Pds5, cohesin rings remain stably associated with chromosomes. Moreover, their distribution throughout yeast genome remains unaffected. However, the destabilization of Scc3 and Pds5 significantly weakens sister chromatid cohesion and causes chromosomal mis-segregation, suggesting that the essential func-

tion of these proteins is in cohesion establishment rather than the maintenance of cohesin on DNA.

Results

Interaction of Scc3, Pds5 and Wpl1 with the cohesin ring subunits *in vitro*

The arrangement of Scc3 and Pds5 proteins within cohesin complex is poorly understood. Recombinant yeast and human Scc3 proteins were reported to interact respectively with the C-terminal part of Scc1 [28] or central region of Scc1 which is poorly conserved between yeast and humans [29]. Recently, it was reported that a deletion of nine amino acids (319–327) at the end of the central region of Scc1 in budding yeast disrupts its association with Scc3 *in vivo* [30]. It has also been proposed that Scc3 facilitates the interaction between Pds5/Wpl1 and the cohesin ring [29].

We investigated interactions of Scc3, Pds5 and Wpl1 with cohesin ring subunits using glycerol gradient centrifugation of recombinant yeast proteins purified from *E. coli*. All proteins were purified using gel filtration chromatography and were confirmed not to be aggregated. In agreement with a previous study [18], we were able to detect a strong interaction between Wpl1 and Pds5. Both proteins migrate in the same fractions, which are significantly faster than Pds5 alone, the larger of the two subunits (Figure 1A). Binding between Scc3 and Wpl1 appeared to be weaker. Wpl1 was detected in the later fractions containing Scc3 but there was little change in Scc3 migration on the gradient possibly due to low stability of the complex. Addition of Scc3 to the Pds5-Wpl1 complex resulted in a further shift towards the bottom of the gradient consistent with the formation of a trimeric complex, which has been previously proposed [18]. However, this shift was very small considering an expected 1.7 fold increase in the estimated molecular weight of the trimeric complex (354 kDa) compared to the Pds5/Wpl1 dimer (221 kDa). It is possible that the Scc3/Pds5/Wpl1 complex assumes a very extended conformation that results in unexpectedly slow migration through glycerol gradients. Alternatively, Scc3 might only weakly associate with the complex making the interaction too unstable to survive the long centrifugation.

We next explored interactions between the subunits of the cohesin complex and Scc3, Pds5, and Wpl1 *in vitro* using gradient centrifugation. We could not detect any interaction of these cohesin-associated proteins with the Smc1 and Smc3 head and hinge domains or with the Smc3 coiled coil (data not shown). Because recombinant Scc1 has poor solubility and could not be used in gradient centrifugation experiments, we expressed its N-terminal, middle and C-terminal regions as GST-fusions and employed a GST pull-down assay to test their interaction with the Scc3, Pds5 and Wpl1. The Scc3/Wpl1 complex was found to interact with the C-terminal part of Scc1 (Figure 1B), consistent with an earlier study [28]. Interestingly, the Pds5/Wpl1 complex bound to the N-terminal region of Scc1 (Figure 1B), which has previously been demonstrated to interact with the Smc3 head [28]. Remarkably, although Scc3, Pds5, and Wpl1 were mixed together in these experiments, they interacted with Scc1 as separate Scc3/Wpl1 and Pds5/Wpl1 heterodimers rather than as a single trimeric complex. Accordingly, only a small amount of Scc3 was detected in the pull-down with N-terminal region of Scc1 and very little Pds5 was found to interact with Scc1 C-terminus. These observations further highlight the poor stability of the Scc3/Pds5/Wpl1 complex, even at the low salt concentrations that were used in our experiments.

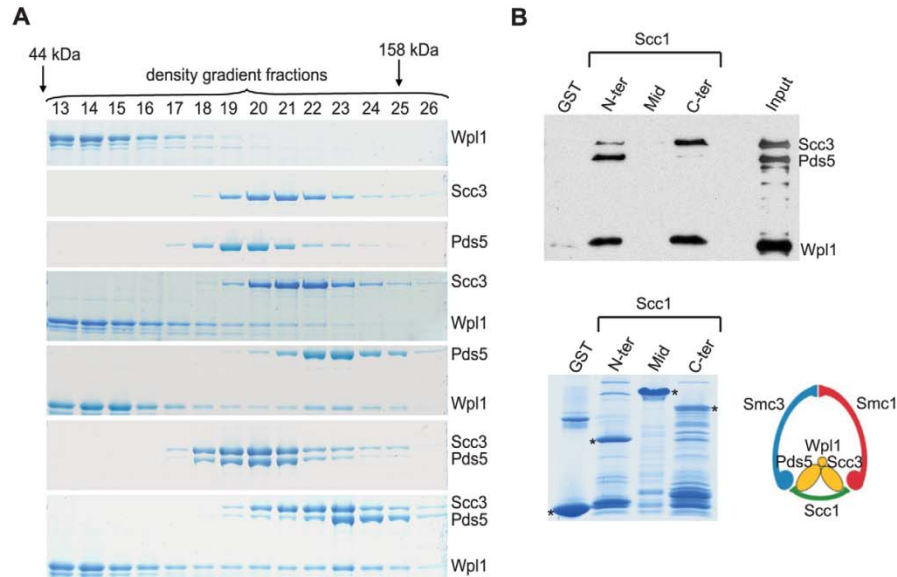


Figure 1. Scc3, Pds5, and Wpl1 form a complex and associate with Scc1 “core” subunit of cohesin. (A) Purified recombinant Scc3, Pds5 and Wpl1 proteins were mixed as indicated and separated by ultracentrifugation on a 10–30% glycerol gradient. A total of 44 gradient fractions were collected and analyzed on a Coomassie-stained 6% SDS-PAGE. Only fractions containing the proteins are shown. Positions of molecular size markers are indicated. (B) Recombinant His6-tagged Scc3, Pds5, and Wpl1 were mixed together and incubated with glutathione-agarose beads charged with GST or GST-fused to the N-terminal (aa 1–168), middle (aa 169–337) or C-terminal (aa 338–566) regions of Scc1. Beads eluates were analyzed by Western blotting with Penta-His antibody (QIAGEN) (upper panel). Coomassie-stained GST-beads are shown in the lower panel. doi:10.1371/journal.pgen.1002856.g001

The interaction sites of Scc1 that we observed for Scc3 and Pds5 suggest a possible role for these proteins in stabilizing the cohesin ring. Pds5 bound close to the interface between the Scc1 N-terminal domain and the Smc3 head while Scc3 binding was adjacent to the interface between the Scc1 C-terminal domain and the Smc1 head. Thus, Pds5 and Scc3 can potentially re-enforce the interaction of Scc1 with Smc3 and/or affect the interaction between the Smc heads, which is required for ATP hydrolysis and opening of the hinge during cohesin loading on DNA [31].

Pds5 depletion has no effect on cohesin association with chromosomes

In order to examine whether Scc3 and Pds5 stabilize cohesin rings on DNA *in vivo* we wanted to deplete them from yeast cells. Since both proteins are essential in budding yeast, we constructed *SCC3* and *PDS5* gene fusions to an N-terminal “degron” sequence. In these experiments we utilized a “conventional” DHFR-based degron in a strain that overexpresses an ubiquitin ligase Ubr1 from the *GALI* promoter [32,33]. Upon shifting to 37°C the degron unfolds and is recognized by Ubr1, which leads to ubiquitinylation and degradation of the target protein. The target gene is placed under the control of the *CUP1* promoter which is shut down in the absence of CuSO_4 in the medium. When applied to Scc3 and Pds5, this “conventional” degron approach resulted in a very moderate decrease in protein abundance and strains were able to grow at 37°C on galactose-containing medium without CuSO_4 (data not shown). Therefore we utilized an alternative approach to silence *SCC3* and *PDS5* transcription described in

[34]. Tet operator sequences were introduced in the promoter. In the absence of doxycycline, transactivator (tTA) activates transcription of the gene while in the presence of doxycycline a Tet repressor (tetR-SSN6) replaces transactivator and silences transcription. This approach resulted in an efficient depletion of Scc3 and Pds5 proteins in the cell, as judged by Western blot analysis (Figure S1) and chromosomal spreads (Figure 2). Strains were unable to grow at 37°C on galactose-containing medium with doxycycline. However, protein levels of Scc1, a “core” subunit of cohesin complex, were also reduced when the degron was induced. The reduction of Scc1 abundance was only modest in the case of Pds5 but very significant when Scc3 was destabilized (Figure 2B and E). This result implied that the Scc3-degron targets Scc1 for degradation and precluded further analysis of the role of Scc3 *in vivo* using a “conventional” degron approach. Surprisingly, the destruction of Pds5 had little or no effect on the amount of Scc1 detected in chromosomal spreads regardless of whether the degron was induced in cells arrested in G2 with nocodazole (Figure 2A) or already in G1 prior to cohesin loading on DNA (Figure 2D). Destruction of Pds5 in a single cycle experiment had little effect on sister chromatid cohesion regardless of when the degron was induced (Figure S2).

The Eco1 protein contains degron sequences that can be used to specifically deplete Scc3 and Pds5 from the cell

In experiments employing a Scc1-Eco1 fusion construct, we discovered that the fusion protein was destroyed in cells arrested in G2 by nocodazole treatment (Figure S3A), which resulted in

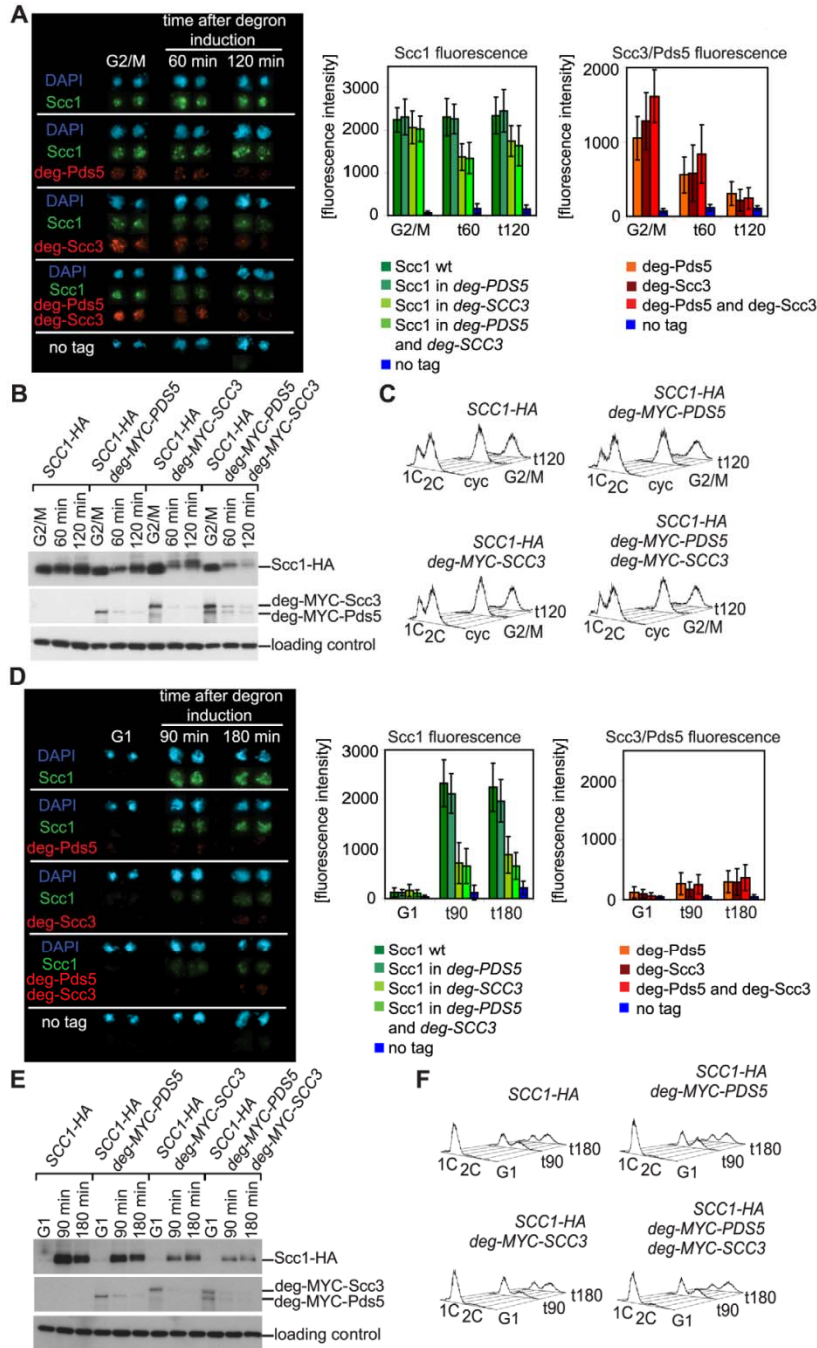


Figure 2. Depletion of Scc3 and Pds5 with a “conventional” temperature-sensitive degron. (A–C) Strains 2395 (*SCC1-HA6*), 2452 (*SCC1-HA6*, *degron-MYC18-PDS5*), 2455 (*SCC1-HA6*, *degron-MYC18-SCC3*) and 2456 (*SCC1-HA6*, *degron-MYC18-PDS5*, *degron-MYC18-SCC3*) were arrested with nocodazole in YEP raffinose at 30°C for 2 hours, resuspended in YEP galactose containing nocodazole and incubated for 45 minutes at 30°C to induce the expression of Ubr1. Cells were shifted to 37°C in YEP galactose containing nocodazole and doxycycline to deplete Pds5 and/or Scc3. (A) Chromosomal spreads were prepared at the indicated time points and stained with DAPI for DNA, anti-HA (mouse, 16B12) and anti-MYC (rabbit, 71D10) antibodies. The secondary antibodies were Alexa Fluor 488 anti-mouse and Alexa Fluor 568 anti-rabbit. Protein fluorescence was quantified using Metamorph software. At every time point fluorescence of 50 nuclei was determined. Error bars represent standard deviation. (B) Western blot of TCA protein extracts probed with anti-HA (16B12), anti-MYC (71D10) and anti-Cdc28 (sc-28550, Santa Cruz). (C) FACS analysis of cellular DNA content. (D–F) Strains were staged in G1 with α -factor in YEP raffinose at 30°C, resuspended in YEP galactose containing α -factor and incubated for 45 minutes at 30°C to induce the expression of Ubr1. Cells were then shifted to 37°C in YEP galactose containing doxycycline and α -factor, incubated for 90 minutes to deplete Pds5 and/or Scc3 and subsequently released in YEP galactose containing nocodazole and doxycycline at 37°C. Chromosomal spreads (D), Western blot (E), and FACS analysis of cellular DNA content (F) are shown. doi:10.1371/journal.pgen.1002856.g002

lethality unless an “unfused” wild type version of Scc1 was co-expressed. This observation led us to examine the abundance of the Eco1 protein throughout the cell cycle. We found that Eco1 is down-regulated when cells exit S-phase and is dramatically reduced in G2 arrested cells (Figure 3A). During the preparation of this manuscript, the existence of a Cdk1-dependent degron was reported for Eco1 [35].

Surprisingly, and in contrast to the *SCC1-ECO1* strain, a *SCC3-ECO1* strain was viable when endogenous *SCC3* and *ECO1* genes were both deleted, indicating that the fusion protein can fulfill the essential functions of both Scc3 and Eco1. Nevertheless, the Scc3-Eco1 fusion protein was destroyed in nocodazole arrested cells similarly to the Scc1-Eco1 fusion (Figure S3C).

The Eco1 protein is comprised of three domains: an N-terminal region containing the PCNA-interacting PIP box and C₂H₂ Zinc-finger, the presumably unstructured S/P-rich middle region and the C-terminal acetyltransferase domain (Figure S3B). In order to determine the localization of degron sequences within Eco1 we fused *SCC3* and *SCC1* genes to each of the three domains of *ECO1*. Fusion of the N-terminal domain had no effect on the abundance of the fusion proteins while fusion of either the middle region or the acetyltransferase domain led to reduced protein levels throughout the cell cycle and disappearance of the fusion proteins after S phase (Figure 3B and Figure S3C).

In further experiments we exploited the ability of the middle region of Eco1 to induce protein degradation in order to address the function of Scc3 and Pds5. Endogenous *SCC3* and *PDS5* genes were tagged at their C-terminus with an HA6 sequence followed by amino acids 63–109 from the middle region of *ECO1*, hereafter referred to as “degron”. This system allowed us to monitor the abundance of Scc3 and Pds5 proteins throughout the cell cycle (Figure 3B). Fusion of *SCC3* and *PDS5* to a degron resulted in a dramatic reduction of the native levels of the respective proteins. However, the decrease in protein abundance was observed throughout the cell cycle. These results suggest that when fused to other proteins, the Eco1-derived degron does not necessarily have an ability to specifically induce protein degradation after the completion of S phase but rather reduces protein stability throughout the cell cycle. Importantly for our study, the amount of Scc1 reduced only slightly in the *PDS5* degron strain and even modestly elevated in the *SCC3* degron strain (Figure 3C). With the use of N-terminal Myc tag in addition to C-terminal HA tag and degron we were able to confirm that degradation of Scc3 and Pds5 proceeded to completion and no stable fragments could be detected in the degron fusion strains (Figure S3D).

We estimated the absolute numbers of Scc3 and Pds5 molecules per cell remaining in degron strains. Serial dilutions of highly purified recombinant Scc3-HA6 and Pds5-HA6 proteins were compared to dilutions of cell lysates from the wild type and degron strains on a Western blot (Figure 3D and E). This analysis allows us to estimate that in nocodazole arrested budding yeast there are

approximately 4500 molecules of Scc3 and 10000 molecules of Pds5 per cell, which is in agreement with the numbers provided in the yeast database (www.yeastgenome.org). In the respective degron strains, there are approximately 250 molecules of Scc3 and Pds5 each, or about 15 molecules per chromosome assuming that 100% of Scc3 and Pds5 are associated with cohesin complexes and loaded on the DNA which is most likely an overestimate. A similar analysis performed with Scc1 resulted in an estimate of 4000 Scc1 molecules per haploid yeast genome [36]. Therefore in the degron strains only 6% or less of cohesin complexes can be associated with Scc3 or Pds5.

To confirm that Scc3 and Pds5 levels decreased due to protein turnover in degron strains, we incubated nocodazole-arrested cultures with cyclohexamide, an inhibitor of protein synthesis. As expected, the levels of wild type Scc3 and Pds5 as well as those of the Scc1 and Smc3 cohesin subunits remained stable throughout the 120 minutes incubation. In contrast, the abundance of the Scc3-degron and Pds5-degron proteins was significantly reduced upon inhibition of protein synthesis (Figure S4).

Pds5 and Scc3 recruit Wpl1 to cohesin complexes

To determine the effects of Scc3 and Pds5 depletion on the architecture of cohesin complexes, we performed the immunoprecipitation experiments (Figure 4). Scc3 could be efficiently co-immunoprecipitated with Scc1 or Smc3 in *PDS5*-degron strains and Pds5 could be co-immunoprecipitated with Scc1 and Smc3 in *SCC3*-degron strains, indicating that Scc3 and Pds5 associate with the cohesin ring independently of each other.

In order to determine whether binding of Wpl1 to cohesin rings requires Scc3 or Pds5, we immunoprecipitated Scc1 (Figure 4C and D) and Smc3 (Figure 4G and H) from wild type, *SCC3*-degron or *PDS5*-degron strains and detected Wpl1 in the pull-down fraction by Western blot. Wpl1 was co-immunoprecipitated with “core” cohesin subunits in the wild type strain. However, the amount of cohesin-bound Wpl1 was reduced in the absence of Pds5 indicating that Pds5 is important for Wpl1 recruitment to cohesin. Depletion of Scc3 resulted in a less pronounced reduction of cohesin-associated Wpl1 suggesting a minor role of Scc3 in Wpl1 recruitment.

Scc3 and Pds5 are not required for the maintenance of the bulk of cohesin on DNA

To confirm that most of the cohesin complexes loaded onto chromosomes in the degron strains are devoid of Scc3 and Pds5, we compared the amounts of Scc3 and Pds5 wild type and degron-fused proteins in chromosome spreads (Figure 5A) and in chromatin pellets (Figure S5). While wild type Scc3 and Pds5 were readily detectable on chromosomes during S phase and G2, the fusion proteins were non-detectable throughout the cell cycle. Remarkably, a dramatic reduction in the amounts of Scc3 and Pds5 bound to chromosomes in the degron-fusion strains did not

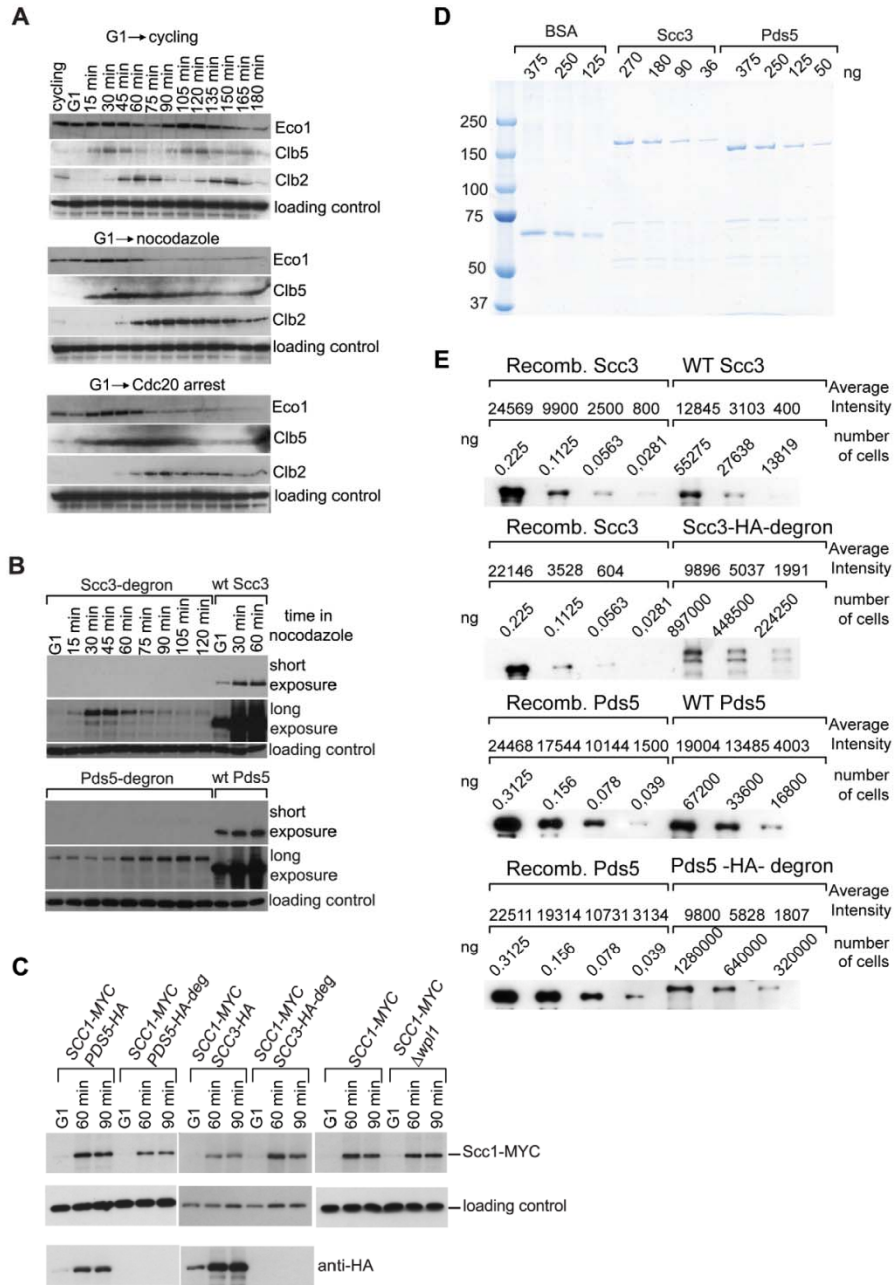


Figure 3. Eco1 contains a degron. (A) 1222 strain with *CDC20* expressed from a methionine-repressible promoter (*Eco1-TAP*) was staged in G1 with α -factor and then released into three different media. Release into the medium without methionine allows cell cycling (top) while release into full medium with methionine or nocodazole (middle and bottom) results in progression through replication and eventual G2 arrest. Expression of S

phase cyclin Clb5 is induced during DNA replication while cyclin Clb2 accumulates in G2 and is destroyed in mitosis. TCA protein extracts were prepared and analyzed by Western blot. Eco1 was detected with peroxidase-anti-peroxidase, Clb5 with sc-6704, Clb2 with sc-9071, loading control with anti-Cdc28 (sc-28550, Santa Cruz). (B) Depletion of Scc3 and Pds5 with an Eco1-derived degron. G1-staged strains 12544 (*SCC3-HA6*), 1323 (*SCC3-HA6-degron*), 1677 (*PDS5-HA6*) and 1675 (*SCC3-HA6-degron*) were released into full media with nocodazole. Western blot was probed with anti-HA antibody. (C) Scc1 protein level is unchanged in the strains with Eco1-derived degron. Strains 1815 (*SCC1-Myc18, PDS5-HA6*), 1818 (*SCC1-Myc18, PDS5-HA6-degron*), 1813 (*SCC1-Myc18, SCC3-HA6*), 1625 (*SCC1-Myc18, SCC3-HA6-degron*), 10589 (*SCC1-MYC18*) and 1906 (*SCC1-MYC18, Awpl1*) were staged in G1 with α -factor and released into media with nocodazole. Western blot was probed with anti-HA, anti-Myc and anti-Cdc28 antibodies. The same yeast cultures were used for chromosomal spreads (Figure 5) and for FACS analysis of cellular DNA content (Figure S13A). (D and E) Determination of Scc3 and Pds5 copy number per yeast cell. (D) Coomassie-stained gel with serial dilutions of purified recombinant Scc3-HA6, Pds5-HA6 and BSA (NEB #B9001) as a standard. (E) Protein extracts were prepared from nocodazole-arrested strains 1323 (*SCC3-HA6-degron*), 1479 (*SCC3-HA6*), 1675 (*PDS5-HA6-degron*) and 1677 (*PDS5-HA6*). Extracts from the indicated number of cells were analyzed by Western blot with anti-HA antibody. Known quantities of recombinant Scc3-HA6 and Pds5-HA6 were used as standards. Bands were quantified with MetaMorph. doi:10.1371/journal.pgen.1002856.g003

result in the reduction of chromosome-associated Scc1 (Figure 5A and Figure S5) or Smc3 (Figure S6). We conclude that stoichiometric quantities of Scc3 and Pds5 are not required to maintain cohesin on DNA. In addition, we could not detect any reduction in the amount of Pds5 bound to chromosomes in the *SCC3*-degron strain or any reduction in the amount of Scc3 bound to chromosomes in the *PDS5*-degron strain (Figure 5B), suggesting that they bind to DNA independently of each other. In order to address whether Scc3 and Pds5 can bind to chromatin independently of cohesin rings we performed chromosome spreads as the cells were released from G1 arrest in the absence of Scc1 (Figure S7). A yeast strain expressing Scc1 from the *GAL* promoter was arrested in G1 with α -factor and then released from the arrest into media containing galactose or glucose. No cohesin was detected on chromatin during G1 arrest. In galactose the appearance of full length Scc1 correlated with Scc1, Scc3 and Pds5 being detected on chromosome spreads while in glucose-containing media the level of Scc1 remained very low and no Scc3 and Pds5 were detected on chromosomes. Therefore, most if not all Scc3 and Pds5 are recruited to chromosomes by cohesin rings.

As Scc3 and Pds5 were both reported to associate with Wpl1, we examined whether Wpl1 affects the association of Scc3 and Pds5 with chromosomes. We could not detect any change in the amounts of Scc3, Pds5, Smc3 or Scc1 on chromosomes in the *Awpl1* strain compared to wild type (Figure 5C and Figure S6). We were not able to detect Wpl1 in chromosome spreads under our experimental conditions which precluded the reciprocal experiment.

Since fluorescence measurements performed on chromosomal spreads provide only crude estimates of the quantity of cohesin associated with chromosomes, we performed ChIP-qPCR analysis on the Scc1 associated with the centromere-adjacent region, or with cohesin positive or negative sites on chromosomal arms (Figure S8). The Scc1 ChIP was normalized to the efficiency of histone H3 IP at the same loci as described in [15]. Using this careful analysis we could detect a marginal decrease in the amount of Scc1 associated with the centromere-adjacent region or chromosomal arm sites in the *SCC3*-degron strain compared to wild type. Consistent with a previous report [15], we observed a 2–3 fold reduction in the amount of Scc1 bound to chromatin in the *Awpl1* and *PDS5*-degron strains. Remarkably, *wpl1* deletion has a very similar effect on the amount of Scc1 associated with chromosomal loci as does the depletion of Pds5, although *WPL1* is non-essential and its deletion results in a relatively small sister chromatid cohesion defect (see below).

To determine whether Scc3 or Pds5 target cohesin rings to distinct sites on chromosomes, we investigated the genome-wide distribution of cohesin in wild type, *SCC3*-degron, *PDS5*-degron and *Awpl1* strains arrested in G2 with nocodazole. Using a ChIP-Seq approach, we found that the overall Scc1 distribution was very similar in *SCC3*-degron, *PDS5*-degron and *Awpl1* strains compared

to wild type with correlation coefficients 0.88, 0.80 and 0.83, respectively (Figure 6A and Figure S9A). We also could not detect any reproducible differences in cohesin distribution around the centromeres (Figure 6B) and at the tDNA genes (Figure S9B) which serve as the sites of cohesin loading onto DNA and are associated with cohesin loader Scc2/Scc4 complex [30].

Scc3 and Pds5 are not required for the stable association of cohesin with DNA

Although the amount of cohesin on chromosomes in *SCC3*-degron and *PDS5*-degron strains was similar to the wild type strain, it remained possible that the association of cohesin rings with DNA is less stable when Scc3 or Pds5 are missing. To test this possibility we performed a fluorescence recovery after photobleaching (FRAP) experiment. We used yeast strains in which endogenous *SCC1* (Figure 7A) or *SMC3* (Figure S10) genes were tagged with *GFP*. It was previously reported that, in metaphase cells, Smc3-GFP is concentrated between the separated spindle poles and forms a cylindrical array where it is stably bound to DNA. It does not recover fluorescence after photobleaching [18,37]. In contrast, an ATP hydrolysis-defective Smc3-GFP mutant that is unstably bound to centromeres, forms distinct foci in the nucleus instead of the cylindrical “barrel” and rapidly recovers fluorescence, $t_{1/2} = 3.4$ s [30]. In our experiments we photobleached a portion of the GFP fluorescence in metaphase cells and did not observe fluorescence recovery for the duration of the experiment (5 minutes) in either the wild type, *SCC3*-degron, *PDS5*-degron or *Awpl1* strains. Histone H2B-GFP was used as a control and recovered fluorescence in parallel experiments (Figure 7B). Thus, cohesin rings are capable of maintaining a stable association with DNA in vivo in the absence of Wpl1 and when the amounts of Scc3 and Pds5 are greatly reduced. We conclude that the essential function of Pds5 and Scc3 cannot be the maintenance of cohesin rings in the closed state when on DNA.

As Pds5 associates with cohesin rings in a salt-sensitive manner and is present in sub-stoichiometric amounts in cohesin immunoprecipitates from cells, we used FRAP to determine whether there is significant turn-over of Pds5 and Scc3 on chromosomes. We did not observe any fluorescence recovery of Pds5-GFP and Scc3-GFP in our experiments (Figure 7B). Therefore, Pds5 and Scc3 are likely to be stable subunits of DNA-bound cohesin complexes in the cell under physiological conditions. Wpl1-GFP does not form a cylindrical array in metaphase cells and thus could not be photobleached. The diffuse fluorescent pattern observed for Wpl1-GFP suggests that it is not a stable cohesin subunit in the cell or that it is associated with only a small fraction of the cohesin complexes.

To demonstrate that cohesin rings devoid of Scc3 and Pds5 are topologically embracing DNA we employed a minichromosome-based assay that was described earlier [38]. Circular minichromo-

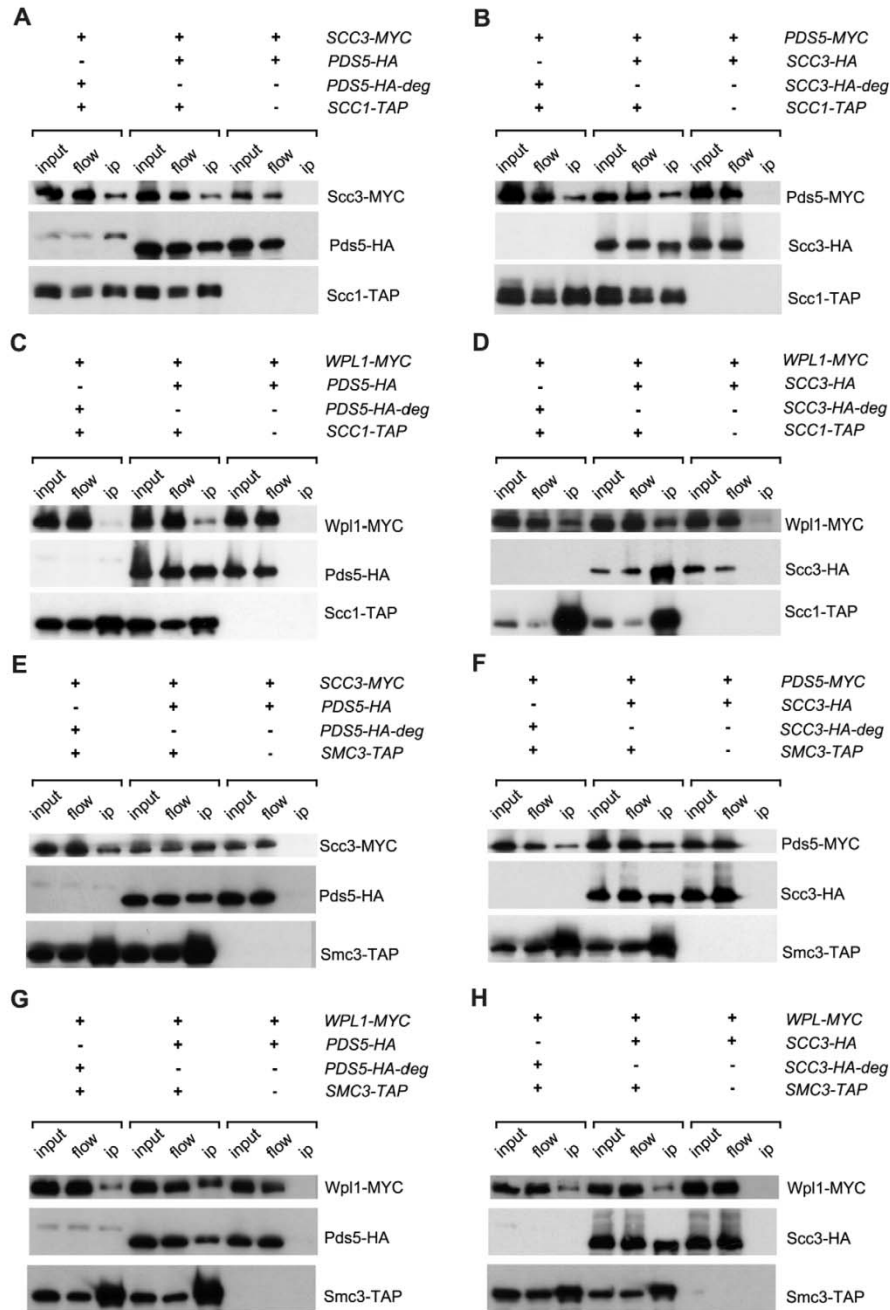


Figure 4. Interaction of Pds5, Scc3 and Wpl1 with cohesin ring. Lysates of nocodazole/benomyl arrested yeast cultures were incubated with IgG sepharose to precipitate Scc1-TAP or Smc3-TAP. The presence of different proteins on the IgG beads was analysed by Western blot probed with anti-HA (12CA5), anti-MYC (71D10) and PAP (P1291, Sigma). The strains were in (A): 1771 (*SCC3-MYC18, PDS5-HA6*), 1829 (*SCC3-MYC18, PDS5-HA6*).

degron, *SCC1-TAP*), 1958 (*SCC3-MYC18*, *PDS5-HA6*, *SCC1-TAP*); in (B): 1734 (*PDS5-MYC18*, *SCC3-HA6*), 1834 (*PDS5-MYC18*, *SCC3-HA6-degron*, *SCC1-TAP*), 1956 (*PDS5-MYC18*, *SCC3-HA6*, *SCC1-TAP*); in (C): 1882 (*WPL1-MYC18*, *PDS5-HA6*), 2014 (*WPL1-MYC18*, *PDS5-HA6*, *SCC1-TAP*), 2016 (*WPL1-MYC18*, *PDS5-HA6-degron*, *SCC1-TAP*); in (D): 1880 (*WPL1-MYC18*, *SCC3-HA6*), 2012 (*WPL1-MYC18*, *SCC3-HA6*, *SCC1-TAP*), 2018 (*WPL1-MYC18*, *SCC3-HA6-degron*, *SCC1-TAP*); in (E): 1771 (*SCC3-MYC18*, *PDS5-HA6*), 2251 (*SCC3-MYC18*, *PDS5-HA6*, *SMC3-TAP*), 2290 (*SCC3-MYC18*, *PDS5-HA6-degron*, *SMC3-TAP*); in (F): 1734 (*PDS5-MYC18*, *SCC3-HA6*), 2249 (*PDS5-MYC18*, *SCC3-HA6*, *SMC3-TAP*), 2264 (*PDS5-MYC18*, *SCC3-HA6-degron*, *SMC3-TAP*); in (G): 1882 (*WPL1-MYC18*, *PDS5-HA6*), 2253 (*WPL1-MYC18*, *PDS5-HA6*, *SMC3-TAP*), 2265 (*WPL1-MYC18*, *PDS5-HA6-degron*, *SMC3-TAP*); in (H): 1882 (*WPL1-MYC18*, *PDS5-HA6*), 2261 (*WPL1-MYC18*, *SCC3-HA6*, *SMC3-TAP*), 2271 (*WPL1-MYC18*, *SCC3-HA6-degron*, *SMC3-TAP*).
doi:10.1371/journal.pgen.1002856.g004

comes from the wild type, *SCC3*-degron and *PDS5*-degron strains could be co-immunoprecipitated with Scc1. However, the linearization of minichromosomes resulted in the dissociation of cohesin from the DNA due to sliding of the cohesin ring off the DNA end (Figure 8). We conclude that cohesin rings devoid of Scc3 or Pds5 maintain their topological association with the DNA.

Scc3 and Pds5 are required for efficient sister chromatid cohesion

Although we found no obvious defects in cohesin association with DNA, sister chromatid cohesion was significantly weakened in *SCC3*-degron and *PDS5*-degron strains (Figure 9A). Premature sister separation in the *Δwpl1* strain was less frequent than in the degron strains. In order to test whether the cohesion defect could be at least partially due to lack of Smc3 head acetylation we generated an antibody that specifically recognizes acetylated Smc3 (Figure S11) and examined the level of Smc3 acetylation in synchronized yeast cultures that were progressing from G1 into S phase. The acetylated form of Smc3 was readily detectable in S phase and was reduced in the *SCC3*-degron, *PDS5*-degron and *Δwpl1* strains when compared to wild type (Figure 9B). This reduction in Smc3 acetylation might contribute to the sister chromatid cohesion defect observed for these strains.

Deletion of *wpl1* was reported to make *ECO1* dispensable for viability in yeast [39]. To determine whether down-regulation of Scc3 or Pds5 alleviated the requirement of *ECO1*, we crossed *SCC3*-degron and *PDS5*-degron strains to a strain in which *eco1* deletion was rescued by a wild type *ECO1* transgene integrated at an unlinked ectopic locus. All of the resultant spores with the *eco1* deletion also carried a wild type *ECO1* transgene (38 spores in case of *PDS5*-degron and 26 spores in case of *SCC3*-degron) indicating that *ECO1* remains essential in *SCC3*-degron and *PDS5*-degron strains. It is possible that down-regulation of Scc3 and Pds5 weakened cohesion in the degron strains and that the Eco1 contribution to cohesion establishment became crucial even though Wpl1 could not efficiently associate with cohesin rings in these strains. We were unable to combine the *SCC3*-degron and *PDS5*-degron in one strain or to delete *WPL1* in either *SCC3*-degron or *PDS5*-degron strains.

Sister chromatid cohesion plays a key role in ensuring that sister kinetochores attach to opposite spindle poles (i.e. bi-orient) during cell division. The tug of war between microtubules pulling sister kinetochores to opposite spindle poles and cohesin rings resisting their splitting force generates tension across sister kinetochores. Only microtubule-kinetochore attachments that result in tension are stabilized, ensuring proper chromosomal segregation. To test whether the cohesion defect we observed resulted in the reduced ability of cells to bi-orient sister kinetochores in mitosis, we used a bi-orientation assay developed by [40]. Strains that carry an array of Tet operators integrated 2 kb from the centromere on chromosome IV and express a Tet repressor-GFP fusion are used to visualize kinetochores as fluorescent green dots. The spindle pole body component, Spc42, is tagged with tomato and can be detected as red dots. The anaphase promoting complex subunit, Cdc20, is expressed from a methionine-repressible promoter,

which generates metaphase arrest in the presence of microtubules in methionine-containing media. The strains were arrested in G1 with α -factor and released into nocodazole and benomyl containing media. After cells arrested in G2 in the absence of microtubules, the drugs were washed out and cells were allowed to build mitotic spindles and establish kinetochore-microtubule attachments while remaining arrested in metaphase due to depletion of Cdc20. Split GFP dots aligned between red spindle pole bodies indicated that bi-orientation was established while two GFP dots at the same spindle pole or one dot at the pole and another at some distance from a pole signified a microtubule attachment defect (Figure 9C). *SCC3*-degron and *PDS5*-degron strains display an obvious sister chromatid cohesion defect and split kinetochores are frequently located at the spindle poles rather than being aligned in the middle of the spindle as in wild type cells. *SCC3*-degron and *PDS5*-degron strains were generally less efficient at establishing bi-orientation. However, about 50% of the cells in either of the degron strains do attach sister kinetochores to opposite spindle poles within 120 minutes of release from microtubule poison arrest indicating that sister chromatid cohesion is still sufficient to establish bi-orientation. As expected from its relatively small sister chromatid cohesion defect, the bi-orientation defect observed in the *Δwpl1* strain was less pronounced than in *SCC3*-degron and *PDS5*-degron strains.

While crossing *SCC3*-degron and *PDS5*-degron strains we noticed that they display an unusual phenotype. The *MAT α* versions of these strains readily mated with not only *MAT a*, but also with *MAT α* partners. The explanation of this “a-faker” phenotype could be the frequent loss of chromosome III carrying the mating type locus. *MAT α* cells that lose their *MAT* locus mate as if they are *MAT a*, the default state of budding yeast with a *MAT* deletion [41]. We confirmed that the illegitimate mating was indeed the result of the loss of chromosome III and not an epigenetic inactivation of the *MAT* locus or mating type switch. First, most of the resulting α/α diploids were unable to sporulate but mated with a *MAT a* tester strain indicating that there was no mating type switch. Second, when mating a degron strain with a TetR-GFP fusion integrated into *LEU2* locus on the opposite arm of chromosome III, no GFP expression could be detected in the illegitimate diploids. The frequency of α to α mating in the *SCC3*-degron strain was estimated to be about 200 times higher than for wild type (Figure S12A). Thus depletion of Scc3 and Pds5 results in elevated rates of chromosomal mis-segregation consistent with sister chromatid cohesion and bi-orientation defects.

SCC3-degron and *PDS5*-degron strains were extremely sensitive to X-ray irradiation (Figure S12B) while the *Δwpl1* strain demonstrated a rather modest increase in sensitivity and only at very high doses, in agreement with an earlier study [42]. As homologous recombination is the preferred pathway of double-strand break repair in post-replicative cells and depends on sister chromatid cohesion [43], it is possible that the observed sensitivity can be fully accounted for by weakened sister chromatid cohesion in these strains. It was reported that human cells depleted of cohesin accumulate spontaneous double-strand breaks because of defects in DNA damage repair [44]. We monitored the formation of Rad52-YFP foci [45] as *SCC3*-degron and *PDS5*-degron strains

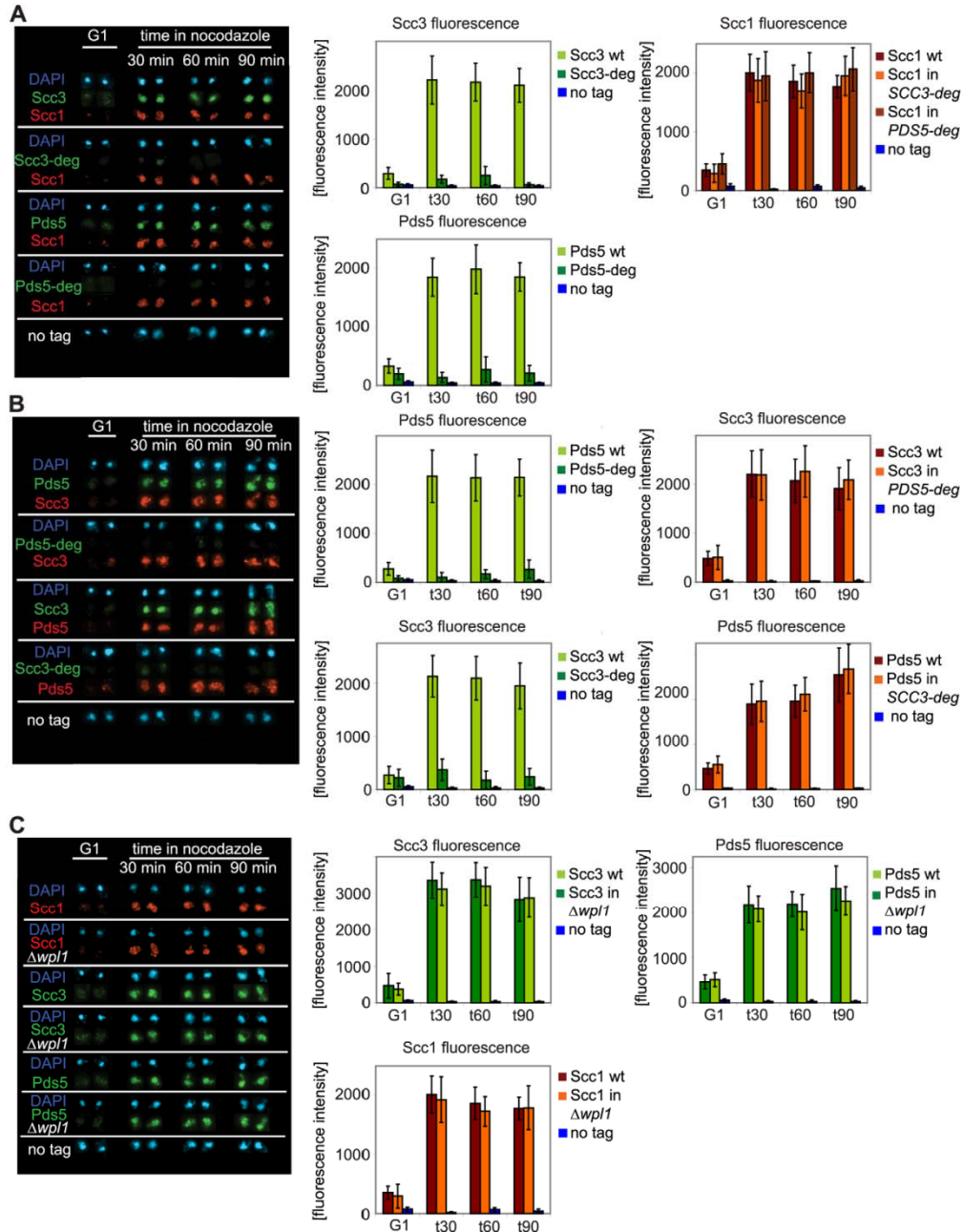


Figure 5. Depletion of Scc3 and Pds5 does not affect cohesin association with chromatin. Yeast strains were staged in G1 with α -factor and released into media with nocodazole. Chromosomal spreads were prepared as in Figure 2. At every time point fluorescence of 50 nuclei was determined. Error bars represent standard deviation. FACS analysis of cellular DNA content is shown in Figure S13. The strains were in (A): 1813 (*SCC1-*

Myc18, SCC3-HA6), 1625 (*SCC1-Myc18, SCC3-HA6-deg*), 1815 (*SCC1-Myc18, PDS5-HA6*), 1818 (*SCC1-Myc18, PDS5-HA6-deg*), in (B): 1771 (*SCC3-Myc18, PDS5-HA6*), 1796 (*SCC3-Myc18, PDS5-HA6-deg*), 1734 (*PDS5-MYC18, SCC3-HA6*) and 1744 (*PDS5-Myc18, SCC3-HA6-deg*) in (C): 1479 (*SCC3-HA6*), 1864 (*SCC3-HA6, Δwpl1*), 1677 (*PDS5-HA6*), 1866 (*PDS5-HA6, Δwpl1*), 10589 (*SCC1-Myc18*) and 1906 (*SCC1-Myc18, Δwpl1*). doi:10.1371/journal.pgen.1002856.g005

progressed through S phase. We did not detect any increase in the frequency of Rad52-YFP foci in these strains compared to wild type (data not shown). Therefore it appears that in the absence of radiation damage there is no dramatic increase in the DNA double strand breaks in Scc3 or Pds5-depleted strains indicative of an ongoing repair process. In human cells cohesin, but not sister chromatid cohesion, is required for the activation of DNA damage-induced intra-S and G2/M checkpoints [44]. In budding yeast, a reduction in chromosomal cohesin resulted in hypersensitivity to DNA damage under conditions where sister chromatid cohesion was unaffected [46]. At this moment we cannot exclude the possibility that Scc3 and Pds5 themselves might have specific functions in double-strand break repair or checkpoint activation.

Discussion

Scc3 and Pds5 do not “lock” cohesin rings on DNA

Cohesin rings are composed of two Smc subunits, Smc1 and Smc3, which are locked together by the third subunit, Scc1. The integrity of all three subunits of the ring is a requirement for its stable association with DNA [38,47]. The function of the additional proteins that associate with the ring, Scc3 and Pds5, appears to be much less clear. Both Scc3 and Pds5 are essential in *S. cerevisiae* and mutations in either results in sister chromatid cohesion defects. This in principle might indicate that these proteins also form an indispensable part of cohesin ring, e.g., prevent its spontaneous re-opening. In this study we tested the requirements of Scc3 and Pds5 for cohesin association with DNA.

Scc3 is stably associated with cohesin rings when they are purified from cells and yeast circular minichromosomes can be co-immunoprecipitated with Scc3 [38], indicating that it is bound to cohesin complexes both in solution and on DNA. In mammalian cells, the Scc3 orthologue SA1 was reported to be bound to DNA with a half-life similar to that of Scc1 [48]. In these experiments both Scc3 and Scc1 were dynamically bound to DNA prior to S phase. After S phase a more stably bound fraction was detected that was implicated in holding sister chromatids together. This would indicate that under normal circumstances there is little exchange of Scc3 subunits between cohesin rings. Pds5, on another hand, was reported to associate with cohesin rings less stably since it readily dissociates from them under elevated salt conditions in vitro [21]. Yeast circular minichromosomes could not be co-immunoprecipitated with Pds5 under conditions which allowed their co-immunoprecipitation with Scc1, Scc3 and Smc1 ([38] and Figure 8B). However, in our experiments no turn-over of Scc3 or Pds5 could be detected in the FRAP experiment in vivo, strongly suggesting that under physiological conditions in the cell both of these proteins are stably associated with chromosomal cohesin complexes. The diffuse fluorescence pattern observed for Wpl1-GFP, on another hand, indicates that Wpl1 is not stably bound to cohesins on DNA.

We investigated the consequences of destabilizing the Scc3 and Pds5 proteins and discovered that their total amounts in the cell can be greatly decreased without causing lethality. It was recently reported that a reduction in the cellular level of the Scc1 subunit of cohesin to 13% of wild type levels resulted in an obvious decrease in the amount of Scc1 detected on chromosomal spreads as well as in chromatin immunoprecipitation assays at chromosomal arm sites [46]. Remarkably, this reduction did not lead to defects in

sister chromatid cohesion or chromosomal segregation indicating that sister chromatid cohesion can be accomplished by a much smaller number of cohesin complexes than are normally associated with yeast chromosomes. In contrast, the reduction of Scc3 and Pds5 levels in our experiments resulted in premature separation of sister chromatids and chromosomal mis-segregation, underscoring their crucial importance for cohesin function. At the same time, while Scc3 and Pds5 could not be detected by immunostaining on chromosome spreads, little or no decrease in the amount of Scc1 on chromosomes could be observed. Most of the chromosomal cohesin complexes in *SCC3*- and *PDS5*-degron strains are not associated with these proteins but remain stably bound to chromosomes at usual cohesin sites. The 50% reduction of chromosomal Scc1 detected in *PDS5*-degron strain with ChIP-qPCR approach can possibly be attributed to the less efficient recruitment of Wpl1 to cohesin complexes in this strain since *wpl1* deletion caused similar if not more pronounced effect.

Because our EcoI-derived degron is non-inducible, it does not allow us to specifically eliminate Scc3 or Pds5 in G2 of the cell cycle once cohesion has been established. Such an approach would allow us to test whether these proteins are required for the maintenance of sister chromatid cohesion, i.e., the capacity of the cohesin complex to hold sisters over a period of time once both sisters are captured. When we performed this experiment with a “conventional” inducible degron, destruction of Pds5 in G2 arrested cells had no obvious effect on cohesion or cohesin association with DNA. Destruction of Scc3 was accompanied by the destabilization of Scc1 and cohesin loss from chromosomes while the effect on sister chromatid cohesion was very modest. This result is in agreement with a previous study which demonstrated that an 8 fold decrease in the abundance of chromosomal Scc1 does not result in premature sister separation [46]. Overall, experiments performed using the “conventional” degron are consistent with our conclusion that Scc3 and Pds5 are not functioning as a cohesin lock on DNA.

It is unlikely that Scc3 and Pds5 act redundantly, that is, that they both contribute to the maintenance of cohesin rings on DNA but either one is sufficient. Although we were not able to combine the EcoI-derived *SCC3* and *PDS5*-degrons in one strain, in experiments with “conventional” degron depletion of both Scc3 and Pds5 closely mimicked the effect of Scc3 depletion alone, which was likely due to the induction of Scc1 degradation. Depletion of Pds5 alone using the “conventional” degron had little or no effect on cohesin association with DNA.

In our experiments, depletion of Scc3 and Pds5 produced a phenotype that is not dissimilar to that of an *eco1* mutant, i.e., a defect in sister chromatid cohesion without a major effect on cohesin association with DNA (Figure 10). This correlation implies a role for Scc3 and Pds5 in cohesion establishment in spite of their reported role as counteracting factors of Eco1. Additionally, the essential functions of Scc3 and Pds5 can be accomplished by a much smaller number of molecules than normally present in the cell. It is possible that only very small number of cohesin rings actually hold sister chromatids together in our degron strains and that those rings do contain Scc3 and Pds5 subunits while the bulk of cohesin is bound to chromosomes without embracing both of the sisters. In this case, the amount of “cohesive” cohesin in our degron strains is limited to less than 15 complexes per chromosome. Importantly, the majority of cohesin complexes in

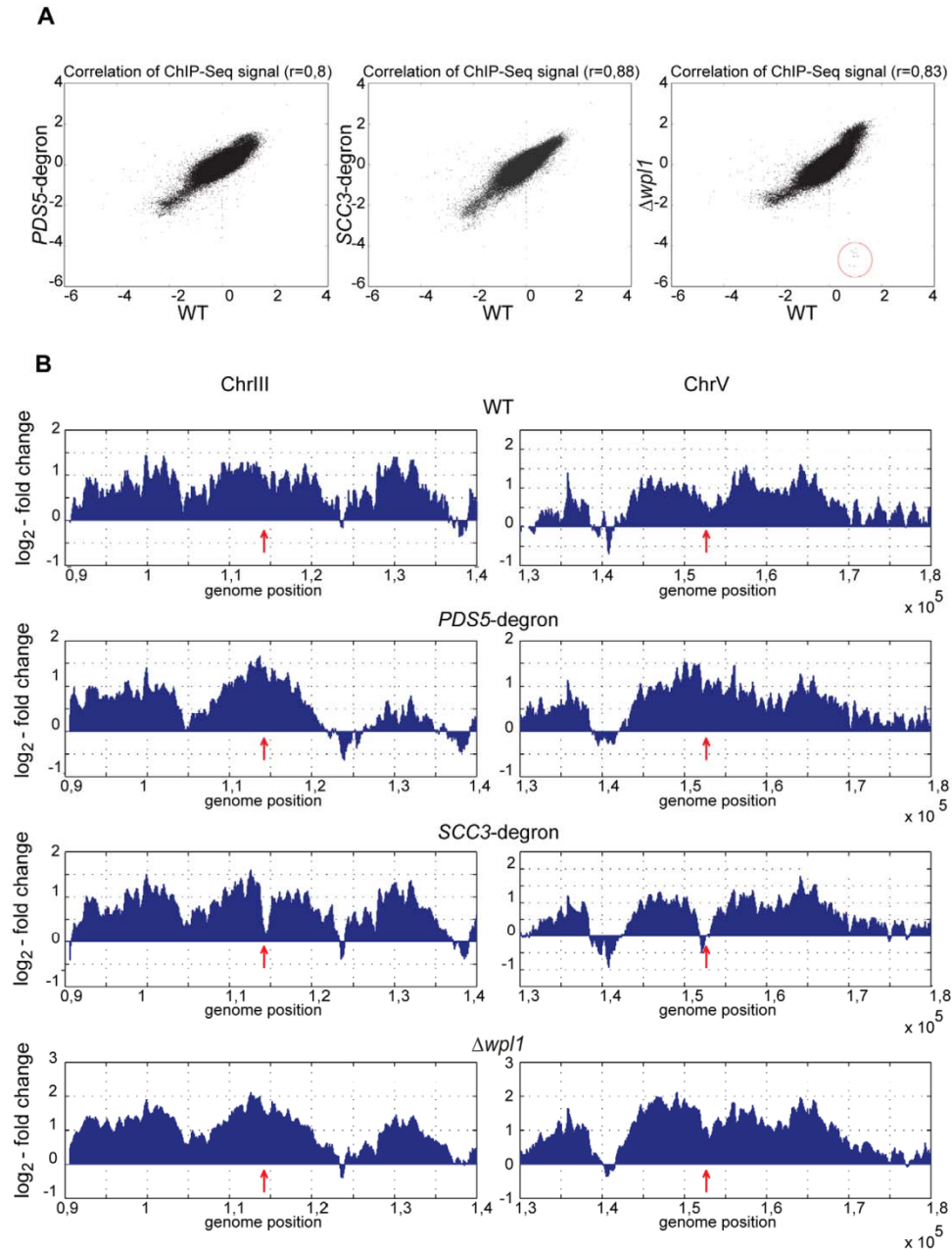


Figure 6. Genome-wide distribution of cohesin in the strains depleted of Scc3, Pds5, and Wpl1. Scc1-Myc18 ChIP was performed with nocodazole arrested 10589 (wild type, *SCC1-Myc18*), 1625 (*SCC3-HA6*-degron, *SCC1-Myc18*), 1818 (*PDS5-HA6*-degron, *SCC1-Myc18*), and 1906 ($\Delta wpl1$, *SCC1-Myc18*) strains. Untagged 1021 (wild type) strain was used as a control to determine signal log ratio. A running 500 bp window with a 50 bp

step size was used to estimate local Scc1 abundance on chromosomal DNA. (A) Scatter plot between chromosomal Scc1 distributions in wild type vs *SCC3*-degron, *PDS5*-degron and *Wpl1* strains. Regions corresponding to *WPL1* gene that are absent in *Wpl1* strain are circled. (B) Scc1 distribution in the pericentromeric regions of chromosomes 3 and 5. Position of the core centromere is marked with an arrow.
doi:10.1371/journal.pgen.1002856.g006

these strains are devoid of Scc3 or Pds5 but still able to maintain stable association with DNA. It is possible that Scc3 and Pds5 are required transiently. For example, they may only be essential during ring loading on DNA and/or cohesin establishment and become non-essential once both sisters have been trapped inside the ring. Intriguingly, no premature separation of sister chromatids or significant effects on the cell cycle were observed in *Drosophila* cells depleted of SA/Scc3 using dsRNAi, although the protein was barely detectable [49].

Scc3 was implicated in the recruitment of cohesin to heterochromatic regions in fission yeast [50] and possibly in recruitment of cohesin to CTCF sites in human cells [51]. We tested whether Scc3 functions in determining the location of cohesin sites on chromosomes in budding yeast that lack pericentric heterochromatin or CTCF. We found that depletion of Scc3, Pds5, or Wpl1 did not have any major effect on the chromosomal addresses of the cohesin complex.

Scc3, Pds5, Wpl1 and the architecture of cohesin complex

The immunoprecipitation experiments conducted in this study demonstrate that Pds5 and Scc3 associate with cohesin rings independently of each other. Scc3 is known to be recruited to cohesin via its interaction with Scc1 while the interacting partner of Pds5 on cohesin rings remains to be confirmed. While recombinant human Pds5 can directly bind to Scc1 in vitro, this interaction is enhanced in the presence of Scc3 [29]. In yeast, Pds5 binds to the cohesin ring in a Scc1-dependent manner. However, an analysis of intra-cohesin interactions in live yeast cells using fluorescence resonance energy transfer (FRET) revealed an unexpected interaction between Pds5 and the Smc1 hinge at the opposite side of the cohesin ring [52]. Since Pds5-Wpl1 and the Smc3 head bind to the same region of Scc1, Pds5 might reinforce the Scc1-Smc3 interface helping to maintain the integrity of the ring. However, a covalent Smc3-Scc1 fusion did not rescue *pds5* deletion (data not shown). The Smc3-Scc1 fusion was previously reported to suppress the lethality of mutations in the Scc1 N-terminal domain that reduce its interaction with the Smc3 head [31]. Therefore, maintaining the integrity of the cohesin ring at the Smc3-Scc1 interface cannot be the essential function of Pds5.

Of all the cohesin associated proteins, Wpl1 associates with the ring in the least stable fashion and displays a complicated pattern of interactions with the cohesin subunits. Wpl1 association with the cohesin ring in human cells is dependent on Scc3 and Scc1 with which it forms a stable ternary complex [17]. At the same time Wpl1 and Pds5 form another stable subcomplex that only weakly binds to the cohesin ring [16]. To complicate the matters, the N-terminal half of the vertebrate Wpl1, which is primarily responsible for its binding to cohesin, and the central region of Scc1, which is implicated in the interaction of Scc1 with Scc3, Pds5 and Wpl1, are conserved only in vertebrates [29]. Nevertheless, recombinant yeast Scc3, Pds5 and Wpl1 were reported to form a stable trimeric complex [18]. In this study we confirmed that Scc3, Pds5 and Wpl1 form a complex, although it is very unstable. Interestingly, the Pds5-Wpl1 dimer binds to the N-terminal region of Scc1 while the Scc3-Wpl1 dimer binds to the C-terminal region. Thus, Wpl1 may physically connect Scc3 with Pds5 and enable the trimeric complex to effectively span the length

of Scc1. The functional importance of this architecture remains to be addressed experimentally.

The results of our immunoprecipitation experiments from *SCC3*-degron and *PDS5*-degron strains are consistent with the model that in yeast Wpl1 is primarily recruited to the cohesin ring via Pds5. Very little Wpl1 could be co-purified with the cohesin ring in the absence of Pds5. This result is in agreement with an earlier report in which the amount of Wpl1 on chromatid was reduced in the *pds5-r10* mutant [15]. Importantly, although *ECO1* can be deleted in the *Wpl1* mutant or in yeast carrying certain specific point mutations in the *PDS5* or *SCC3* genes [9,15,18], simple destabilization of Scc3 or Pds5 proteins is insufficient to permit Eco1-independent growth (this study). Intriguingly, none of the *Aeco1* suppressor mutations in the *SCC3* and *PDS5* genes affected their interaction with Wpl1 in an in vitro assay [18]. It appears that *scc3* and *pds5* suppressor mutations influence the functions of the respective proteins in a more subtle way and do not result in partial loss-of-function alleles as was proposed earlier [15]. Rather, it is possible that these are the separation-of-functions alleles that selectively allow Scc3 and Pds5 to function in the establishment of cohesin while making them resistant to Wpl1 action that converts them from establishment to anti-establishment factors.

Interestingly, the level of Smc3 head acetylation was reduced when Scc3, Pds5 or Wpl1 were depleted. This reduction in Smc3 acetylation is unlikely to be the only reason for the observed cohesin defect since the *Wpl1* strain displays a similar reduction in acetylation but only a very modest cohesin defect. In a previous study, reduced Smc3 acetylation in a *Wpl1* strain was attributed to a decrease in chromosomal cohesin [39]. However, in our *SCC3*-degron strain, the amount of Scc1 associated with chromosomes is virtually unchanged despite diminished Smc3 acetylation.

In conclusion, we discovered a new and very efficient degron sequence and were able to employ it to study the effect of destabilization of Scc3 and Pds5. Our results demonstrate that Scc3 and Pds5 are not required for the maintenance of cohesin on DNA but are important for sister chromatid cohesion.

Materials and Methods

Strains and plasmids

Yeast strains are listed in Table S1.

Plasmid pYM27 [53] which was used for GFP-tagging of *SMC3*, *SCC1*, *SCC3*, *PDS5*, and *WPL1* as well as strain YKL200 and plasmids pKL187 [32,33] and pCM324 [34] that were used for the construction of "conventional" temperature-sensitive degron strains were obtained from EUROSCARF.

Protein expression and purification

Codon optimized sequences (Genescript) encoding Scc3, Pds5 and Wpl1 were cloned into pET21a or pET28b (Novagen). Sequences encoding N-terminal (aa 1-168), middle (aa 169-337) and C-terminal (aa 338-566) regions of Scc1 were cloned into pGEX-2T [7].

Proteins were tagged C-terminally with a His6 tag and expressed in *E. coli* BL21 (DE3) RIL according to common auto-induction protocols [54]. Cells were harvested and resuspended in lysis buffer (20 mM HEPES-KOH (pH 7.5), 300 mM NaCl, 5% glycerol, 5 mM imidazole, 1 mM β -ME, 1 mM PMSF

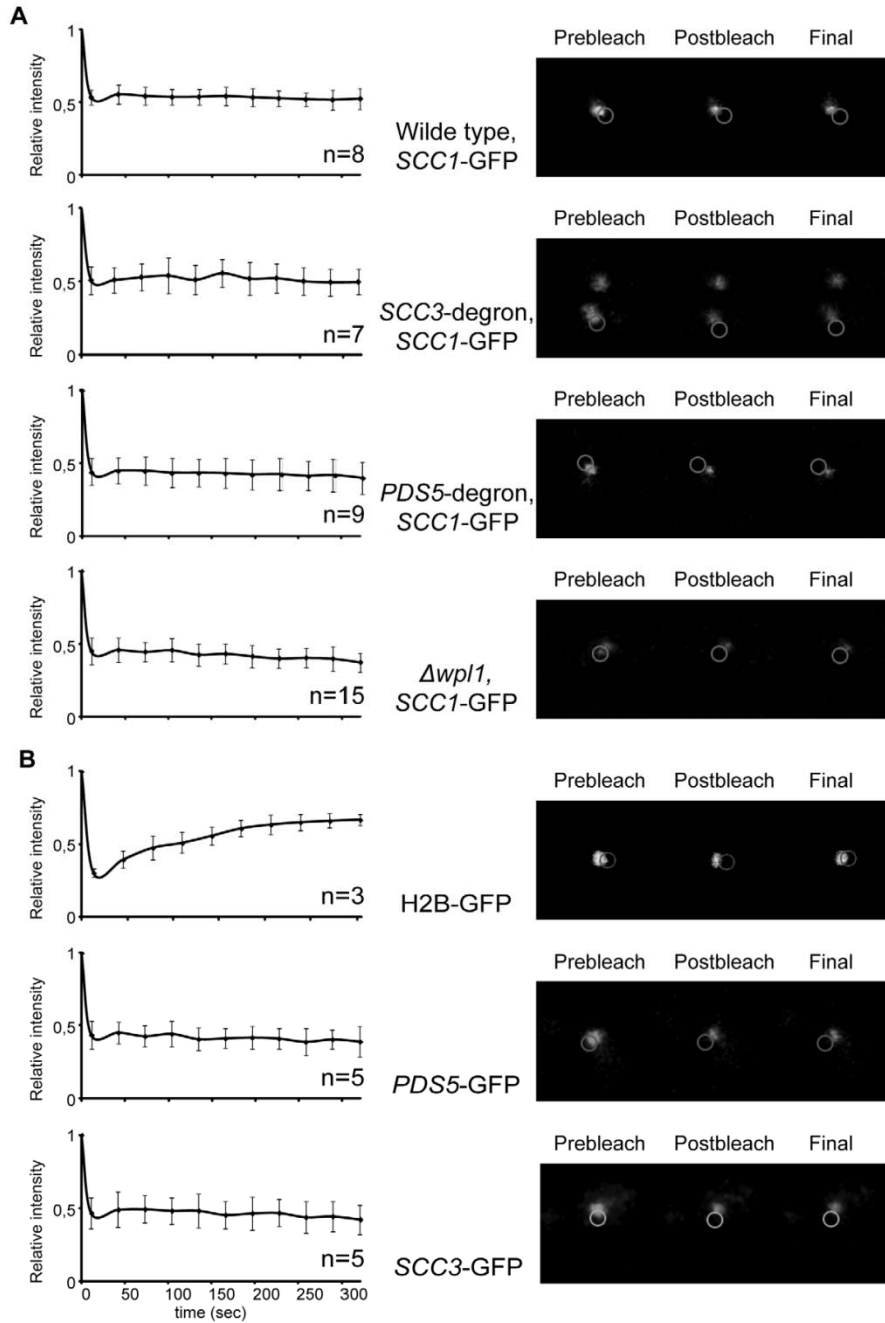


Figure 7. Depletion of Scc3, Pds5, and Wpl1 does not affect cohesin turnover rate on chromosomes. (A) A fluorescence recovery after photobleaching experiment was performed on mitotic cells of 2353 (wild type), 2390 (*SCC3-HA6*-degron), 2389 (*PDS5-HA6*-degron), and 2391 ($\Delta wpl1$) strains with endogenous *SCC1* tagged with GFP. No recovery of the bleached pericentric cohesin was observed during the experiment. (B) Scc3 and

Pds5 stably associate with chromatin. A FRAP experiment was performed on mitotic cells of 2281 (*SCC3-GFP*) and 2417 (*PDS5-GFP*) strains. Histone H2B-GFP strain (1904) was used as control. No recovery of bleached Scc3-GFP and Pds5-GFP was observed during experiment in contrast with H2B-GFP. The mean and standard deviation were calculated from independent experiments (numbers of observed cells for each strain are indicated on the graphs).
doi:10.1371/journal.pgen.1002856.g007

and 1× complete EDTA-free protease inhibitor mix (Roche). Cells were lysed (French Press, 17 kpsi), the cleared supernatant was incubated with Ni-NTA agarose beads (Quiagen) for 2 h at 4°C. Beads were washed with lysis buffer containing 500 mM NaCl and 30 mM imidazole and proteins were eluted with lysis buffer containing 100 mM NaCl and 250 mM imidazole. Subsequently, proteins were loaded onto a 16/60 Superdex200 or a 16/60 Superdex75 size exclusion column equilibrated with GF buffer (20 mM HEPES-KOH (pH 7.5), 100 mM NaCl, 5% glycerol, 1 mM β-ME). Peak fractions were analysed by SDS-PAGE and Coomassie staining and stored at -80°C.

10 30% Glycerol density gradients were performed in 10 mM HEPES-KOH (pH 7.5), 75 mM NaCl, 0.25 mM EDTA and 1× complete EDTA-free protease inhibitor mix (Roche). Proteins were mixed and preincubated for 1 h at 4°C, loaded on a preformed gradient and centrifuged at 38000 rpm for 38 h at 4°C using a SW40 Ti rotor (Beckman Coulter). 300 µl fractions

(44 fractions total) were harvested using a Gradient Station (Biocomp).

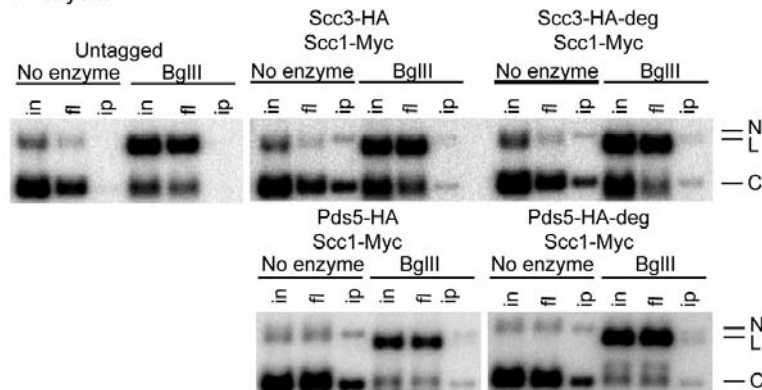
GST pull-down

GST and GST-fusions with Scc1 were purified as described [55]. For GST pull-downs beads were equilibrated with binding buffer (20 mM HEPES (pH 7.5), 100 mM NaCl, 5% glycerol and 5 mM 2-mercaptoethanol). Wpl1, Scc3 and Pds5 were mixed and pre-incubated for 30 minutes at 4°C. GST-beads were then added and incubated with rotation for 2 hours at 4°C. Beads were washed three times with binding buffer containing 0.5% NP-40 and eluted by boiling in SDS-PAGE loading buffer.

Immunoprecipitations

Yeast strains were grown in 200 mls of YEPD and arrested with 15 µg/ml nocodazole and 10 µg/ml benomyl for 2 hours at 30°C. Cells were harvested and lysates were prepared by beating with

A Myc IP



B HA IP

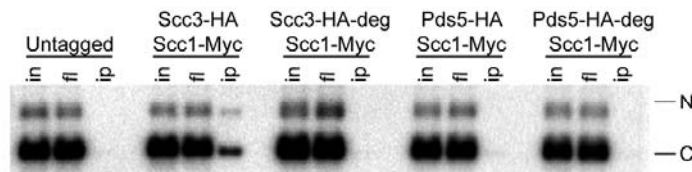


Figure 8. Cohesin rings devoid of Scc3 and Pds5 topologically embrace circular DNA. Strains 1021 (untagged), 1813 (*SCC3-HA6*, *SCC1-Myc18*), 1625 (*SCC3-HA6-deg*, *SCC1-Myc18*), 2525 (*PDS5-HA6*, *SCC1-Myc18*) and 1818 (*PDS5-HA6-deg*, *SCC1-Myc18*) carried the centromeric minichromosomes. (A) Yeast lysates were incubated with BgIII restriction enzyme as indicated. Minichromosomes were co-immunoprecipitated with Scc1-Myc18. DNA was prepared by phenol/chloroform extraction and separated on a 1% agarose gel with ethidium bromide. Southern blot probed with a *TRP1*-specific probe is shown. Nicked (N), linear (L), and closed circular (C) forms of the minichromosome are indicated. (B) Minichromosomes were immunoprecipitated with anti-HA antibody. Minichromosomes from *SCC3-HA6* but not *SCC3-HA6-deg* strains could be co-immunoprecipitated with Scc3 indicating the efficient depletion of Scc3 from the minichromosomes in the *SCC3-HA6-deg* strain. Since Pds5 association with minichromosomes is very salt-sensitive, they could not be co-immunoprecipitated with Pds5-HA6 in either the wild type or *PDS5-HA6-deg* strains under our experimental conditions.
doi:10.1371/journal.pgen.1002856.g008

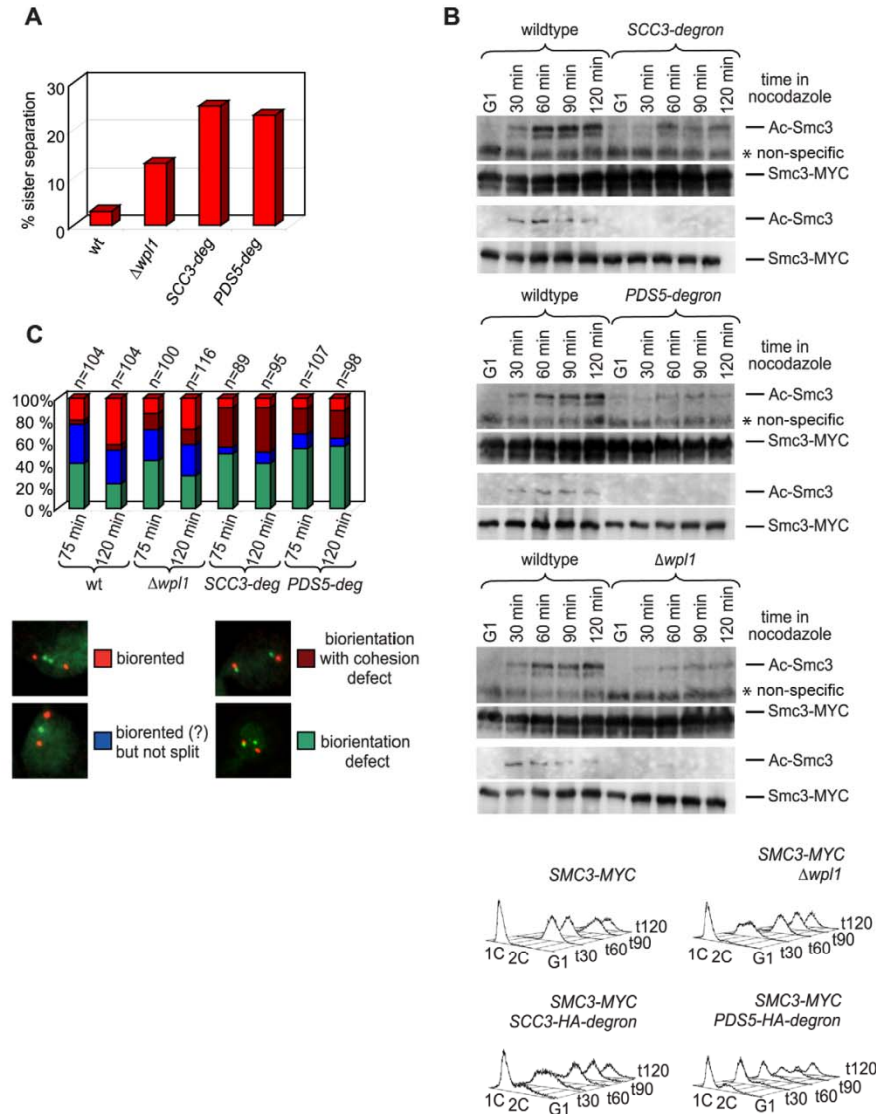


Figure 9. Sister chromatid cohesion defect in yeast depleted of Scc3 and Pds5. (A) Yeast strains 1417 (wild type), 2190 ($\Delta wpl1$), 1621 (SCC3-deg) and 1678 (PDS5-deg) have an array of 200 Tet operators integrated into *URA3* locus 35 kb from the centromere on chromosome V and express TetR-GFP. Cells were staged in G1 with α -factor and released into media with nocodazole for 100 minutes. Separation of sister chromatids was scored as one (non-separated) versus two (separated) GFP dots. Dots separation was scored in 300 cells per strain. (B) 1759 (wild type), 1776 (SCC3-deg), 1779 (PDS5-deg) and 1769 ($\Delta wpl1$) strains with Myc-tagged endogenous *SMC3* gene were released from α -factor arrest into nocodazole containing media. Samples were collected at the indicated time points and processed for Western blot probed with anti-acetyl-Smc3 antibody (see Figure S11). The same blot was re-probed with anti-MYC to detect Smc3 (71D10). Western blots with different amounts of samples are shown to demonstrate both the actual levels of Ac-Smc3 in different strains and equal loading. FACS analysis of cellular DNA content is shown. (C) 1822 (wild type), 2436 ($\Delta wpl1$), 1832 (SCC3-deg) and 1833 (PDS5-deg) strains with CENIV GFP dots and Spc42-Tomato were expressing Cdc20 from methionine-repressible promoter. Strains were arrested in G1 with α -factor and methionine was then added for 1 hour to shut down Cdc20 expression. Cells were released from G1 arrest into methionine and nocodazole containing media for 2 hours. Microtubule poisons were washed out and samples taken at indicated times, fixed in methanol and analyzed by fluorescence microscopy. doi:10.1371/journal.pgen.1002856.g009

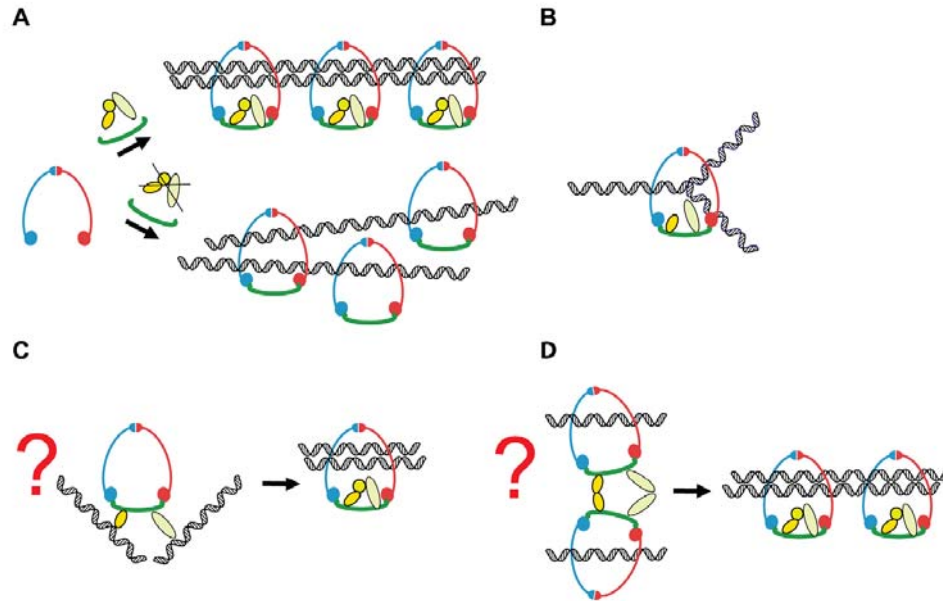


Figure 10. A model of how Scc3 and Pds5 play a role in the establishment of sister chromatid cohesion but are not required to stabilize cohesin rings on the DNA. In the normal cell cycle of budding yeast Scc1 subunit is synthesized in the late G1 or early S phase. Scc1 binds to Smc1/Smc3 heterodimer and completes the cohesin ring. Scc3 and Pds5 stably associate with cohesin via Scc1 subunit. Cohesin complexes are loaded on the chromosomes. During DNA replication two newly generated sister chromatids are captured inside a single cohesin ring in a process which remains poorly understood. Scc3 and Pds5 function to ensure that two sister chromatids are captured inside a cohesin ring. In their absence, cohesin complexes are stably loaded on the DNA but fail to embrace both of the sister chromatids resulting in defective sister chromatid cohesion (A). We can speculate that Pds5 and Scc3 could stabilize cohesin rings specifically during the replication fork passage (B) or transiently bind sister chromatids during the establishment of cohesion (C). Alternatively they could mediate a transient interaction between two cohesin rings as proposed by [61] (D).

doi:10.1371/journal.pgen.1002856.g010

glass beads in buffer I (50 mM HEPES-KOH (pH 7.3), 70 mM Potassium Acetate, 5 mM Magnesium Acetate, 10% glycerol, 0.1% Triton X-100, 1× complete EDTA-free protease inhibitor mix (Roche), 2 mM PMSF, 1× PhosSTOP phosphatase inhibitor mix (Roche), 5 μg/ml aprotinin, 5 μg/ml pepstatin, 0.5 mM DTT). Protein concentrations of the lysates were adjusted and they were incubated with IgG Sepharose 6 beads (Amersham) for 2 hours or overnight. Beads were washed two times with buffer I, once with buffer I/100 mM Potassium Acetate, once with buffer I/120 mM Potassium Acetate, once with buffer I/150 mM Potassium Acetate. For detection of Wpl1 association with cohesin higher salt concentration washes were omitted and beads were washed three times with buffer I and two times with buffer I/100 mM Potassium Acetate.

Minichromosome immunoprecipitation

Minichromosome immunoprecipitation was performed as described in [38]. Yeast strains were transformed with the 2310 bp plasmid [56] containing an 850 bp long *CEN4* sequence from YCplac22 and *TRP1ARS1* sequence. Strains were grown overnight in synthetic medium without tryptophan at 30°C, were diluted into 300 ml YEPD at OD₆₀₀ of 0.2 and grown till OD₆₀₀ reached 0.65. Cells were arrested with 10 μg/ml nocodazole for 1.5 hour. Spheroplasting was carried out with lyticase (L-2524, Sigma). Spheroplasts were lysed in 4.5 ml of lysis buffer (25 mM

Hepes/KOH [pH 8.0], 50 mM KCl, 10 mM MgSO₄, 10 mM Na citrate, 25 mM Na sulfite, 0.25% TritonX-100, 1 mM PMSF, 3 mM DTT, and 1× complete EDTA-free inhibitors [Roche]) supplemented with 100 ng/ml RNase A (Fermentas). DNA digest was performed with 1000 units of Bgl II per 1 ml of lysate for 2 hours at 4°C. The reaction was stopped by the addition of 5 M NaCl to a final concentration of 200 mM. Minichromosomes were immunoprecipitated with 12.5 μg/ml of anti-HA (12CA5, Roche) or anti-Myc (9E11, Santa Cruz) antibodies and 0.25 ml suspension of protein A dynabeads (Invitrogen). Minichromosomes were then eluted off the beads two times with 0.25 ml of 50 mM Tris (pH 8.0), 10 mM EDTA, 1% SDS at 65°C, extracted with phenol/chloroform/isoamyl alcohol (25:24:1) and ethanol precipitated. Samples were dissolved in 40 μg of TE and separated on a 1% agarose gel with ethidium bromide. Southern transfer was performed under denaturing conditions using Hybond-XL membrane (GE Healthcare). Blots were hybridized with a *TRP1* probe and scanned on Storm 840 (Molecular Dynamics).

FRAP

Fluorescence microscopy and photobleaching were performed according to the protocol described in [37] with modifications. Cells were immobilized in a slab of media supplemented with 10% low melting point agarose (NuSieve GTG Agarose, Lonza) and imaged at the room temperature (20°C) with Olympus fv1000

laser scan confocal microscope with standard eGFP band pass filter (500–550 nm) and argon laser (488 nm excitation line). Seven z sections were acquired in 750 nm steps and analyzed with Imapris software. The mean and the standard deviation of the acquired intensity were calculated using MatLAB (Mathworks Inc., Natick, MA).

ChIP-Seq

Chromatin immunoprecipitation was performed as in [57] using strains with Myc-tagged Scc1 subunit of cohesin, anti-Myc 9E11 antibody and rat anti-mouse IgG2a Dynabeads M-450 (Dyna). Immunoprecipitated DNA was ligated to the adaptors, size fractionated (150–500 bp) and amplified using ChIPSeq DNA Sample Prep Kit (Illumina) according to the manufacturer's instructions. DNA libraries were analysed on High Sensitivity DNA Chips with Bioanalyzer 2100 (Agilent Technologies). Cluster generation and sequencing analysis were performed on Illumina Genome Analyzer II with the help of Standard Cluster Generation V4-GA II and 36 cycle Sequencing v4 kits (Illumina). Reads were aligned against the *Saccharomyces cerevisiae* reference genome using Palmapper v0.5 [58] reporting all alignments with at most three mismatches and one gap. To reduce the effect of possible contamination with human DNA, we also aligned the reads against the human genome and only considered reads uniquely mapping to the yeast genome. We then used the multimapper resolution tool (<http://bioweb.me/mmr>) to identify the best location of reads mapping to multiple locations. For further analysis we only considered reads mapping to the chromosomal DNA of *Saccharomyces cerevisiae*. The summary of counts of aligned reads is presented in Table S2. We then computed and plotted the log-ratios between the samples' read coverages and the negative control (untagged strain) at equi-spaced genomic locations using Matlab.

ChIP-qPCR

ChIP DNA was quantified by quantitative PCR using LightCycler 480 SYBR Green I Master mix and LightCycler 480 (Roche) according to manufacturer's instructions. Primers, used for quantification of the centromeric region of chromosome VI and a cohesin site on the arm of chromosome VI (172 kb) were described in [30]. Primers for a cohesin-low site on the arm of chromosome V (141 kb) were described in [15]. Histone H3 ChIP was performed with an anti-H3 rabbit polyclonal antibody (Abcam, ab1791) and Protein A Dynabeads (Invitrogen).

Chromosome spreading

Chromosome spreading was performed as described in [59]. Images were taken with an Axio Imager fluorescence microscope (Zeiss) with a 63× objective and scaled with MetaMorph image analysis software version 7.1.3.0 (Molecular Devices). All the images were taken with the same exposure time and scaled using the minimum and maximum intensities recorded in the given data set as lower and upper limits respectively. Z stacks (7–9 planes with 0.3 micron step) were acquired and projected on one plane by averaging. An area of fixed size was placed over the chromatin region and the average intensity was recorded. Background was measured outside the chromatin area and subtracted. The same nuclei were used for quantification of Scc1 and Scc3/Pds5 signals. Figures were assembled with the help of Adobe Photoshop software.

Other techniques

Rabbit polyclonal anti-acetyl Smc3 antibody was raised against a peptide CRTVGLK(Ac)K(Ac)DDYQL and affinity purified (Eurogentec).

Chromatin pellets were prepared as described in [60].

Supporting Information

Figure S1 An induction of the “conventional” N-terminal ts degnon results in a complete degradation of Pds5 and Scc3. To test if any stable fragments were remaining after the degnon induction *PDS5* and *SCC3* were tagged at the C-termini with HA6. Degrons were induced in nocodazole-arrested yeast as in Figure 2A C. Strain numbers are indicated in brackets in the figure. Western blots probed with anti-HA (16B12) antibody and anti-Cdc28 (sc-28550, Santa Cruz) as a loading control are shown. No stable fragments could be detected. (TIFF)

Figure S2 Sister chromatid cohesion defect in yeast depleted of Scc3 and Pds5 using a “conventional” N-terminal ts degnon. (A) Strains 2418 (wild type), 2419 (degnon-*PDS5*), 2420 (degnon-*SCC3*), and 2449 (degnon-*PDS5* and degnon-*SCC3*) have an array of Lac operators integrated into *URA3* locus 35 kb from the centromere on chromosome V and express LacI-GFP. To induce the degnon in G1, strains were staged with α -factor in YEP raffinose. Cells were resuspended in YEP galactose containing α -factor and incubated for 45 minutes at 30°C to induce the expression of Ubr1. Cells were then shifted to 37°C in YEP galactose containing doxycycline and α -factor and incubated for additional 90 minutes to destroy Pds5 and/or Scc3. Cells were released from α -factor arrest into YEP galactose containing nocodazole and doxycycline at 25°C for 3 hours. To induce degnon in G2/M, strains were synchronized with α -factor and released into nocodazole containing YEP raffinose medium for 2 hours. Cells were resuspended in YEP galactose containing nocodazole and incubated for 45 minutes at 30°C to induce the expression of Ubr1. Cells were then shifted to 37°C in YEP galactose containing doxycycline and nocodazole and incubated for 90 minutes to destroy Pds5 and/or Scc3. Cells were then chased in YEP galactose containing nocodazole and doxycycline at 25°C for 3 hours. This last incubation step was found necessary since the dots signal was weakened under the conditions of degnon induction. Separation of sister chromatids was scored as one (non-separated) versus two (separated) GFP dots in 300 cells. (B) FACS analysis of cellular DNA content. (C) Western blot demonstrating the depletion of Pds5 and Scc3. TCA protein extracts were prepared at indicated time points. Blots were probed with anti-Myc antibody (71D10) and anti-Cdc28 (sc-28550, Santa Cruz) for loading control. (TIFF)

Figure S3 Eco1 contains degnon sequences. (A) 1188 (*GAL-SCC1*), 1176 (*GAL-SCC1 SCC1-HA6*) and 1177 (*GAL-SCC1 SCC1-HA6-ECO1*) strains were synchronized in G1 with α -factor and then released into media with glucose and nocodazole for 90 minutes. Western blot was probed with anti-HA antibody (12CA5). (B) Schematic representation of Eco1 domains. N-terminal region with the PCNA-interacting PIP box and C2H2 Zinc finger, middle region rich in serines and prolines and C-terminal acetyltransferase domain are indicated. (C) *GAL-SCC3* strains carrying transgenes *SCC3-HA6* (1257), *SCC3-HA6-ECO1* (1258), *SCC3-HA6-ECO1(aa1 63)* (1259) and *SCC3-HA6-ECO1(aa111 281)* (1260) were staged in G1 with α -factor and then released into galactose-containing media with nocodazole. Western blot was probed with anti-HA antibody (12CA5) to detect Scc3 or Scc3-Eco1 fusions. Loading control was anti-Cdc28 sc-28550 (Santa Cruz). (D) No stable fragments of Pds5 and Scc3 can be detected in the degnon strains. *PDS5* and *SCC3* were tagged at the N-termini with Myc9. Strains were arrested in G2/M with

nocodazole for 3 hours and TCA protein extracts were prepared. Strain numbers are indicated in brackets in the figure. Western blots probed with anti-Myc (71D10) antibody and anti-Cdc28 (sc-28550, Santa Cruz) as a loading control are shown.

(TIF)

Figure S4 Protein stability assay in nocodazole arrested cells. Strains 1323 (*SCC3-HA6*-degron), 1479 (*SCC3-HA6*), 1675 (*PDS5-HA6*-degron), 1677 (*PDS5-HA6*), 1759 (*SMC3-MYC18*), and 10589 (*SCC1-HA6*) were arrested with nocodazole for 2 hours. Cycloheximide was added at a final concentration of 0.1 mg/ml, samples were taken at the indicated time points and TCA protein extracts prepared. Western blot was probed with anti-HA (16B12) or anti-MYC (71D10) and anti-Cdc28 (sc-28550, Santa Cruz) antibodies as a loading control.

(TIF)

Figure S5 Chromatin-bound fraction of cohesin is not affected by the depletion of Scc3 and Pds5. Strains 1813 (*SCC1-Myc18*, *SCC3-HA6*), 1625 (*SCC1-Myc18*, *SCC3-HA6*-degron), 2525 (*SCC1-Myc18*, *PDS5-HA6*), 1818 (*SCC1-Myc18*, *PDS5-HA6*-degron) and 1906 (*SCC1-Myc18*, *Δwpl1*) were arrested in G2/M with nocodazole. Whole cell extracts (WCE) were fractionated into soluble supernatant (sup) and chromatin pellet (pell). Equivalent amounts of protein samples were separated on SDS-PAGE. Western blot was probed with anti-HA (16B12), anti-Myc (71D10), as well as with anti-Cdc28 (sc-28550, Santa Cruz) and anti-Hmo1 antibodies [S2] as loading controls for the soluble fraction and chromatin pellet, respectively.

(TIF)

Figure S6 Depletion of Scc3 and Pds5 does not affect cohesin association with chromatin. (A) Yeast strains 1759 (*SMC3-MYC18*), 1769 (*SMC3-MYC18*, *Δwpl1*), 1776 (*SMC3-MYC18*, *SCC3-HA6*-degron), 1779 (*SMC3-MYC18*, *PDS5-HA6*-degron), 2197 (*SMC3-MYC18*, *PDS5-HA6*), 2227 (*SMC3-MYC18*, *SCC3-HA6*) were staged in G1 with α -factor and released into media with nocodazole. Chromosomal spreads were prepared at indicated time points as in Figure 2. At every time point fluorescence of 50 nuclei was determined. Error bars represent standard deviation. Cellular DNA content was analyzed by FACS (B).

(TIF)

Figure S7 Scc3 and Pds5 associate with chromosomes in Scc1-dependent manner. (A) Strains 1835 (*GAL-SCC1-Myc18*, *SCC3-HA6*), 1813 (*SCC1-Myc18*, *SCC3-HA6*), 1839 (*GAL-SCC1-Myc18*, *PDS5-HA6*), and 1815 (*SCC1-Myc18*, *PDS5-HA6*) were grown in media with galactose and arrested with α -factor for 2 hours. Media was then changed to YEP glucose and cells were incubated in the presence of α -factor for additional 60 minutes before release in YEP glucose with nocodazole. Chromosomal spreads were prepared at indicated times as in Figure 2. Samples from the same experiment were processed for Western blot shown in (B) and FACS analysis of cellular DNA content shown in (C).

(TIF)

Figure S8 ChIP-qPCR assay of Scc1. (A) Strains 10589 (wild type), 1625 (*SCC3*-degron), 1818 (*PDS5*-degron), 1906 (*Δwpl1*) with endogenous *SCC1* tagged with Myc18, and untagged strain (1021) were arrested with nocodazole. Chromatin immunoprecipitation was performed with anti-Myc and anti-histone H3 antibodies. ChIP DNA was quantified by quantitative PCR using 3 pairs of primers amplifying centromere adjacent region of chromosome VI, cohesin-high site on the arm of chromosome VI (172 kb), and cohesin-low site on the arm of chromosome V (141 kb). (B) The immunoprecipitation ratios of Scc1 were normalized between the strains using the control IP ratios of H3 and divided by the

resultant IP ratio of wild type. (C) Schematic of the analyzed chromosomal regions.

(TIF)

Figure S9 Scc3, Pds5, and Wpl1 depletion does not affect the genome-wide distribution of cohesin. (A) Scc1 distribution on chromosome VII is shown. A window of 5,000 bps (i.e., 2,500 bps in each direction) was used for smoothing. The data sets for the wild type and one of the mutant strains are plotted on the same graph to facilitate comparison. (B) Scc1 distribution at the tDNA loci of chromosomes VII. Position of the tDNA genes is marked with red lines. A window of 500 bp with a 50 bp step was used.

(TIF)

Figure S10 Depletion of Scc3, Pds5, and Wpl1 does not affect Smc3 turnover rate on chromosomes. A FRAP experiment was performed on mitotic cells of 2003 (wild type), 2040 (*SCC3*-degron), 2004 (*PDS5*-degron), and 2034 (*Δwpl1*) strains with endogenous *SMC3* tagged with GFP. No recovery of the bleached pericentric cohesin was observed during experiment. The mean and standard deviation were calculated from independent experiments (numbers of observed cells for each strain are indicated on the graphs).

(TIF)

Figure S11 Specificity of the rabbit polyclonal anti-acetyl Smc3 antibody. The antibody was raised against a peptide CRTVGLK(Ac)K(Ac)DDYQL and affinity purified (Eurogentec). Strains 1021 (wild type), 1759 (*SMC3-MYC18*), 1752 (*Δwpl1*, *Δwco1*) and 1578 (*smc3* (K113N)) were grown until early log phase in YEPD. TCA protein extracts were analyzed by Western blot. The * indicates a non-specific band.

(TIF)

Figure S12 Chromosomal loss and X-ray sensitivity of strains depleted of Scc3 and Pds5. (A) Chromosomal loss in *SCC3*-degron strain. Cell suspensions containing 12×10^6 cells from 1480 (*SCC3-HA6::HIS3*) and 1326 (*SCC3*-degron::*NAT*) *MAT* α strains were mixed with an equivalent number of cells from *MAT* α or *MAT* α tester strains (*his1*, otherwise prototrophic) on Millipore nitrocellulose filters. Filters were placed on YEPD plates and incubated for 8 hours at 25°C. Cells were washed off the surface of the filter, diluted and plated on minimal media to select for diploids and selective media to select for diploids and one of the parents. Selective media was media without histidine to select for *SCC3-HA6::HIS3* or YEPD with nourseothricin to select for *SCC3*-degron::*NAT*. The mating titer was calculated from the ratio between the numbers of colonies on minimal versus selective plates and dilution factor. The error bars represent standard deviation calculated from the results of two independent experiments. (B) Depletion of Scc3 and Pds5 results in X-ray hypersensitivity. Exponentially growing strains 1021 (wild type), 1366 (*Δwpl1*), 1323 (*SCC3*-degron), and 1675 (*PDS5*-degron) were plated on YEPD and exposed to X-ray irradiation for 40, 80, 120 and 160 minutes. Emerging colonies were counted after two days incubation and % survival was calculated.

(TIF)

Figure S13 FACS analysis of cellular DNA content from the experiment in Figure 3C and Figure 5.

(TIF)

Table S1 List of yeast strains.

(DOC)

Table S2 Summary of ChIP-seq reads alignment against the *Saccharomyces cerevisiae* genome.

(DOC)

Acknowledgments

We thank Kerry Bloom, Kevin Hardwick, Tomoyuki Tanaka, Rodney Rothstein, Susan Gasser, Steven J. Brill and Kim Nasmyth for strains, plasmids and antibodies; Maria Langeegger and Silke Hauf for help with fluorescence microscopy; Berit Lochmann for help with the experiments; Olga Zhukova and Adrian Streit for assistance with qPCR; Susanne Hanel for technical assistance and Olaf-Oliver Wolz for help with manuscript preparation.

References

- Nasmyth K, Haering CH (2009) Cohesin: its roles and mechanisms. *Annu Rev Genet* 43: 525–558.
- Haering CH, Farcas AM, Arumugam P, Metson J, Nasmyth K (2008) The cohesin ring concatenates sister DNA molecules. *Nature* 454: 297–301.
- Onn I, Heidinge-Pauli JM, Guacci V, Unal E, Koshland DE (2008) Sister chromatid cohesion: a simple concept with a complex reality. *Annu Rev Cell Dev Biol* 24: 105–129.
- Haering CH, Schoffnegger D, Nishino T, Helmhart W, Nasmyth K, et al. (2004) Structure and Stability of Cohesin's Smc1-Kleisin Interaction. *Mol Cell* 15: 951–964.
- Skibbens RV, Corson LB, Koshland D, Hieter P (1999) Ctf7p is essential for sister chromatid cohesion and links mitotic chromosome structure to the DNA replication machinery. *Genes Dev* 13: 307–319.
- Toth A, Ciosk R, Uhlmann F, Galova M, Schleiffer A, et al. (1999) Yeast cohesin complex requires a conserved protein, Eco1p(Ctf7), to establish cohesion between sister chromatids during DNA replication. *Genes Dev* 13: 320–333.
- Ivanov D, Schleiffer A, Eisenhaber F, Mechler K, Haering CH, et al. (2002) Eco1 is a novel acetyltransferase that can acetylate proteins involved in cohesion. *Curr Biol* 12: 323–328.
- Zhang J, Shi X, Li Y, Kim BJ, Jia J, et al. (2008) Acetylation of Smc3 by Eco1 is required for S phase sister chromatid cohesion in both human and yeast. *Mol Cell* 31: 143–151.
- Rofel Ben-Shahar T, Heeger S, Lehane C, East P, Flynn H, et al. (2008) Eco1-dependent cohesin acetylation during establishment of sister chromatid cohesion. *Science* 321: 563–566.
- Unal E, Heidinge-Pauli JM, Kim W, Guacci V, Onn I, et al. (2008) A molecular determinant for the establishment of sister chromatid cohesion. *Science* 321: 566–569.
- Heidinge-Pauli JM, Unal E, Koshland D (2009) Distinct targets of the Eco1 acetyltransferase modulate cohesion in S phase and in response to DNA damage. *Mol Cell* 34: 311–321.
- Beckouet F, Hu B, Roig MB, Sutani T, Komata M, et al. (2011) An Smc3 acetylation cycle is essential for establishment of sister chromatid cohesion. *Mol Cell* 39: 689–699.
- Borges V, Lehane C, Lopez-Serra L, Flynn H, Shekel M, et al. (2011) Hos1 deacetylates Smc3 to close the cohesin acetylation cycle. *Mol Cell* 39: 677–688.
- Xiong B, Lu S, Gerton JL (2011) Hos1 is a lysine deacetylase for the smc3 subunit of cohesin. *Curr Biol* 20: 1660–1665.
- Sutani T, Kawaguchi T, Kanno R, Itoh T, Shirahige K (2009) Budding yeast Wpl1(Rad61)-Pds5 complex counteracts sister chromatid cohesion-establishing reaction. *Curr Biol* 19: 492–497.
- Kueng S, Hegemann B, Peters BH, Lipp JJ, Schleiffer A, et al. (2006) Wapl controls the dynamic association of cohesin with chromatin. *Cell* 127: 955–967.
- Gandhi R, Gillespie PJ, Hirano T (2006) Human Wapl is a cohesin-binding protein that promotes sister-chromatid resolution in mitotic prophase. *Curr Biol* 16: 2406–2417.
- Rowland BD, Roig MB, Nishino T, Kurze A, Uhuocak P, et al. (2009) Building sister chromatid cohesion: smc3 acetylation counteracts an antiestablishment activity. *Mol Cell* 33: 763–774.
- Panizza S, Tanaka T, Hochwagen A, Eisenhaber F, Nasmyth K (2000) Pds5 cooperates with cohesin in maintaining sister chromatid cohesion. *Curr Biol* 10: 1557–1564.
- Hartman T, Stead K, Koshland D, Guacci V (2000) Pds5p is an essential chromosomal protein required for both sister chromatid cohesion and condensation in *Saccharomyces cerevisiae*. *J Cell Biol* 151: 613–626.
- Sumara I, Vorlaufer E, Gieffers C, Peters BH, Peters JM (2000) Characterization of vertebrate cohesin complexes and their regulation in prophase. *J Cell Biol* 151: 749–762.
- Losada A, Yokochi T, Kobayashi R, Hirano T (2000) Identification and characterization of SA/SCC3p subunits in the *Xenopus* and human cohesin complexes. *J Cell Biol* 150: 405–416.
- Losada A, Yokochi T, Hirano T (2005) Functional contribution of Pds5 to cohesin-mediated cohesion in human cells and *Xenopus* egg extracts. *J Cell Sci* 118: 2133–2141.
- Tanaka K, Hao Z, Kai M, Okayama H (2001) Establishment and maintenance of sister chromatid cohesion in fission yeast by a unique mechanism. *Embo J* 20: 5779–5790.
- Neuwald AF, Hirano T (2000) HEAT repeats associated with condensins, cohesins, and other complexes involved in chromosome-related functions. *Genome Res* 10: 1445–1452.

Author Contributions

Conceived and designed the experiments: DI IK. Performed the experiments: IK MRS VV JR DI. Analyzed the data: VTS GR. Contributed reagents/materials/analysis tools: CL AVF. Wrote the paper: DI. Constructed strains: JM.

- Hauf S, Roitinger E, Koch B, Dittrich CM, Mechler K, et al. (2005) Dissociation of cohesin from chromosome arms and loss of arm cohesion during early mitosis depends on phosphorylation of SA2. *PLoS Biol* 3: e69.
- Bernard F, Schmidt CK, Vaur S, Dheur S, Drogat J, et al. (2000) Cell-cycle regulation of cohesin stability along fission yeast chromosomes. *Embo J* 27: 111–121.
- Haering CH, Lowe J, Hochwagen A, Nasmyth K (2002) Molecular architecture of SMC proteins and the yeast cohesin complex. *Mol Cell* 9: 773–788.
- Shintomi K, Hirano T (2009) Releasing cohesin from chromosome arms in early mitosis: opposing actions of Wapl-Pds5 and Sgo1. *Genes Dev* 23: 2224–2236.
- Hu B, Itoh T, Mishra A, Katoh Y, Chan KL, et al. (2011) ATP hydrolysis is required for relocating cohesin from sites occupied by its Scc2/4 loading complex. *Curr Biol* 21: 12–24.
- Gruber S, Arumugam P, Katou Y, Kuglitsch D, Helmhart W, et al. (2006) Evidence that Loading of Cohesin Onto Chromosomes Involves Opening of Its SMC Hinge. *Cell* 127: 523–537.
- Kanemaki M, Sanchez-Diaz A, Gambus A, Labib K (2003) Functional proteomic identification of DNA replication proteins by induced proteolysis in vivo. *Nature* 423: 720–724.
- Sanchez-Diaz A, Kanemaki M, Marchesi V, Labib K (2004) Rapid depletion of budding yeast proteins by fusion to a heat-inducible degron. *Sci STKE* 2004: PL8.
- Yen K, Gitsham P, Wishart J, Oliver SG, Zhang N (2003) An improved tetO promoter replacement system for regulating the expression of yeast genes. *Yeast* 20: 1255–1262.
- Lyons NA, Morgan DO (2011) Cdk1-dependent destruction of Eco1 prevents cohesin establishment after S phase. *Mol Cell* 42: 378–389.
- Weitzer S, Lehane C, Uhlmann F (2003) A model for ATP hydrolysis-dependent binding of cohesin to DNA. *Curr Biol* 13: 1930–1940.
- Yeh E, Haase J, Paliulis LV, Joglekar A, Bond L, et al. (2008) Pericentric chromatin is organized into an intramolecular loop in mitosis. *Curr Biol* 18: 81–90.
- Ivanov D, Nasmyth K (2005) A topological interaction between cohesin rings and a circular minichromosome. *Cell* 122: 849–860.
- Ben-Shahar TR, Heeger S, Lehane C, East P, Flynn H, et al. (2008) Eco1-dependent cohesin acetylation during establishment of sister chromatid cohesion. *Science* 321: 563–566.
- Fernius J, Hardwick KG (2007) Bub1 kinase targets Sgo1 to ensure efficient chromosome biorientation in budding yeast mitosis. *PLoS Genet* 3: e213.
- Warren GD, Eckley DM, Lee MS, Hanna JS, Hughes A, et al. (2004) S-phase checkpoint genes safeguard high-fidelity sister chromatid cohesion. *Mol Cell Biol* 24: 1724–1735.
- Game JC, Burrell GW, Brown JA, Shibata T, Baccari C, et al. (2003) Use of a genome-wide approach to identify new genes that control resistance of *Saccharomyces cerevisiae* to ionizing radiation. *Radiat Res* 160: 14–24.
- Sjogren C, Nasmyth K (2001) Sister chromatid cohesion is required for postreplicative double-strand break repair in *Saccharomyces cerevisiae*. *Curr Biol* 11: 991–995.
- Watrin E, Peters JM (2009) The cohesin complex is required for the DNA damage-induced G2/M checkpoint in mammalian cells. *Embo J* 28: 2625–2635.
- Lisby M, Mortensen UH, Rothstein R (2003) Colocalization of multiple DNA double-strand breaks at a single Rad52 repair centre. *Nat Cell Biol* 5: 572–577.
- Heidinge-Pauli JM, Mert O, Davenport C, Guacci V, Koshland D (2011) Systematic reduction of cohesin differentially affects chromosome segregation, condensation, and DNA repair. *Curr Biol* 20: 957–963.
- Gruber S, Haering CH, Nasmyth K (2003) Chromosomal cohesin forms a ring. *Cell* 112: 765–777.
- Gerlich D, Koch B, Dupeux F, Peters JM, Ellenberg J (2006) Live-cell imaging reveals a stable cohesin-chromatin interaction after but not before DNA replication. *Curr Biol* 16: 1571–1578.
- Vass S, Gotterill S, Valdeolmillos AM, Barbero JL, Lin E, et al. (2003) Depletion of Drad21/Sccl in *Drosophila* cells leads to instability of the cohesin complex and disruption of mitotic progression. *Curr Biol* 13: 208–218.
- Nonaka N, Kitajima T, Yokobayashi S, Xiao G, Yamamoto M, et al. (2002) Recruitment of cohesin to heterochromatic regions by Swi6/HP1 in fission yeast. *Nat Cell Biol* 4: 89–93.
- Rubio ED, Reiss DJ, Welch PL, Distchev CM, Filippova GN, et al. (2008) CTCF physically links cohesin to chromatin. *Proc Natl Acad Sci U S A* 105: 8309–8314.

52. Mc Intyre J, Muller EG, Weitzer S, Snyderman BE, Davis TN, et al. (2007) In vivo analysis of cohesin architecture using FRET in the budding yeast *Saccharomyces cerevisiae*. *Embo J* 26: 3783–3793.
53. Janke C, Magiera MM, Rathfelder N, Taxis C, Reber S, et al. (2004) A versatile toolbox for PCR-based tagging of yeast genes: new fluorescent proteins, more markers and promoter substitution cassettes. *Yeast* 21: 947–962.
54. Studier FW (2005) Protein production by auto-induction in high density shaking cultures. *Protein Expr Purif* 41: 207–234.
55. Ivanov D, Kwak YT, Nee E, Guo J, Garcia-Martinez LF, et al. (1999) Cyclin T1 domains involved in complex formation with Tat and TAR RNA are critical for tat-activation. *J Mol Biol* 288: 41–56.
56. Ivanov D, Nasmyth K (2007) A physical assay for sister chromatid cohesion in vitro. *Mol Cell* 27: 300–310.
57. Tanaka T, Cosma MP, Wirth K, Nasmyth K (1999) Identification of cohesin association sites at centromeres and along chromosome arms. *Cell* 98: 847–858.
58. Ossowski S, Schneeberger K, Clark RM, Lanz C, Warthmann N, et al. (2008) Sequencing of natural strains of *Arabidopsis thaliana* with short reads. *Genome Res* 18: 2024–2033.
59. Michaelis C, Ciosk R, Nasmyth K (1997) Cohesins: chromosomal proteins that prevent premature separation of sister chromatids. *Cell* 91: 35–45.
60. Liang C, Stillman B (1997) Persistent initiation of DNA replication and chromatin-bound MCM proteins during the cell cycle in *cdc6* mutants. *Genes Dev* 11: 3375–3386.
61. Zhang N, Kuznetsov SG, Sharan SK, Li K, Rao PH, et al. (2008) A handcuff model for the cohesin complex. *J Cell Biol* 183: 1019–1031.

CURRICULUM VITAE

Personal

Name Irina Kulemzina
Address Kirchentellinsfurter Straße 1
 72074 Tübingen
 Germany
Date of birth 3rd December 1986
Place of birth Rovno, USSR

Education

1994 – 2004 High School, Protvino, Russia

2005 – 2010 Studies in Bioinformatics and Bioengineering, Diploma, Lomonosov
Moscow State University, Moscow, Russia
Diploma thesis: ‘Studying the mechanisms of programmed cell death in
Saccharomyces cerevisiae involving Ydr391 and Ysp2 proteins’.
Supervisor: Prof. Dr. Fedor Severin, Lomonosov Moscow State
University and Belozersky Institute of Physico-Chemical Biology,
Moscow, Russia

2010 – 2012 Graduate studies, Eberhard Karls Universität Tübingen, Tübingen,
Germany
PhD thesis: ‘The role of cohesin associated factors, Pds5, Scc3, and
Wpl1 during cohesion establishment and maintenance in budding yeast’.
Supervisor: Dr. Dmitri Ivanov, Friedrich Miescher Laboratory of the
Max Planck Society, Tübingen, Germany